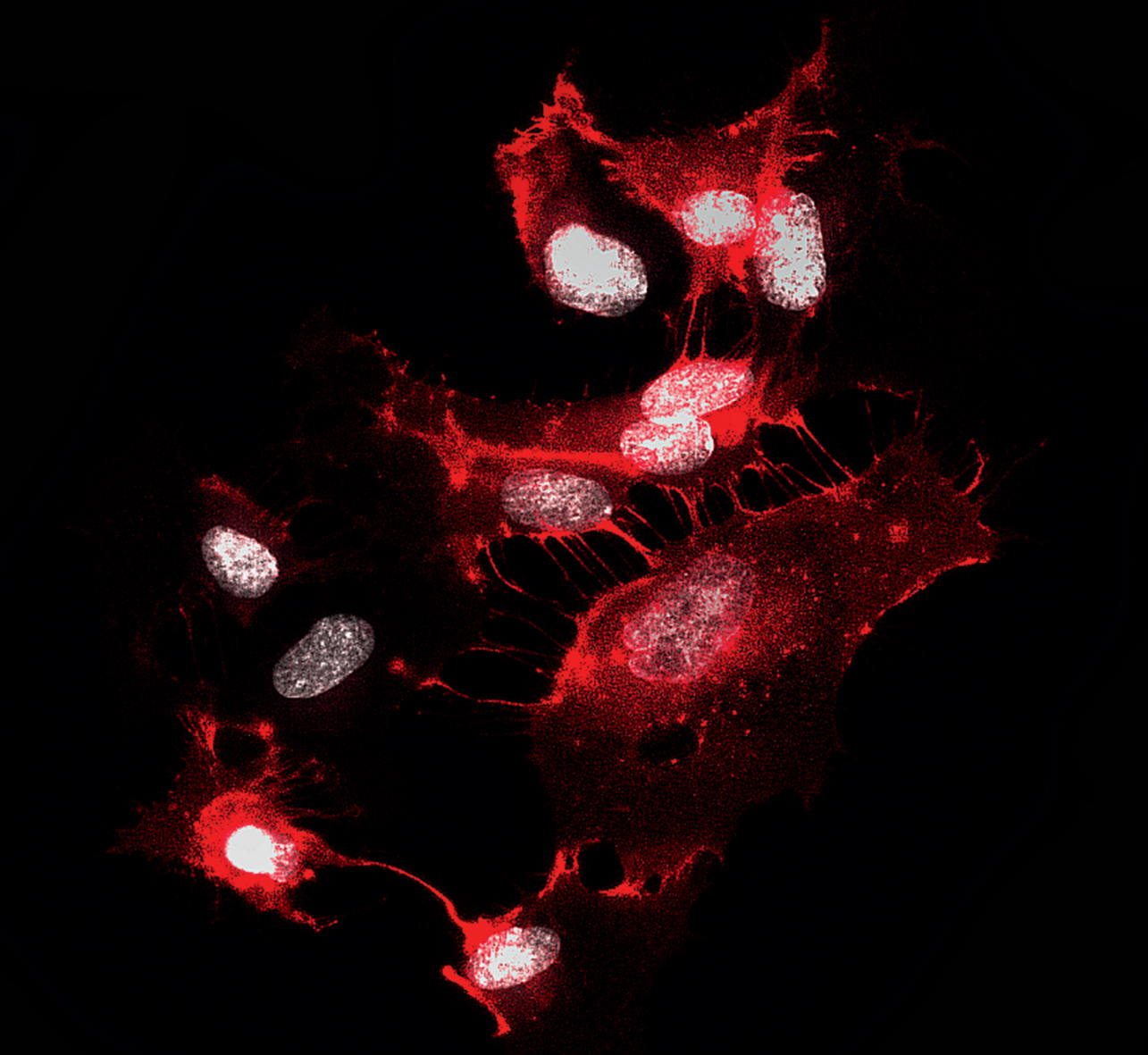
Intraplaque Angiogenesis and Therapeutic Targeting of Angiogenesis

Laura Parma



Intraplaque Angiogenesis and Therapeutic Targeting of Angiogenesis

Laura Parma

© L. Parma, 2020

Printing: Ridderprint BV, The Netherlands
ISBN: 978-94-6416-111-3
All rights reserved. No part of this thesis may be reproduced, distributed or transmitted in any form or by any means, without prior written permission of the author.

Intraplaque Angiogenesis and Therapeutic Targeting of Angiogenesis

Proefschrift

ter verkrijging van de graad van doctor
aan de Universiteit Leiden op gezag van rector magnificus prof. mr. C.J.J.M. Stolker,
volgens besluit van het College voor Promoties
te verdedigen op donderdag 15 oktober 2020
klokke 13:45 uur

door

Laura Parma
geboren op 29 januari 1990
te Vimercate, Italy

Promotor:	Prof. dr. P.H.A. Quax
Co-promotor:	Dr. M.R. de Vries Dr. S. Bellosta (University of Milano)
Leden promotiecommissie:	Prof. dr. M.J.T.H. Goumans Prof. dr. J.W. Jukema Prof. dr. J.D. van Buul (Sanquin, Amsterdam) Dr. J.C. Sluimer (CARIM Maastricht, University of Edinburgh)

The research presented in this thesis was performed at the Department of Surgery and the Einthoven Laboratory for Experimental Vascular Medicine, Leiden University Medical Center, Leiden, the Netherlands. The work was financially supported by the Horizon 2020 Marie Slodowska Curie Action (Grant number 675527).

Financial support by the Dutch Heart Foundation for the publication of this thesis is gratefully acknowledged.

Alla mia nonna Angelina

Table of Contents

Chapter 1: **General introduction**

Chapter 2: **Plaque angiogenesis and intraplaque hemorrhage in atherosclerosis.**
Parma L*, Baganha F*, Quax PHA, de Vries MR.
Eur J Pharmacology. 2017; 816:107-115.

Chapter 3: **Prolonged hyperoxygenation treatment improves vein graft patency and decreases macrophage content in atherosclerotic lesions in ApoE3*Leiden mice.**
Parma L, Peters HAB, Baganha F, Sluimer JC, de Vries MR and Quax PHA.
Cells. 2020 Feb 1;9(2).

Chapter 4: **Blockade of vascular endothelial growth factor receptor 2 inhibits intraplaque haemorrhage by normalization of plaque neovessels.**
de Vries MR*, Parma L*, Peters HAB, Schepers A, Hamming JF, Jukema JW, Goumans MJTH, Guo L, Finn AV, Virmani R, Ozaki CK, Quax PHA.
J Internal Medicine. 2018; 285(1):59-74.

Chapter 5: **Small molecule mediated inhibition of bFGF reduces intraplaque angiogenesis and macrophage infiltration in accelerated atherosclerotic vein graft lesions in ApoE3*Leiden mice.**
Parma L, Peters HAB, Simons KH, Lazzari P, de Vries MR, Quax PHA.
Manuscript under review.

Chapter 6: **Transketolase blockade reduces inflammation and angiogenesis in vitro.**
Parma L, MC Schmit, S Van Den Bogaert, de Vries MR, Quax PHA.
Manuscript in preparation.

Chapter 7: **BMOV induces angiogenesis via phosphorylation of VEGFR2 independently of VEGF addition.**
Parma L, Peters HAB, Meijerink H, de Vries MR, Quax PHA.
Int J Mol Sci. 2020 Jul; 21(13): 4643.

Chapter 8: **General summary and future perspectives**

Appendices: **Nederlandse samenvatting**
Riassunto in Italiano
List of publications
Curriculum Vitae
Acknowledgements

CHAPTER 1

GENERAL INTRODUCTION

General introduction

Atherosclerosis

Cardiovascular diseases (CVDs) are the major cause of death globally, taking an estimated 17.9 million lives each year [1]. CVDs is a broad term that comprises pathological conditions affecting heart and blood vessels. The most common cause underlying cardiovascular diseases is atherosclerosis, a chronic disease marked by the formation of plaques in the intimal layer of the arteries.

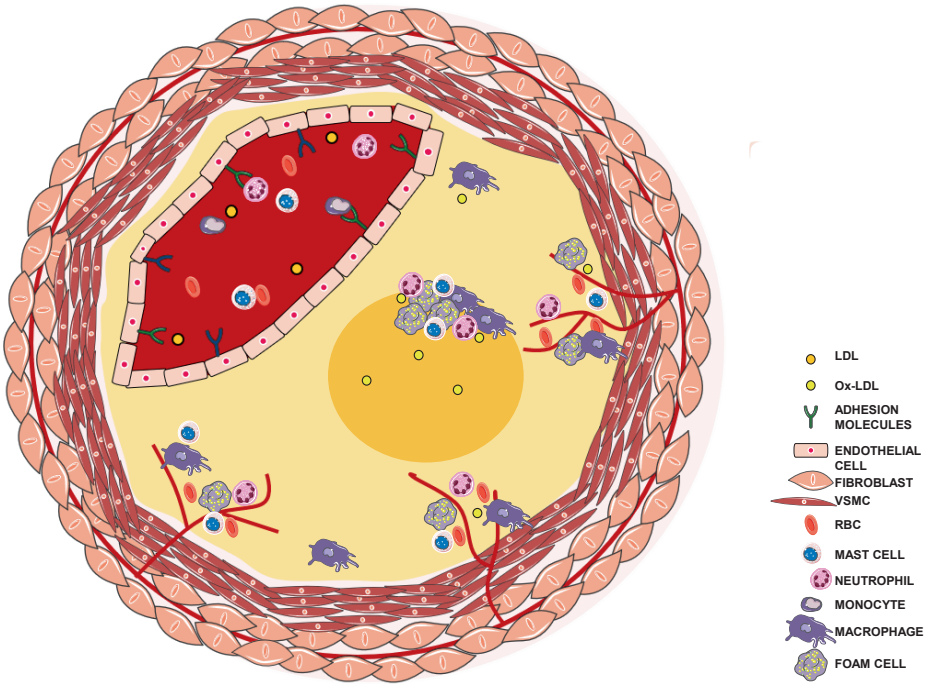


Figure 1. Unstable atherosclerotic plaque. Schematic representation of an advanced unstable atherosclerotic plaque. Features of plaque instability like intraplaque angiogenesis, haemorrhage, high inflammation and a large necrotic core are presents.

The earliest feature of atherosclerosis is characterized by oxidized low-density lipoproteins (oxLDL) accumulation in the aortic wall that provokes the expression of adhesion molecules on the dysfunctional endothelium and the production of inflammatory mediators resulting in the recruitment of monocytes [2,3]. Monocytes accumulate in the sub-intimal layer and differentiate into macrophages that engulf oxLDL and convert into lipid filled foam cells [4].

Engulfing of modified LDL by macrophages activates cytokine production that on its turn, promote the influx and activation of other inflammatory cells and their retention in the plaque [5]. Macrophages in atherosclerosis can be broadly divided in two groups. M1 pro-inflammatory macrophages play an important role in plaque progression by secreting pro-inflammatory cytokines and matrix metalloproteinases (MMPs) that drive the plaque toward an unstable phenotype [3,6]. In contrast, M2 anti-inflammatory macrophages promote tissue repair and hence favour plaque stability by reducing plaque size and cholesterol content [7,8].

As the plaque enlarges, the ensuing hypoxia and inflammation are thought to promote neovascularization [9]. These nascent immature blood vessels are leaky and permit extravasation of inflammatory cells and red blood cells into the plaque, a process called intraplaque haemorrhage, further contributing to necrotic core enlargement and plaque instability [9].

Intraplaque angiogenesis, intraplaque haemorrhage, high macrophage content and a large necrotic core are typical features of advanced unstable atherosclerotic plaques [10]. These plaques are more prone to rupture and the rupture of an unstable atherosclerotic plaque often results in thrombus formation and cessation of the blood flow, leading to the manifestation of severe clinical symptoms like myocardial infarction and stroke. The majority of acute cardiovascular events in patients is caused by occlusive thrombosis formed by rupture or erosion of an atherosclerotic plaque [11]. Despite improved insights into disease pathogenesis and therapeutic options, additional treatment strategies are required to block mechanisms involved in plaque destabilization [5].

Therefore, the aim of this thesis was to investigate the effects of new potential therapeutic strategies on the process of angiogenesis.

Angiogenesis

The formation of new blood vessels, angiogenesis, is a complex process that plays important roles in development, tissue and organ regeneration, as well as numerous pathological conditions [12,13]. The key players in this process are endothelial cells (ECs). Endothelial cells form the endothelium, a thin monolayer that lines the interior surface of a blood vessel.

During healthy adulthood most ECs are quiescent. During wound healing and in disorders fuelled by angiogenesis (for example cancer and atherosclerosis), quiescent ECs become proliferative and start rapidly to form new vessels [14]. The initial stimulus that triggers the process of angiogenesis is hypoxia [2,15]. Hypoxia is a state of lack of oxygen in which the tissue is in need for new vessels to restore its physiologic levels of oxygen. Hypoxia leads to the stabilization of the transcription factor Hypoxia-inducible factor 1-alpha (HIF1a), via preventing its degradation, and promotes its dimerization with the Hif1b subunit [16]. This complex activates the transcription of different genes, among which the pro-angiogenic factors like vascular endothelial growth factor (VEGF) and basic fibroblast growth factor (bFGF). These angiogenic growth factors work as stimuli that trigger the mobilization of endothelial cells and the formation of a new angiogenic sprout. Activated ECs release proteases that degrade the underlying basement membrane. Afterward, leading ECs start to migrate toward the angiogenic stimulus while the cells behind them proliferate and elongate the neovessel. At the end of the process a new mature vessel with a basement membrane and pericyte coverage is formed [14].

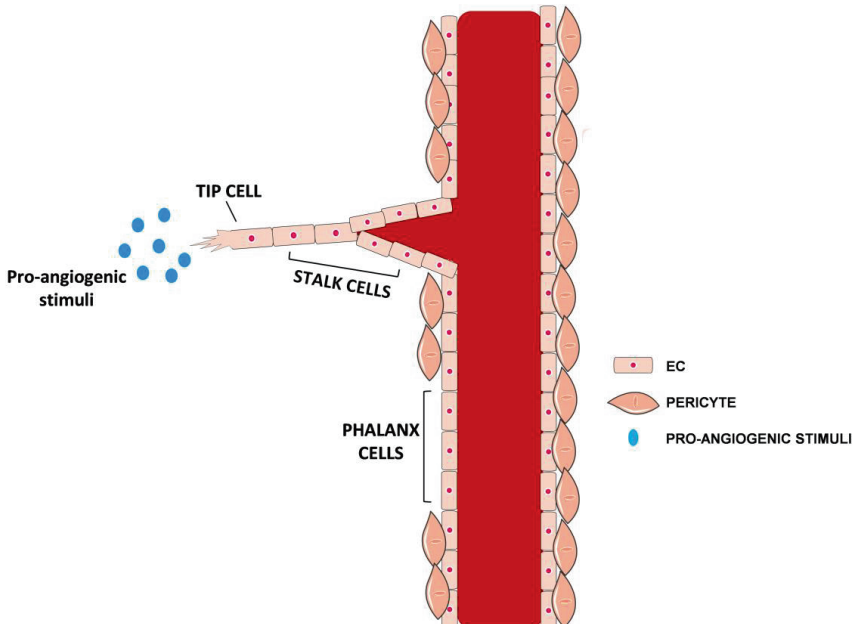


Figure 2. Process of angiogenesis. Schematic representation of the angiogenic process. Migrating tip cells migrate toward an angiogenic stimulus while stalk cells, through proliferation, elongate the nascent sprout. Phalanx cells line the lumen of quiescent vessels.

In a new vessel ECs with three distinct functions can be distinguished: phalanx, stalk and tip cells. Tip cells are motile and invasive and they quickly protrude filopodia that pull the cell forward. Tip cells lead the way to the nascent sprout sensing and migrating toward an angiogenic stimulus. Stalk cells are positioned behind the tip cells and elongate the stalk of the sprout. These cells proliferate, form junctions, lay down extracellular matrix and form a lumen [5]. However the EC phenotype is not static but dynamic. In fact, a stalk cell can become a tip cell, making sure that the fittest cell always leads the sprout [17]. The differentiation of tip versus stalk cell occurs via a Notch mediated lateral inhibition mechanism. Tip cells express high levels of VEGF receptor 2 (VEGFR2) in their filopodia following the VEGF pro-angiogenic signal. At the same time VEGF induces the expression of delta-like canonical Notch ligand 4 (Dll4). Dll4 activates Notch signalling in neighbouring cells and thereby suppresses VEGFR2 expression and tip cell behaviour and induces a stalk cell phenotype [18].

Once the new vessel has been formed, proliferating endothelial cells become quiescent phalanx cells. These cells form a cobblestone monolayer by sticking to each other through tight junctions, are covered by pericytes and are embedded in a thick basement membrane [19].

Phalanx, stalk and tip cells can also be characterized by their metabolism used mainly for redox homeostasis, biomass and energy production respectively [17]. Quiescent phalanx cells, exposed to high oxygen levels have to protect themselves from oxidative stress. To do so, phalanx cells have a 3-fold increase in their fatty acid oxidation (FAO), compared to proliferating cells, to ensure redox homeostasis via production of NADPH [20]. Proliferating stalk cells use the pentose phosphate pathway (PPP), the glutamine and serine pathways and FAO/TCA cycles for nucleotide and biomass production [21-23]. In contrast tip cells rely on PFKFB3-driven glycolysis to obtain fast energy to migrate [21].

Intraplaque angiogenesis in atherosclerosis

Intraplaque angiogenesis is the formation of neovessels inside an atherosclerotic plaque. During the process of plaque formation, large numbers of inflammatory cells enter the plaque. These cells are highly metabolic active and consume a great quantity of oxygen [24]. This process determines the status of intraplaque hypoxia, a status in which the oxygen demand is higher than the oxygen available. As explained above, hypoxia triggers the

recruitment of pro-angiogenic molecules that work as stimulus attracting endothelial cells coming from the vasa vasora. Most neovessels appear to originate from the adventitial vasa vasora, however in-growth of new vessels from the luminal endothelium has also been observed [25,26]. Endothelial cells migrate and proliferate from the existing vasculature of the vasa vasora toward the hypoxic area inside of the plaque following a gradient of pro-angiogenic cues and form new vessels.

An important feature of these vessels is that they are immature and therefore leaky [27]. They lack a complete pericyte coverage and moreover the tight junctions between endothelial cells are not completely formed leading to the extravasation of red blood cells and inflammatory cells from the neovessels to the inside the plaque, a process called intraplaque haemorrhage (IPH) [28]. Red blood cells in particular constitute the main cellular component of intraplaque haemorrhage [29]. Once red blood cells reach the highly oxidative intraplaque environment they lyse and their cellular membranes release un-esterified cholesterol [29]. At the same time extravasated inflammatory cells are rich sources of cytokines, growth factors, and proteases such as matrix metalloproteinases (MMPs), and can influence both plaque stability and plaque angiogenesis [2]. In addition, macrophages can secrete pro-angiogenic factors, like VEGF, and can therefore fuel intraplaque angiogenesis [30]. These processes contribute to increased plaque inflammation and instability, making the atherosclerotic plaque more prone to rupture.

One approach to stabilize atherosclerotic plaques and prevent their rupture is targeting intraplaque angiogenesis with the aim to reduce the number and/or increase the maturation of the neovessels.

Murine models of angiogenesis and atherosclerosis

Murine models are the preferred animal model to study atherosclerosis due to their rapid reproduction and ease of genetic manipulation. However naive atherosclerotic lesions in most of the traditionally used strains, ApoE KO, LDLR KO and ApoE3*Leiden, do not develop intraplaque angiogenesis most probably due to the small size of the lesions in which the hypoxia that occurs can be resolved by the regular levels of diffusion of oxygen via the lumen [5]. Currently two murine models have been developed with atherosclerotic lesions that show intraplaque angiogenesis. One model is based on vein graft surgery in ApoE3*Leiden mice on

high fat, high cholesterol diet. In this model, 28 days after surgery the lesions show typical characteristics of unstable human plaques, including intraplaque angiogenesis and haemorrhage, foam cells, calcification and cholesterol clefts [31]. The other is the ApoE KO Fbn1C1039G$^{+/-}$ mice model. A heterozygous mutation C1039G$^{+/-}$ in the Fbn1 gene results in the fragmentation of elastic fibers in the media of the vessel wall [32]. Those mice, if fed with a Western diet for 20 weeks, develop plaques that show intraplaque neovessels and intraplaque haemorrhage that can result in plaque rupture [33]. Both models are characterized by large atherosclerotic lesions and lack of elastic lamina together the cause of the displayed plaque angiogenesis. In this thesis we use one model of accelerated atherosclerosis, namely the vein graft model, that presents intraplaque angiogenesis. In this thesis two more animal models are used; to study intimal hyperplasia the femoral artery cuff model has been used and for studying in vivo angiogenesis, the murine Matrigel plug model was used.

Vein graft accelerated atherosclerosis in ApoE3*Leiden mice

Vein graft bypass surgery is mimicked in a mouse model of vein graft surgery. When this procedure is performed in mice that are prone to develop atherosclerosis, like the ApoE3*Leiden mice on a hypercholesterolemic diet, the lesion within the vein graft develop with an accelerated form of atherosclerosis [34,35]. During the surgical procedure the thoracic caval vein from a donor mouse is inter-positioned within the right carotid artery of a recipient mouse. Pulsatile flow through the venous conduit confirms a successful procedure. Donor mice are on chow diet until T=0, time point at which they are sacrificed. Recipient mice are on high cholesterol, high fat diet from three weeks prior the surgery until the day of sacrifice 28 days after surgery [35].

28 days after surgery the lesions formed highly resemble human native atherosclerotic lesions including intraplaque angiogenesis and haemorrhage, calcification, cholesterol clefts and the presence of foam cells [31].

Femoral artery cuff placement in C57BL/6 mice

A murine model to study intimal hyperplasia is the femoral artery cuff placement in C57BL/6 mice. In this model of intimal hyperplasia a non-constrictive cuff around the femoral artery of C57BL/6 mice is placed. Briefly, the left and right femoral arteries are isolated and a rigid, non-

constrictive polyethylene cuff is placed around the artery [36]. In response to this injury a smooth muscle cells (SMCs) rich neointima is formed within three weeks if this model is used under normocholesterolemic conditions. After 21 days, accelerated atherosclerotic lesions are formed in which is present a strong predominance of SMCs and no presence of intraplaque angiogenesis.

Matrigel plug model of in vivo angiogenesis in C57BL/6 mice

A widely used in vivo assay for the evaluation of pro- or anti-angiogenic factors is the in vivo angiogenesis plug assay, which makes use of the basement membrane Matrigel [12]. ECs migrate and proliferate in the Matrigel and here they form neovessels. During this procedure Matrigel extracellular matrix is injected into the subcutaneous space on the dorsal side of C57BL/6 mice on both flanks [37]. Matrigel is liquid at 4 °C and gels at higher temperatures and therefore it solidifies after injection forming a plug at body temperature. Over time, blood vessels will sprout into the plug and after 21 days new angiogenic sprouts are visible in the plugs [37].

Potential angiogenic targets for therapeutic interventions

In the past years, the number of compounds targeting different pathways to counteract angiogenic growth has greatly increased, mainly in the oncological field [38]. Due to their role in angiogenesis, growth factors and their receptors, as well as protein tyrosine kinases (PTKs) and protein tyrosine phosphatases (PTPs), families of proteins that regulate the phosphorylation of these receptors, are main targets for angiogenic therapies. More recently, several studies showed that endothelial cell metabolism is a driver of angiogenesis and therefore the enzymes involved in different metabolic pathways, such as PFKFB3, represent new targets for anti-angiogenic therapies [17].

VEGF/VEGFR2 signalling

The VEGF family is composed of five structurally related factors: VEGF-A, VEGF-B, VEGF-C, VEGF-D and the placenta growth factor (PlGF) [39]. These ligands bind with different affinities to three VEGF receptor tyrosine kinases (VEGFR1-3) [39]. The receptors show an overlapping but distinct expression pattern with mainly VEGFR1 expressed in monocytes and macrophages, VEGFR2 in vascular endothelial cells, and VEGFR3 in lymphatic endothelial cells.

VEGFR1 signalling is involved in inhibition of angiogenesis, immune cell recruitment, fatty acid uptake, while VEGFR2 signalling activation promotes angiogenesis and VEGFR3 promotes lymph-angiogenesis [39,40]. VEGFR2 is part of the receptor tyrosine kinases family (RTKs). VEGF binding to VEGFR results in autophosphorylation of specific tyrosine residues in the cytoplasmic domain of VEGFR2 [41]. Phosphorylated VEGFR2 initiates downstream signalling pathways relevant to angiogenesis and produces several cellular responses in ECs including a strong mitogenic signal and survival signal [42]. The signalling network comprises the activation of signalling molecules and the cross talks involving these molecules modulates the process of angiogenesis [42].

Due to their important role in angiogenesis therapeutics targeting VEGF/VEGFR2 signalling were developed to block vessel growth in retinopathy and cancer [43]. In the context of atherosclerosis, it was shown that treatment with axitinib (inhibitor of VEGFR1, 2 and 3) attenuated plaque angiogenesis in ApoE$^{-/-}$Fbn1C1039G$^{+/-}$ mice [44]. Therefore, anti-VEGFR2 antibody treatment may have beneficial effects in stabilizing advanced atherosclerotic plaques, which is discussed in chapter 4.

bFGF/FGFR signalling

The basic fibroblast growth factor (bFGF), also called FGF2, is part of the fibroblast growth factors family that comprises 18 members that act as ligands and 4 members that represents the receptors (FGFR1-4) [45]. It is a very well-known regulator of angiogenesis and exerts is function by binding to one of the four FGFR. When promoting angiogenesis, bFGF binds primarily to FGFR1 on the surface of ECs [46,47]. bFGF has been shown to be involved in the pathogenesis of atherosclerosis [48] as well as in the regulation of processes that drive plaque instability [49,50].

Several studies showed that targeting FGF/FGFR axis could be beneficial for atherosclerosis. A study from Raj et al., showed that inhibiting FGFR signalling with the RTK inhibitor SU5402 in ApoE$^{-/-}$ mice fed a high-fat diet inhibited neointimal thickening by almost 85 % [51]. SSR128129E, a small-molecule multi-FGF receptor blocker was tested in a vein graft model in C57BL/6J mice and in ApoE$^{-/-}$ mice [52]. SSR128129E decreased neointima proliferation in both models [52]. However, it has been shown that a tight regulation of FGF signalling is necessary for vascular homeostasis and therefore the complete blockade of all the four

receptors could have adverse effects. To overcome this problem, we collaborated in the synthesis of the small molecule 3'-(propane-1,3-diyilbis(azanediyl)bis(oxomethylene)bis(1-(2,4-dichlorophenyl)-1,4-dihydro-thieno[3',2':4,5]cyclohepta[1,2-c]pyrazole-8-sulfonic acid), namely K5 that binds to bFGF and inhibits the bFGF/FGFR signalling [53]. The effects of K5 treatment on accelerated vein graft atherosclerosis in ApoE3*Leiden mice are described in chapter 5.

Pentose phosphate pathway

Besides the glycolysis, an alternative metabolic process for the breakdown of glucose is the pentose phosphate pathway (PPP) [54]. This pathway has two distinct phases: the oxidative phase and the non-oxidative phase. First, glucose-6-phosphate (G6P) is converted into ribose-5-phosphate (R5P) in the oxidative branch, generating NADPH [54]. The non-oxidative branch provides precursors for nucleotide synthesis and glycolytic metabolites by interconverting fructose-6-phosphate (F6P) and glyceraldehyde-3-phosphate (G3P) generating R5P [54].

A key enzyme involved in the pentose phosphate pathway is transketolase (TKT), which is a thiamine-dependent enzyme. This enzyme reversibly links the non-oxidative branch of the PPP to the glycolysis controlling nucleotide biosynthesis and energy production. Both ECs and macrophages rely on this metabolic pathway to carry out proliferation [55]. Intraplaque angiogenesis and inflammation are strongly connected in atherosclerosis. The interaction between these two processes forms a vicious cycle that modifies the microenvironment composition of the plaque and drives the plaque towards an unstable phenotype. It has been shown that PPP blockade in macrophages reduces cytokine secretion and inflammation [56]. The result of TKT blockade in macrophages and its effects on angiogenesis are described in chapter 6.

Protein tyrosine Phosphatases

The activation of receptor tyrosine kinases is controlled not only by the binding of specific ligands, but it is also regulated by protein tyrosine phosphatases (PTPs) [57]. PTPs are a family of endogenous modulators of RTKs-mediated signalling pathways that carry out the dephosphorylation of phospho-tyrosine residues [57]. Among RTKs regulated by PTPs there are some master regulators of angiogenesis like VEGFR, FGFR and PDGFR. PTPs acts by either

direct dephosphorylation of particular receptor tyrosine residues or of downstream signalling components [57].

Due to their broad function, the regulation or blockade of PTPs could be an approach to increase RTKs activation and subsequently angiogenesis. We investigated the effect of PTPs blockade using bis(maltolato)oxidovanadium (IV) (BMOV) on in vitro angiogenesis and VEGFR2 signalling in **chapter 7**.

Outline of the thesis

The aim of this thesis was to investigate the effects of new potential therapeutic strategies on angiogenesis. The first part of this thesis focusses on new possibilities to inhibit or decrease intraplaque angiogenesis in atherosclerosis. **Chapter 2** consist of a review on intraplaque angiogenesis and intraplaque haemorrhage in atherosclerosis. In this review we discuss the processes that drive intraplaque angiogenesis as well as new imaging techniques to detect intraplaque angiogenesis in patients. Moreover, we give an overview of angiogenesis targets and animal models used for the study of atherosclerosis.

In **Chapter 3** we study how restoring hypoxia via hyperoxygenation treatment using carbogen gas (95%O_2, 5%CO_2) in ApoE3*Leiden mice that underwent vein graft surgery, affects intraplaque angiogenesis and vascular remodelling.

In **Chapter 4** we describe the effect of VEGFR2 blockade using a monoclonal antibody, DC101, on accelerated atherosclerotic lesions in ApoE3*Leiden mice. We investigate the role of VEGFR2 blockade on vascular remodelling as well as on intraplaque angiogenesis and on the maturation of neovessels. Due to the great importance of growth factors receptors and their ligands in angiogenesis, in **Chapter 5** we examine the effect of bFGF blockade on the stability of advanced atherosclerotic plaques. We describe how a new small molecule, K5, by binding and inhibiting bFGF have effects on the remodelling of accelerated atherosclerotic vein graft lesions and their compositions, including intraplaque angiogenesis and haemorrhage. In **Chapter 6** we study how TKT inhibition affects the production of pro-inflammatory and pro-angiogenic cytokines in cultured human macrophages. Additionally, we show the functional consequences of macrophage TKT blockade on angiogenesis in vitro. The second part of this thesis focusses on a new strategy to increase in vitro angiogenesis. In **Chapter 7** we unravel the effect of BMOV mediated PTPs blockade on in vitro angiogenesis using human endothelial

cells. Moreover, we examine how this influences the activation of VEGFR2 and its downstream signalling.

References

1. (WHO), W.H.O. Cardiovascular Diseases. **2018**.
2. de Vries, M.R.; Quax, P.H. Plaque angiogenesis and its relation to inflammation and atherosclerotic plaque destabilization. *Curr Opin Lipidol* **2016**, *27*, 499-506, doi:10.1097/mol.0000000000000339.
3. Thomas, A.C.; Eijgelaar, W.J.; Daemen, M.J.; Newby, A.C. Foam Cell Formation In Vivo Converts Macrophages to a Pro-Fibrotic Phenotype. *PloS one* **2015**, *10*, e0128163, doi:10.1371/journal.pone.0128163.
4. Chistiakov, D.A.; Bobryshev, Y.V.; Orekhov, A.N. Macrophage-mediated cholesterol handling in atherosclerosis. *Journal of cellular and molecular medicine* **2016**, *20*, 17-28, doi:10.1111/jcmm.12689.
5. Parma, L.; Baganha, F.; Quax, P.H.A.; de Vries, M.R. Plaque angiogenesis and intraplaque hemorrhage in atherosclerosis. *Eur J Pharmacol* **2017**, *816*, 107-115, doi:10.1016/j.ejphar.2017.04.028.
6. Huang, W.C.; Sala-Newby, G.B.; Susana, A.; Johnson, J.L.; Newby, A.C. Classical macrophage activation up-regulates several matrix metalloproteinases through mitogen activated protein kinases and nuclear factor-kappaB. *PloS one* **2012**, *7*, e42507, doi:10.1371/journal.pone.0042507.
7. Lee, S.G.; Oh, J.; Bong, S.K.; Kim, J.S.; Park, S.; Kim, S.; Park, S.; Lee, S.H.; Jang, Y. Macrophage polarization and acceleration of atherosclerotic plaques in a swine model. *PloS one* **2018**, *13*, e0193005, doi:10.1371/journal.pone.0193005.
8. Llodra, J.; Angeli, V.; Liu, J.; Trogan, E.; Fisher, E.A.; Randolph, G.J. Emigration of monocyte-derived cells from atherosclerotic lesions characterizes regressive, but not progressive, plaques. *Proceedings of the National Academy of Sciences of the United States of America* **2004**, *101*, 11779-11784, doi:10.1073/pnas.0403259101.
9. Virmani, R.; Kolodgie, F.D.; Burke, A.P.; Finn, A.V.; Gold, H.K.; Tulenko, T.N.; Wrenn, S.P.; Narula, J. Atherosclerotic plaque progression and vulnerability to rupture: angiogenesis as a source of intraplaque hemorrhage. *Arterioscler Thromb Vasc Biol* **2005**, *25*, 2054-2061, doi:10.1161/01.Atv.0000178991.71605.18.
10. Jain, R.K.; Finn, A.V.; Kolodgie, F.D.; Gold, H.K.; Virmani, R. Antiangiogenic therapy for normalization of atherosclerotic plaque vasculature: a potential strategy for plaque stabilization. *Nature clinical practice. Cardiovascular medicine* **2007**, *4*, 491-502, doi:10.1038/ncpcardio0979.
11. Hansson, G.K.; Libby, P.; Tabas, I. Inflammation and plaque vulnerability. *Journal of internal medicine* **2015**, *278*, 483-493, doi:10.1111/joim.12406.
12. Nowak-Sliwinska, P.; Alitalo, K.; Allen, E.; Anisimov, A.; Aplin, A.C.; Auerbach, R.; Augustin, H.G.; Bates, D.O.; van Beijnum, J.R.; Bender, R.H.F., et al. Consensus guidelines for the use and interpretation of angiogenesis assays. *Angiogenesis* **2018**, *21*, 425-532, doi:10.1007/s10456-018-9613-x.
13. Bikfalvi, A. History and conceptual developments in vascular biology and angiogenesis research: a personal view. *Angiogenesis* **2017**, *20*, 463-478, doi:10.1007/s10456-017-9569-2.
14. Carmeliet, P.; Jain, R.K. Molecular mechanisms and clinical applications of angiogenesis. *Nature* **2011**, *473*, 298-307, doi:10.1038/nature10144.
15. Lee, E.S.; Bauer, G.E.; Caldwell, M.P.; Santilli, S.M. Association of artery wall hypoxia and cellular proliferation at a vascular anastomosis. *The Journal of surgical research* **2000**, *91*, 32-37, doi:10.1006/jsre.2000.5891.
16. Jain, T.; Nikolopoulou, E.A.; Xu, Q.; Qu, A. Hypoxia inducible factor as a therapeutic target for atherosclerosis. *Pharmacology & therapeutics* **2018**, *183*, 22-33, doi:10.1016/j.pharmthera.2017.09.003.
17. Li, X.; Sun, X.; Carmeliet, P. Hallmarks of Endothelial Cell Metabolism in Health and Disease. *Cell metabolism* **2019**, *30*, 414-433, doi:10.1016/j.cmet.2019.08.011.
18. De Bock, K.; Georgiadou, M.; Schoors, S.; Kuchnio, A.; Wong, B.W.; Cantelmo, A.R.; Quaegebeur, A.; Ghesquiere, B.; Cauwenberghs, S.; Eelen, G., et al. Role of PFKFB3-driven glycolysis in vessel sprouting. *Cell* **2013**, *154*, 651-663, doi:10.1016/j.cell.2013.06.037.
19. Carmeliet, P.; De Smet, F.; Loges, S.; Mazzone, M. Branching morphogenesis and antiangiogenesis candidates: tip cells lead the way. *Nature reviews. Clinical oncology* **2009**, *6*, 315-326, doi:10.1038/nrclinonc.2009.64.
20. Kalucka, J.; Bierhansl, L.; Conchinha, N.V.; Missiaen, R.; Elia, I.; Bruning, U.; Scheinok, S.; Treps, L.; Cantelmo, A.R.; Dubois, C., et al. Quiescent Endothelial Cells Upregulate Fatty Acid beta-Oxidation for Vasculoprotection via Redox Homeostasis. *Cell metabolism* **2018**, *28*, 881-894.e813, doi:10.1016/j.cmet.2018.07.016.

21. Cantelmo, A.R.; Conradi, L.C.; Brajic, A.; Goveia, J.; Kalucka, J.; Pircher, A.; Chaturvedi, P.; Hol, J.; Thienpont, B.; Teuwen, L.A., et al. Inhibition of the Glycolytic Activator PFKFB3 in Endothelium Induces Tumor Vessel Normalization, Impairs Metastasis, and Improves Chemotherapy. *Cancer cell* **2016**, *30*, 968-985, doi:10.1016/j.ccell.2016.10.006.
22. Leopold, J.A.; Walker, J.; Scribner, A.W.; Voetsch, B.; Zhang, Y.Y.; Loscalzo, A.J.; Stanton, R.C.; Loscalzo, J. Glucose-6-phosphate dehydrogenase modulates vascular endothelial growth factor-mediated angiogenesis. *J Biol Chem* **2003**, *278*, 32100-32106, doi:10.1074/jbc.M301293200.
23. Vandekeere, S.; Dubois, C.; Kalucka, J.; Sullivan, M.R.; Garcia-Caballero, M.; Goveia, J.; Chen, R.; Diehl, F.F.; Bar-Lev, L.; Souffreau, J., et al. Serine Synthesis via PHGDH Is Essential for Heme Production in Endothelial Cells. *Cell metabolism* **2018**, *28*, 573-587.e513, doi:10.1016/j.cmet.2018.06.009.
24. Tawakol, A.; Singh, P.; Mojena, M.; Pimentel-Santillana, M.; Emami, H.; MacNabb, M.; Rudd, J.H.; Narula, J.; Enriquez, J.A.; Traves, P.G., et al. HIF-1alpha and PFKFB3 Mediate a Tight Relationship Between Proinflammatory Activation and Anerobic Metabolism in Atherosclerotic Macrophages. *Arterioscler Thromb Vasc Biol* **2015**, *35*, 1463-1471, doi:10.1161/atvbaha.115.305551.
25. Khurana, R.; Simons, M.; Martin, J.F.; Zachary, I.C. Role of angiogenesis in cardiovascular disease: a critical appraisal. *Circulation* **2005**, *112*, 1813-1824, doi:10.1161/circulationaha.105.535294.
26. Sueishi, K.; Yonemitsu, Y.; Nakagawa, K.; Kaneda, Y.; Kumamoto, M.; Nakashima, Y. Atherosclerosis and angiogenesis. Its pathophysiological significance in humans as well as in an animal model induced by the gene transfer of vascular endothelial growth factor. *Annals of the New York Academy of Sciences* **1997**, *811*, 311-322; 322-314, doi:10.1111/j.1749-6632.1997.tb52011.x.
27. Xu, J.; Lu, X.; Shi, G.P. Vasa vasorum in atherosclerosis and clinical significance. *International journal of molecular sciences* **2015**, *16*, 11574-11608, doi:10.3390/ijms160511574.
28. Jeney, V.; Balla, G.; Balla, J. Red blood cell, hemoglobin and heme in the progression of atherosclerosis. *Frontiers in physiology* **2014**, *5*, 379, doi:10.3389/fphys.2014.00379.
29. Michel, J.B.; Martin-Ventura, J.L.; Nicoletti, A.; Ho-Tin-Noe, B. Pathology of human plaque vulnerability: mechanisms and consequences of intraplaque haemorrhages. *Atherosclerosis* **2014**, *234*, 311-319, doi:10.1016/j.atherosclerosis.2014.03.020.
30. Ribatti, D.; Crivellato, E. Immune cells and angiogenesis. *Journal of cellular and molecular medicine* **2009**, *13*, 2822-2833, doi:10.1111/j.1582-4934.2009.00810.x.
31. Lardenoye, J.H.; de Vries, M.R.; Löwik, C.W.; Xu, Q.; Dhore, C.R.; Cleutjens, J.P.; van Hinsbergh, V.W.; van Bockel, J.H.; Quax, P.H. Accelerated atherosclerosis and calcification in vein grafts: a study in APOE*3 Leiden transgenic mice. *Circ Res* **2002**, *91*, 577-584.
32. Van der Veken, B.; De Meyer, G.R.; Martinet, W. Intraplaque neovascularization as a novel therapeutic target in advanced atherosclerosis. *Expert opinion on therapeutic targets* **2016**, *20*, 1247-1257, doi:10.1080/14728222.2016.1186650.
33. Van der Donckt, C.; Van Herck, J.L.; Schrijvers, D.M.; Vanhoutte, G.; Verhoye, M.; Blockx, I.; Van Der Linden, A.; Bauters, D.; Lijnen, H.R.; Sluimer, J.C., et al. Elastin fragmentation in atherosclerotic mice leads to intraplaque neovascularization, plaque rupture, myocardial infarction, stroke, and sudden death. *European heart journal* **2015**, *36*, 1049-1058, doi:10.1093/eurheartj/ehu041.
34. Parma, L.; Peters, H.A.B.; Baganha, F.; Sluimer, J.C.; de Vries, M.R.; Quax, P.H.A. Prolonged Hyperoxygenation Treatment Improves Vein Graft Patency and Decreases Macrophage Content in Atherosclerotic Lesions in ApoE3*Leiden Mice. *Cells* **2020**, *9*, doi:10.3390/cells9020336.
35. de Vries, M.R.; Parma, L.; Peters, H.A.B.; Schepers, A.; Hamming, J.F.; Jukema, J.W.; Goumans, M.; Guo, L.; Finn, A.V.; Virmani, R., et al. Blockade of vascular endothelial growth factor receptor 2 inhibits intraplaque haemorrhage by normalization of plaque neovessels. *Journal of internal medicine* **2019**, *285*, 59-74, doi:10.1111/joim.12821.
36. de Vries, M.R.; Niessen, H.W.; Lowik, C.W.; Hamming, J.F.; Jukema, J.W.; Quax, P.H. Plaque rupture complications in murine atherosclerotic vein grafts can be prevented by TIMP-1 overexpression. *PloS one* **2012**, *7*, e47134, doi:10.1371/journal.pone.0047134.
37. Doorn, J.; Fernandes, H.A.; Le, B.Q.; van de Peppel, J.; van Leeuwen, J.P.; De Vries, M.R.; Aref, Z.; Quax, P.H.; Myklebost, O.; Saris, D.B., et al. A small molecule approach to engineering vascularized tissue. *Biomaterials* **2013**, *34*, 3053-3063, doi:10.1016/j.biomaterials.2012.12.037.
38. Vasudev, N.S.; Reynolds, A.R. Anti-angiogenic therapy for cancer: current progress, unresolved questions and future directions. *Angiogenesis* **2014**, *17*, 471-494, doi:10.1007/s10456-014-9420-y.
39. Koch, S.; Claesson-Welsh, L. Signal transduction by vascular endothelial growth factor receptors. *Cold Spring Harbor perspectives in medicine* **2012**, *2*, a006502, doi:10.1101/cshperspect.a006502.

40. Simons, M.; Gordon, E.; Claesson-Welsh, L. Mechanisms and regulation of endothelial VEGF receptor signalling. *Nature reviews. Molecular cell biology* **2016**, *17*, 611-625, doi:10.1038/nrm.2016.87.
41. Cebe-Suarez, S.; Zehnder-Fjallman, A.; Ballmer-Hofer, K. The role of VEGF receptors in angiogenesis; complex partnerships. *Cellular and molecular life sciences : CMLS* **2006**, *63*, 601-615, doi:10.1007/s00018-005-5426-3.
42. Abhinand, C.S.; Raju, R.; Soumya, S.J.; Arya, P.S.; Sudhakaran, P.R. VEGF-A/VEGFR2 signaling network in endothelial cells relevant to angiogenesis. *Journal of cell communication and signaling* **2016**, *10*, 347-354, doi:10.1007/s12079-016-0352-8.
43. Apte, R.S.; Chen, D.S.; Ferrara, N. VEGF in Signaling and Disease: Beyond Discovery and Development. *Cell* **2019**, *176*, 1248-1264, doi:10.1016/j.cell.2019.01.021.
44. Van der Veken, B.; De Meyer, G.R.Y.; Martinet, W. Axitinib attenuates intraplaque angiogenesis, haemorrhages and plaque destabilization in mice. *Vascular pharmacology* **2018**, *100*, 34-40, doi:10.1016/j.vph.2017.10.004.
45. Beenken, A.; Mohammadi, M. The FGF family: biology, pathophysiology and therapy. *Nature reviews. Drug discovery* **2009**, *8*, 235-253, doi:10.1038/nrd2792.
46. Javerzat, S.; Auguste, P.; Bikfalvi, A. The role of fibroblast growth factors in vascular development. *Trends in molecular medicine* **2002**, *8*, 483-489, doi:10.1016/s1471-4914(02)02394-8.
47. Bastaki, M.; Nelli, E.E.; Dell'Era, P.; Rusnati, M.; Molinari-Tosatti, M.P.; Parolini, S.; Auerbach, R.; Ruco, L.P.; Possati, L.; Presta, M. Basic fibroblast growth factor-induced angiogenic phenotype in mouse endothelium. A study of aortic and microvascular endothelial cell lines. *Arterioscler Thromb Vasc Biol* **1997**, *17*, 454-464, doi:10.1161/01.atv.17.3.454.
48. Lindner, V.; Lappi, D.A.; Baird, A.; Majack, R.A.; Reidy, M.A. Role of basic fibroblast growth factor in vascular lesion formation. *Circ Res* **1991**, *68*, 106-113, doi:10.1161/01.res.68.1.106.
49. Takahashi, J.C.; Saiki, M.; Miyatake, S.; Tani, S.; Kubo, H.; Goto, K.; Aoki, T.; Takahashi, J.A.; Nagata, I.; Kikuchi, H. Adenovirus-mediated gene transfer of basic fibroblast growth factor induces in vitro angiogenesis. *Atherosclerosis* **1997**, *132*, 199-205, doi:10.1016/s0021-9150(97)00102-0.
50. Sigala, F.; Savvari, P.; Liontos, M.; Sigalas, P.; Pateras, I.S.; Papalampros, A.; Basdra, E.K.; Kolettas, E.; Papavassiliou, A.G.; Gorgoulis, V.G. Increased expression of bFGF is associated with carotid atherosclerotic plaques instability engaging the NF-kappaB pathway. *Journal of cellular and molecular medicine* **2010**, *14*, 2273-2280, doi:10.1111/j.1582-4934.2010.01082.x.
51. Raj, T.; Kanellakis, P.; Pomilio, G.; Jennings, G.; Bobik, A.; Agrotis, A. Inhibition of fibroblast growth factor receptor signaling attenuates atherosclerosis in apolipoprotein E-deficient mice. *Arterioscler Thromb Vasc Biol* **2006**, *26*, 1845-1851, doi:10.1161/01.ATV.0000227689.41288.5e.
52. Dol-Gleizes, F.; Delesque-Touchard, N.; Mares, A.M.; Nestor, A.L.; Schaeffer, P.; Bono, F. A new synthetic FGF receptor antagonist inhibits arteriosclerosis in a mouse vein graft model and atherosclerosis in apolipoprotein E-deficient mice. *PloS one* **2013**, *8*, e80027, doi:10.1371/journal.pone.0080027.
53. Lazzari P., Z.M., Sani M. United States patent number US9181196B2. **2014**.
54. Ramos-Martinez, J.I. The regulation of the pentose phosphate pathway: Remember Krebs. *Archives of biochemistry and biophysics* **2017**, *614*, 50-52, doi:10.1016/j.abb.2016.12.012.
55. Tang, C.Y.; Mauro, C. Similarities in the Metabolic Reprogramming of Immune System and Endothelium. *Frontiers in immunology* **2017**, *8*, 837, doi:10.3389/fimmu.2017.00837.
56. Baardman, J.; Verberk, S.G.S.; Prange, K.H.M.; van Weeghel, M.; van der Velden, S.; Ryan, D.G.; Wust, R.C.I.; Neele, A.E.; Speijer, D.; Denis, S.W., et al. A Defective Pentose Phosphate Pathway Reduces Inflammatory Macrophage Responses during Hypercholesterolemia. *Cell reports* **2018**, *25*, 2044-2052.e2045, doi:10.1016/j.celrep.2018.10.092.
57. Buschmann, I.; Hackbusch, D.; Gatzke, N.; Dulsner, A.; Trappiel, M.; Dagnell, M.; Ostman, A.; Hooft van Huijsduijnen, R.; Kappert, K. Inhibition of protein tyrosine phosphatases enhances cerebral collateral growth in rats. *Journal of molecular medicine (Berlin, Germany)* **2014**, *92*, 983-994, doi:10.1007/s00109-014-1164-z.

CHAPTER 2

PLAQUE ANGIOGENESIS AND INTRAPLAQUE HEMORRHAGE IN ATHEROSCLEROSIS

L Parma[1,2*], F Baganha[1,2*], MR de Vries[1,2], PHA Quax[1,2]

[*]Authors contributed equally to this work
[1]Department of Surgery and [2]Einthoven Laboratory for Experimental Vascular Medicine, Leiden University Medical Center, Leiden, The Netherlands

Eur J Pharmacol. 2017;816:107-115.

ABSTRACT

Acute cardiovascular events, due to rupture or erosion of an atherosclerotic plaque, represent the major cause of morbidity and mortality in patients. Growing evidence suggests that plaque neovascularization is an important contributor to plaque growth and instability. The vessels' immaturity, with profound structural and functional abnormalities, leads to recurrent intraplaque hemorrhage.

This review discusses new insights of atherosclerotic neovascularization, including the effects of leaky neovessels on intraplaque hemorrhage, both in experimental models and humans. Furthermore, modalities for in vivo imaging and therapeutic interventions to target plaque angiogenesis will be discussed.

INTRODUCTION

The majority of acute cardiovascular events in patients is caused by occlusive thrombosis formed by rupture or erosion of an atherosclerotic plaque.[1] Despite improved insight into disease pathogenesis and therapeutic options, additional treatment strategies are required to block mechanisms involved in plaque destabilization.

Advanced atherosclerotic lesions are characterized by large necrotic cores with thin fibrous caps, cholesterol deposits, inflammatory cells and calcifications [2]. Recent insights in the pathophysiology of atherosclerotic lesions have shed new light on the formation of unstable lesions. For instance, it has been shown that, of the total number of foam cells a significant portion is derived from smooth muscle cells (SMCs) rather than from macrophages [3]. Also the role of calcification is more clarified, it has been shown that extended calcification can stabilize atherosclerotic plaques [4], whereas spotty micro-calcifications contribute to plaque destabilization [5-7]. Furthermore, it is becoming more and more clear that plaque angiogenesis and intraplaque hemorrhage (IPH) are important contributors to unstable lesions [8,9]. Plaque angiogenesis is a physiological response to the increased oxygen demand in the plaque but can have adverse effects by facilitating IPH and influx of inflammatory mediators [10].

This review is focused on plaque angiogenesis, the relation with inflammatory mediators, and the subsequent effects of IPH on plaque instability, both in experimental models and in humans. Moreover, options to target plaque angiogenesis for imaging and therapeutic purposes will be discussed.

ANGIOGENESIS-DRIVING PROCESSES

Hypoxia

The molecular mechanism regulating angiogenesis in atherosclerosis involves signaling pathways that are mainly driven by the lack of oxygen [11]. Hypoxia occurs when oxygen supply is decreased and or oxygen demand is increased. The ability to sense and respond to changes in O2 concentration is a fundamental feature of all nucleated cells. Cell survival in a hypoxic environment leads to a general shut-down of energy-consuming transcription and translation, with one major exception — the hypoxia-inducible factor (HIF) pathway [12,13].

Hypoxia promotes monocyte/ macrophage survival and oxLDL uptake by macrophages [14]. It also enhances the expression of matrix metalloproteases by a variety of cells in the plaque contributing to the instability of the plaque [15]. Furthermore, due to the hypoxic state of macrophages ATP depletion occurs, causing cell death and expansion of the necrotic core leading to a feedback cycle between plaque expansion and hypoxia. Fong et al. has shown that exposure to hypoxia accelerates the plaque growth of ApoE KO mice fed with a high cholesterol diet [16]. In contrast, when atherosclerosis prone mice were exposed to carbogen (95% O2, 5 % CO2) oxygenation, plaque growth was inhibited [12]. Sluimer et al. showed extensive hypoxia in the center of advanced human carotid atherosclerotic plaques [17]. Pimonidazole, a hypoxia marker, was co-localized with CD68 positive macrophages, HIF1-α and VEGF expression, suggesting the involvement of the HIF pathway in the regulation of human plaque angiogenesis and lesion progression [17].

HIF is a heterodimeric protein composed of α and β subunits. The α chain confers oxygen regulation on the complex and its expression is hypoxia-dependent and has three isoforms, HIF-1α, 2α and 3α of which only HIF-1α and HIF-1β are widely expressed in normal tissues [18-20]. The beta chain (three isoforms) is constitutively expressed and works as an aryl receptor nuclear translocator. Under normoxic conditions, the synthesized HIF-1α is rapidly degraded and the co-activators are blocked by oxygen-dependent enzymes, the prolyl-hydroxylases domain (PHD) enzymes [21,22]. During hypoxia, PHD activity is reduced, allowing the dimerization of HIF-1α and HIF-1β [23,24]. This active complex binds to DNA starting the transcription of downstream genes involved in angiogenesis and inflammation [25]. HIF-1α mediates inflammation by promoting pro-inflammatory cytokines expression (stromal cell-derived factor 1, VEGF-A) and consequently inflammatory cell recruitment [26,27]. Arrup et al. have shown that HIF-1α expression also modulates the macrophage glycolytic pathway, by increasing glucose uptake and glucose transporter 1 mRNA expression, enhancing oxygen consumption. In addition, HIF-1α reduces the mRNA expression of the major cholesterol transporters [28] and activates the lectin-like OxLDL receptor-1 scavenger receptors that mediates oxLDL uptake in macrophages [29], leading to the expansion of the foam cell population. Interestingly, hypoxia can also reduce macrophage migration, by mediating the expression of retention molecules that stimulate their accumulation and prevent egression from the plaque [30]. Thus, hypoxia induced overexpression of HIF-1α not only regulates

plaque angiogenesis, but also has additional effects stimulating the growth of atherosclerotic plaques.

Moreover, an extensive crosstalk between HIF and nuclear factor-kB (NF-κB), two important molecular players in atherosclerosis, has been reported. They have common activating stimuli and share regulators and targets [31,32]. Only the canonical NF-κB pathway is sensitive to hypoxia, while both the inhibitor of NF-κB subunit alpha (IKKα) and the inhibitor of NF-κB subunit beta (IKKβ) can be hydroxylated by PHD [33,34]. Marsch et al. shows that PHD1 knockout mice display a protective cardiovascular metabolic phenotype with lower plasma cholesterol levels and glucose tolerance improvement [35]. Furthermore, NF-κB has been shown to play a role in basal and stimulated HIF-1α mRNA expression. The p50 and p65 NF-κB subunits can bind to the HIF-1α promoter in response to hypoxia and when these subunits are overexpressed, an increase in HIF-1α mRNA levels and promoter activity is observed [36]. The full mechanism between HIF and NF-κB in hypoxia is not yet completely understood but these features highlight the complex and interrelated hypoxia and inflammatory signaling cascades in atherosclerosis.

Endothelial Cells Sprouting

Angiogenic sprouting involves the invasion of avascular areas by proliferating and migrating ECs. The mechanism of angiogenesis has been deeply studied and the process of neovessel formation has been described in detail [37] [38], [39] [40]. In a nascent sprout, three phenotypically distinct EC types can be recognized: tip, stalk and phalanx cells. Tip cells are motile and invasive, protrude filopodia and lead the way to the nascent sprout since they are located at the forefront of the vessel branches, sensing and responding to guidance cues in the microenvironment, while migrating toward an angiogenic stimulus. Stalk cells trail behind the tip cells and elongate the stalk of the sprout. These cells proliferate, form junctions, lay down extracellular matrix and form a lumen. Phalanx cells are the most quiescent ECs, lining vessels once the new vessel branches have been consolidated [41].

The differentiation of tip versus stalk cell occurs via a Notch mediated lateral inhibition mechanism. VEGF-A and VEGF receptor 2 (VEGFR-2) signaling induces tip cells formation and delta-like canonical Notch ligand 4 (Dll4) upregulation. Expression of Dll4 in tip cells activates Notch in adjacent ECs, thereby decreasing the expression of VEGFR-2 and inducing stalk cell differentiation [42]. Interestingly, it was shown that Notch signaling promotes the progression

of atherosclerosis in vivo [42]. Blockade of Dll4–Notch signaling by anti-Dll4 antibody administration, suppresses atheroma progression in the aorta of LDLR KO mice that were fed high-cholesterol/high-fat diet for 24 weeks. Blockade of this angiogenesis related pathway leads to a reduction in the accumulation of macrophages in the aorta of the mice treated with neutralizing anti-Dll4 antibody [42], showing the tight interaction of these processes.

VEGF-A, VEGF-C and their receptors VEGFR-2 and VEGFR-3 participate in the detachment process of ECs from the ECM and guide the behavioral switching of the ECs. To ensure optimal fitness of the tip cell leading the sprout, the EC with the highest responsiveness to VEGF will occupy the tip position. Chronic inflammatory cell infiltration in the atherosclerotic plaque activates ECs and enhances the expression of different cell adhesion molecules like vascular cell adhesion protein 1 (VCAM-1) and intercellular Adhesion Molecule 1 (ICAM-1), which recruit monocytes and lymphocytes [43].

A stabilized and mature vascular plexus includes adoption of a quiescent endothelial phalanx phenotype, branch regression, basement membrane deposition and coverage with pericytes that will stabilize the endothelial tubes and help regulating the capillary diameter and vessel permeability. Fusion of sprouting neovessels, which is necessary to form vascular networks, is controlled by bridging-macrophages [44]. Macrophages accumulate at sites of vessel anastomosis and interact with filopodia of neighboring tip cells during fusion. It was shown in zebrafish embryos that macrophages can act as cellular chaperones for endothelial cell fusion by bridging tip cells from different vessel segments [45].

Although it is widely accepted that angiogenesis is mainly regulated by hypoxia, other factors like hemodynamic forces may also regulate angiogenesis.

Hemodynamic forces

Blood flow plays crucial roles in angiogenesis by generating frictional force that develops between flowing blood and the vascular endothelium [46]. ECs covering the inner surface of blood vessels are constantly exposed to different types of shear stress. Shear stress is pulsatile in normal physiology, but can be oscillatory in pathologies such as atherosclerosis, affecting endothelial function and morphology. The EC response to shear stress is closely linked to the regulation of vascular tone, blood coagulation and fibrinolysis, angiogenesis, and vascular remodelling, and it plays an important role in maintaining the homoeostasis of the circulatory

system [47]. Shear stress induces collateral artery growth as well as capillary growth and it was shown that endoglin played a crucial role in this process [48]. Furthermore, it is known that shear stress modulates the expression of thrombospondin 1 and its receptor CD36 during angiogenesis in vivo [49]. Impairment of the EC response to shear stress leads to the development of vascular diseases such as hypertension, thrombosis, aneurysms, and atherosclerosis [47]. The mechanisms and sensors by which ECs initially recognize shear stress have yet to be confirmed, but the sensors most likely involved in angiogenesis are Piezo1 [50], calcium [51] and primary cilia [52].

ANGIOGENESIS IN THE ATHEROSCLEROTIC PLAQUE

Pathological angiogenesis of the vessel wall is a consistent feature of atherosclerotic plaque development and progression of the disease [53] however the source of plaque neovessels is not fully established. The general idea is that endothelial cells (ECs) grow from the existing adventitial vasa vasorum triggered by a gradient of VEGF, into the plaque. [54].

Adventitial angiogenesis is thought to be the main source of neovessels. In addition, it has been suggested that angiogenesis may also occur from the luminal side. However, clear evidence for the extent of this phenomenon is lacking.

Due to its important role in atherosclerotic plaques, vasa vasorum has been studied as a therapeutical target. Langheinrich et al. reported a significant decrease of lesion size in ApoE KO LDL KO mice treated with 3-Deazaadenosine, an anti-inflammatory and anti-proliferative drug. This was accompanied by a significant decrease of vasa vasorum neovascularization, although no effects on intraplaque angiogenesis were reported [55].

Descriptive and cross-sectional studies in humans suggest a clear association between the neovessel density and atherosclerotic progression and vulnerability [11]. A large longitudinal atherosclerosis plaque biobank study (AtheroExpress) demonstrated that plaque neovascularization but also IPH significantly relate to adverse cardiovascular outcome during clinical follow-up [54].

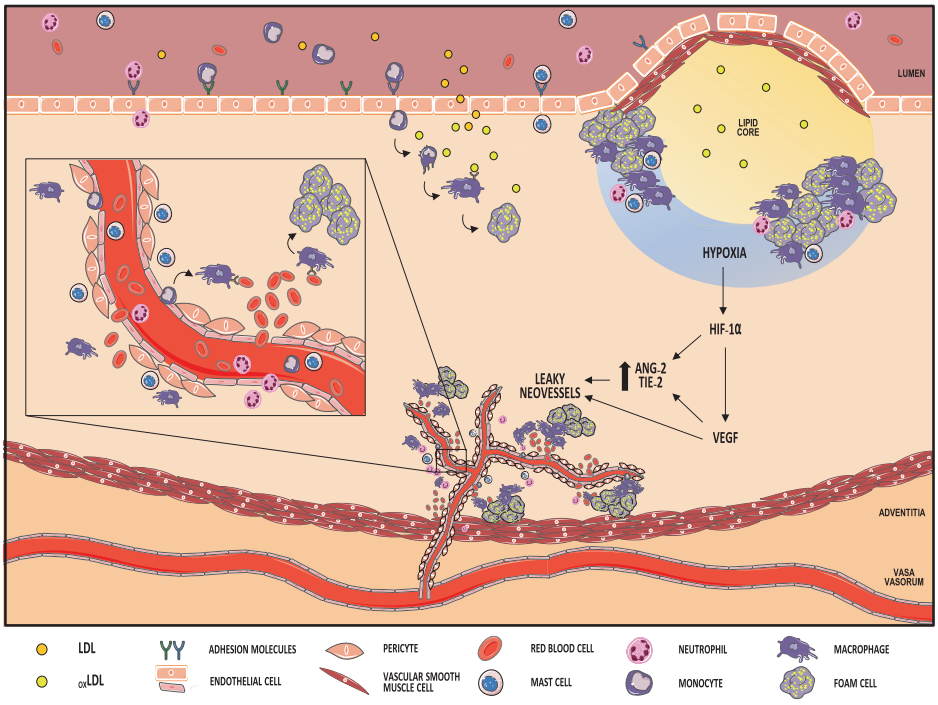


Figure. 1. Plaque angiogenesis. Once in the plaque macrophages engulf oxLDL and become lipid filled foam cells. Their accumulation activates cytokine production that promotes the influx of neutrophils, mast cells and monocytes. The high oxygen consumption of these inflammatory cells leads to hypoxia. HIF-1α and VEGF, together with an unbalanced presence of the destabilizing factor Ang2 bound to its receptor Tie2, trigger the formation of leaky neovessels. (Magnification) Intraplaque hemorrhage, with extravasation of red blood cells and inflammatory cells, is due to immature neovessels, lacking proper enveloping pericytes and poor tight junctions between endothelial cells. Macrophages accumulate cholesterol to the point of becoming foam cells by phagocytizing extravasated red blood cells.

Intraplaque hemorrhage

Neovessels in vulnerable plaques are immature, irregular and fragile due to the compromised structural integrity [56]. In fact, they are characterized by discontinuous basement membrane and a low number of tight junctions between ECs [57]. Moreover these premature vessels are relatively poor in pericytes coverage and are therefore immature and highly susceptible to leakage of circulating cells [58], leading to intraplaque hemorrhage (IPH). In the oncological field, newly formed vessels have been reported to have the same features. Tumor vessels are heterogeneous [59], and many are hyperpermeable [60]. In their walls, there are inter endothelial openings and trans endothelial channels, resulting in a wide range of pore sizes [61]. The hyperpermeability of tumor vessels allows plasma to flow to the interstitial space [61]. Moreover tumor vessels are organized in a chaotic fashion and do not follow the

hierarchical branching pattern of normal vascular networks [62]. Of interest is that compared to normal individuals, patients with acute coronary syndrome have red blood cells with higher amounts of cholesterol in the membranes. Consequently the leakage of these red blood cells may lead to an increased cholesterol deposition, atheroma growth and decreasing plaque stability. Thus, the cholesterol content in the red blood cell membrane could be a marker for the growth and vulnerability of the atherosclerotic plaque [63,64].

The key players in vessel maturation are VEGF its receptors and the members of the angiopoietin system. VEGF and its main receptors VEGFR-1 and VEGFR-2 drive EC proliferation and tube formation as well as the attachment and detachment of pericytes during the maturation of neovessels [37]. Angiopoietin-1 (Ang-1) and angiopoietin-2 (Ang-2) are ligands of the endothelial receptor Tie-2, and both have a major role in the final maturation phase of neovascularization with opposite functions. HIF-1α and VEGF-A, induce Ang-2 to destabilize the interactions between pericytes and ECs, and thus allows vessels to grow. Ang-1 together with platelet derived growth factor (PDGF) acts as a major stabilizing factor that increases the stability of the junctions between the EC, thus promoting vessel maturity and stability and reducing leakiness [65]. The balance between Ang-1 and Ang-2 expression was explored in human plaques. A positive correlation was observed between Ang-2 expression and microvascular density within the plaque, as well as with the ratio Ang-2/Ang-1 [66]. Also, PDGF-BB and its receptor (PDGFR)-β are known to be important in vessel permeability, fragility, and impaired perfusion [43], because of their pivotal role in the establishment of functional blood vessels by recruiting and stabilizing perivascular cells.

These findings suggest that the neovessels are subjected to regular leakage associated with extravasation of red blood cells, leucocytes and plasma lipids to the neighborhood.

Red blood cells

Extravasated red blood cells (RBCs) constitute the main cellular component of IPH, which with their hemoglobin content and cell membrane components, enriched in unesterified cholesterol, participate in both the cholesterol accumulation and the oxidative process [67]. Once trapped in the highly oxidative environment of the atherosclerotic plaques, RBCs tend to lyse quickly [68]. The cytoplasm of RBCs is rich in hemoglobin, which can attract multiple monocytes and neutrophils to the plaque [58].

Cholesterol retention in the atherosclerotic plaque leads to cholesterol crystal formation. This can originate directly from free cholesterol or from cholesterol esters endocytosed by foam cells. RBCs membrane have a high cholesterol content with a percentage of lipids up to 40% of the total weight of the cells [69]. It has been suggested that RBC membranes are very important contributors to lipid deposition and lipid core expansion upon IPH. This is further illustrated by the presence of iron and glycophorin A, a characteristic protein of the RBC membrane, which co-localizes with cholesterol crystals within the plaques, suggesting that cholesterol crystals could originate from erythrocytes phagocytized by macrophages [70].

Inflammation

Inflammation is a key factor in all stages of atherosclerosis progression.

In the initial phase of atherosclerosis, oxidized low-density lipoproteins (oxLDL) accumulation in the aortic wall triggers the expression of adhesion molecules that facilitate the migration of monocytes into the aortic wall [10]. Monocytes differentiate into macrophages that engulf oxLDL and convert into lipid filled foam cells. Accumulation of modified LDL by macrophages activates cytokine production that promote the influx and activation of other inflammatory cells and their retention in the plaque. Most inflammatory cells in the plaque, and especially macrophages, are metabolic very active cells that exhibit high oxygen consumption which leads to oxygen deprivation in the plaque [71]. In addition, monocytes/macrophages release pro-angiogenic factors such as VEGF and by interacting with vascular smooth muscle cells (VSMC), macrophages induce unbalanced synthesis of the extracellular matrix (ECM) leading to secretion of VEGF by VSMC [72]. Furthermore, in endarterectomy samples obtained during surgery an accumulation of mast cells was observed in neovessel-rich areas of atherosclerotic plaques [73]. Whereas, in animal experiments it was demonstrated that mast cells situated near the newly formed vessels contained fibroblast growth factor (FGF), a potent pro-angiogenic factor [74]. In line with these reports, it was stated that vasa vasorum vessel density in atherosclerotic lesions of ApoE KO mice highly correlates with the occurrence of inflammatory cells foci [72,75-77].

In advanced lesions, neovessels leakage constitutes the main entrance for inflammatory cells. The influx of RBCs facilitate the extravasation of circulating inflammatory cells. The influx of RBCs facilitate the extravasation of circulating inflammatory cells. RBCs can change the forces on an interacting cell, by giving the ability to interact with the endothelium at higher shear

stress, increasing the contact frequency and duration with the endothelium [78]. RBCs increase the numbers of rolling and adhering monocytes by increasing the normal force and/or the frequency of collision of monocytes interacting with the endothelium. The increase in cell capture requires the physical presence of RBCs, indicating that RBC-induced mechanical forces may facilitate leukocyte-endothelial cell interactions in vivo [78]. This invasion leads to reactive, inflammatory and apoptotic environment where the instability of the plaque is profoundly affected. Not only monocytes are increased, also neutrophils and mast cells were increased, that can release their granular content rich in serine proteases and matrix metalloproteases [67]. These proteases digest components of elastic fibers (elastin) and of the basement membrane (collagen, laminin and fibronectin). This high proteolytic activity can ultimately lead to fibrous cap thinning and plaque erosion [79,80]. Furthermore, the influx and lysis of RBCs drives a higher request of macrophage activity in order to phagocytose the RBC remainders. In combination with the hampered efferocytosis response in the atherosclerotic lesions causing an impaired clearance of these apoptotic cells by lesional macrophages this may explain why these macrophage accumulate in the atherosclerotic necrotic core, and may potentiate vascular inflammation [81,82]. Also, their ability to efferocytosis, phagocytosis of dying/dead cells, is defective. This malfunctioning increases the inflammation state and reduces cholesterol efflux contributing to necrotic core expansion and ultimately, the increase of risk of plaque rupture [83].

IMAGING OF ANGIOGENESIS

The detection of patients with atherosclerotic plaques at risk is a major challenge for the cardiovascular research field. It has inspired the development of invasive and non-invasive imaging technologies to visualize the atheroma in detail. The significant investments in these imaging technologies are not only justified by the need to early diagnose patients with atherosclerosis but also by the development of drug programs [84].

The most prominent imaging technologies are already in used in clinical studies and their value to identify crucial characteristics of vulnerable plaques is undeniable [85]. Plaque angiogenesis is one of these features and its detection in vivo can represent a step forward in diagnosis and follow up of atherosclerosis.

The most advanced technique in humans to visualize angiogenesis is positron emission tomography, PET [86-88]. This high sensitive tool uses 18F-fluorodeoxyglucose (FDG), a glucose analogue tracer. After intravenous injection, 18F-FDG is taken up by cells that metabolize glucose, where it becomes trapped after phosphorylation. Due to the high glycolytic rate of endothelial cells, plaque neovascularization can be monitored by 18F-FDG uptake [85]. However, PET images do not give structural information. This has to be assessed using PET with combined techniques such as computed tomography (CT), magnetic resonance imaging (MRI) [89]. Another disadvantage is the low resolution, as a result of this imaging of angiogenesis in small size animal models is still a challenge.

Near-infrared fluorescence (NIRF) appears to be a highly versatile platform for in vivo molecular imaging due to their picomolar sensitivity and microscopic resolution [90]. Matter et al. developed a sensor for NIRF that targets the extra-domain B of fibronectin, inserted into fibronectin during angiogenesis. In this study, blood vessels were visualized with a good target-to-background ratio[91]. NIRF can also be used for the identification of specific plaque features, such as MMP activity [92] or flow patterns [93,94]. NIRF however does not provide any structural information on the plaque. This limitation can, in part, be overcome by multimodal imaging such as NIRF–optical coherence tomography (OCT) and others [95,96].
OCT is an imaging technique also based on infrared light, which can be used to study atherosclerotic plaques with extreme spatial accuracy. OCT imaging presents a strong correlation to histology and specificity to distinguish plaque phenotypes. OCT has been used to identify patients with risk of plaque rupture by measuring calcified nodules, fibrous cap thickness, lipid pool extension and also neovascularization [97]. However, contrary to PET and NIRF, OCT does not allow specific molecular targeting.

No perfect technique is yet available but the combination of multimodal technologies seems to be a promising opportunity for imaging [95]. Furthermore, the strong correlation between angiogenesis and plaque progression suggests a useful application of imaging technologies as a therapeutic approach for patients with atherosclerosis.

ANGIOGENESIS TARGETS

VEGF, Ang2 and Endostatin

In the last decade, there has been a substantial increase in compounds targeting different pathways to counteract angiogenic growth, mainly investigated in the oncological field. Interestingly, lately more emphasis is put on stabilizing neovessels rather than blockade of angiogenesis due to unwanted side effects [98,99]. Several approaches have been investigated in order to block angiogenesis in the atherosclerotic plaques, such as the use of anti-angiogenic agents and blocking pro-angiogenic factors.

Endostar is a novel modified recombinant human endostatin [100] a broad-spectrum angiogenesis inhibitor that interferes with the pro-angiogenic action of growth factors such as basic fibroblast growth factor (bFGF/FGF-2) and VEGF. A study in ApoE KO mice study showed that prolonged treatment with endostatin reduced plaque growth [101]. More recently, Endostar has been tested in a swine model [102]. The combination of hypercholesterolemic diet with balloon injury resulted in early atherosclerotic lesions. The use of Endostar in this model attenuates vasa vasorum neovascularization, vessel wall inflammation and the progression of atherosclerosis.

A different therapeutic approach, besides the use of anti-angiogenic agents, could be the blockage of pro-angiogenic factors.

Bevacizumab, a fully humanized anti-VEGF antibody is a well-known inhibitor of angiogenesis and is widely used in clinical oncology. Although Bevacizumab does not recognize murine VEGF [103], it showed profound effects in a murine model by causing disruption of the endothelium and consequently accelerated atherosclerosis in ApoE KO mice [104].

In a New Zealand rabbits model, Bevacizumab-eluting stent implantation in iliac arteries inhibits neovascularization without affecting re-endothelialization. Local gene delivery of VEGFR-1 in the iliac artery of a rabbit in which an atherosclerotic plaque was induced by high-lipid diet in combination with balloon catheter injury, reduced lesion formation. This occurred most likely via an inhibitory effect on atherosclerotic plaque angiogenesis, which hints at the clinical utility of sFlt-1 in atherosclerosis therapy [105].

Apart from VEGF, another angiogenic target under study is Ang-2. Blockade of Ang-2 on experimental atherosclerosis in LDLR-/- ApoB100/100 mice on high cholesterol diet was shown to result in delayed fatty streak formation and decreased plasma triglyceride levels.

However, Ang-2 deletion did not prevent plaque progression or changes in plaque stability and did not affect adventitial neovessel density [106].

So far, the right anti-angiogenic target in atherosclerosis is yet to be found, but the potential of anti-angiogenic approaches in the tumor field, suggest that anti-angiogenic treatments in atherosclerosis will be defined in the near future. Of note should be that targeting the vaso vasorum neovascularization is a different approach than blocking the intraplaque angiogenesis, despite the fact that the intraplaque angiogenic capillaries have their origin in the vasa vasorum.

EC Metabolism

In the field of (tumor) angiogenesis, it is well recognized that endothelial cell metabolism changes during hypoxia, switching to glycolysis-dependent ATP production [107]. In atherosclerosis, plaque progression is associated with macro and micro endothelial dysfunction, which is attributed to EC metabolic maladaptation [108]. Therefore, targeting the endothelial glycolytic metabolism might be a promising therapeutic approach. To date, no treatments are available yet, however some targets have been described: tetrahydrobiopterin (BH4), NADPH oxidase 1 (NOX1) and NADPH oxidase 2 (NOX2) and 6-phosphofructo-2-kinase/fructose-2,6-biphosphatase 3 (PFKFB3) [108].

BH4, an endothelial NOS (eNOS) cofactor, is metabolic inactivated during endothelial dysfunction. Strategies to restore vascular BH4 availability is being tested in ongoing studies. In ApoE KO mice with reduced nitric oxide (NO) synthesis, supplementation with BH4 precursors reduces reactive oxygen species (ROS) production and fosters NO synthesis [109]. However, clinical trials in patients with coronary heart disease and myocardial infarction have shown mixed results for BH4 supplementation [110].

NOX enzymes are another important source of ROS in atherosclerosis which strongly affects plaque angiogenesis. NOX use NADPH, another eNOS cofactor, for ROS production, compromising NO levels [111]. In addition, NOX activate redox-sensitive transcriptional factors such as NF-κB and HIF1α [112,113]. Based on those findings, NOX antagonists have been developed for the treatment of cardiovascular diseases and are currently in preclinical testing.

PFKFB3, a key activator of glycolysis (the main pathway source for energy in EC), is highly expressed in proliferating ECs. Interestingly, genetic or pharmacological inhibition of PFKFB3

impairs the ability of ECs to sprout *in vitro* and to form vessels *in vivo* [114,115]. Pharmacological PFKFB3 blockade, leads to a partial and transient reduction of glycolysis, capable of reducing pathological angiogenesis in inflamed skin, colon and eye disease, without evoking systemic effects [116]. In addition, overexpression of PFKFB3 overrules the pro-stalk cell effect of Notch signaling, thereby making the stalk cell more competitive for the tip position [115]. Altogether, these findings illustrate the pivotal role of glycolysis in angiogenesis and the therapeutic potential of blocking glycolysis in plaque angiogenesis inhibition.

ANIMAL MODELS

Among the different animal models used to study atherosclerosis, pigs and rats are rarely suitable for exploring plaque neovascularization in the atherosclerotic plaque because they seldom display plaque neovessels [43]. In contrast, induced advanced atherosclerotic plaques in the thoracic descending aorta of New Zealand white rabbits show intra plaque angiogenesis, as detected using contrast-enhanced ultrasound [117].

Mice are a preferred model to study atherosclerosis since there are all kinds of transgenic strains available. Unfortunately most of the traditionally used strains, ApoE KO, LDLR KO and ApoE3*Leiden, do not develop extensive neovessels in their atherosclerotic plaques. Recently two models have been developed with atherosclerotic lesions that are more unstable and prone to rupture.

One model is based on murine vein graft atherosclerosis. Human atherosclerotic lesions in saphenous vein bypass grafts are vulnerable and have a higher risk to disrupt than native atherosclerotic lesions [2,118]. The murine vein graft model is performed by the interposition of a caval vein from a donor mouse into the carotid artery of an atherosclerosis prone recipient mouse. Hypercholesterolemia in ApoE3*Leiden mice resulted in a significant increase in accelerated atherosclerosis in vein grafts with profound vein graft thickening within 4 weeks after surgery. These lesions are rich in neovessels and are most likely formed through angiogenesis from the vasa vasora and consist of CD31 positive endothelial cells [92]. In a substantial number of vein grafts, a considerable amount of RBCs could be found in the extracellular matrix, adjacent to the neovessels, suggesting leakiness and intraplaque hemorrhage (Fig. 1). Foam cell accumulation was even observed within seven days after vein

bypass grafting, which illustrates the extreme fast initiation of this accelerated atherosclerosis [119]. Reducing inflammatory responses in this model could inhibit IPH, as well as erosions and plaque dissection thereby increasing plaque stability [120].

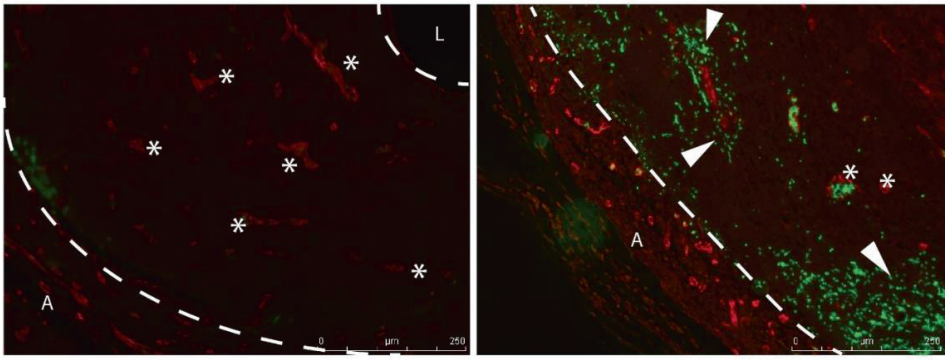


Figure. 2. Vein graft lesions in hypercholesterolemic ApoE3*Leiden mice 28 days after surgery. (a) Vein graft lesions show extensive neovessels (*). (b) Red blood cells dispersed in the extracellular matrix outside the neovessels demonstrate intraplaque hemorrhage (arrow head) in a vein graft lesion. CD31 positive endothelial cells (red), TER119 positive red blood cells (green) (A) adventitia, (L) lumen .

Another example of animal model with spontaneous plaque rupture is the ApoE KO Fbn1C1039G+/− mice model. A heterozygous mutation C1039G+/− in the Fbn1 gene results in the fragmentation of elastic fibers in the media of the vessel wall [43]. The effect of increased arterial stiffness, due to progressive elastic fiber degeneration, on atherosclerosis was studied in this model. ApoE KO Fbn1C1039G+/− mice fed with a Western diet for 20 weeks, show sign of plaque destabilization, such as increased number of fibrous caps and enlargement of the necrotic core [121]. The atherosclerotic plaques of ApoE KO Fbn1C1039G+/− mice contained highly leaky plaque neovessels and IPH, resulting in plaque rupture, myocardial infarction, stroke, and sudden death [122].

CONCLUSIONS

In this review, we described the pathological processes associated with angiogenesis in atherosclerotic plaques and illustrate how plaque neovascularization and IPH are strongly correlated with atherosclerotic plaque progression, instability and rupture. The established impact of plaque neovascularization on the evolution of atherothrombotic events, together with improved animal models and new imaging technologies, provide a new basis for the

development of anti-angiogenic strategies to prevent atherosclerotic plaque progression and instability.

REFERENCES

1. Hansson, G.K.; Libby, P.; Tabas, I. Inflammation and plaque vulnerability. *Journal of internal medicine* **2015**, *278*, 483-493, doi:10.1111/joim.12406.
2. Yahagi, K.; Kolodgie, F.D.; Otsuka, F.; Finn, A.V.; Davis, H.R.; Joner, M.; Virmani, R. Pathophysiology of native coronary, vein graft, and in-stent atherosclerosis. *Nature reviews. Cardiology* **2016**, *13*, 79-98, doi:10.1038/nrcardio.2015.164.
3. Chaabane, C.; Coen, M.; Bochaton-Piallat, M.L. Smooth muscle cell phenotypic switch: implications for foam cell formation. *Current opinion in lipidology* **2014**, *25*, 374-379, doi:10.1097/mol.0000000000000113.
4. Imoto, K.; Hiro, T.; Fujii, T.; Murashige, A.; Fukumoto, Y.; Hashimoto, G.; Okamura, T.; Yamada, J.; Mori, K.; Matsuzaki, M. Longitudinal structural determinants of atherosclerotic plaque vulnerability: a computational analysis of stress distribution using vessel models and three-dimensional intravascular ultrasound imaging. *J Am Coll Cardiol* **2005**, *46*, 1507-1515, doi:10.1016/j.jacc.2005.06.069.
5. Ehara, S.; Kobayashi, Y.; Yoshiyama, M.; Shimada, K.; Shimada, Y.; Fukuda, D.; Nakamura, Y.; Yamashita, H.; Yamagishi, H.; Takeuchi, K., et al. Spotty calcification typifies the culprit plaque in patients with acute myocardial infarction: an intravascular ultrasound study. *Circulation* **2004**, *110*, 3424-3429, doi:10.1161/01.cir.0000148131.41425.e9.
6. Ruiz, J.L.; Hutcheson, J.D.; Aikawa, E. Cardiovascular calcification: current controversies and novel concepts. *Cardiovascular pathology : the official journal of the Society for Cardiovascular Pathology* **2015**, *24*, 207-212, doi:10.1016/j.carpath.2015.03.002.
7. Hutcheson, J.D.; Goettsch, C.; Bertazzo, S.; Maldonado, N.; Ruiz, J.L. Genesis and growth of extracellular-vesicle-derived microcalcification in atherosclerotic plaques. **2016**, *15*, 335-343, doi:10.1038/nmat4519.
8. Michel, J.B.; Virmani, R.; Arbustini, E.; Pasterkamp, G. Intraplaque haemorrhages as the trigger of plaque vulnerability. *Eur Heart J* **2011**, *32*, 1977-1985, 1985a, 1985b, 1985c, doi:10.1093/eurheartj/ehr054.
9. Haasdijk, R.A.; Den Dekker, W.K.; Cheng, C.; Tempel, D.; Szulcek, R.; Bos, F.L.; Hermkens, D.M.; Chrifi, I.; Brandt, M.M.; Van Dijk, C., et al. THSD1 preserves vascular integrity and protects against intraplaque haemorrhaging in ApoE-/- mice. *Cardiovascular research* **2016**, *110*, 129-139, doi:10.1093/cvr/cvw015.
10. de Vries, M.R.; Quax, P.H. Plaque angiogenesis and its relation to inflammation and atherosclerotic plaque destabilization. *Curr Opin Lipidol* **2016**, *27*, 499-506, doi:10.1097/mol.0000000000000339.
11. Sluimer, J.C.; Daemen, M.J. Novel concepts in atherogenesis: angiogenesis and hypoxia in atherosclerosis. *J Pathol* **2009**, *218*, 7-29, doi:10.1002/path.2518.
12. Pouyssegur, J.; Dayan, F.; Mazure, N.M. Hypoxia signalling in cancer and approaches to enforce tumour regression. *Nature* **2006**, *441*, 437-443, doi:10.1038/nature04871.
13. Semenza, G.L. Targeting HIF-1 for cancer therapy. *Nature reviews. Cancer* **2003**, *3*, 721-732, doi:10.1038/nrc1187.
14. Roiniotis, J.; Dinh, H.; Masendycz, P.; Turner, A.; Elsegood, C.L.; Scholz, G.M.; Hamilton, J.A. Hypoxia prolongs monocyte/macrophage survival and enhanced glycolysis is associated with their maturation under aerobic conditions. *Journal of immunology (Baltimore, Md. : 1950)* **2009**, *182*, 7974-7981, doi:10.4049/jimmunol.0804216.
15. Nakano, D.; Hayashi, T.; Tazawa, N.; Yamashita, C.; Inamoto, S.; Okuda, N.; Mori, T.; Sohmiya, K.; Kitaura, Y.; Okada, Y., et al. Chronic hypoxia accelerates the progression of atherosclerosis in apolipoprotein E-knockout mice. *Hypertension research : official journal of the Japanese Society of Hypertension* **2005**, *28*, 837-845, doi:10.1291/hypres.28.837.
16. Fong, G.H. Potential contributions of intimal and plaque hypoxia to atherosclerosis. *Current atherosclerosis reports* **2015**, *17*, 510, doi:10.1007/s11883-015-0510-0.
17. Sluimer, J.C.; Gasc, J.M.; van Wanroij, J.L.; Kisters, N.; Groeneweg, M.; Sollewijn Gelpke, M.D.; Cleutjens, J.P.; van den Akker, L.H.; Corvol, P.; Wouters, B.G., et al. Hypoxia, hypoxia-inducible transcription factor, and macrophages in human atherosclerotic plaques are correlated with intraplaque angiogenesis. *J Am Coll Cardiol* **2008**, *51*, 1258-1265, doi:10.1016/j.jacc.2007.12.025.
18. Pugh, C.W.; Ratcliffe, P.J. Regulation of angiogenesis by hypoxia: role of the HIF system. *Nature medicine* **2003**, *9*, 677-684, doi:10.1038/nm0603-677.
19. Tian, H.; McKnight, S.L.; Russell, D.W. Endothelial PAS domain protein 1 (EPAS1), a transcription factor selectively expressed in endothelial cells. *Genes & development* **1997**, *11*, 72-82.

20. Wiesener, M.S.; Turley, H.; Allen, W.E.; Willam, C.; Eckardt, K.U.; Talks, K.L.; Wood, S.M.; Gatter, K.C.; Harris, A.L.; Pugh, C.W., et al. Induction of endothelial PAS domain protein-1 by hypoxia: characterization and comparison with hypoxia-inducible factor-1alpha. *Blood* **1998**, *92*, 2260-2268.
21. Lando, D.; Peet, D.J.; Gorman, J.J.; Whelan, D.A.; Whitelaw, M.L.; Bruick, R.K. FIH-1 is an asparaginyl hydroxylase enzyme that regulates the transcriptional activity of hypoxia-inducible factor. *Genes & development* **2002**, *16*, 1466-1471, doi:10.1101/gad.991402.
22. Lando, D.; Peet, D.J.; Whelan, D.A.; Gorman, J.J.; Whitelaw, M.L. Asparagine hydroxylation of the HIF transactivation domain a hypoxic switch. *Science (New York, N.Y.)* **2002**, *295*, 858-861, doi:10.1126/science.1068592.
23. Lee, J.W.; Bae, S.H.; Jeong, J.W.; Kim, S.H.; Kim, K.W. Hypoxia-inducible factor (HIF-1)alpha: its protein stability and biological functions. *Experimental & molecular medicine* **2004**, *36*, 1-12, doi:10.1038/emm.2004.1.
24. Lijkwan, M.A.; Hellingman, A.A.; Bos, E.J.; van der Bogt, K.E.; Huang, M.; Kooreman, N.G.; de Vries, M.R.; Peters, H.A.; Robbins, R.C.; Hamming, J.F., et al. Short hairpin RNA gene silencing of prolyl hydroxylase-2 with a minicircle vector improves neovascularization of hindlimb ischemia. *Human gene therapy* **2014**, *25*, 41-49, doi:10.1089/hum.2013.110.
25. Ho, T.K.; Abraham, D.J.; Black, C.M.; Baker, D.M. Hypoxia-inducible factor 1 in lower limb ischemia. *Vascular* **2006**, *14*, 321-327, doi:10.2310/6670.2006.00056.
26. Folco, E.J.; Sukhova, G.K.; Quillard, T.; Libby, P. Moderate hypoxia potentiates interleukin-1beta production in activated human macrophages. *Circulation research* **2014**, *115*, 875-883, doi:10.1161/circresaha.115.304437.
27. Ramkhelawon, B.; Yang, Y.; van Gils, J.M.; Hewing, B.; Rayner, K.J.; Parathath, S.; Guo, L.; Oldebeken, S.; Feig, J.L.; Fisher, E.A., et al. Hypoxia induces netrin-1 and Unc5b in atherosclerotic plaques: mechanism for macrophage retention and survival. *Arteriosclerosis, thrombosis, and vascular biology* **2013**, *33*, 1180-1188, doi:10.1161/atvbaha.112.301008.
28. Aarup, A.; Pedersen, T.X.; Junker, N.; Christoffersen, C.; Bartels, E.D.; Madsen, M.; Nielsen, C.H.; Nielsen, L.B. Hypoxia-Inducible Factor-1alpha Expression in Macrophages Promotes Development of Atherosclerosis. *Arterioscler Thromb Vasc Biol* **2016**, *36*, 1782-1790, doi:10.1161/atvbaha.116.307830.
29. Crucet, M.; Wust, S.J.; Spielmann, P.; Luscher, T.F.; Wenger, R.H.; Matter, C.M. Hypoxia enhances lipid uptake in macrophages: role of the scavenger receptors Lox1, SRA, and CD36. *Atherosclerosis* **2013**, *229*, 110-117, doi:10.1016/j.atherosclerosis.2013.04.034.
30. Ramkhelawon, B.; Yang, Y.; van Gils, J.M.; Hewing, B.; Rayner, K.J.; Parathath, S.; Guo, L.; Oldebeken, S.; Feig, J.L.; Fisher, E.A., et al. Hypoxia induces netrin-1 and Unc5b in atherosclerotic plaques: a mechanism for macrophage retention and survival. *Arteriosclerosis, thrombosis, and vascular biology* **2013**, *33*, 1180-1188, doi:10.1161/ATVBAHA.112.301008.
31. D'Ignazio, L.; Bandarra, D.; Rocha, S. NF-kappaB and HIF crosstalk in immune responses. *The FEBS journal* **2016**, *283*, 413-424, doi:10.1111/febs.13578.
32. Palazon, A.; Goldrath, A.W.; Nizet, V.; Johnson, R.S. HIF transcription factors, inflammation, and immunity. *Immunity* **2014**, *41*, 518-528, doi:10.1016/j.immuni.2014.09.008.
33. Cummins, E.P.; Berra, E.; Comerford, K.M.; Ginouves, A.; Fitzgerald, K.T.; Seeballuck, F.; Godson, C.; Nielsen, J.E.; Moynagh, P.; Pouyssegur, J., et al. Prolyl hydroxylase-1 negatively regulates IkappaB kinase-beta, giving insight into hypoxia-induced NFkappaB activity. *Proceedings of the National Academy of Sciences of the United States of America* **2006**, *103*, 18154-18159, doi:10.1073/pnas.0602235103.
34. Oliver, K.M.; Garvey, J.F.; Ng, C.T.; Veale, D.J.; Fearon, U.; Cummins, E.P.; Taylor, C.T. Hypoxia activates NF-kappaB-dependent gene expression through the canonical signaling pathway. *Antioxidants & redox signaling* **2009**, *11*, 2057-2064, doi:10.1089/ars.2008.2400.
35. Marsch, E.; Demandt, J.A.; Theelen, T.L.; Tullemans, B.M.; Wouters, K.; Boon, M.R.; van Dijk, T.H.; Gijbels, M.J.; Dubois, L.J.; Meex, S.J., et al. Deficiency of the oxygen sensor prolyl hydroxylase 1 attenuates hypercholesterolaemia, atherosclerosis, and hyperglycaemia. *Eur Heart J* **2016**, *37*, 2993-2997, doi:10.1093/eurheartj/ehw156.
36. van Uden, P.; Kenneth, N.S.; Rocha, S. Regulation of hypoxia-inducible factor-1alpha by NF-kappaB. *The Biochemical journal* **2008**, *412*, 477-484, doi:10.1042/bj20080476.
37. Carmeliet, P.; Jain, R.K. Molecular mechanisms and clinical applications of angiogenesis. *Nature* **2011**, *473*, 298-307, doi:10.1038/nature10144.

38. Eelen, G.; Cruys, B.; Welti, J.; De Bock, K.; Carmeliet, P. Control of vessel sprouting by genetic and metabolic determinants. *Trends in Endocrinology and Metabolism* **2013**, *24*, 589-596, doi:10.1016/j.tem.2013.08.006.
39. Cantelmo, A.R.; Brajic, A.; Carmeliet, P. Endothelial Metabolism Driving Angiogenesis Emerging Concepts and Principles. *Cancer Journal* **2015**, *21*, 244-249, doi:10.1097/ppo.0000000000000133.
40. Coulon, C.; Georgiadou, M.; Roncal, C.; De Bock, K.; Langenberg, T.; Carmeliet, P. From vessel sprouting to normalization: role of the prolyl hydroxylase domain protein/hypoxia-inducible factor oxygen-sensing machinery. *Arterioscler Thromb Vasc Biol* **2010**, *30*, 2331-2336, doi:10.1161/ATVBAHA.110.214106.
41. De Smet, F.; Segura, I.; De Bock, K.; Hohensinner, P.J.; Carmeliet, P. Mechanisms of vessel branching: filopodia on endothelial tip cells lead the way. *Arterioscler Thromb Vasc Biol* **2009**, *29*, 639-649, doi:10.1161/ATVBAHA.109.185165.
42. Herbert, S.P.; Stainier, D.Y. Molecular control of endothelial cell behaviour during blood vessel morphogenesis. *Nature reviews. Molecular cell biology* **2011**, *12*, 551-564, doi:10.1038/nrm3176.
43. Van der Veken, B.; De Meyer, G.R.; Martinet, W. Intraplaque neovascularization as a novel therapeutic target in advanced atherosclerosis. *Expert Opin Ther Targets* **2016**, 10.1080/14728222.2016.1186650, 1-11, doi:10.1080/14728222.2016.1186650.
44. Jaipersad, A.S.; Lip, G.Y.; Silverman, S.; Shantsila, E. The role of monocytes in angiogenesis and atherosclerosis. *Journal of the American College of Cardiology* **2014**, *63*, 1-11, doi:10.1016/j.jacc.2013.09.019.
45. Fantin, A.; Vieira, J.M.; Gestri, G.; Denti, L.; Schwarz, Q.; Prykhozhij, S.; Peri, F.; Wilson, S.W.; Ruhrberg, C. Tissue macrophages act as cellular chaperones for vascular anastomosis downstream of VEGF-mediated endothelial tip cell induction. *Blood* **2010**, *116*, 829-840, doi:10.1182/blood-2009-12-257832.
46. Sewduth, R.; Santoro, M.M. "Decoding" Angiogenesis: New Facets Controlling Endothelial Cell Behavior. *Frontiers in physiology* **2016**, *7*, 306, doi:10.3389/fphys.2016.00306.
47. Ando, J.; Yamamoto, K. Flow detection and calcium signalling in vascular endothelial cells. *Cardiovascular research* **2013**, *99*, 260-268, doi:10.1093/cvr/cvt084.
48. Seghers, L.; de Vries, M.R.; Pardali, E.; Hoefer, I.E.; Hierck, B.P.; ten Dijke, P.; Goumans, M.J.; Quax, P.H. Shear induced collateral artery growth modulated by endoglin but not by ALK1. *Journal of cellular and molecular medicine* **2012**, *16*, 2440-2450, doi:10.1111/j.1582-4934.2012.01561.x.
49. Bongrazio, M.; Da Silva-Azevedo, L.; Bergmann, E.C.; Baum, O.; Hinz, B.; Pries, A.R.; Zakrzewicz, A. Shear stress modulates the expression of thrombospondin-1 and CD36 in endothelial cells in vitro and during shear stress-induced angiogenesis in vivo. *International journal of immunopathology and pharmacology* **2006**, *19*, 35-48.
50. Li, J.; Hou, B.; Tumova, S.; Muraki, K.; Bruns, A.; Ludlow, M.J.; Sedo, A.; Hyman, A.J.; McKeown, L.; Young, R.S., et al. Piezo1 integration of vascular architecture with physiological force. *Nature* **2014**, *515*, 279-282, doi:10.1038/nature13701.
51. Qiu, W.; Kass, D.A.; Hu, Q.; Ziegelstein, R.C. Determinants of shear stress-stimulated endothelial nitric oxide production assessed in real-time by 4,5-diaminofluorescein fluorescence. *Biochemical and biophysical research communications* **2001**, *286*, 328-335, doi:10.1006/bbrc.2001.5401.
52. Goetz, J.G.; Steed, E.; Ferreira, R.R.; Roth, S.; Ramspacher, C.; Boselli, F.; Charvin, G.; Liebling, M.; Wyart, C.; Schwab, Y., et al. Endothelial cilia mediate low flow sensing during zebrafish vascular development. *Cell reports* **2014**, *6*, 799-808, doi:10.1016/j.celrep.2014.01.032.
53. van Hinsbergh, V.W.M.; Eringa, E.C.; Daemen, M. Neovascularization of the atherosclerotic plaque: interplay between atherosclerotic lesion, adventitia-derived microvessels and perivascular fat. *Current Opinion in Lipidology* **2015**, *26*, 405-411, doi:10.1097/mol.0000000000000210.
54. Hellings, W.E.; Peeters, W.; Moll, F.L.; Piers, S.R.; van Setten, J.; Van der Spek, P.J.; de Vries, J.P.; Seldenrijk, K.A.; De Bruin, P.C.; Vink, A., et al. Composition of carotid atherosclerotic plaque is associated with cardiovascular outcome: a prognostic study. *Circulation* **2010**, *121*, 1941-1950, doi:10.1161/circulationaha.109.887497.
55. Langheinrich, A.C.; Sedding, D.G.; Kampschulte, M.; Moritz, R.; Wilhelm, J.; Haberbosch, W.G.; Ritman, E.L.; Bohle, R.M. 3-Deazaadenosine inhibits vasa vasorum neovascularization in aortas of ApoE(-/-)/LDL(-/-) double knockout mice. *Atherosclerosis* **2009**, *202*, 103-110, doi:10.1016/j.atherosclerosis.2008.04.008.
56. Xu, J.Y.; Lu, X.T.; Shi, G.P. Vasa Vasorum in Atherosclerosis and Clinical Significance. *International Journal of Molecular Sciences* **2015**, *16*, 11574-11608, doi:10.3390/ijms160511574.

57. Sluimer, J.C.; Kolodgie, F.D.; Bijnens, A.P.; Maxfield, K.; Pacheco, E.; Kutys, B.; Duimel, H.; Frederik, P.M.; van Hinsbergh, V.W.; Virmani, R., et al. Thin-walled microvessels in human coronary atherosclerotic plaques show incomplete endothelial junctions relevance of compromised structural integrity for intraplaque microvascular leakage. *J Am Coll Cardiol* **2009**, *53*, 1517-1527, doi:10.1016/j.jacc.2008.12.056.
58. Jeney, V.; Balla, G.; Balla, J. Red blood cell, hemoglobin and heme in the progression of atherosclerosis. *Frontiers in physiology* **2014**, *5*, 379, doi:10.3389/fphys.2014.00379.
59. Nagy, J.A.; Chang, S.H.; Shih, S.C.; Dvorak, A.M.; Dvorak, H.F. Heterogeneity of the tumor vasculature. *Semin Thromb Hemost* **2010**, *36*, 321-331, doi:10.1055/s-0030-1253454.
60. Nagy, J.A.; Dvorak, A.M.; Dvorak, H.F. Vascular hyperpermeability, angiogenesis, and stroma generation. *Cold Spring Harb Perspect Med* **2012**, *2*, a006544, doi:10.1101/cshperspect.a006544.
61. Martin, J.D.; Fukumura, D.; Duda, D.G.; Boucher, Y.; Jain, R.K. Reengineering the Tumor Microenvironment to Alleviate Hypoxia and Overcome Cancer Heterogeneity. *Cold Spring Harb Perspect Med* **2016**, *6*, doi:10.1101/cshperspect.a027094.
62. Jain, R.K. Molecular regulation of vessel maturation. *Nat Med* **2003**, *9*, 685-693, doi:10.1038/nm0603-685.
63. Giannoglou, G.D.; Koskinas, K.C.; Tziakas, D.N.; Ziakas, A.G.; Antoniadis, A.P.; Tentes, I.K.; Parcharidis, G.E. Total cholesterol content of erythrocyte membranes and coronary atherosclerosis: an intravascular ultrasound pilot study. *Angiology* **2009**, *60*, 676-682, doi:10.1177/0003319709337307.
64. Tziakas, D.N.; Chalikias, G.K.; Stakos, D.; Tentes, I.K.; Papazoglou, D.; Thomaidi, A.; Grapsa, A.; Gioka, G.; Kaski, J.C.; Boudoulas, H. Independent and additive predictive value of total cholesterol content of erythrocyte membranes with regard to coronary artery disease clinical presentation. *International journal of cardiology* **2011**, *150*, 22-27, doi:10.1016/j.ijcard.2010.02.022.
65. Goel, S.; Wong, A.H.; Jain, R.K. Vascular normalization as a therapeutic strategy for malignant and nonmalignant disease. *Cold Spring Harbor perspectives in medicine* **2012**, *2*, a006486, doi:10.1101/cshperspect.a006486.
66. Post, S.; Peeters, W.; Busser, E.; Lamers, D.; Sluijter, J.P.; Goumans, M.J.; de Weger, R.A.; Moll, F.L.; Doevendans, P.A.; Pasterkamp, G., et al. Balance between angiopoietin-1 and angiopoietin-2 is in favor of angiopoietin-2 in atherosclerotic plaques with high microvessel density. *J Vasc Res* **2008**, *45*, 244-250, doi:10.1159/000112939.
67. Michel, J.B.; Martin-Ventura, J.L.; Nicoletti, A.; Ho-Tin-Noe, B. Pathology of human plaque vulnerability: mechanisms and consequences of intraplaque haemorrhages. *Atherosclerosis* **2014**, *234*, 311-319, doi:10.1016/j.atherosclerosis.2014.03.020.
68. Nagy, E.; Eaton, J.W.; Jeney, V.; Soares, M.P.; Varga, Z.; Galajda, Z.; Szentmiklósi, J.; Méhes, G.; Csonka, T.; Smith, A., et al. Red cells, hemoglobin, heme, iron, and atherogenesis. *Arterioscler Thromb Vasc Biol* **2010**, *30*, 1347-1353, doi:10.1161/ATVBAHA.110.206433.
69. Kolodgie, F.D.; Burke, A.P.; Nakazawa, G.; Cheng, Q.; Xu, X.; Virmani, R. Free cholesterol in atherosclerotic plaques: where does it come from? *Curr Opin Lipidol* **2007**, *18*, 500-507, doi:10.1097/MOL.0b013e3282efa35b.
70. Kolodgie, F.D.; Gold, H.K.; Burke, A.P.; Fowler, D.R.; Kruth, H.S.; Weber, D.K.; Farb, A.; Guerrero, L.J.; Hayase, M.; Kutys, R., et al. Intraplaque hemorrhage and progression of coronary atheroma. *The New England journal of medicine* **2003**, *349*, 2316-2325, doi:10.1056/NEJMoa035655.
71. Marsch, E.; Sluimer, J.C.; Daemen, M.J. Hypoxia in atherosclerosis and inflammation. *Curr Opin Lipidol* **2013**, *24*, 393-400, doi:10.1097/MOL.0b013e32836484a4.
72. Khurana, R.; Simons, M.; Martin, J.F.; Zachary, I.C. Role of Angiogenesis in Cardiovascular Disease. *A Critical Appraisal* **2005**, *112*, 1813-1824, doi:10.1161/circulationaha.105.535294.
73. Willems, S.; Vink, A.; Bot, I.; Quax, P.H.A.; de Borst, G.J.; de Vries, J.-P.P.M.; van de Weg, S.M.; Moll, F.L.; Kuiper, J.; Kovanen, P.T., et al. Mast cells in human carotid atherosclerotic plaques are associated with intraplaque microvessel density and the occurrence of future cardiovascular events. *European Heart Journal* **2013**, *34*, 3699-3706, doi:10.1093/eurheartj/eht186.
74. Lappalainen, H.; Laine, P.; Pentikainen, M.O.; Sajantila, A.; Kovanen, P.T. Mast cells in neovascularized human coronary plaques store and secrete basic fibroblast growth factor, a potent angiogenic mediator. *Arteriosclerosis, thrombosis, and vascular biology* **2004**, *24*, 1880-1885, doi:10.1161/01.ATV.0000140820.51174.8d.
75. Butoi, E.; Gan, A.M.; Tucureanu, M.M.; Stan, D.; Macarie, R.D.; Constantinescu, C.; Calin, M.; Simionescu, M.; Manduteanu, I. Cross-talk between macrophages and smooth muscle cells impairs collagen and metalloprotease synthesis and promotes angiogenesis. *Biochimica et Biophysica Acta*

(BBA) - Molecular Cell Research **2016**, *1863*, 1568-1578, doi:http://dx.doi.org/10.1016/j.bbamcr.2016.04.001.

76. Eriksson, E.E. Intravital microscopy on atherosclerosis in apolipoprotein e-deficient mice establishes microvessels as major entry pathways for leukocytes to advanced lesions. *Circulation* **2011**, *124*, 2129-2138, doi:10.1161/CIRCULATIONAHA.111.030627.
77. Rademakers, T.; Douma, K.; Hackeng, T.M.; Post, M.J.; Sluimer, J.C.; Daemen, M.J.; Biessen, E.A.; Heeneman, S.; van Zandvoort, M.A. Plaque-associated vasa vasorum in aged apolipoprotein E-deficient mice exhibit proatherogenic functional features in vivo. *Arterioscler Thromb Vasc Biol* **2013**, *33*, 249-256, doi:10.1161/atvbaha.112.300087.
78. Melder, R.J.; Yuan, J.; Munn, L.L.; Jain, R.K. Erythrocytes enhance lymphocyte rolling and arrest in vivo. *Microvascular research* **2000**, *59*, 316-322, doi:10.1006/mvre.1999.2223.
79. Leclercq, A.; Houard, X.; Philippe, M.; Ollivier, V.; Sebbag, U.; Meilhac, O.; Michel, J.B. Involvement of intraplaque hemorrhage in atherothrombosis evolution via neutrophil protease enrichment. *Journal of leukocyte biology* **2007**, *82*, 1420-1429, doi:10.1189/jlb.1106671.
80. Dorweiler, B.; Torzewski, M.; Dahm, M.; Kirkpatrick, C.J.; Lackner, K.J.; Vahl, C.F. Subendothelial infiltration of neutrophil granulocytes and liberation of matrix-destabilizing enzymes in an experimental model of human neo-intima. *Thrombosis and haemostasis* **2008**, *99*, 373-381, doi:10.1160/th07-06-0387.
81. Schrijvers, D.M.; De Meyer, G.R.; Kockx, M.M.; Herman, A.G.; Martinet, W. Phagocytosis of apoptotic cells by macrophages is impaired in atherosclerosis. *Arteriosclerosis, thrombosis, and vascular biology* **2005**, *25*, 1256-1261, doi:10.1161/01.ATV.0000166517.18801.a7.
82. Kojima, Y.; Volkmer, J.P.; McKenna, K.; Civelek, M.; Lusis, A.J.; Miller, C.L.; Direnzo, D.; Nanda, V.; Ye, J.; Connolly, A.J., et al. CD47-blocking antibodies restore phagocytosis and prevent atherosclerosis. *Nature* **2016**, *536*, 86-90, doi:10.1038/nature18935.
83. Tabas, I.; Bornfeldt, K.E. Macrophage Phenotype and Function in Different Stages of Atherosclerosis. *Circulation research* **2016**, *118*, 653-667, doi:10.1161/circresaha.115.306256.
84. Goncalves, I.; den Ruijter, H.; Nahrendorf, M.; Pasterkamp, G. Detecting the vulnerable plaque in patients. *Journal of internal medicine* **2015**, *278*, 520-530, doi:10.1111/joim.12414.
85. Taqueti, V.R.; Di Carli, M.F.; Jerosch-Herold, M.; Sukhova, G.K.; Murthy, V.L.; Folco, E.J.; Kwong, R.Y.; Ozaki, C.K.; Belkin, M.; Nahrendorf, M., et al. Increased microvascularization and vessel permeability associate with active inflammation in human atheromata. *Circulation. Cardiovascular imaging* **2014**, *7*, 920-929, doi:10.1161/circimaging.114.002113.
86. Perez-Medina, C.; Binderup, T.; Lobatto, M.E.; Tang, J.; Calcagno, C.; Giesen, L.; Wessel, C.H.; Witjes, J.; Ishino, S.; Baxter, S., et al. In Vivo PET Imaging of HDL in Multiple Atherosclerosis Models. *JACC. Cardiovascular imaging* **2016**, *9*, 950-961, doi:10.1016/j.jcmg.2016.01.020.
87. Calcagno, C.; Mulder, W.J.M.; Nahrendorf, M.; Fayad, Z.A. Systems Biology and Noninvasive Imaging of Atherosclerosis. *Arteriosclerosis, thrombosis, and vascular biology* **2016**, *36*, e1-e8, doi:10.1161/atvbaha.115.306350.
88. Alie, N.; Eldib, M.; Fayad, Z.A.; Mani, V. Inflammation, Atherosclerosis, and Coronary Artery Disease: PET/CT for the Evaluation of Atherosclerosis and Inflammation. *Clinical Medicine Insights. Cardiology* **2014**, *8*, 13-21, doi:10.4137/cmc.s17063.
89. Magnoni, M.; Ammirati, E.; Camici, P.G. Non-invasive molecular imaging of vulnerable atherosclerotic plaques. *Journal of Cardiology* **2015**, *65*, 261-269, doi:http://dx.doi.org/10.1016/j.jjcc.2015.01.004.
90. Bourantas, C.V.; Garcia-Garcia, H.M.; Torii, R.; Zhang, Y.J.; Westwood, M.; Crake, T.; Serruys, P.W. Vulnerable plaque detection: an unrealistic quest or a feasible objective with a clinical value? *Heart (British Cardiac Society)* **2016**, *102*, 581-589, doi:10.1136/heartjnl-2015-309060.
91. Matter, C.M.; Schuler, P.K.; Alessi, P.; Meier, P.; Ricci, R.; Zhang, D.; Halin, C.; Castellani, P.; Zardi, L.; Hofer, C.K., et al. Molecular Imaging of Atherosclerotic Plaques Using a Human Antibody Against the Extra-Domain B of Fibronectin. *Circulation research* **2004**, *95*, 1225-1233, doi:10.1161/01.RES.0000150373.15149.ff.
92. de Vries, M.R.; Niessen, H.W.; Lowik, C.W.; Hamming, J.F.; Jukema, J.W.; Quax, P.H. Plaque rupture complications in murine atherosclerotic vein grafts can be prevented by TIMP-1 overexpression. *PloS one* **2012**, *7*, e47134, doi:10.1371/journal.pone.0047134.
93. Wong, C.Y.; de Vries, M.R.; Wang, Y.; van der Vorst, J.R.; Vahrmeijer, A.L.; van Zonneveld, A.J.; Roy-Chaudhury, P.; Rabelink, T.J.; Quax, P.H.; Rotmans, J.I. Vascular remodeling and intimal hyperplasia in a novel murine model of arteriovenous fistula failure. *J Vasc Surg* **2014**, *59*, 192-201.e191, doi:10.1016/j.jvs.2013.02.242.

94. Wong, C.; Bezhaeva, T.; Rothuizen, T.C.; Metselaar, J.M.; de Vries, M.R.; Verbeek, F.P.; Vahrmeijer, A.L.; Wezel, A.; van Zonneveld, A.J.; Rabelink, T.J., et al. Liposomal prednisolone inhibits vascular inflammation and enhances venous outward remodeling in a murine arteriovenous fistula model. *Scientific reports* **2016**, *6*, 30439, doi:10.1038/srep30439.
95. Bourantas, C.V.; Jaffer, F.A.; Gijsen, F.J.; van Soest, G.; Madden, S.P.; Courtney, B.K.; Fard, A.M.; Tenekecioglu, E.; Zeng, Y.; van der Steen, A.F., et al. Hybrid intravascular imaging: recent advances, technical considerations, and current applications in the study of plaque pathophysiology. *Eur Heart J* **2016**, 10.1093/eurheartj/ehw097, doi:10.1093/eurheartj/ehw097.
96. Wang, H.; Gardecki, J.A.; Ughi, G.J.; Jacques, P.V.; Hamidi, E.; Tearney, G.J. Ex vivo catheter-based imaging of coronary atherosclerosis using multimodality OCT and NIRAF excited at 633 nm. *Biomedical Optics Express* **2015**, *6*, 1363-1375, doi:10.1364/BOE.6.001363.
97. Tsujita, K.; Kaikita, K.; Araki, S.; Yamada, T.; Nagamatsu, S.; Yamanaga, K.; Sakamoto, K.; Kojima, S.; Hokimoto, S.; Ogawa, H. In Vivo optical coherence tomography visualization of intraplaque neovascularization at the site of coronary vasospasm: a case report. *BMC cardiovascular disorders* **2016**, *16*, 235, doi:10.1186/s12872-016-0408-y.
98. Goel, S.; Wong, A.H.K.; Jain, R.K. Vascular Normalization as a Therapeutic Strategy for Malignant and Nonmalignant Disease. *Cold Spring Harbor Perspectives in Medicine* **2012**, *2*, 24, doi:10.1101/cshperspect.a006486.
99. Jain, R.K. Antiangiogenesis strategies revisited: from starving tumors to alleviating hypoxia. *Cancer Cell* **2014**, *26*, 605-622, doi:10.1016/j.ccell.2014.10.006.
100. O'Reilly, M.S.; Boehm, T.; Shing, Y.; Fukai, N.; Vasios, G.; Lane, W.S.; Flynn, E.; Birkhead, J.R.; Olsen, B.R.; Folkman, J. Endostatin: an endogenous inhibitor of angiogenesis and tumor growth. *Cell* **1997**, *88*, 277-285.
101. Moulton, K.S.; Heller, E.; Konerding, M.A.; Flynn, E.; Palinski, W.; Folkman, J. Angiogenesis inhibitors endostatin or TNP-470 reduce intimal neovascularization and plaque growth in apolipoprotein E-deficient mice. *Circulation* **1999**, *99*, 1726-1732.
102. Xu, X.; Mao, W.; Chai, Y.; Dai, J.; Chen, Q.; Wang, L.; Zhuang, Q.; Pan, Y.; Chen, M.; Ni, G., et al. Angiogenesis Inhibitor, Endostar, Prevents Vasa Vasorum Neovascularization in a Swine Atherosclerosis Model. *J Atheroscler Thromb* **2015**, *22*, 1100-1112, doi:10.5551/jat.26906.
103. Bogdanovich, S.; Kim, Y.; Mizutani, T.; Yasuma, R.; Tudisco, L.; Cicatiello, V.; Bastos-Carvalho, A.; Kerur, N.; Hirano, Y.; Baffi, J.Z., et al. Human IgG1 antibodies suppress angiogenesis in a target-independent manner. *Signal Transduct Target Ther* **2016**, *1*, doi:10.1038/sigtrans.2015.1.
104. Winnik, S.; Lohmann, C.; Siciliani, G.; von Lukowicz, T.; Kuschnerus, K.; Kraenkel, N.; Brokopp, C.E.; Enseleit, F.; Michels, S.; Ruschitzka, F., et al. Systemic VEGF inhibition accelerates experimental atherosclerosis and disrupts endothelial homeostasis - implications for cardiovascular safety. *International Journal of Cardiology* **2013**, *168*, 2453-2461, doi:10.1016/j.ijcard.2013.03.010.
105. Wang, Y.; Zhou, Y.; He, L.; Hong, K.; Su, H.; Wu, Y.; Wu, Q.; Han, M.; Cheng, X. Gene delivery of soluble vascular endothelial growth factor receptor-1 (sFlt-1) inhibits intra-plaque angiogenesis and suppresses development of atherosclerotic plaque. *Clin Exp Med* **2011**, *11*, 113-121, doi:10.1007/s10238-010-0112-7.
106. Theelen, T.L.; Lappalainen, J.P.; Sluimer, J.C.; Gurzeler, E.; Cleutjens, J.P.; Gijbels, M.J.; Biessen, E.A.; Daemen, M.J.; Alitalo, K.; Ylä-Herttuala, S. Angiopoietin-2 blocking antibodies reduce early atherosclerotic plaque development in mice. *Atherosclerosis* **2015**, *241*, 297-304, doi:10.1016/j.atherosclerosis.2015.05.018.
107. Cruys, B.; Wong, B.W.; Kuchnio, A.; Verdegem, D.; Cantelmo, A.R.; Conradi, L.-C.; Vandekeere, S.; Bouché, A.; Cornelissen, I.; Vinckier, S., et al. Glycolytic regulation of cell rearrangement in angiogenesis. *Nature Communications* **2016**, *7*, 12240, doi:10.1038/ncomms12240.
108. Pircher, A.; Treps, L.; Bodrug, N.; Carmeliet, P. Endothelial cell metabolism: A novel player in atherosclerosis? Basic principles and therapeutic opportunities. *Atherosclerosis* **2016**, *253*, 247-257, doi:10.1016/j.atherosclerosis.2016.08.011.
109. Ozaki, M.; Kawashima, S.; Yamashita, T.; Hirase, T.; Namiki, M.; Inoue, N.; Hirata, K.; Yasui, H.; Sakurai, H.; Yoshida, Y., et al. Overexpression of endothelial nitric oxide synthase accelerates atherosclerotic lesion formation in apoE-deficient mice. *The Journal of clinical investigation* **2002**, *110*, 331-340, doi:10.1172/jci15215.
110. Bendall, J.K.; Douglas, G.; McNeill, E.; Channon, K.M.; Crabtree, M.J. Tetrahydrobiopterin in Cardiovascular Health and Disease. *Antioxidants & redox signaling* **2014**, *20*, 3040-3077, doi:10.1089/ars.2013.5566.

111. Drummond, G.R.; Sobey, C.G. Endothelial NADPH oxidases: which NOX to target in vascular disease? *Trends in Endocrinology & Metabolism* **2014**, *25*, 452-463, doi:http://dx.doi.org/10.1016/j.tem.2014.06.012.
112. Diebold, I.; Petry, A.; Sabrane, K.; Djordjevic, T.; Hess, J.; Gorlach, A. The HIF1 target gene NOX2 promotes angiogenesis through urotensin-II. *J Cell Sci* **2012**, *125*, 956-964, doi:10.1242/jcs.094060.
113. Menden, H.; Welak, S.; Cossette, S.; Ramchandran, R.; Sampath, V. Lipopolysaccharide (LPS)-mediated angiopoietin-2-dependent autocrine angiogenesis is regulated by NADPH oxidase 2 (Nox2) in human pulmonary microvascular endothelial cells. *The Journal of biological chemistry* **2015**, *290*, 5449-5461, doi:10.1074/jbc.M114.600692.
114. De Bock, K.; Georgiadou, M.; Carmeliet, P. Role of Endothelial Cell Metabolism in Vessel Sprouting. *Cell Metabolism* **2013**, *18*, 634-647, doi:http://dx.doi.org/10.1016/j.cmet.2013.08.001.
115. Schoors, S.; De Bock, K.; Cantelmo, Anna R.; Georgiadou, M.; Ghesquière, B.; Cauwenberghs, S.; Kuchnio, A.; Wong, Brian W.; Quaegebeur, A.; Goveia, J., et al. Partial and Transient Reduction of Glycolysis by PFKFB3 Blockade Reduces Pathological Angiogenesis. *Cell Metabolism* **2014**, *19*, 37-48, doi:http://dx.doi.org/10.1016/j.cmet.2013.11.008.
116. De Bock, K.; Georgiadou, M.; Schoors, S.; Kuchnio, A.; Wong, Brian W.; Cantelmo, Anna R.; Quaegebeur, A.; Ghesquière, B.; Cauwenberghs, S.; Eelen, G., et al. Role of PFKFB3-Driven Glycolysis in Vessel Sprouting. *Cell* **2013**, *154*, 651-663, doi:http://dx.doi.org/10.1016/j.cell.2013.06.037.
117. Giannarelli, C.; Ibanez, B.; Cimmino, G.; Garcia Ruiz, J.M.; Faita, F.; Bianchini, E.; Zafar, M.U.; Fuster, V.; Garcia, M.J.; Badimon, J.J. Contrast-enhanced ultrasound imaging detects intraplaque neovascularization in an experimental model of atherosclerosis. *JACC Cardiovasc Imaging* **2010**, *3*, 1256-1264, doi:10.1016/j.jcmg.2010.09.017.
118. de Vries, M.R.; Simons, K.H.; Jukema, J.W.; Braun, J.; Quax, P.H. Vein graft failure: from pathophysiology to clinical outcomes. *Nat Rev Cardiol* **2016**, *13*, 451-470, doi:10.1038/nrcardio.2016.76.
119. Lardenoye, J.H.; de Vries, M.R.; Löwik, C.W.; Xu, Q.; Dhore, C.R.; Cleutjens, J.P.; van Hinsbergh, V.W.; van Bockel, J.H.; Quax, P.H. Accelerated atherosclerosis and calcification in vein grafts: a study in APOE*3 Leiden transgenic mice. *Circ Res* **2002**, *91*, 577-584.
120. Wezel, A.; de Vries, M.R.; Maassen, J.M.; Kip, P.; Peters, E.A.; Karper, J.C.; Kuiper, J.; Bot, I.; Quax, P.H. Deficiency of the TLR4 analogue RP105 aggravates vein graft disease by inducing a pro-inflammatory response. *Scientific reports* **2016**, *6*, 24248, doi:10.1038/srep24248.
121. Van Herck, J.L.; De Meyer, G.R.; Martinet, W.; Van Hove, C.E.; Foubert, K.; Theunis, M.H.; Apers, S.; Bult, H.; Vrints, C.J.; Herman, A.G. Impaired fibrillin-1 function promotes features of plaque instability in apolipoprotein E-deficient mice. *Circulation* **2009**, *120*, 2478-2487, doi:10.1161/circulationaha.109.872663.
122. Van der Donckt, C.; Van Herck, J.L.; Schrijvers, D.M.; Vanhoutte, G.; Verhoye, M.; Blockx, I.; Van Der Linden, A.; Bauters, D.; Lijnen, H.R.; Sluimer, J.C., et al. Elastin fragmentation in atherosclerotic mice leads to intraplaque neovascularization, plaque rupture, myocardial infarction, stroke, and sudden death. *European heart journal* **2015**, *36*, 1049-1058, doi:10.1093/eurheartj/ehu041.

CHAPTER 3

PROLONGED HYPEROXYGENATION TREATMENT IMPROVES VEIN GRAFT PATENCY AND DECREASES MACROPHAGE CONTENT IN ATHEROSCLEROTIC LESIONS IN APOE3*LEIDEN MICE

L Parma[1,2], HAB Peters[1,2], F Baganha[1,2], JC Sluimer[3,4], MR de Vries[1,2], PHA Quax[1,2]

[1]Department of Surgery and [2]Einthoven Laboratory for Experimental Vascular Medicine, Leiden University Medical Center, Leiden, The Netherlands [3]Cardiovascular Research Institute Maastricht, Department of Pathology, Maastricht University Medical Center, Maastricht, The Netherlands. [4]Centre for Cardiovascular Science, University of Edinburgh, Edinburgh, UK.

Cells. 2020 Feb 1;9(2)

Abstract

Unstable atherosclerotic plaques frequently show plaque angiogenesis which increases the chance of rupture and thrombus formation leading to infarctions. Hypoxia plays a role in angiogenesis and inflammation, two processes involved in the pathogenesis of atherosclerosis. We aim to study the effect of resolution of hypoxia using carbogen gas (95% O_2, 5% CO_2) on the remodeling of vein graft accelerated atherosclerotic lesions in ApoE3*Leiden mice which harbor plaque angiogenesis. Single treatment resulted in a drastic decrease of intraplaque hypoxia, without affecting plaque composition. Daily treatment for three weeks resulted in 34.5% increase in vein graft patency and increased lumen size. However, after three weeks intraplaque hypoxia was comparable to the controls, as were the number of neovessels and the degree of intraplaque hemorrhage. To our surprise we found that three weeks of treatment triggered ROS accumulation and subsequent Hif1a induction, paralleled with a reduction in the macrophage content, pointing to an increase in lesion stability. Similar to what we observed in vivo, in vitro induction of ROS in bone marrow derived macrophages lead to increased Hif1a expression and extensive DNA damage and apoptosis. Our study demonstrates that carbogen treatment did improve vein graft patency and plaque stability and reduced intraplaque macrophage accumulation via ROS mediated DNA damage and apoptosis but failed to have long term effects on hypoxia and intraplaque angiogenesis.

Introduction

The (in)stability of atherosclerotic plaques determines the incidence of major cardiovascular events such as myocardial infarction and stroke [1]. Lack of oxygen within the plaque, or intraplaque hypoxia, has been identified as one of the major contributors to plaque instability [2,3]. [4]It has been detected in advanced human atherosclerotic lesions [5] as well as in murine atherosclerotic lesions [6,7].

The intraplaque lack of oxygen is provoked by progressive thickening of the neointimal layer [8] and overconsumption of O_2 by plaque inflammatory cells [5]. The key regulator of hypoxia is the transcription factor Hif1a [9]. Low oxygen levels, or hypoxia, prevents degradation of Hif1a, promoting its dimerization with the Hif1b subunit. This complex activates the transcription of multiple genes, the most important being Vegfa, that triggers the formation of neovessels in the plaque. Intraplaque neovessels are often immature and therefore leaky, leading to intraplaque hemorrhage, a phenomenon characterized by extravasation of inflammatory cells and red blood cells inside the plaque. Hypoxia also upregulates the expression of transcription factors that cause vascular calcification in vascular smooth muscle cells [10], a characteristic feature of atherosclerosis. Both intraplaque neovessels and vascular calcification are regulated by hypoxia [10] and contribute to plaque instability. The combination of those processes results in a larger plaque which is more unstable and prone to rupture [11,12]. Hif1a was shown to be present in macrophage-rich and foam cell-rich areas and its expression in macrophages was correlated with accelerated atherosclerosis development in $LDLR^{-/-}$ mice [13]. Moreover, it has been shown that hypoxia can influence gene expression in macrophages, leading to an inflammatory response with increased production of pro-inflammatory cytokines [14,15].

Thus, the reoxygenation of the atherosclerotic plaque would be expected to prevent intraplaque hypoxia and atherosclerotic plaque progression. Previously, Marsch et al. showed that plaque reoxygenation in $LDLR^{-/-}$ mice via breathing of the hyperoxic gas carbogen, composed of 95% O_2 and 5% CO_2, prevented necrotic core expansion by enhancing efferocytosis [16]. The response of intraplaque angiogenesis to reoxygenation could not be studied in this model, as intraplaque angiogenesis is virtually nonexistent in plaques of $LDLR^{-/-}$ mice. To examine the effect of carbogen treatment on intraplaque angiogenesis we used vein grafts in hypercholesterolemic ApoE3*Leiden mice that do harbor extensive intraplaque angiogenesis, and have been shown to be morphologically similar to rupture-prone plaques

in humans. The lesions in this model have the typical characteristics of late stage atherosclerosis, including the presence of foam cells, intraplaque neovascularization, calcification and cholesterol clefts [17] and eventually also occlusion of the graft.

We hypothesized that carbogen gas exposure would reduce hypoxia in vein grafts in the ApoE3* Leiden mice and consequently would reduce intraplaque angiogenesis and increase lesion stability. Thus, we used this model to study plaque reoxygenation and its effect on vein graft remodeling, intraplaque neovascularization, inflammation and vein graft patency. Moreover, since prolonged hyperoxia has the risk of introducing reactive oxygen species [18], we investigated the effect of reactive oxygen species in vitro on bone marrow derived macrophages and in vivo in the atherosclerotic lesions and their effect on the plaque environment.

Materials and Methods

Mice

This study was performed in compliance with Dutch government guidelines and the Directive 2010/63/EU of the European Parliament. All animal experiments were approved by the animal welfare committee of the Leiden University Medical Center. Male ApoE3*Leiden mice, crossbred in our own colony on a C57BL/background, 8 to 16 weeks old, were fed a diet containing 15% cacao butter, 1% cholesterol and 0.5% cholate (100193, Triple A Trading, Tiel, The Netherlands) for three weeks prior to surgery until sacrifice.

Vein Graft Surgery

Vein graft surgery was performed by donor mice caval vein inter-positioning in the carotid artery of recipient mice as previously described [6,19]. Briefly, thoracic caval veins from donor mice were harvested. In recipient mice, the right carotid artery was dissected and cut in the middle. The artery was everted around the cuffs that were placed at both ends of the artery and ligated with 8.0 sutures. The caval vein was sleeved over the two cuffs, and ligated. On the day of surgery and on the day of sacrifice mice were anesthetized with midazolam (5 mg/kg, Roche Diagnostics, Basel, Switzerland), medetomidine (0.5 mg/kg, Orion, Espoo, Finland) and fentanyl (0.05 mg/kg, Janssen Pharmaceutical Beerse, Belgium). The adequacy of the anesthesia was monitored by keeping track of the breathing frequency and the response to toe pinching of the mice. After surgery, mice were antagonized with atipamezol (2.5 mg/kg, Orion Espoo, Finland) and fluminasenil (0.5 mg/kg, Fresenius Kabi, Bad Homburg vor der Ho¨he, Germany). Buprenorphine (0.1 mg/kg, MSD Animal Health, Keniworth, NJ, USA) was given after surgery to relieve pain.

Carbogen Treatment

Acute reoxygenation was investigate in ApoE3*Leiden mice on day 28 after vein graft surgery. Mice were randomized in two groups, a control group (n = 13) and a carbogen treated group (n = 12) and exposed for 90 min to air (21% O_2) or carbogen gas (95% O_2, 5% CO_2) respectively. Halfway during the treatment, the mice received intraperitoneal injection of hypoxia specific marker pimonidazole (100 mg/kg, hypoxyprobe Omni kit, Hypoxyprobe Inc., Burlington, MA, USA) and anesthesia. Directly after the end of the treatment, mice were sacrificed after 5 min

of in vivo perfusion-fixation under anesthesia. Vein grafts were harvested, fixated in 4% formaldehyde, dehydrated and paraffin-embedded for histology.

Chronic reoxygenation was investigated in ApoE3*Leiden mice starting on day 7 after vein graft surgery. The decision for this timepoint was based on our previous finding that intraplaque angiogenesis is detectable in ApoE3*Leiden mice starting from day 14 after vein graft surgery [6]. Mice were randomized based on their plasma cholesterol levels (Roche Diagnostics, kit 1489437, Basel, Switzerland) and body weight in two groups, a control group (n = 16) and a carbogen treated group (n = 16) and exposed daily for 90 min to air (21% O_2) or carbogen (95% O_2, 5% CO_2) respectively, until the day of sacrifice. On day 28 after surgery, mice received the last treatment and halfway during this last treatment they received intraperitoneal injection of hypoxia specific marker pimonidazole (100 mg/kg, hypoxyprobe Omni kit, Hypoxyprobe Inc., Burlington, MA, USA) and anesthesia. Immediately after the end of the treatment, mice were sacrificed as previously described for the acute reoxygenation experiment.

Histological and Immunohistochemical Assessment of Vein Grafts

Vein graft samples were embedded in paraffin, and sequential cross-sections (5 µm thick) were made throughout the embedded vein grafts. To quantify the vein graft thickening (vessel wall area), MOVAT pentachrome staining was performed. Total size of the vein graft and lumen were measured. Thickening of the vessel wall (measured as intimal thickening + media thickening) was defined as the area between lumen and adventitia and determined by subtracting the luminal area from the total vessel area. The optimal lumen area was calculated by converting the luminal circumference, measured as the luminal perimeter, into luminal area.

Intraplaque angiogenesis was measured as the amount of $CD31^+$ vessels in the vessel wall area and intraplaque hemorrhage (IPH) was monitored by the amount of erythrocytes outside the (neo)vessels and scored as either not present, low, moderate or high.

Antibodies directed at alpha smooth muscle cell actin (αSMActin, Sigma, Santa Clara, CA, USA), Mac-3 (BD Pharmingen, Franklin Lakes, NJ, USA), Pimonidazole (mouse IgG1 monoclonal antibody, clone 4.3.11.3, Hypoxyprobe Inc., Burlington, MA, USA), 8OHdG (bs-1278R , Bioss antibodies,, Woburn, MA, USA), CD31 (sc-1506-r, Santa Cruz, Dallas, TX, USA), Ter119 (116202, Biolegend, , San Diego, CA, USA), Ki67 (ab16667, Abcam, Cambridge, UK) and

cleaved caspase 3 (, 9661-S, Cell SignalingDanvers, MA, USA) were used for immunohistochemical staining. Sirius red staining (80115, Klinipath, Amsterdam, The Netherlands) was performed to quantify the amount of collagen present in the vein grafts. The immuno-positive areas are expressed as a total area or percentage of the lesion area. Stained slides were photographed using microscope photography software (Axiovision, Carl Zeiss Microscopy, White Plains, NY, USA) or Ultrafast Digital Pathology Slide Scanner and associated software (Philips, Cambridge, Massachusetts, USA) and image analysis softwares were used to quantify the vein graft intimal hyperplasia and composition (Qwin, Leica, Wetzlar, Germany and Imagej, Bethesda, MD, USA).

RNA Isolation, cDNA Synthesis and qPCR

Total RNA was isolated from 10 (20 µm thick) paraffin sections (at least *n* = 6/group) following the manufacture's protocol (FFPE RNA isolation kit, Qiagen, Venlo, the Netherlands). cDNA was synthesized using the Superscript IV VILO kit according to the manufacture's protocol (TermoFisher, Waltham, Massachusetts, USA).

Commercially available TaqMan gene expression assays for the housekeeping gene hypoxanthine phosphoribosyl transferase (Hprt) (Mm01545399_m1), and selected genes were used (Applied Biosystems, Foster City, CA, USA); Vegfa (Mm03015193_m1), Hif1a (Mm00468869_m1), Cxcl12 (Mm00445553_m1), Epas1 (Mm01236112_m1), Il6 (Mm00446190_m1), Tnf (Mm00443258_m1) and Ccl2 (Mm00441242_m1). Q-PCRs were performed on the ABI 7500 Fast system (Applied Biosystems). The 2-ΔΔCt method was used to analyze the relative changes in gene expression.

Bone Marrow Derived Macrophages Isolation and In Vitro Experiments

Monocytes were isolated from bone marrow of tibias and femurs of male ApoE3*Leiden mice (*n* = 4) and cultured in RPMI 1640 medium (52400-025, ThermoFisher, GIBCO, Waltham, Massachusetts, USA,) supplemented with 25% heat inactivated fetal calf serum (Gibco® by Life Technologies), 100 U/mL Penicillin/Streptomycin (ThermoFisher, GIBCO, Waltham, Massachusetts, USA) and 0.1 mg/mL macrophage colony-stimulating factor (, 14-8983-80, ThermoFisher, E-Bioscience Waltham, Massachusetts, USA). After eight days the derived macrophages were seeded in a 12 wells plate for RNA isolation and in a chamber slide for immunocytochemistry (ICC) (NUNC LAB-TEK II, 154534, ThermoFisher, Waltham, Massachusetts, USA). 24 h later, when BMM were fully attached, BMM were stimulated with

either 200 or 400 µm tert-butylhydroperoxide, t-BHP, (Luperox, 458139, Sigma Aldrich, St. Louis, Missouri, USA) as a ROS mimic for 6 h.

RNA was isolated according to standard protocol using TRIzol® (Ambion®, ThermoFisher,Waltham, Massachusetts, USA) after which sample concentration and purity were examined by nanodrop (Nanodrop Technologies, ThermoFisher, Waltham, Massachusetts, USA). Complementary DNA (cDNA) was prepared using the High Capacity cDNA Reverse Transcription Kit (Applied Biosystems, ThermoFisher, Waltham, Massachusetts, USA) according to manufacturer's protocol. For qPCR, commercially available TaqMan gene expression assays for the selected genes were used as explained above.

For ICC cells were fixated in 4% formaldehyde and antibodies directed at Mac-3 (BD Pharmingen, Franklin Lakes, NJ, USA), 8OHdG (bs-1278R, Bioss antibodies, Woburn, MA, USA) and cleaved caspase 3 (9661-S, Cell Signaling, Danvers, MA, USA) were used for immunocytochemical staining. Tile-scans of stained slides were photographed using a fluorescent microscope (Leica AF-6000, Leica, Wetzlar, Germany) and Fiji image analysis software was used to quantify the mean grey value expression of the targets (Imagej, Bethesda, MD, USA).

Statistical Analysis

Results are expressed as mean ± SEM. A 2-tailed Student's t-test was used to compare individual groups. Non-Gaussian distributed data were analyzed using a Mann-Whitney U test using GraphPad Prism version 6.00 for Windows (GraphPad Software). Probability-values < 0.05 were regarded significant.

Results

Acute Carbogen Exposure Reduces Intraplaque Hypoxia

To evaluate the effect of acute carbogen treatment on advanced atherosclerotic vein graft lesions, ApoE3*Leiden mice that underwent vein graft surgery were exposed for 90 min to carbogen gas or normal breathing air. Mice exposed to carbogen gas (*n* = 8) showed a significant reduction of intraplaque (IP) hypoxia in the vein graft lesion compared to the air breathing group (*n* = 8) as shown by a 84% decrease in the immuno-area positive for pimonidazole in the lesions of carbogen treated mice compared to the control (*p*-value = 0.027) (Figure 1A–C).

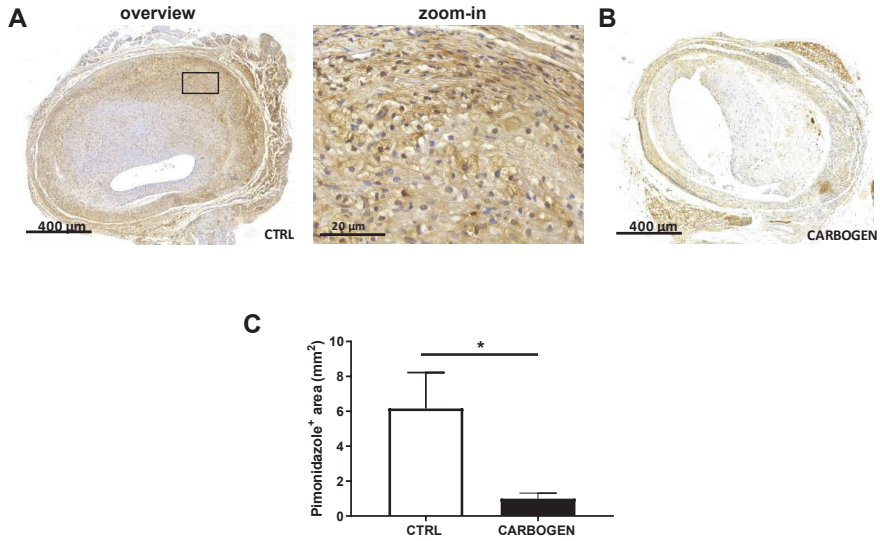


Figure 1. Short term carbogen exposure drastically reduces intraplaque hypoxia. (**A**) Representative pictures of sections from vein graft lesions in ApoE3* Leiden mice stained for pimonidazole in the control group (*n* = 8) and (**B**) one-time carbogen treated group (*n* = 8). (**C**) Quantification of pimonidazole positive area. Data are presented as mean ± SEM. * $p < 0.05$; by two-sided Student's t test.

Regarding the aspect of vein graft patency, single 90-min carbogen exposure directly before sacrifice did not affect vein graft patency (Figure 2A), vessel wall area, lumen perimeter, lumen area or optimal lumen area (Figure 2B,C). Furthermore, weight nor cholesterol levels were changed (Figure S1).

The percentage of collagen present in the lesion was comparable between the two groups (Figure 2D) and at a cellular level, the percentage of macrophages (Figure 2E) and SMCs (Figure 2F) were not altered by the acute exposure to carbogen.

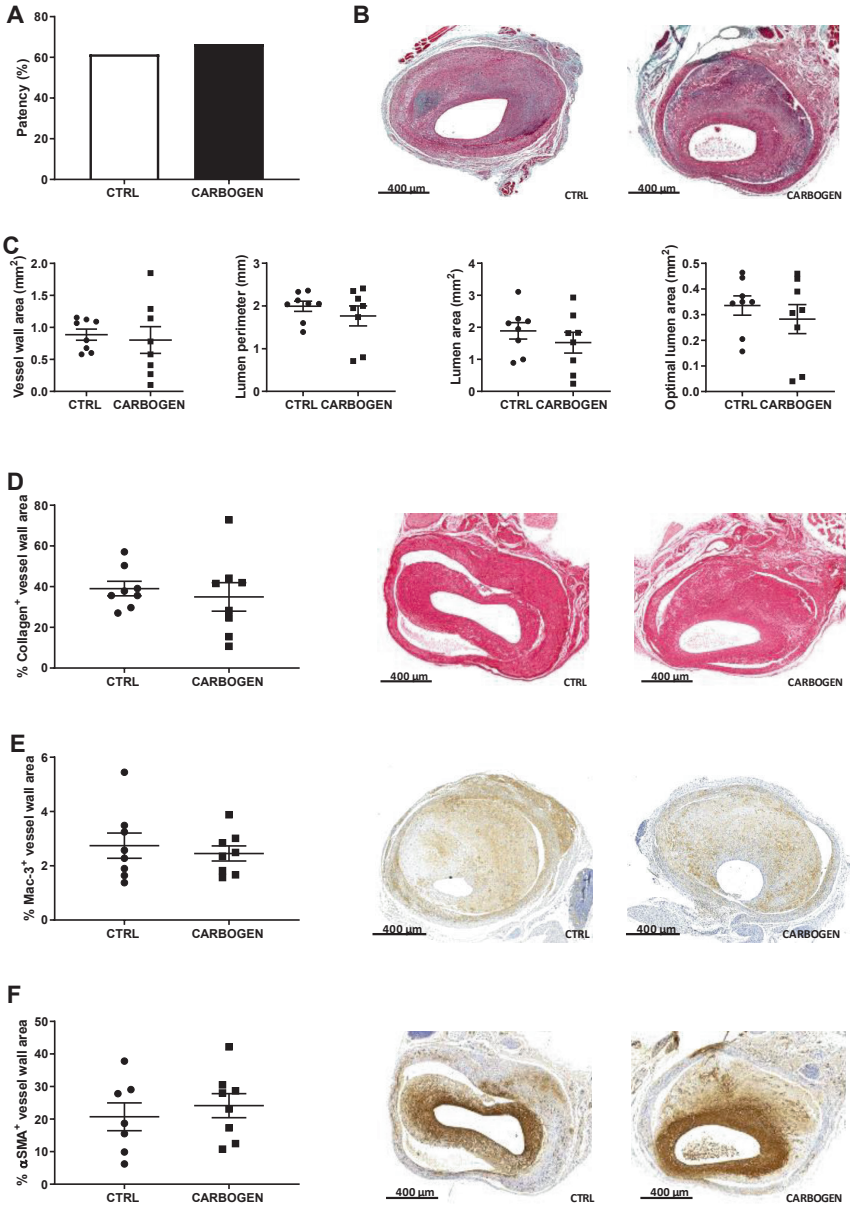


Figure 2. Short term exposure to carbogen gas does not influence plaque size nor composition. (**A**) Quantitative measurement of vein graft patency in ApoE3*Leiden mice from the control and one-time carbogen treated groups. Data are analyzed by Chi-square test (**B**) Representative pictures of MOVAT staining of vein graft sections from control (n = 8) and carbogen group (n = 8). (**C**) Quantification of vessel wall area, lumen perimeter, lumen area and optimal lumen area. Percentage of positive vessel wall area and representative pictures for (**D**) collagen (n = 8 for control and carbogen groups), (**E**) macrophages (n = 8 for control and carbogen groups) and

(**F**) smooth muscle cells staining (*n* = 8 for control and *n* = 7 for carbogen groups). Data are presented as mean ± SEM.

Chronic Carbogen Exposure Does not Influence Intraplaque Hypoxia

To evaluate the effect of hyperoxic carbogen treatment on plaque composition and remodeling we performed a chronic carbogen treatment on ApoE3*Leiden mice with advanced atherosclerotic vein graft lesions. Mice were exposed for 90 min daily to carbogen gas (*n* = 13) or normal breathing air (*n* = 12) for 21 days. Neither weight or cholesterol levels were affected by the treatment (Figure S2).

Surprisingly chronic exposure to carbogen gas did not reduce intraplaque hypoxia in the treated group when compared to the air breathing group (Figure 3). In fact, the degree of pimonidazole staining in the vein graft area was not different between the two groups (Figure 3).

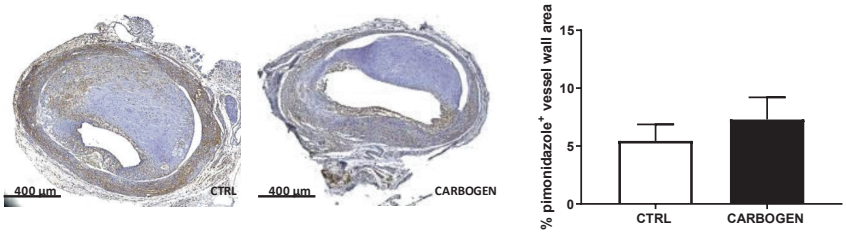


Figure 3. Chronic carbogen treatment does not affect intraplaque hypoxia. Representative pictures of vein graft cross sections stained for pimonidazole in control (*n* = 8) and chronic-treated carbogen groups (*n* = 13) and quantitative measurement of percentage of vessel wall area positive for pimonidazole staining. Data are presented as mean ± SEM.

Chronic Exposure to Carbogen Plays a Protective Role Against Occlusions

Chronic carbogen treatment resulted in a beneficial effect on vein graft patency, increasing the rate of vein graft patency by 34.5% (Figure 4A). In fact, only 53% of the mice of the control group presented a patent vein graft (Figure 4A), while 87.5% of the mice exposed to carbogen gas had a patent vein graft.

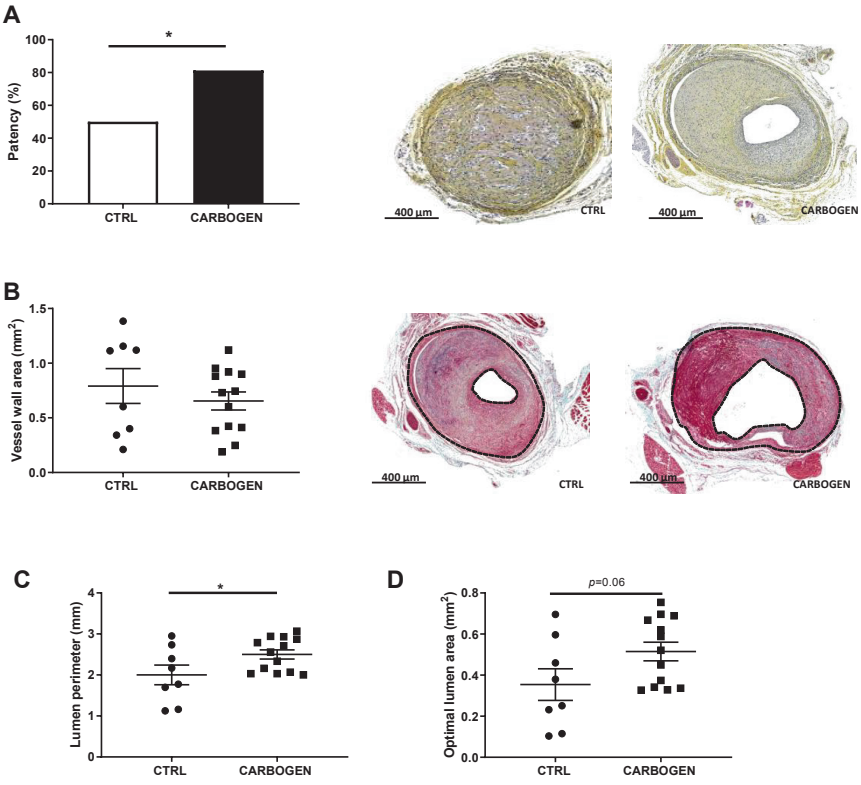


Figure 4. Chronic exposure to carbogen plays a protective role against vein graft occlusions. (**A**) Quantitative measurement of vein graft patency in ApoE3*Leiden mice from the control and prolonged carbogen treated groups. Data are analyzed by Chi-square test. * $p < 0.05$. Representative pictures of non-patent and patent vein grafts in ApoE3* Leiden mice at day 28 after surgery in the right panel. (**B**) Quantitative measurements of vein graft thickening. In the right panel, representative pictures of MOVAT staining in vein grafts from control ($n = 8$) and long term carbogen treated mice ($n = 13$), with vessel wall area as the area between the two dotted lines. (**C**) Quantification of lumen perimeter and (**D**) optimal lumen area. Data are presented as mean ± SEM. * $p < 0.05$; by two-sided Student's t test.

Vessel wall area thickening was not affected by exposure to carbogen gas since no differences could be detected between the two groups when taken only the patent grafts into account (Figure 4B). More importantly lumen size was affected by carbogen gas. In fact, carbogen treated mice presented a significant increase in the lumen perimeter when compared to control (Figure 4C,E, *p*-value = 0.048), and an increase in the optimal lumen area (Figure 4D, *p*-value = 0.067).

Chronic Carbogen Treatment Does Not Have an Effect on Intraplaque Angiogenesis and Intraplaque Hemorrhage

To see whether exposure to carbogen gas had an effect on the hypoxia triggered IP angiogenesis, the amount of $CD31^+$ vessels in the vein graft lesions (white arrows in Figure 5A zoom in) was evaluated and no difference in the number of neovessels in the carbogen group was observed when compared to the control group (*p*-value > 0.99).

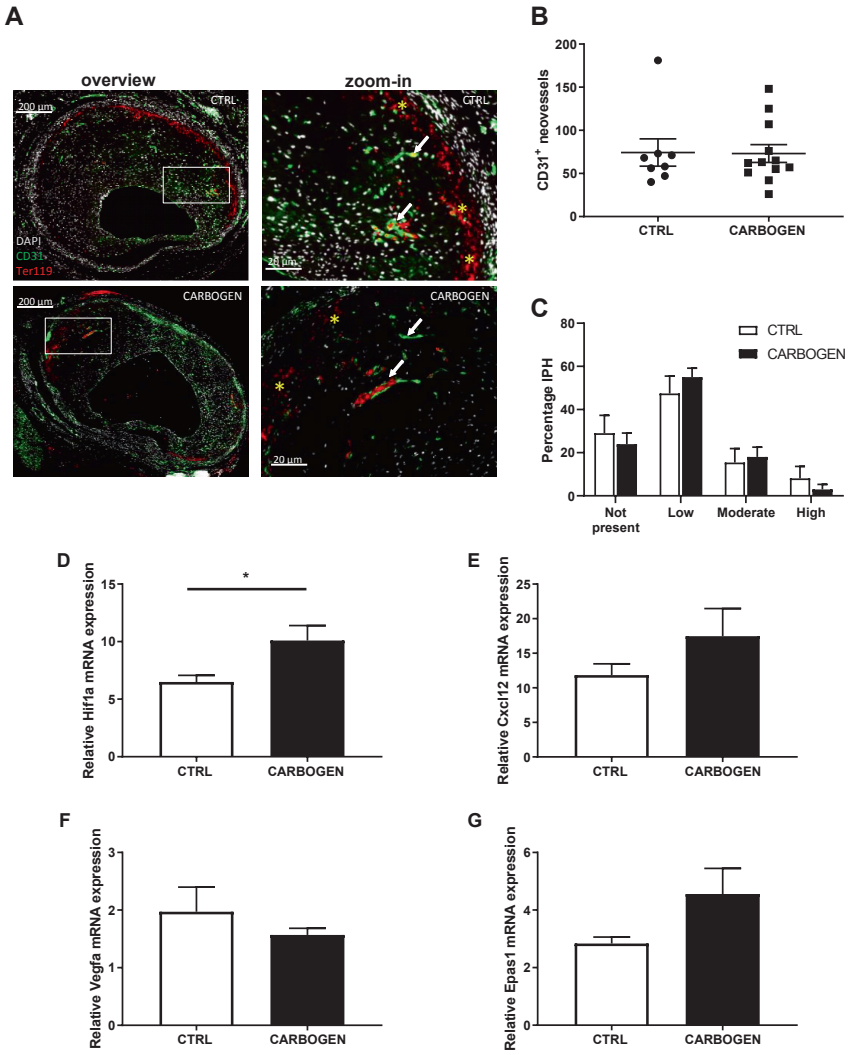


Figure 5. Chronic carbogen treatment does not affect intraplaque neovascularization. (**A**) Representative pictures of vein grafts lesions stained for DAPI (white), CD31 (green) and Ter119 (red). (**B**) Quantification of CD31 positive neovessels in the vessel wall area in the control group (n = 8) and in the carbogen treated group (n = 12). (**C**) Bar graphs representing the quantitative measurements for IPH in the control and long term carbogen treated groups. IPH was scored as not present, low, moderate or high. Total vessel wall gene expression of (**D**) Hif1a, (**E**) Cxcl12, (**F**) Vegfa and (**G**) Hif2a, relative to Hprt, was measured in the control and long term carbogen treated groups. Data are presented as mean ± SEM. * $p < 0.05$; by two-sided Student's t test.

In addition, when corrected for intimal thickness no differences were observed between the groups (p-value = 0.91) (Figure 5A,B). As a measure of the quality of the IP angiogenesis the degree of intraplaque hemorrhage was analyzed (yellow stars in Figure 5A zoom-in) as the amount of $Ter119^+$ cells found outside the neovessels and quantified as not present, low, moderate or high, and no differences could be seen when comparing the two groups (Figure 5C).

To determine the effects of hyperoxia on angiogenesis related genes the expression of Hif1a was analyzed. We surprisingly found a significant upregulation of Hif1a mRNA expression in the carbogen treated group when compared to the control (Figure 5D, p-value = 0.05), while mRNA expression of Cxcl12, Vegfa and Epas1 were not altered (Figure 5E–G). No differences between control and one-time carbogen treated group were found when analyzing gene expression in vein grafts from the acute carbogen treatment (Figure S3).

Chronic Carbogen Treatment Induces Accumulation of Reactive Oxygen Species and Apoptosis

Although an effect on Hif1a upregulation was observed, surprisingly no effect on angiogenesis could be seen. Therefore, we looked into other mechanisms that could possibly regulate Hif1a. We hypothesized that the mRNA upregulation of Hif1a in the carbogen treated group (Figure 5D) was caused by an accumulation of reactive oxygen species (ROS) induced by the carbogen treatment. ROS is known to be induced by prolonged hyperoxia [18] and to regulate the transcription of different genes involved in hypoxia and in inflammation such as Hif1a and Il6.

Il6 mRNA expression was studied as a representative for ROS induced factors and quantification of its expression showed a trend towards increased expression in the carbogen group of the chronic exposure study when compared to the control group (Figure 6A, p-value = 0.09).

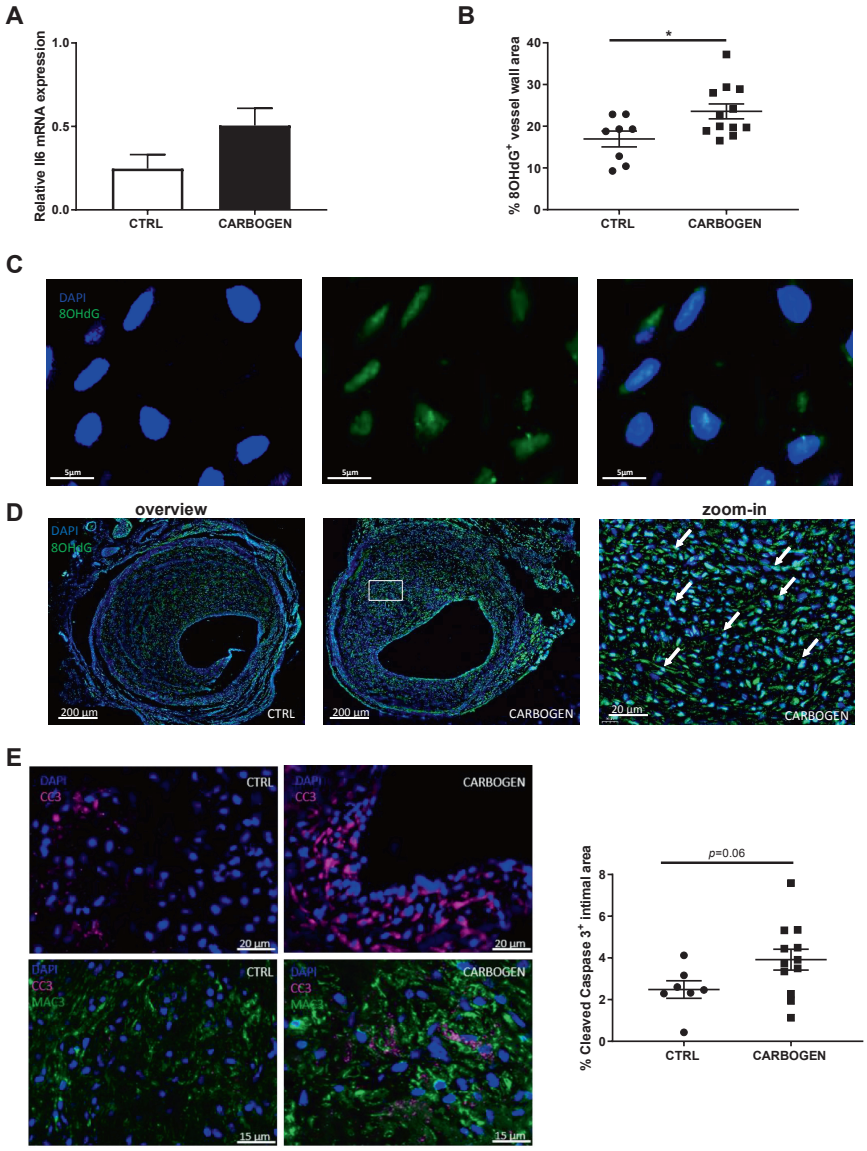


Figure 6. Chronic carbogen treatment induces accumulation of ROS. (**A**) Il6 gene expression relative to Hprt in the total vessel wall of control and chronic carbogen treated groups. (**B**) Quantification of the percentage of vessel wall area positive for 8OHdG. (**C**) Representative pictures of DAPI (in blue, left panel), 8OHdG (in green, central panel) and merged (right panel) staining in the vein graft lesions. (**D**) representative pictures of DAPI (blue) and 8OHdG (green) staining in vein graft lesions from control (n = 8) and carbogen treated (n = 12) mice. Light blue staining represents nuclei positive for 8OHdG and examples are indicated by white arrows. (**E**) In the top panels, representative pictures of DAPI (blue) and cleaved caspase 3 (CC3, in magenta) staining and in the bottom panels representative pictures of DAPI (blue), CC3 (magenta) and Mac3 (green) staining in control and

carbogen groups respectively. In the right panel quantification of percentage of intimal area positive for cleaved caspase 3. Data are presented as mean ± SEM. * $p < 0.05$ by two-sided Student's t test.

Next the presence of ROS was studied in the vein graft lesions by quantifying the amount of ROS–mediated DNA damage, analyzed by 8-hydroxy-2'deoxy-guanosine (8OHdG) immunohistochemical staining. We determined the subcellular location of the staining of 8OHdG. As observed in Figure 6C, a strong 8OHdG positive staining was found in the nuclei of the cells, with an occasional staining outside of the nuclei in the mitochondria, seen as cytoplasmic staining (Figure 6C, right panel). This suggests that the main site of ROS induced DNA damage is nuclear, and not mitochondrial. 8OHdG positive staining could be seen as light blue staining in the nuclei of the cells as a results of co-localized DAPI and 8OHdG staining (Figure 6D zoom-in) and the quantification corrected for the vessel wall area resulted in an increase of DNA damage in the carbogen treated group when compared to the control group (Figure 6B,D), supporting the idea that ROS levels are increased.

ROS is known to induce apoptosis as a consequence of DNA damage. Therefore, the amount of cells positive for cleaved caspase 3 (CC3) in the atherosclerotic vein graft lesions was determined in the carbogen treated and in the control groups (Figure 6E). Due to their high oxygen consumption we hypothesized that macrophages could possibly be the main cell type affected by DNA damage induced by ROS and subsequent apoptosis. As shown in the bottom panel of Figure 6D, macrophages rich areas in the lesions of mice treated with carbogen were found to be strongly positive for CC3 when compared to control (Figure 6E bottom panel).

When looking at the total amount of cells positive for cleaved caspase 3 in the intimal area, an increase in apoptotic cells $CC3^+$ in the lesions of mice exposed to carbogen gas was found compared to the air breathing group (Figure 6E, *p*-value = 0.06).

Chronic Carbogen Exposure Reduces Inflammatory Cell Content

The effects of chronic carbogen gas treatment on intraplaque inflammation were studied on macrophages since they produce high amounts of ROS, consume elevate amounts of O_2 and are known to be hypoxic [7]. Interestingly, the group of mice exposed daily to carbogen for 21 days showed a significant reduction in macrophage content when compared to the control group breathing normal air (*p*-value = 0.0126).When corrected for the differences in vein graft thickening, the relative percentage of macrophages was significantly decreased in the carbogen exposed group by the 15.2% (Figure 7A, *p*-value = 0.0044).

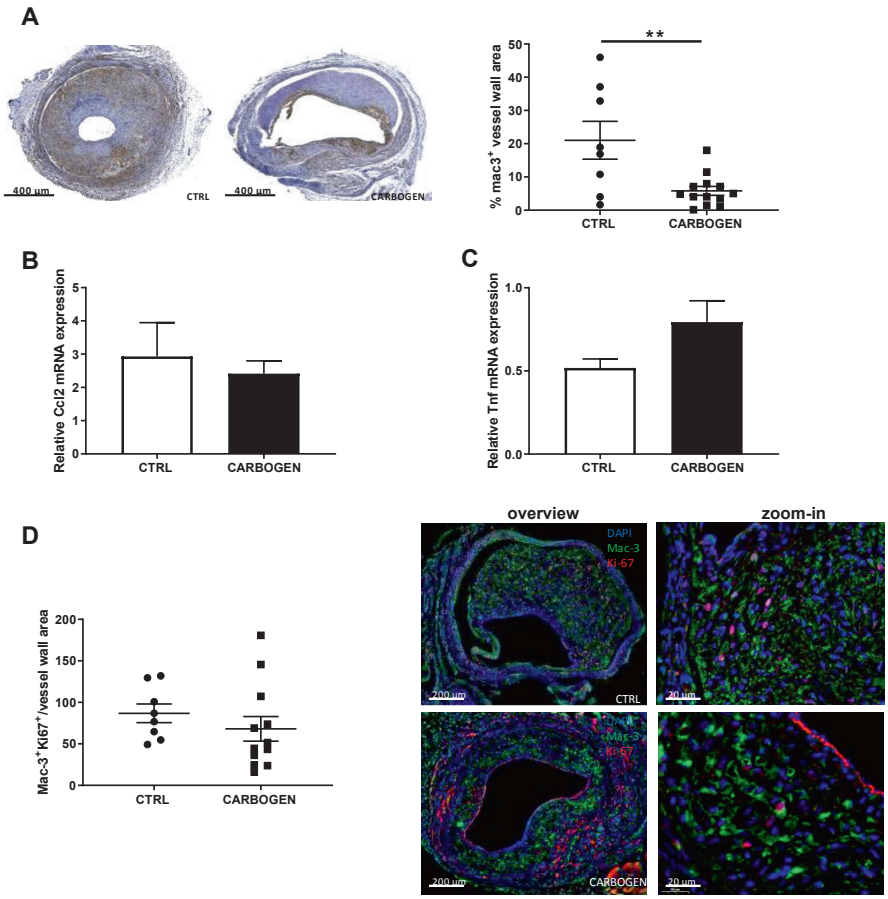


Figure 7. Chronic carbogen treatment reduces macrophages infiltration in the plaque. (**A**) Representative pictures of ApoE3* Leiden mice vein grafts from control (n = 8) and chronic carbogen treated (n = 13) groups stained for Mac-3. In the right panel quantitative measurements of the percentage of vessel wall area positive for Mac-3. Data are presented as mean ± SEM. * $p < 0.05$, ** $p < 0.01$; by two-sided Student's t test. Total wall gene expression of (**B**) Ccl2 and (**C**) Tnf relative to Hprt. (**D**) Quantification of the number of cells positive for Mac-3 and Ki67 in the vessel wall area of control (n = 8) and carbogen treated group (n = 13) and representative pictures of the staining with DAPI presented in blue, Mac-3 in green and Ki67 in red. Data are presented as mean ± SEM. ** $p < 0.01$ by 2-sided Student t test.

To study whether the decrease in macrophages was not due to a reduced infiltration of macrophages, nor a reduced proliferation of resident macrophages, local cytokines expression in the vein grafts was studied and the proliferation of macrophages was analyzed. First, the mRNA expression levels of Ccl2 and Tnf in the vein graft atherosclerotic lesions were examined. The mRNA levels of Ccl2 and Tnf did not differ between the carbogen treated group and the control (Figure 7B,C).

Using a triple IHC staining for Mac-3, Ki-67 and DAPI the amount of proliferating macrophages was determined. As shown in Figure 7D and, there was no difference in the number of proliferative macrophages corrected for the vessel wall thickening (*p*-value = 0.16).
Thus, the data suggest that the reduction of plaque macrophages could be due to enhanced macrophage apoptosis.

Chronic Carbogen Treatment Does Not Affect Plaque Size but Increases Plaque Stability

To evaluate the effect of prolonged carbogen treatment and accumulation of ROS on plaque composition, the amount of collagen (positive collagen area in the total vessel wall) and smooth muscle cells (positive αSMA area in the total vessel wall) was analyzed, two main predictors of plaque stability.

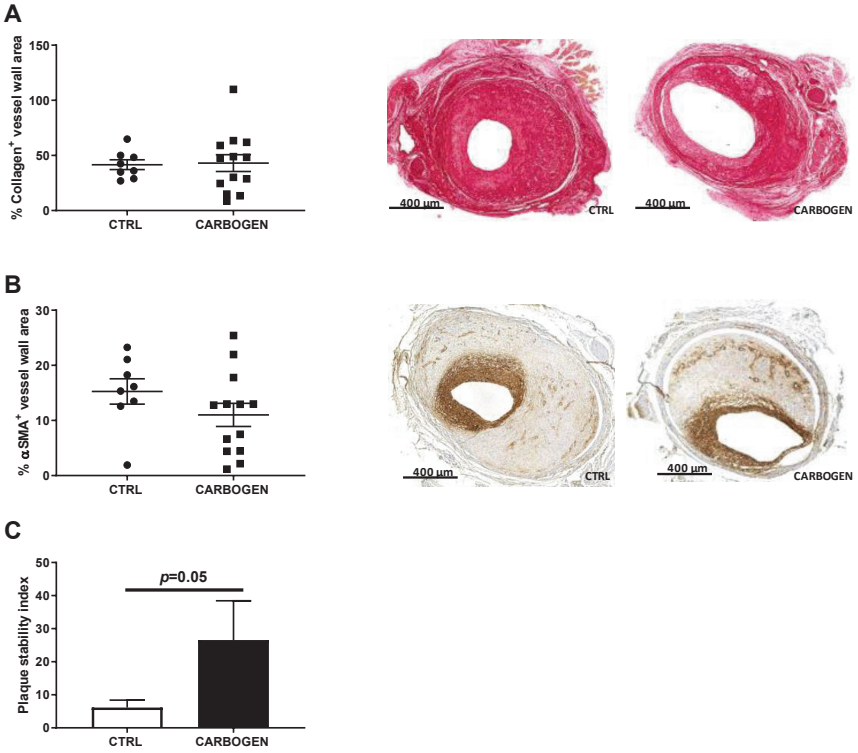


Figure 8. Chronic carbogen treatment does not affect collagen nor smooth muscle cells content in the lesion but increases plaque stability. (**A**) Quantitative measurement vessel wall area positive for collagen in ApoE3*Leiden mice from the control (*n* = 8) and carbogen treated (*n* = 13) groups. In the right panel representative pictures for collagen staining. (**B**) Quantification of percentage of vessel wall area positive for smooth muscle cell actin and representative pictures from the control (*n* = 8) and carbogen treated (*n* = 13) groups. (**C**) Quantification of plaque stability index. Data are presented as mean ± SEM.

The collagen content in the plaque was not affected by carbogen treatment, and was comparable between the two groups (Figure 8A). Similarly, SMCs content in the carbogen group was not different from the control group (Figure 8B). Interestingly, when calculating the plaque stability index, defined as the amount of collagen and SMCs divided by the vessel wall area, atherosclerotic plaques of the mice daily exposed to carbogen resulted to be more stable than the lesion of the control group (Figure 8C, *p*-value = 0.05).

ROS Increases DNA Damage and Apoptosis in Bone Marrow Derived Macrophages In Vitro

To unravel the molecular and cellular mechanism underlying the observed changes in macrophage content, in particular whether this could be due to hyperoxia induced ROS accumulation, we treated macrophages derived from bone marrow of APOE3*Leiden mice with t-BHP, a known ROS mimic [20]. t-BHP treatment increased the occurrence of DNA damage in BMM as measured by 8-OHdG immunocytochemical staining (Figure 9A), confirming its activity as a ROS mimic and the induction of DNA damage by ROS. We then evaluated the effect of the ROS mimic t-BHP on the expression of several genes. Similar to changes in expression in vivo, we found that t-BHP-induced ROS caused a significant increase of Hif1a mRNA expression (*p*-value = 0.007 and 0.02 respectively) when compared to control (Figure 9C). Interestingly, we also found that ROS caused an increase in the expression of pro-inflammatory genes Ccl2 and Tnf, but decreased Epas1 expression compared to control (Figure S4).

To assess if ROS ultimately causes apoptosis in cultured BMM, we examined the expression of CC3 and found a significant and dose dependent increase in CC3 expression, thus apoptosis, in t-BHP treated BMM when compared to control (Figure 9F). The group treated with 200 µm t-BHP showed a 10% increase (*p*-value = 0.03) and the group treated with 400 µm t-BHP a 27% increase (*p*-value = 0.01) in CC3 expression when compared to control (Figure 9D). Moreover, we observed a drastic reduction in the total number of cells by 72% and 70% in the groups treated with 200 and 400 µm t-BHP, respectively, when compared to control (Figure 9E, *p*-value = 0.01 for both groups). Combined these data demonstrate that ROS directly affects gene expression in macrophages and causes DNA damage and apoptosis.

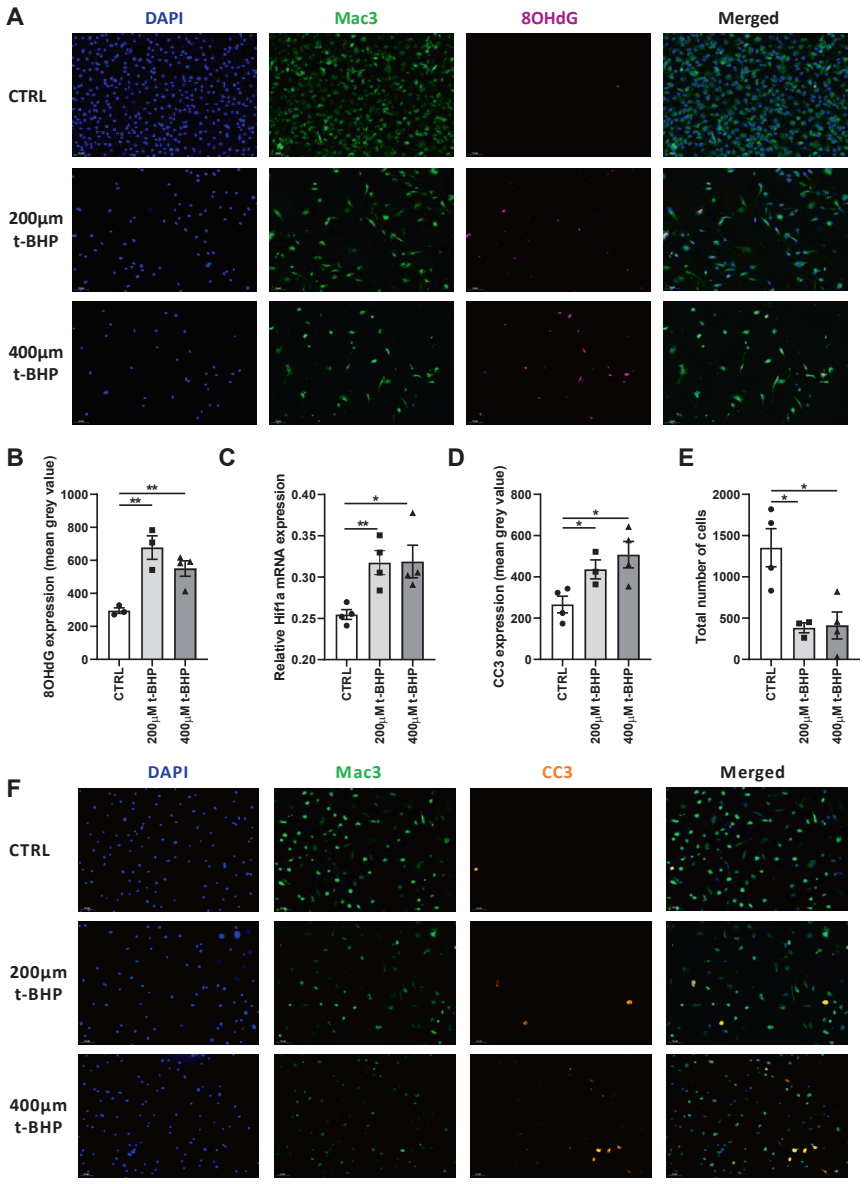


Figure 9. ROS induces DNA damage and apoptosis on in vitro bone marrow macrophages (BMM) (**A**) Representative pictures of CTRL BMM and BMM treated with 200 or 400 µm t-BHP respectively are shown. Examples images stained for DAPI (blue), Mac3 (green) and 8OHdG (magenta) as well as a merged image are shown per each condition tested. (**B**) Quantification of 8OHdG expression as mean intensity is shown. (**C**) Total mRNA expression of Hif1a relative to Hprt. (**D**) Quantification of CC3 expression as mean intensity is shown. (**E**) Quantification of total amount of cells per condition tested expressed as total amount of positive DAPI nuclei. (**F**) Representative pictures of CTRL BMM and BMM treated with 200 or 400 µm t-BHP respectively. Examples images stained for DAPI (blue), Mac3 (green) and cleaved caspase 3 (CC3) (orange) as well as a merged image are shown

per each condition tested. Data are presented as mean ± SEM. * $p < 0.05$, ** $p < 0.01$,; by two-sided Student's t test.

Discussion

The results of the present study show that carbogen treatment in an acute short term setting resulted in a profound reduction of intraplaque hypoxia in murine vein grafts lesions in vivo. Long term treatment with carbogen resulted in a beneficial effect on vein graft patency in ApoE3*Leiden mice, but surprisingly, had no effect on hypoxia, intraplaque angiogenesis and intraplaque hemorrhage. On the other hand, long term carbogen treatment resulted in hyperoxia-induced ROS formation with consequent effects on HIF1a mRNA levels and macrophage apoptosis. A reduction in macrophage content in the vein graft lesions was observed, resulting in less unstable lesions. Moreover, comparable to what was observed in vivo, in vitro induction of ROS using the ROS mimic t-BHP in BMM resulted in a strong increment in DNA damage and apoptosis.

Carbogen inhalation is widely used in the oncological field [21,22]. It has been shown that the time to achieve a maximal increase in tumor oxygenation with carbogen inhalation depends on various factors such as the type of cell involved, the location, and the size of the tumor [23,24]. Moreover, Hou et al. observed an effect of carbogen treatment comparable to what was observed in the present study, both in the short and the long term experiments. Single carbogen inhalation significantly increased tumor oxygenation, while during multiple administrations of carbogen the effect was reduced, indicating that the response to chronic carbogen is not consistent over days [23]. Nevertheless, we showed that prolonged carbogen treatment has a protective role against vein graft occlusions. Vein graft occlusion is a phenomenon often seen after vein grafting in which the vessel lumen is narrowed due to extensive intimal hyperplasia that progress to stenosis and occlusion [25]. This phenomenon is also observed in ApoE3*Leiden mice that undergo vein graft surgery. Besides the reduction in vein graft occlusions, an increase in vein graft patency due to an increase in lumen perimeter and optimal lumen area of the hyperoxic vein grafts was observed, similar to the study by Fowler et al. [26]. In that study carbogen is used in the treatment of central retinal artery occlusion to increase blood oxygen maintaining oxygenation of the retina [26]. This effect of hyperoxygenation on retinal artery remodeling can be related to the effect of carbogen on patency and increase in lumen perimeter and increase in the optimal lumen found in the present study.

We did not observe a reduction in hypoxia nor an effect on intraplaque angiogenesis in the prolonged carbogen study. Furthermore, no changes in local gene expression of Vegfa were observed in the vein grafts, but interestingly Hif1a was upregulated in the prolonged carbogen exposure study and not downregulated as expected. In fact following our initial hypothesis we would have expected a reduction in intraplaque angiogenesis in parallel with a reduction in Hif1a and Vegfa expression. For this reason, we studied other known processes that regulate Hif1a and observed an accumulation of ROS in the carbogen exposed group when compared to the control group. Repeated exposure to hyperoxia is known to be associated at a cellular level with an accumulation of ROS [27,28]. When the exposure is repeated too often, the oxidant insult is no longer compensated by the host's antioxidant defense mechanisms and therefore cell injury and death ensue [29]. Cell injury induced by ROS comprises lipid peroxidation, protein oxidation and DNA damage [30,31]. We observed an increase in DNA damage measured as an augmented presence of 8OHdG staining in the long term carbogen treated group when compared to the control group, indicating that a daily long term treatment with carbogen gas results in accumulation of ROS that in turns induces DNA damage in the atherosclerotic lesions. Moreover, we also observed an increase in DNA damage in bone marrow macrophages in vitro under ROS stimulation. It is known that DNA damage can be found in the nuclei and in the mitochondria [32,33]. Both in the vein graft lesions in vivo and in the cultured t-BHP treated macrophages in vitro, a strong 8OHdG positive staining in the nuclei of the cells, with an occasional cytoplasmic staining could be seen. The subcellular location of the staining of 8OHdG suggests that the main site of ROS induced DNA damage is nuclear, and not mitochondrial. ROS generated by repeated hyperoxia treatment can alter gene expression by modulating transcription factor activation, like NF-kβ, which then impact downstream targets [34]. It has been shown that hyperoxia also results in nuclear translocation of NF-kβ and NF-kβ activation in several cell types [35]. Our results show that long term carbogen treatment result in Hif1a gene expression upregulation. In addition, in vitro BMM treated with the ROS mimic t-BHP also showed an upregulation of Hif1a gene expression. Interestingly, the transcription of this gene is known to be regulated by NF-kβ transcription factor. In fact, Bonello et al., demonstrated that ROS induced Hif1a transcription via binding of NF-kβ to a specific site in the Hif1a promoter [36]. Those findings could be further investigated in future experiments using antioxidants such as NAC to see whether it can reverse the carbogen treatment.

We showed that the accumulation of ROS in the carbogen treated group caused an increase in apoptosis, accumulated in macrophages rich areas, and resulted in a decrease in the amount of macrophages. Even though we cannot exclude that the association of macrophages with cleaved caspase 3 could be due to efferocytosis of apoptotic cells, macrophage efferocytosis is frequently hampered in atherosclerotic lesions, therefore it is likely that these macrophages are apoptotic. Previously, in contrast with our findings, a strong correlation between macrophage content and hypoxia was shown by Marsch et al. [16]. Moreover, hypoxia potentiates macrophage glycolytic flux in a Hif1a dependent manner [37] in order to fulfill the need of ATP for protein production and migration. Taken together, this points to a high request and high use of O_2 by plaque macrophages and a consequent high exposure of these inflammatory cells to ROS accumulated during hyperoxia. We demonstrated that ROS causes accumulation of DNA damage and subsequently an increase in apoptosis and cell death in BMM in vitro. The link between ROS induced DNA damage and apoptosis detected in vitro might explain the observed apoptosis in macrophages in vivo. Moreover, a reduction in the number of macrophages is associated with plaque stability and plaque stability is reflected in an increase in vein graft patency as observed in the present study.

Previously Marsch et al. showed that repeated carbogen treatment in $LDLR^{-/-}$ mice lead to reduction in intraplaque hypoxia, necrotic core size and apoptosis [16]. In the present study we showed that repeated carbogen treatment in accelerated vein graft atherosclerotic lesions in ApoE3* Leiden mice resulted in increased apoptosis and unaltered intraplaque hypoxia when compared to controls. Accelerated atherosclerotic lesions in ApoE3*Leiden mice highly resemble human atherosclerotic lesions and, differently from $LDLR^{-/-}$ mice, do present intraplaque angiogenesis. Our results show that although we did not observe reduced intraplaque angiogenesis and IPH daily hyperoxia treatment with carbogen gas in this murine model lead to accumulation of ROS that could not be cleared by anti-oxidant agents and the ROS build-up lead to DNA damage and induced apoptosis. In fact, differently from Marsch et al., who treated mice daily for five days, followed by two days of no carbogen exposure we performed the treatment daily and started our treatment seven days after mice underwent vein graft surgery, when the atherosclerotic lesions already started forming. This starting time point was based on our previous findings [6] in which we found that intraplaque neovascularization in ApoE3*Leiden mice that underwent vein graft surgery is visible 14 days

after surgery. Therefore, we were able to study the effect of carbogen treatment on lesion stabilization rather than on lesion formation.

One of the limitations of the current study may be the choice of the model used, the ApoE3*Leiden mice vein grafts. However, since in most mouse models for spontaneous atherosclerosis intraplaque angiogenesis is absent, and the lesions observed in the ApoE3*Leiden mice vein grafts show many features that can also be observed in advanced human lesions, including intraplaque hypoxia, angiogenesis and intraplaque hemorrhage, we believe this model is suitable for the current studies. The fact that the most prominent effects observed relate to hyperoxygenation induced ROS production, macrophage apoptosis and vein graft patency, whereas the experimental set-up was initially designed to identify effects on intraplaque angiogenesis, might indicate another limitation in our study set-up.

Based on the results obtained in the present study we can conclude that although short term carbogen gas treatment leads to a profound reduction in intraplaque hypoxia, the treatment has mixed effects. Despite the beneficial effects of the hyperoxygenation treatment on vein grafts, i.e., improved vein graft patency and a strong trend towards an increased plaque stability index, chronic hyperoxygenation also induced Hif1a mRNA expression, ROS accumulation and apoptosis. That all will harm the vein grafts in the current model under the current conditions. This indicates that in order to define potential therapeutic benefits of hyperoxygenation treatment further research is needed to define optimal conditions for this treatment in vein graft disease.

References

1. Bentzon, J.F.; Otsuka, F.; Virmani, R.; Falk, E. Mechanisms of plaque formation and rupture. *Circ. Res.* **2014**, *114*, 1852–1866, doi:10.1161/circresaha.114.302721.
2. de Vries, M.R.; Quax, P.H. Plaque angiogenesis and its relation to inflammation and atherosclerotic plaque destabilization. *Curr. Opin. Lipidol.* **2016**, *27*, 499–506, doi:10.1097/mol.0000000000000339.
3. Lee, E.S.; Bauer, G.E.; Caldwell, M.P.; Santilli, S.M. Association of artery wall hypoxia and cellular proliferation at a vascular anastomosis. *The Journal of surgical research* **2000**, *91*, 32-37, doi:10.1006/jsre.2000.
4. Sluimer, J.C.; Gasc, J.M.; van Wanroij, J.L.; Kisters, N.; Groeneweg, M.; Sollewijn Gelpke, M.D.; Cleutjens, J.P.; van den Akker, L.H.; Corvol, P.; Wouters, B.G., et al. Hypoxia, hypoxia-inducible transcription factor, and macrophages in human atherosclerotic plaques are correlated with intraplaque angiogenesis. *J. Am. Coll Cardiol.* **2008**, *51*, 1258–1265, doi:10.1016/j.jacc.2007.12.025.
5. de Vries, M.R.; Parma, L.; Peters, H.A.B.; Schepers, A.; Hamming, J.F.; Jukema, J.W.; Goumans, M.; Guo, L.; Finn, A.V.; Virmani, R., et al. Blockade of vascular endothelial growth factor receptor 2 inhibits intraplaque haemorrhage by normalization of plaque neovessels. *Journal of internal medicine* **2019**, *285*, 59-74, doi:10.1111/joim.12821.
6. Marsch, E.; Sluimer, J.C.; Daemen, M.J. Hypoxia in atherosclerosis and inflammation. *Curr. Opin. Lipidol.* **2013**, *24*, 393–400, doi:10.1097/MOL.0b013e32836484a4.
7. Subbotin, V.M. Excessive intimal hyperplasia in human coronary arteries before intimal lipid depositions is the initiation of coronary atherosclerosis and constitutes a therapeutic target. *Drug Discov. Today* **2016**, *21*, 1578–1595, doi:10.1016/j.drudis.2016.05.017.
8. Jain, T.; Nikolopoulou, E.A.; Xu, Q.; Qu, A. Hypoxia inducible factor as a therapeutic target for atherosclerosis. *Pharmacol. Ther.* **2018**, *183*, 22–33, doi:10.1016/j.pharmthera.2017.09.003.
9. Balogh, E.; Toth, A.; Mehes, G.; Trencsenyi, G.; Paragh, G.; Jeney, V. Hypoxia Triggers Osteochondrogenic Differentiation of Vascular Smooth Muscle Cells in an HIF-1 (Hypoxia-Inducible Factor 1)-Dependent and Reactive Oxygen Species-Dependent Manner. *Arter. Thromb. Vasc. Biol.* **2019**, *39*, 1088–1099, doi:10.1161/atvbaha.119.312509.
10. Parma, L.; Baganha, F.; Quax, P.H.A.; de Vries, M.R. Plaque angiogenesis and intraplaque hemorrhage in atherosclerosis. *Eur. J. Pharm.* **2017**, *816*, 107–115, doi:10.1016/j.ejphar.2017.04.028.
11. Sluimer, J.C.; Kolodgie, F.D.; Bijnens, A.P.; Maxfield, K.; Pacheco, E.; Kutys, B.; Duimel, H.; Frederik, P.M.; van Hinsbergh, V.W.; Virmani, R., et al. Thin-walled microvessels in human coronary atherosclerotic plaques show incomplete endothelial junctions relevance of compromised structural integrity for intraplaque microvascular leakage. *J. Am. Coll. Cardiol.* **2009**, *53*, 1517–1527, doi:10.1016/j.jacc.2008.12.056.
12. Aarup, A.; Pedersen, T.X.; Junker, N.; Christoffersen, C.; Bartels, E.D.; Madsen, M.; Nielsen, C.H.; Nielsen, L.B. Hypoxia-Inducible Factor-1alpha Expression in Macrophages Promotes Development of Atherosclerosis. *Arter. Thromb. Vasc. Biol.* **2016**, *36*, 1782–1790, doi:10.1161/atvbaha.116.307830.
13. Hultén, L.M.; Levin, M. The role of hypoxia in atherosclerosis. *Curr. Opin. Lipidol.* **2009**, *20*, 409–414, doi:10.1097/MOL.0b013e3283307be8.
14. Abe, H.; Semba, H.; Takeda, N. The Roles of Hypoxia Signaling in the Pathogenesis of Cardiovascular Diseases. *J. Atheroscler. Thromb.* **2017**, *24*, 884–894, doi:10.5551/jat.RV17009.
15. Marsch, E.; Theelen, T.L.; Demandt, J.A.; Jeurissen, M.; van Gink, M.; Verjans, R.; Janssen, A.; Cleutjens, J.P.; Meex, S.J.; Donners, M.M., et al. Reversal of hypoxia in murine atherosclerosis prevents necrotic core expansion by enhancing efferocytosis. *Arter. Thromb. Vasc. Biol.* **2014**, *34*, 2545–2553, doi:10.1161/atvbaha.114.304023.
16. de Vries, M.R.; Niessen, H.W.; Lowik, C.W.; Hamming, J.F.; Jukema, J.W.; Quax, P.H. Plaque rupture complications in murine atherosclerotic vein grafts can be prevented by TIMP-1 overexpression. *Plos One* **2012**, *7*, e47134, doi:10.1371/journal.pone.0047134.
17. Jamieson, D.; Chance, B.; Cadenas, E.; Boveris, A. The relation of free radical production to hyperoxia. *Annu Rev. Physiol.* **1986**, *48*, 703–719, doi:10.1146/annurev.ph.48.030186.003415.
18. Simons, K.H.; de Vries, M.R.; Peters, H.A.B.; Hamming, J.F.; Jukema, J.W.; Quax, P.H.A. The protective role of Toll-like receptor 3 and type-I interferons in the pathophysiology of vein graft disease. *J. Mol. Cell. Cardiol.* **2018**, *121*, 16–24, doi:10.1016/j.yjmcc.2018.06.001.
19. Han, L.; Wang, Y.L.; Sun, Y.C.; Hu, Z.Y.; Hu, K.; Du, L.B. tert-Butylhydroperoxide induces apoptosis in RAW264.7 macrophages via a mitochondria-mediated signaling pathway. *Toxicol. Res.* **2018**, *7*, 970–976, doi:10.1039/c7tx00282c.

20. Yip, K.; Alonzi, R. Carbogen gas and radiotherapy outcomes in prostate cancer. *Ther. Adv. Urol.* **2013**, *5*, 25–34, doi:10.1177/1756287212452195.
21. Zhang, L.J.; Zhang, Z.; Xu, J.; Jin, N.; Luo, S.; Larson, A.C.; Lu, G.M. Carbogen gas-challenge blood oxygen level-dependent magnetic resonance imaging in hepatocellular carcinoma: Initial results. *Oncol. Lett.* **2015**, *10*, 2009–2014, doi:10.3892/ol.2015.3526.
22. Hou, H.G.; Khan, N.; Du, G.X.; Hodge, S.; Swartz, H.M. Temporal variation in the response of tumors to hyperoxia with breathing carbogen and oxygen. *Med. Gas. Res.* **2016**, *6*, 138–146, doi:10.4103/2045-9912.191359.
23. Chakhoyan, A.; Corroyer-Dulmont, A.; Leblond, M.M.; Gerault, A.; Toutain, J.; Chazaviel, L.; Divoux, D.; Petit, E.; MacKenzie, E.T.; Kauffmann, F., et al. Carbogen-induced increases in tumor oxygenation depend on the vascular status of the tumor: A multiparametric MRI study in two rat glioblastoma models. *J. Cereb. Blood Flow Metab.* **2017**, *37*, 2270–2282, doi:10.1177/0271678x16663947.
24. de Vries, M.R.; Simons, K.H.; Jukema, J.W.; Braun, J.; Quax, P.H. Vein graft failure: from pathophysiology to clinical outcomes. *Nat. Rev. Cardiol.* **2016**, *13*, 451–470, doi:10.1038/nrcardio.2016.76.
25. Fowler, S.B. Carbogen in the management of a central retinal artery occlusion. *Insight (Am. Soc. Ophthalmic Regist. Nurses)* **2012**, *37*, 10–11.
26. Gore, A.; Muralidhar, M.; Espey, M.G.; Degenhardt, K.; Mantell, L.L. Hyperoxia sensing: from molecular mechanisms to significance in disease. *J. Immunotoxicol.* **2010**, *7*, 239–254, doi:10.3109/1547691x.2010.492254.
27. Zhao, M.; Tang, S.; Xin, J.; Wei, Y.; Liu, D. Reactive oxygen species induce injury of the intestinal epithelium during hyperoxia. *Int. J. Mol. Med.* **2018**, *41*, 322–330, doi:10.3892/ijmm.2017.3247.
28. Petrache, I.; Choi, M.E.; Otterbein, L.E.; Chin, B.Y.; Mantell, L.L.; Horowitz, S.; Choi, A.M. Mitogen-activated protein kinase pathway mediates hyperoxia-induced apoptosis in cultured macrophage cells. *Am. J. Physiol.* **1999**, *277*, L589–595, doi:10.1152/ajplung.1999.277.3.L589.
29. Halliwell, B.; Chirico, S. Lipid peroxidation: its mechanism, measurement, and significance. *Am. J. Clin. Nutr.* **1993**, *57*, 715S–724S; discussion 724S-725S, doi:10.1093/ajcn/57.5.715S.
30. Evans, M.D.; Dizdaroglu, M.; Cooke, M.S. Oxidative DNA damage and disease: induction, repair and significance. *Mutat. Res.* **2004**, *567*, 1–61, doi:10.1016/j.mrrev.2003.11.001.
31. Santulli, G.; Xie, W.; Reiken, S.R.; Marks, A.R. Mitochondrial calcium overload is a key determinant in heart failure. *Proc. Natl. Acad. Sci. USA* **2015**, *112*, 11389–11394, doi:10.1073/pnas.1513047112.
32. Xie, W.; Santulli, G.; Reiken, S.R.; Yuan, Q.; Osborne, B.W.; Chen, B.X.; Marks, A.R. Mitochondrial oxidative stress promotes atrial fibrillation. *Sci. Rep.* **2015**, *5*, 11427, doi:10.1038/srep11427.
33. Traenckner, E.B.; Pahl, H.L.; Henkel, T.; Schmidt, K.N.; Wilk, S.; Baeuerle, P.A. Phosphorylation of human I kappa B-alpha on serines 32 and 36 controls I kappa B-alpha proteolysis and NF-kappa B activation in response to diverse stimuli. *EMBO J.* **1995**, *14*, 2876–2883.
34. Michiels, C.; Minet, E.; Mottet, D.; Raes, M. Regulation of gene expression by oxygen: NF-kappaB and HIF-1, two extremes. *Free Radic. Biol. Med.* **2002**, *33*, 1231–1242, doi:10.1016/s0891-5849(02)01045-6.
35. Bonello, S.; Zahringer, C.; BelAiba, R.S.; Djordjevic, T.; Hess, J.; Michiels, C.; Kietzmann, T.; Gorlach, A. Reactive oxygen species activate the HIF-1alpha promoter via a functional NFkappaB site. *Arter. Thromb. Vasc. Biol.* **2007**, *27*, 755–761, doi:10.1161/01.ATV.0000258979.92828.bc.
36. Tawakol, A.; Singh, P.; Mojena, M.; Pimentel-Santillana, M.; Emami, H.; MacNabb, M.; Rudd, J.H.; Narula, J.; Enriquez, J.A.; Traves, P.G., et al. HIF-1alpha and PFKFB3 Mediate a Tight Relationship Between Proinflammatory Activation and Anerobic Metabolism in Atherosclerotic Macrophages. *Arter. Thromb. Vasc. Biol.* **2015**, *35*, 1463–1471, doi:10.1161/atvbaha.115.305551.

Supplemental Material

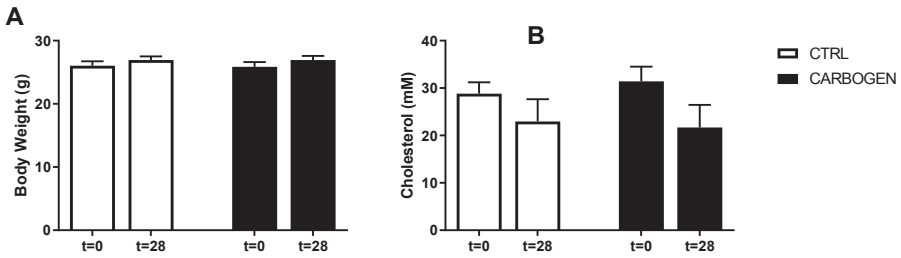


Figure S1. Bodyweight and cholesterol levels acute carbogen treatment. (A). Bodyweight before (t=0) and 28 days after surgery (t=28) of control and one-time carbogen treated mice. (B). Plasma cholesterol levels before (t=0) and 28 days after surgery (t=28) of control and one-time carbogen treated mice.

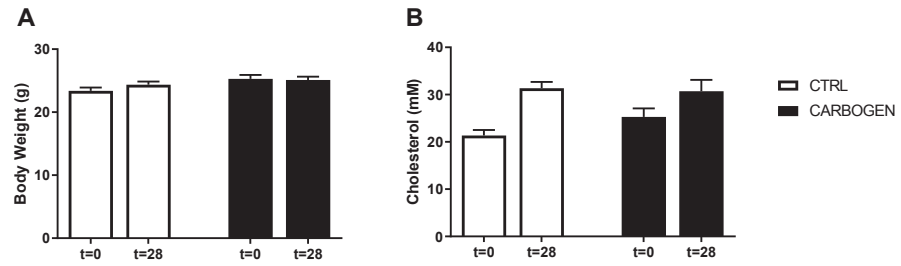


Figure S2. Bodyweight and cholesterol levels chronic carbogen treatment. (A). Bodyweight before (t=0) and 28 days after surgery (t=28) of control and prolonged carbogen treated mice. (B). Plasma cholesterol levels before (t=0) and 28 days after surgery (t=28) of control and prolonged carbogen treated mice.

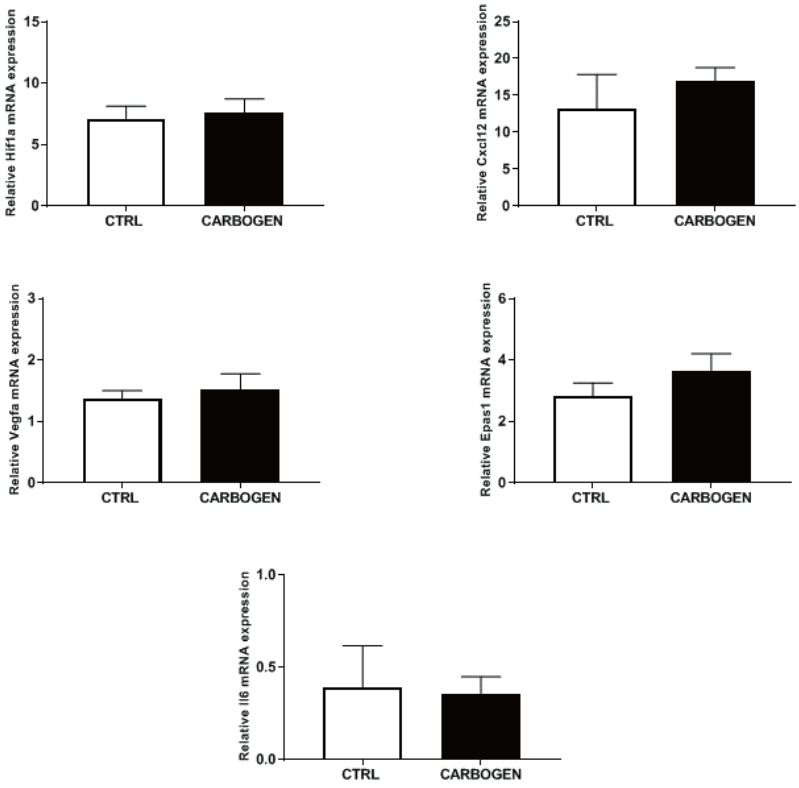


Figure S3. Total wall gene expression. (A) Expression of Hif1a, Cxcl12, Vegfa, Epas1 and Il6 in the mice from the control and one-time carbogen treated groups.

CHAPTER 4

BLOCKADE OF VEGF RECEPTOR 2 INHIBITS INTRAPLAQUE HEMORRHAGE BY NORMALIZATION OF PLAQUE NEOVESSELS

MR de Vries[1,2], L Parma[1,2], EAB Peters [1,2], A Schepers[1], JF Hamming[1], J Jukema[3], MJ Goumans[4], L Guo[5], AV Finn[5], R Virmani[5], CK Ozaki[6], PHA Quax[1,2]

[1]Department of Surgery, [2]Einthoven Laboratory for Experimental Vascular Medicine, [3]Department of Cardiology, [4]Department of Cell and Chemical Biology, Leiden University Medical Center, Leiden, The Netherlands. [5]CVPath Institute Inc. Gaithersburg, Maryland, USA. [6]Department of Surgery, Division of Vascular and Endovascular Surgery, Brigham and Women's Hospital, Harvard Medical School, Boston, Massachusetts, USA

J Internal Medicine. 2018; 285(1):59-74.

Abstract

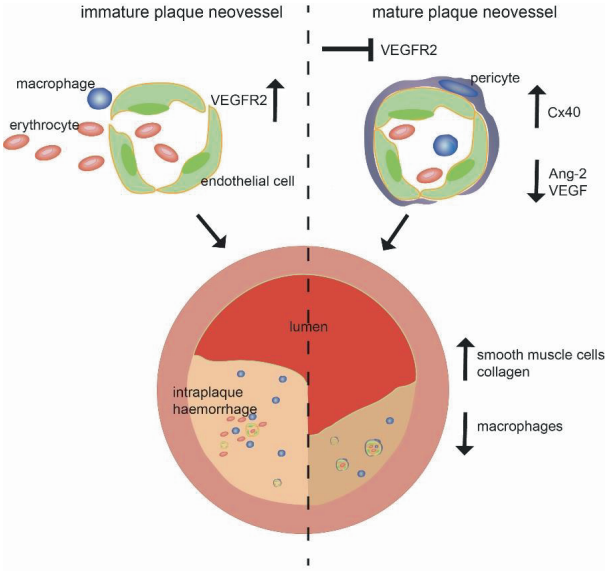
Background: Plaque angiogenesis is associated with atherosclerotic lesion growth, plaque instability and negative clinical outcome. Plaque angiogenesis is a natural occurring process to fulfill the increasing demand of oxygen and nourishment of the vessel wall. However, inadequate formed, immature plaque neovessels are leaky and cause intraplaque hemorrhage.

Objective: Blockade of VEGFR2 normalizes the unbridled process of plaque neovessel formation and induces maturation of nascent vessels resulting in prevention of intraplaque hemorrhage and influx of inflammatory cells into the plaque and subsequently increases plaque stability.

Methods and Results: In human carotid and vein graft atherosclerotic lesions, leaky plaque neovessels and intraplaque hemorrhage co-localize with VEGF/VEGFR2 and angiopoietins. Using hypercholesterolemic ApoE3*Leiden mice that received a donor caval vein interposition in the carotid artery we demonstrate that atherosclerotic vein graft lesions at t28 are associated with hypoxia, Hif1α and Sdf1 up-regulation. Local VEGF administration results in increased plaque angiogenesis. VEGFR2 blockade in this model results in a significant 44% decrease in intraplaque hemorrhage and 80% less extravasated erythrocytes compared to controls. VEGFR2 blockade *in vivo* results in a 32% reduction of vein graft size and more stable lesions with significantly reduced macrophage content (30%), and increased collagen (54%) and smooth muscle cell content (123%). Significant decreased VEGF, Angiopoietin-2 and increased Connexin 40 expression levels demonstrate increased plaque neovessel maturation in the vein grafts. VEGFR2 blockade in an aortic ring assay showed increased pericyte coverage of the capillary sprouts.

Conclusion: Inhibition of intraplaque hemorrhage by controlling neovessels maturation holds promise to improve plaque stability.

Graphical abstract



VEGFR2 blockade results in improved plaque neovessel maturation leading to reduced intraplaque haemorrhage and attenuated lesions with a more stable phenotype.

Introduction

Plaque angiogenesis and intraplaque hemorrhage are critical determinants of plaque instability [1]. Plaque angiogenesis or neovessel formation correlates with lesion progression, plaque inflammation and negative clinical outcome after cardiovascular events [2, 3]. Fragile atherosclerotic plaques do not only cause plaque instability in native atherosclerosis but also in post-interventional lesions such as in vein grafts and in in-stent neoatherosclerosis [4, 5].

Hypoxia in atherosclerotic lesions is a driver of plaque instability[6]. Furthermore, it can induce lesion growth and affect vascular remodeling[7, 8]. Angiogenesis a natural occurring process induced by hypoxia, fulfills the increasing demand of oxygen and nourishment of the vessel wall. Neovessel formation is stimulated by hypoxia-induced up-regulation of vascular endothelial growth factor (VEGF) [9, 10]. VEGF binds to and mediates its activity primarily through VEGF receptor 2 (VEGFR2). Plaque neovessels are frequently found dysfunctional especially, immature plaque neovessels. These neovessels are characterized by increased permeability caused by underdeveloped inter-endothelial junctions, incomplete basement membranes and partial pericyte coverage [11]. As a result, neovessels leak blood components into the lesions i.e. intraplaque hemorrhage. Erythrocytes in the plaque become phagocytosed and their cholesterol-rich membranes contribute to the free cholesterol content of the plaque [12-14]. Leaky neovessels are clearly associated with inflammatory cells[1]. Recently, it was shown by some of the coauthors that especially hemoglobin-haptoglobin receptor CD163+ macrophages interact with plaque neovessels and induce vascular permeability resulting in propagation of the instable character of lesions[15].

Anti-angiogenic therapies are used in cancer and eye diseases. However, these therapies are not always found beneficial [16]. Normalization of the neovasculature i.e. creating healthy mature neovessels is a relatively new strategy to target neovascularization [17]. Generation of a basement membrane and recruitment of pericytes are crucial steps in vessel maturation. These processes are regulated by VEGF-VEGFR2 and the tightly balanced angiopoietin-Tie2 system [18]. High levels of VEGF increase vessel permeability whereas low levels of VEGF are necessary for a stable vessel [19]. Angiopoietin (Ang)-1 mediates pericyte-endothelial cell adhesion and Ang-2 induces vessel permeability and acts as an antagonist to Ang-1, resulting in pericyte loss [19].

In preclinical models, it has been demonstrated that pro-angiogenic strategies augment atherosclerotic plaque growth and vascular inflammation whereas, anti-angiogenic strategies inhibit atherosclerosis [20-22]. Previously, we have shown that lesions induced by vein grafting in atherosclerosis-prone mice display profound plaque neovessels and intraplaque hemorrhage [23]. These plaque neovessels frequently lack pericyte coverage classifying them as immature [23].

We hypothesized that improving the maturation state of plaque neovessels reduces the extent of vascular "leakiness", which results in reduced intraplaque hemorrhage and lesion progression. Since low levels of VEGF are necessary for vessel homeostasis, we investigated the impact of the VEGFR2 blocking antibody (DC101) on plaque angiogenesis, maturation status, and atherosclerotic lesion size and composition in murine vein grafts.

Materials and Methods

Human tissue specimens

Human coronary artery vein graft specimens (n=12) were available from the CVPath Institute. A detailed patient description can be found in table 1 of the on line supplement. The severity of the vein graft lesions were scored as early, intermediate or late as described previously[4]. Anonymous carotid endarterectomy (n=12) specimens obtained at the LUMC in accordance with guidelines set out by the 'Code for Proper Secondary Use of Human Tissue' of the Dutch Federation of Biomedical Scientific Societies (Federa) and conform with the principles outlined in the Declaration of Helsinki. The carotid endarterectomy specimens phenotype was scored based on the Athero Express Biobank classification[2]. Unstable plaques were selected based on relative necrotic core size, foam cell and inflammatory cell infiltration score, and the presence of neovascularization. Specimens were formalin fixed, embedded in paraffin, sectioned and stained as described below.

Animals

All animal experiments were performed in compliance with Dutch government guidelines and the Directive 2010/63/EU of the European Parliament. Male ApoE3*Leiden mice, crossbred in our own colony on a C57BL/6 background for at least 18 generations, 10-16 weeks old, were fed a diet (AB diets) containing 1% cholesterol and 0.05% cholate (VEGF experiment) or 0.5% cholate (time courses and DC101 experiment) from 3 weeks prior to surgery until sacrifice. The mice were housed on regular bedding and nesting material, water and diet were provided at libitum Mice were randomized based on their plasma cholesterol levels (inclusion criteria of cholesterol level >8 mM) (Roche Diagnostics, kit 1489437) and body weight. Mice were anesthetized with midazolam (5 mg/kg, Roche Diagnostics), medetomidine (0.5 mg/kg, Orion,) and fentanyl (0.05 mg/kg, Janssen Pharmaceutical). After the surgery, the anesthesia of the mice was antagonized with atipamezol (2.5 mg/kg, Orion) and fluminasenil (0.5 mg/kg, Fresenius Kabi). Buprenorphine (0.1 mg/kg, MSD Animal Health) was given after surgery to relieve pain.

Vein grafts

Vein graft surgery was performed by a donor caval vein interposition in the carotid artery of recipient mice as described before[23, 24]. At sacrifice, patency of the vein grafts was visually checked for pulsations and blood flow, occluded vein grafts were excluded from the study. animals underwent 3 minutes of *in vivo* perfusion-fixation with PBS and formalin under anesthesia. Vein grafts were harvested, formalin fixed, dehydrated and paraffin-embedded for histology.

Treatment

VEGF experiment: Immediately after vein graft surgery the vein graft was immersed *in vivo* in 100 µl of 40% pluronic gel (F127, Sigma Aldrich) containing 250 ng VEGF (n=7, Sigma Aldrich) or pluronic gel alone (n=6).

DC101 experiment: Mice were treated with IP injections of rat anti-mouse VEGF-R2 IgG monoclonal blocking antibodies (10 mg/kg DC101, Bio X cell)[25] (n=14) or control rat anti-mouse IgG antibodies (10 mg/kg, Bio X cell) (n=14) at day 14, 17, 21 and 25. 2 mice in this group were excluded from analysis due to thrombosis in the vein graft.

In vivo *detection of hypoxia*

One hour prior to sacrifice mice (n=6) received an intraperitoneal injection with the hypoxia marker pimonidazole hydrochloride (100 mg/kg, hypoxyprobe Omni kit, Hypoxyprobe Inc.). Pimonidazole was detected with the in the kit included rabbit polyclonal antibody (clone 2627).

Histological and immunohistochemical assessment of vein grafts

Cross sections were routinely stained with hematoxylin-phloxine-saffron (HPS) or Movat's pentachrome staining. Picrosirius red was used to detect collagen. The following antibodies were used for immunohistochemistry: endothelial cell CD31 (sc-1506-r, Santa Cruz), Glycophorin A (YTH89.1 Thermofisher), VEGF (sc-7269, Santa Cruz), VEGFR2 (55B11, Cell Signalling), Ang-1 (human; A78648, Atlas antibodies; murine LS-B62, LS Bio), Ang-2 (PAB19784, Abnova), intercellular adhesion molecule 1 (ICAM1 sc-1511-r, Santa Cruz), vascular cell adhesion protein 1 (VCAM1, ab27560, Abcam), stromal cell-derived factor 1 (SDF-1, ab9797, Abcam), Hypoxia-

inducible factor 1-alpha (HIF-1α, NB100-473, Novus Biologicals), CD163 (orb13303 Biorbyt), CD3 (ab16669, Abcam), macrophage MAC3 (550292, BD-Pharmingen), smooth muscle cell actin (SMCA, 1A4, Dako) and erythrocyte Ly76 (TER119, 116202, Biolegend). For each antibody isotype-matched antibodies were used as negative controls.

Images of the human lesions were obtained with the Ultrafast Digital Pathology Slide Scanner and associated software (Phillips). Bright field photographs were obtained with a Zeiss microscope and associated software. Fluorescent double and triple staining were acquired with the fluorescent slide scanner (3DHistech) and panoramic viewer software (3DHistech).

Morphometric analysis of vein grafts

Image analysis software (Qwin, Leica) was used for morphometric analysis. For each mouse eight (150 µm spaced) cross-sections were used to determine lesion size and occurrence of intraplaque hemorrhage over a total vein graft length of 1050 µm. Since elastic laminas are non-existent in these venous grafts, we analyzed the putative vessel wall area (or lesion area) by measuring total vessel area (area within the adventitia) and the lumen area. The lesion area was calculated as total vessel area minus lumen area. Immuno-positive areas in vein grafts are expressed as total area or percentage of the lesion area.

Morphologic analyses of intraplaque hemorrhage

Intraplaque hemorrhage was analyzed using CD31/Ly76 double-stained sections. Lesions where erythrocytes were found extravascular, adjacent to neovessels, were regarded as lesions with intraplaque hemorrhage. Using image analysis software (Qwin, Leica) the extravasated erythrocyte content was evaluate by measuring the total erythrocyte area in the lesion, followed by subtraction of the area of erythrocytes within the CD31 stained neovessels.

RNA isolation, cDNA synthesis and RT-PCR

Time course: total RNA was isolated from murine vein grafts harvested at several time points (vein grafts/time point; t0 (caval vein); 24h; 3d; 7d; (n=3 each), 14d (n=4) and 28d (n=5)). RNA was isolated and cDNA was synthesized as described previously[26].

VEGFR2 experiment: total RNA was isolated from 10 (20µm thick) paraffin sections of vein grafts (n=6/group). RNA was isolated according manufacturers protocol (FFPE RNA isolation kit, Qiagen). RNA for Q-PCR was reverse transcribed using a High Capacity RNA-to-cDNA kit (Applied Biosystems). Commercially available TaqMan gene expression assays for the housekeeping gene hypoxanthine phosphoribosyl transferase (HPRT1), and selected genes were used (Applied Biosystems); *Vegfa* (Mm 00437306_m1), *Hif1-α* (Mm 0468869_m1), *Sdf-1 (Mm 00445553_m1), Vegfr2* (Mm01222421_m1), *Vegfr1* (Mm00438980_m1), *Tie2* (Mm00443243_m1), *Icam1* (Mm00516023_m1), *Ang-1* (Mm00456503_m1), *Ang-2* (Mm00545822_m1), *Connexin37* (Mm01179783_m1), *Connexin40* (Mm01265686_m1), *Connexin43* (Mm00439105_m1), *Ccl2* (Mm00441242_m1) and *Il6* (Mm00441242_m1)). Q-PCRs were performed on the ABI 7500 Fast system (Applied Biosystems). The 2-ΔΔCt method was used to analyze the relative changes in gene expression.

Aortic ring assay

3 separate experiments were conducted using 3 mice per experiment. C57BL/6 mice, age between 8- 12 weeks, were anesthetized (as described above) and the aorta was dissected and stored in medium. Each aorta was cut in 1 mm rings, and serum-starved in Opti-MEM + Glutamax (Gibco) overnight at 37 °C and 5% CO2. The next day, each ring was mounted in a well of a 96-well plate in 70 µl of 1.0 mg/ml acid-solubilized rat tail collagen I (Millipore) in DMEM. After collagen polymerization (60 min at 37 °C and 5% CO2), Opti-MEM supplemented with 2.5% FCS and 30 ng/ml VEGF (R&D systems) was added with or without DC101 or control antibodies (30 µg/ml). The rings were cultured for 7 days and pictures were taken (Zeiss). The number of sprouts were counted manually.

For immunohistochemistry rings were formalin fixed and permeabilized with 0.2% Triton X-100. Rings were stained with SMCA, CD31 (BD Pharmingen) and MAC3. Z stack images were captured with a LSM700 confocal laser-scanning microscope (Zeiss) and quantified with image J.

Statistical analysis

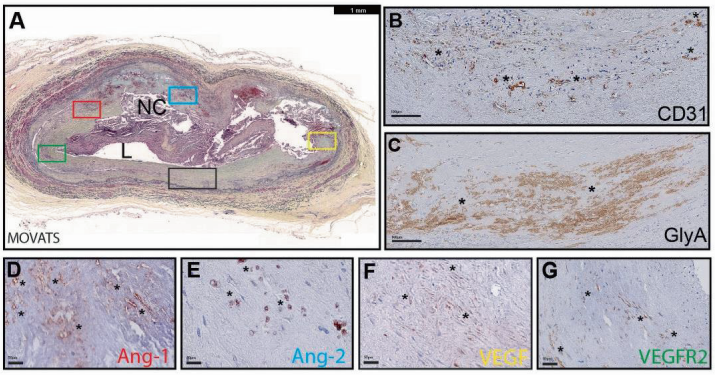
Results are expressed as mean ± SEM. A 2-tailed Student's t-test was used to compare individual groups. Non-Gaussian distributed data were analyzed using a Mann-Whitney U test using

GraphPad Prism version 6.00 for Windows (GraphPad Software). Probability-values <0.05 were regarded significant.

Results

Leaky neovessels in human vein graft and carotid lesions

Both vein graft specimens (Fig 1 panel 1) and carotid atherosclerotic lesions (Fig 1 panel 2) show features of classical atherosclerotic lesions with, foam cells, calcification and necrotic cores. Neovessels were found throughout the lesions in both vein grafts and carotid specimen, with preference for the media and at inflammatory regions around necrotic cores, Fig 1B panel 1&2. Frequently, these neovessels were leaky as demonstrated by the presence of erythrocytes (Glycophorin A expressing cells) outside the neovessels, Fig 1C panel 1&2. Both Ang-1 (Fig 1D panel 1&2) and Ang-2 (Fig 1E panel 1&2) were localized around the neovessels, although not all neovessels were found positive. Most neovessels, also in regions of intraplaque hemorrhage, did express VEGF, Fig 1F panel 1&2. VEGFR2 staining was present around the neovessels but not as strong as VEGF expression, Fig 1G panel 1&2.



Panel 2 Carotid lesion

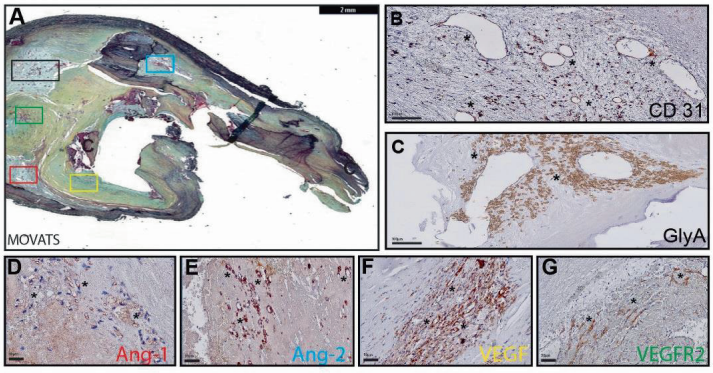


Figure 1. Leaky neovessels in human vein graft and carotid lesions. (A) Human vein grafts (n=12) and (B) carotid plaques (n=12) were stained with Movat's pentachrome for general morphology. (A/B.1) CD31 positive leaky neovessels as revealed by the presence of (A.2/ B.2) glycophorin A (GLyA) positive erythrocytes outside neovessels. (A.3-4, B.3-4) Angiopoietins, Ang-1 and Ang-2, localized around the neovessels as well as VEGF and VEGFR2 (A.5-6, B.5-6). NC, necrotic core. L, Lumen C, Calcification. *neovessels.

Hypoxia drives plaque angiogenesis in vein grafts

In a time-course experiment of murine vein grafts the expression of *Hif1-α* mRNA rapidly and significantly increased in vein grafts at all time points until day 28 (t28), when compared to native caval veins, with the highest level at t7, Fig 2A. *Hif1-α* protein expression was clearly visible at t28, Fig 2B. *Sdf-1* mRNA was significantly up regulated from t7 to t28 when compared to caval veins, Fig 2C. At the latter time point, *Sdf-1* protein expression could be detected especially in SMCs, Fig 2D. Interestingly, while we could not detect an increase of *Vegf-a* mRNA during the time-course, Fig 2E, positive VEGF staining could be seen at t28, especially in plaque neovessels, Fig 2F. *In vivo* we determined hypoxia by injecting the hypoxia probe pimonidazole (n=6). Hypoxia was evident in all layers of the vein graft (t28), especially in macrophages scattered throughout the vein graft, Fig 2G and H.

A histological time course of vein grafts was used to study the timeframe in which the first plaque neovessels appear. From t14 (n=4) the first plaque neovessels were detectable. These neovessels were primarily in the outer region of the vein grafts, suggesting sprouting from the vasa vasorum, Fig 2I. At t28 $CD31^+$ plaque neovessels could be detected throughout all layers of the vein graft (n=4), Fig 2J. The majority of these plaque neovessels have an activated endothelium, demonstrated by the expression of ICAM1 (Fig 2K) and VCAM1, Fig 2L. Up regulation of ICAM1 and VCAM1 can lead to increased interactions with inflammatory cells. Therefore, 28 days old vein grafts were stained with a combination of CD31 and CD163, an exclusive marker for neovessel associated macrophages[15] and CD31 and CD3+T cells. CD163+ macrophages can be abundantly found throughout the vein graft lesion (Fig 2M) but mostly in close proximity of neovessels (Fig 2N). CD3+ T cells are mainly located in the peri-adventitial region of the vein grafts which are highly vascularized (Fig 2O,P).However, CD3+ T cells are not specifically associated with neovessels in other areas within the vein graft lesion (white arrow, Fig 2O).

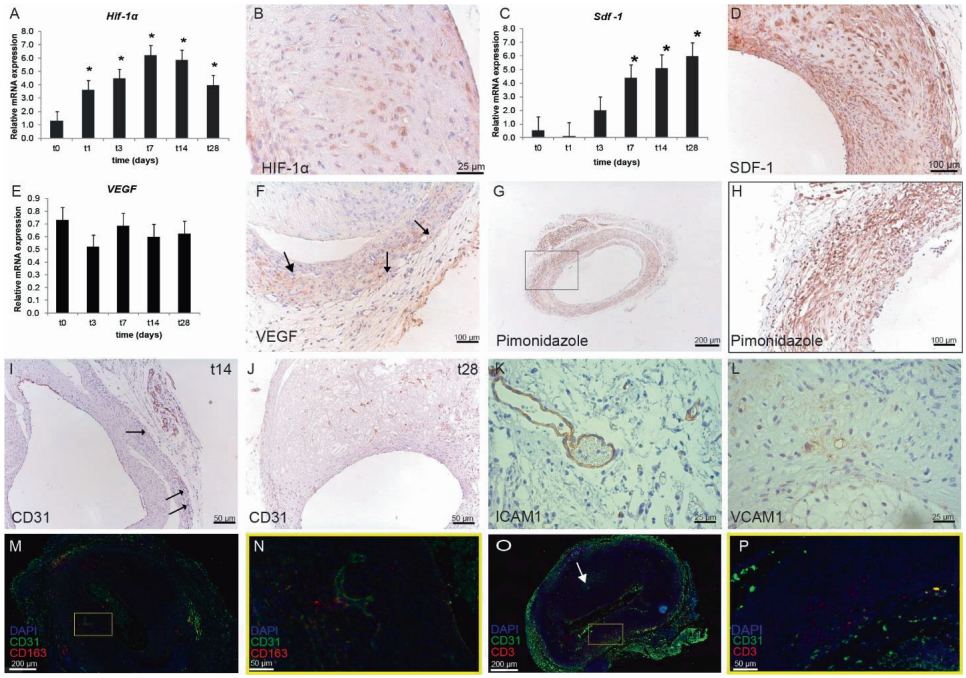


Figure 2. Hypoxia drives plaque angiogenesis. (A) Hypoxia inducible factor (Hif)-1α mRNA regulation over time in vein grafts (t0-t7 n=3, t14 n=4, t28 n=5) in hypercholesterolemic ApoE3*Leiden mice. **(B)** HIF-1α protein is expressed by various cell types in vein grafts (t28). **(C)** Stromal cell-derived factor 1 (Sdf-1) mRNA regulation over time. **(D)** At day 28 SDF-1 is expressed in all layers of the vein graft. **(E)** Vegf mRNA regulation over time. (**F**) VEGF could be seen in neovessels (arrows) in the vessel wall (t28). **(G,H)** Hypoxia (t28) could be detected with pimonidazole throughout the vein graft wall (n=6 mice). **(I)** In a histological time course (n=4 mice/time point) neovessels expressing CD31 could be detected from day 14 (t14) onwards. **(J)** At t28 neovessels could be detected throughout the entire vessel wall. Plaque neovessels show activation by expression of Intercellular Adhesion Molecule 1 (ICAM1) **(K)** and Vascular Cell Adhesion Molecule 1 (VCAM1) **(L)**. CD163+ macrophages are found throughout the t28 vein graft lesion **(M)** and are clearly associated with neovessels **(N)**. CD3+ T cells are found in the peri-adventitial region of the vein grafts but not so much in other regions (white arrow) associated with neovessels **(O,P)** * p<0.05

Perivascular VEGF increases plaque neovessel density

To examine whether in the vein graft model we could target plaque angiogenesis we applied, a pluronic gel containing 250 ng VEGF in the perivascular region of the vein grafts, directly after surgery. Local treatment with VEGF did not affect cholesterol levels or bodyweight, S1A and B. After 28 days, we observed an increase in the number of neovessels in the VEGF treated group compared to controls, Fig 3A. Quantification of the plaque neovessel density per section revealed a significant 60% increase in neovessels in the VEGF group (p=0.014), Fig 3B. However, local

application of VEGF did not result in a significant effect on the vessel wall area (p= 0.628), Fig 3C. Both in the control group as well as in the VEGF treated group 1 out of 6 mice intraplaque hemorrhage was observed.

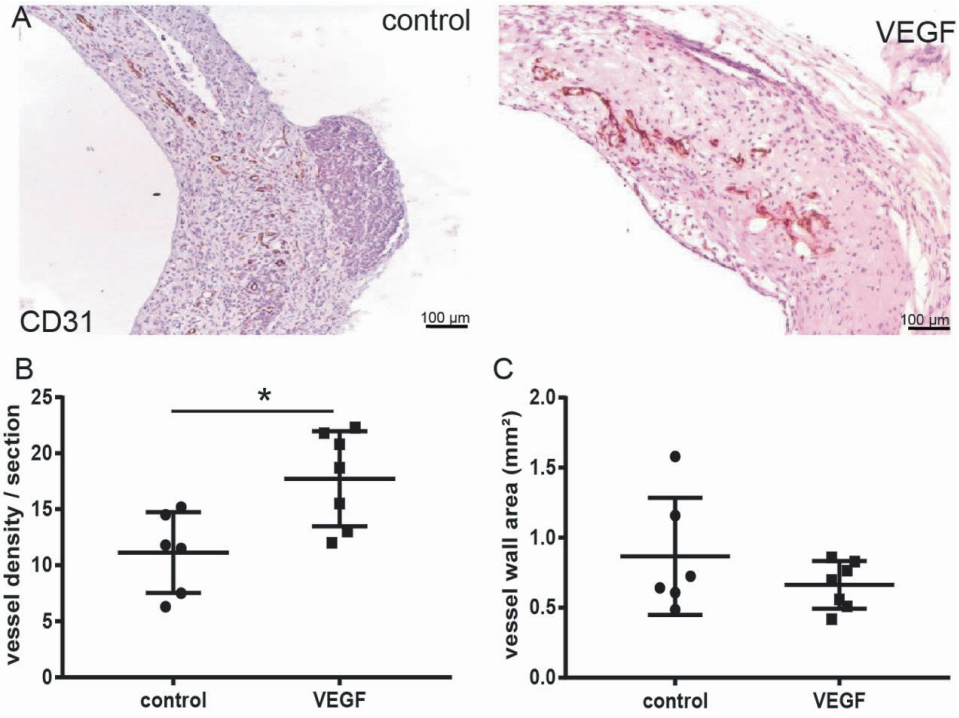


Figure 3. Perivascular VEGF increases plaque angiogenesis. VEGF was applied in pluronic gel (n=7) or pluronic gel alone (n=6) topically on the vein in ApoE3*Leiden mice. **(A)** CD31 staining of plaque neovessels in the control group (n=6) and VEGF group (n=7). **(B)** Quantification of the neovessel density at day 28 **(C)** Quantification of the vessel wall area. * p<0.05

Angiopoietin expression is augmented in intraplaque hemorrhage regions

Neovessels associated with intraplaque hemorrhage are characterized by reduced pericyte coverage. Mature neovessels are covered by SMC actin positive pericytes, Fig 4A. In regions of intraplaque hemorrhage (characterized by perivascular erythrocytes) neovessels were partly devoid of pericyte coverage, Fig 4B. Tie2, the main receptor of the angiopoietins was found to be specifically expressed by endothelial cells of plaque neovessels. The expression of Tie2 did not

differ between mature neovessels (Fig 4C) or neovessels associated with intraplaque hemorrhage, Fig 4D. Increased staining of both Ang-1 and Ang-2 could be observed in areas of intraplaque hemorrhage. Ang-1 was predominantly expressed in intraplaque hemorrhage regions whereas no staining around mature neovessels could be observed, Fig 4E. Ang-2 showed increased expression in lesions with intraplaque hemorrhage in contrast to regions of the lesions without intraplaque hemorrhage, Fig 4F.

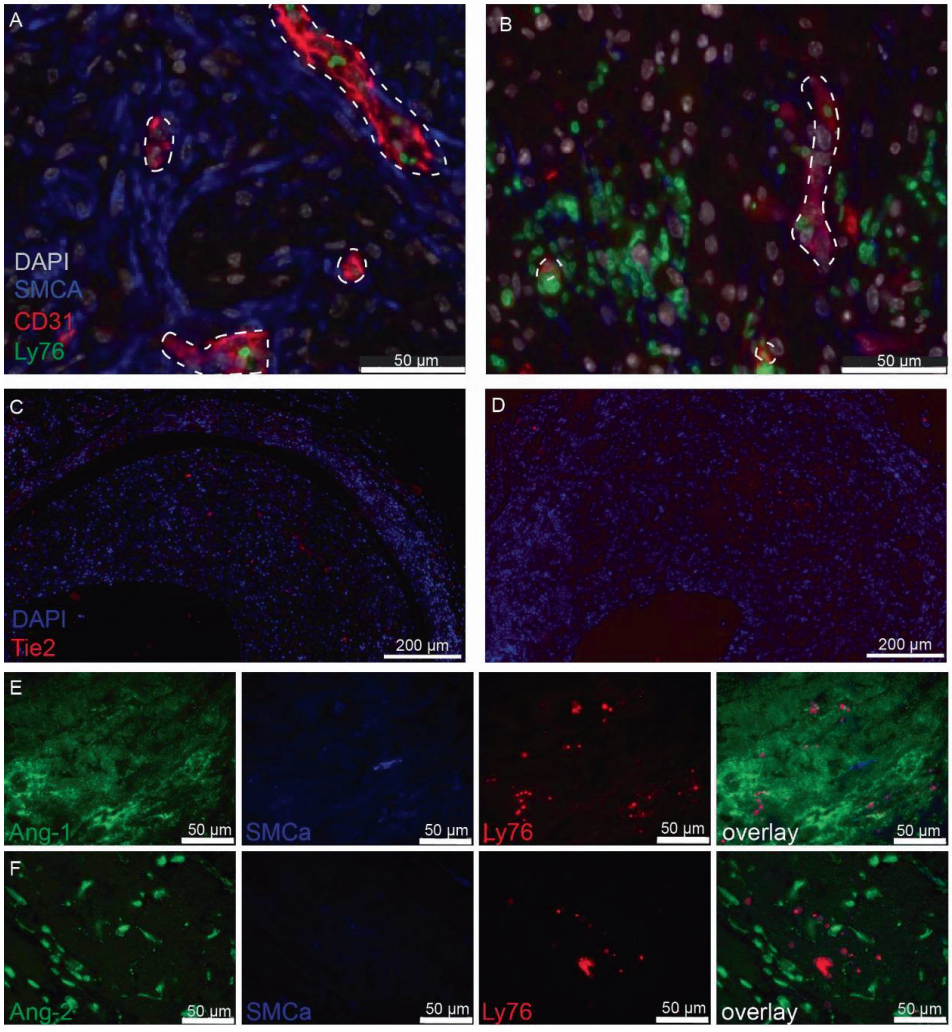


Figure 4. Angiopoietins-Tie2 expression in regions of intraplaque hemorrhage. (A) Staining of smooth muscle cell actin (SMCA), endothelial cells (CD31) and erythrocytes (Ly76) in plaque neovessels (dashed white lining) in lesion without (left panel) and with (right panel) intraplaque hemorrhage (IPH). **(B)** Staining of Tie2 in lesion without (left panel) and with (right panel) IPH. **(C)** Single staining's and overlay of Angiopoietin (Ang)-1 (Ang-1), SMCA and Ly76 in regions of IPH. **(D)** Single staining's and overlay of Ang-2, SMCA and Ly76 in regions of IPH.

VEGFR2 blocking antibodies inhibit intraplaque hemorrhage and erythrocyte extravasation

To interfere in the process of vessel integrity, we treated ApoE3*Leiden receiving a vein graft with the VEGFR2 blocking antibody (DC101). Treatment with DC101 did not change cholesterol levels or bodyweight in comparison to the control group, S1C and D. Intraplaque hemorrhage was less frequently observed in mice treated with DC101 (7 out of 14 mice, 50%) in comparison to control animals (10 out of 12 mice, 83%). In the DC101 group a smaller segment of the vein grafts (242 µm, 26% of the vein graft length) was affected by intraplaque hemorrhage in comparison to the control group (620 µm, 59% of the vein graft length, p=0.037), Fig 5A. In addition, 80% less extravasated erythrocytes were observed in the DC101 group than in the control group (p=0.049), Fig 5B. These extravasated erythrocytes were predominantly observed in the regions near the adventitia and in the mid-portion of the vein graft lesions, Fig 5B.

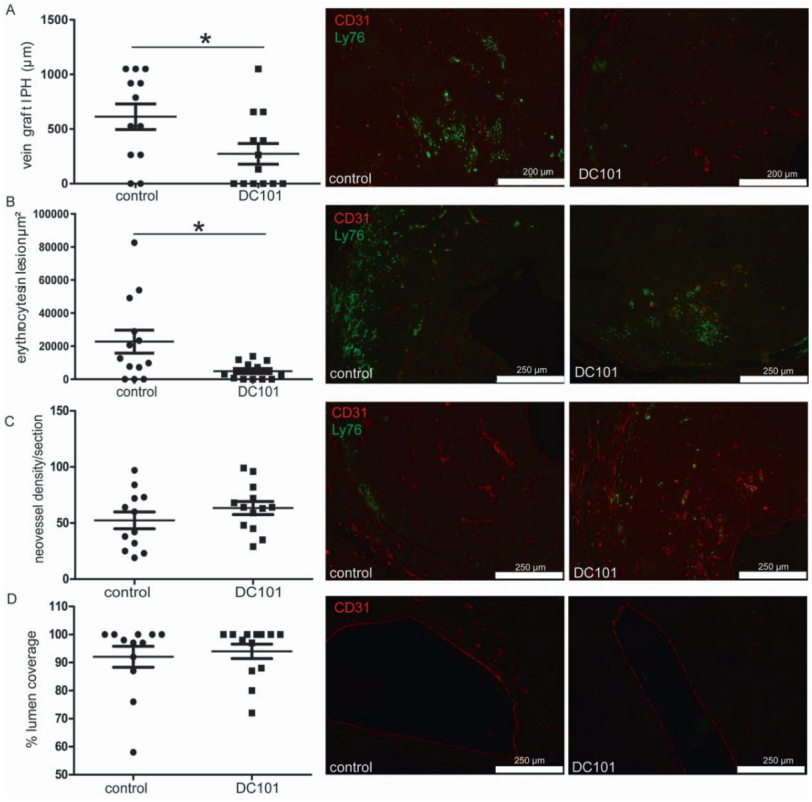


Figure 5. Intraplaque hemorrhage and erythrocyte extravasation after VEGFR2 blockade. Vein grafts in hypercholesterolemic ApoE3*L mice treated with control IgG antibodies (10 mg/kg) n=12 and VEGFR2 blocking antibodies (DC101, 10 mg/kg) n=14, 28 days after surgery **(A)** Quantification of the vein graft length that displayed intraplaque hemorrhage. Representative examples of lesions with intraplaque hemorrhage. **(B)** Quantification of the area of the extravasated erythrocytes and representative images of lesions with extravasated erythrocytes. **(C)** Quantification of the density of neovessels in vein grafts expressed as the number of neovessel per section (10-12 sections/mouse) **(D)**. Quantification of endothelial cell coverage of the lumen expressed as % coverage. * $p<0.05$, L = lumen.

Neovessel density is not reduced by VEGFR2 blocking antibodies in vivo

The anti-angiogenic effect of suppression of VEGF-signaling *in vivo* was analyzed by quantifying the neovessel density in the vein graft lesions. In the DC101 group an average of 63±25 neovessels per vein graft section was observed, whereas in the control IgG treated group 52±19 neovessels per vein graft section were found (p=0.327), Fig 5C. The vein graft model is characterized by denudation of the luminal endothelium in the early days after engraftment, which is restored later in time[5]. Both in the DC101 group and the control group the endothelium was completely restored at 28 days after surgery (p=0.639), Fig 5D.

DC101 prevents vein graft thickening and results in a more stable lesion composition

VEGFR2 blockade resulted in a reduction of the lesion size compared to the control group, Fig 6A. Quantification of these lesions showed that the DC101 treated group had a significant reduction of 32% in vein graft thickening compared to the control IgG treated group (p=0.044), Fig 6A. A decrease in outward remodeling as measured by the total vessel area, was detected in the DC101 treated group (33%, p=0.05), S2A. The luminal area however, was not significantly affected by DC101 treatment (p=0.369), S2B. Next, the effect of DC101 treatment on vein graft lesion composition was assessed. In the DC101 group an increased collagen content was observed in comparison to the control group (46%, p=0.066), S2C. When corrected for the differences in vein graft thickening, the relative percentage of collagen was significantly increased in the DC101 treated group (54% p=0.047), Fig 6B. In addition, a substantial increase in the SMCA area was observed (118% p=0.003) in the DC101 group as well as a significant increase in the percentage of SMCA (123% p=0.0005), Fig 6C and S2D. Plaque macrophages were significantly reduced after DC101 treatment with 30% (p=0.001), Fig 6D whereas, the total macrophage area was reduced by 42% (p=0.018), S2E.

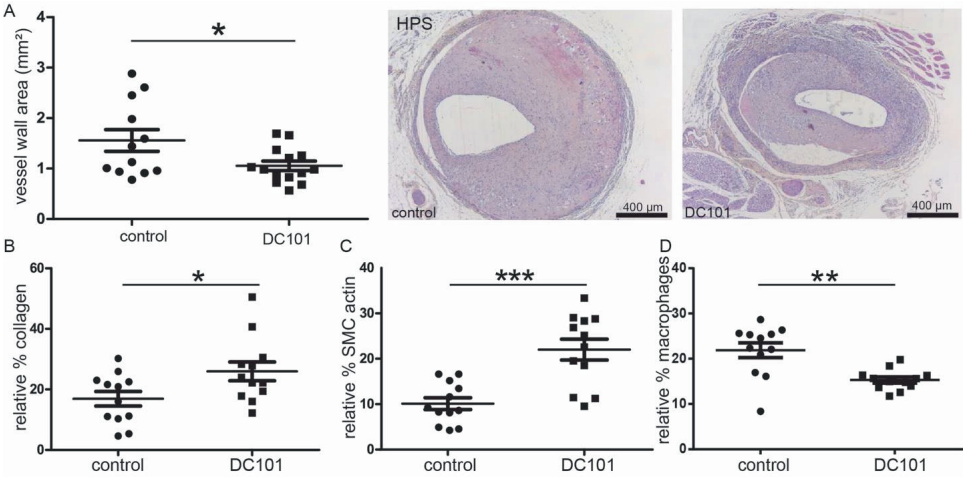


Figure 6. Quantitative measurements of vein graft area and lesion composition. (**A**) Quantitative measurements of vein graft thickening and representative cross-sections of vein
grafts in hypercholesterolemic ApoE3*L mice treated with control IgG antibodies (10 mg/kg) n=12 and VEGFR2 blocking antibodies (DC101, 10 mg/kg) n=14, 28 days after surgery (Hematoxilin-Phloxine-Saffron staining). **(B)** relative percentage collagen, **(C)** relative percentage smooth muscle cell actin, **(D)** relative percentage macrophages. * p<0.05, **p<0.01, ***p<0.005.

VEGFR2 blockade stimulates expression of genes associated with a more mature neovessel phenotype

To investigate the local inflammatory response, we measured the gene expression levels of pro-inflammatory genes *Ccl2, Il6* and *Icam1* in the vein grafts; No differences in expression levels could be detected between the groups, Fig 7A-C. Also, the expression of VEGF/VEGFR mRNA in the vein graft wall was analyzed. Interestingly, the expression of both *Vegfa* (Fig 7D) and *Vegfr1* (Fig 7E) was significantly reduced upon DC101 treatment (24% (p=0.014) and 32% (p=0.048) respectively) whereas, the expression of *Vegfr2* was not affected, Fig 7F. Furthermore, the angiopoietin receptor *Tie2* (Fig 7G) was not differently expressed between the groups, nor was the vessel stabilizing factor *Ang1*, Fig 7H. The vessel destabilizing factor *Ang2* was significantly decreased (p=0.039) after DC101 treatment, Fig 7I. As a measure for proper endothelial function, we measured Connexin (*Cx*43, *Cx37* and *Cx40*) expression. DC101 treatment showed no effect on *Cx43* (Fig 7J) and *Cx37* (Fig 7K) expression levels but remarkably, significantly increased (p=0.047) levels of *Cx40* were observed pointing towards increased inter-endothelial cell connections, Fig 7L.

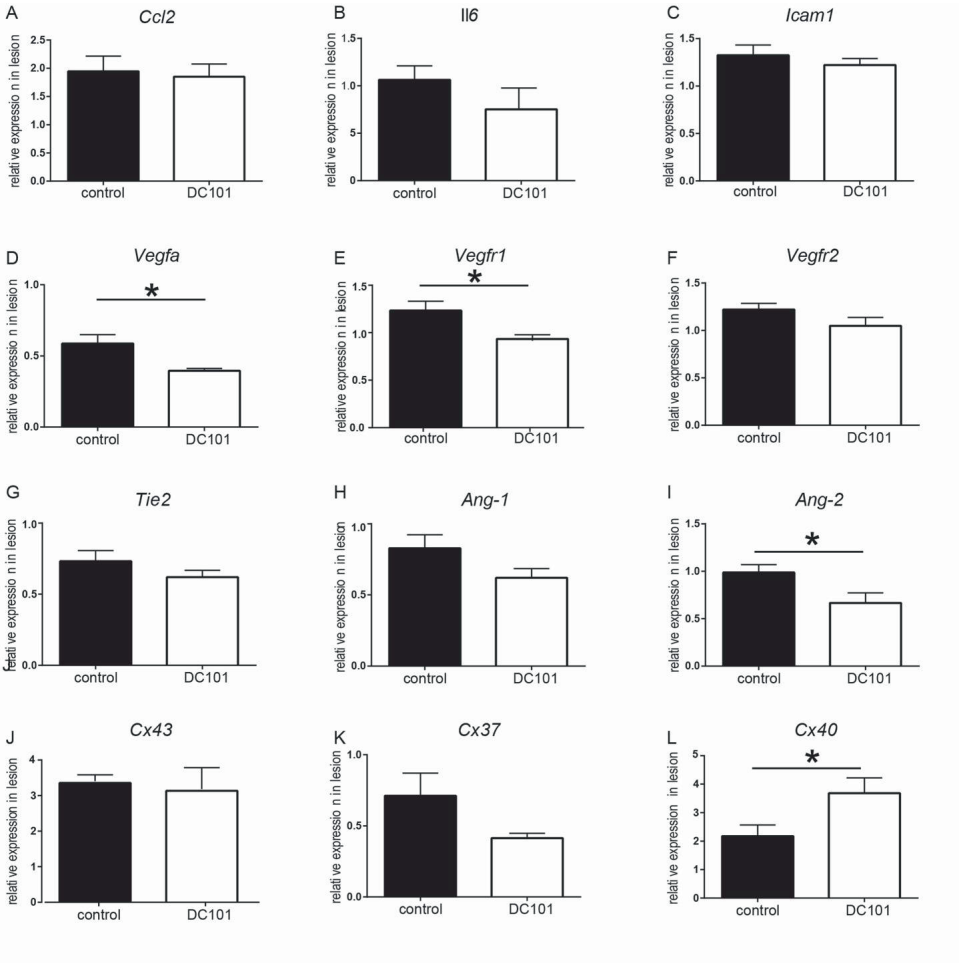


Figure 7. Gene expression in vein grafts. Total wall gene expression was measured in vein grafts of control and VEGFR2 blocking antibodies treated mice (n=6/group). **(A)** Inflammation associated genes. **((B)** VEGF and VEGF receptor genes. **(C)** Tie2 and angiopoietins. **(D)** Connexins. *p<0.05.

VEGFR2 blocking antibodies induce concentration dependent vessel maturation

The effects of VEGFR2 blockade on vessel maturation was further studied in an aortic ring assay. Of the 2 concentrations DC101(10 and 30 µg/ml) tested, only the highest concentration resulted

in a significant reduction (66% p=0.003) of sprout formation when compared to no treatment, Fig 8A. The pericyte coverage of the sprout in the 30 µg/ml DC101 group was not significantly different than the control. Interestingly, the 10 µg/ml DC101 concentration induced a significant increase in SMCA$^+$ pericyte coverage of the CD31$^+$ sprouts (20%, p=0.005), Fig 8B and C.

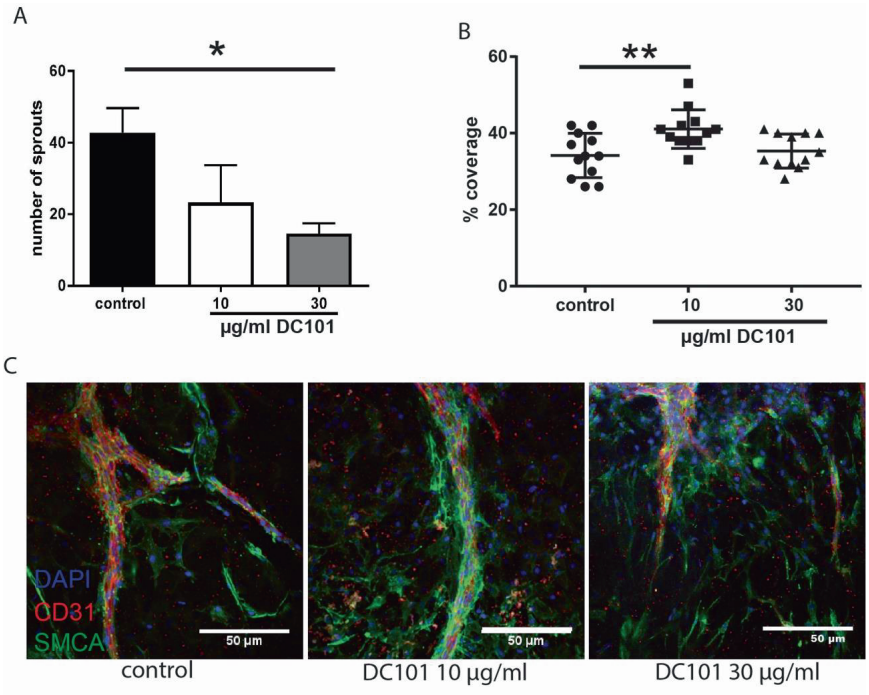


Figure 8. VEGFR2 blockade in aortic ring assay. Representative experiment of 3 separate experiments using 3 mice/condition and 4 rings per mouse. Quantification of the number of sprouts **(A)** and the % coverage of SMCs over the CD31$^+$ sprouts **(B)**. **(C)** Typical examples of sprouts in the control and DC101 treated groups. * p<0.05, ** p<0.01.

Discussion

Immature intraplaque neovessels have been characterized as the main contributors to intraplaque hemorrhage. Intraplaque hemorrhage occurs in native atherosclerosis but also in accelerated atherosclerosis after vein grafting or stenting[4]. However, most of the evidence is descriptive in nature [9, 13]. In the present study, we used an intervention to show that VEGFR2 blockade reduces intraplaque hemorrhage and increases plaque stability by enhancing neovessels maturation in vein graft atherosclerosis.

We observed that neovessels in human carotid and vein graft specimen are associated with VEGF/VEGFR2 and angiopoietins. In both types of atherosclerotic lesions numerous regions with intraplaque hemorrhage and leaky vessels were observed. We demonstrated that plaque neovessels in the vein grafts originate primarily from the adventitia, This is also the general idea for native atherosclerotic lesion however, luminal angiogenesis cannot be excluded [1]. VEGFR2 is involved in this process as the main receptor. VEGFR2 is involved in tip-cell-stalk-cell differentiation in the early phase of angiogenesis and mediates the permeability enhancing effects of VEGF in adult endothelial cells as well as neovessel maturation [16]. We have previously shown that the majority of plaque neovessels in vein grafts express a basement membrane and that pericytes coverage is heterogeneous [23]. Here we demonstrate that incomplete pericyte coverage of murine plaque neovessels is angiopoietin related. Incomplete pericyte coverage in regions of intraplaque hemorrhage is also observed in human instable atherosclerotic plaques [11].

A modest induction in Vegf mRNA expression between 3 and 7 days but no further regulation between other time points was observed. Interestingly, Hamdan et al. showed comparable absent induction of Vegf mRNA in a canine vein graft model between native vein and 4 weeks after surgery, but did see a significant induction after 48 hours [27]. It seems that Vegf mRNA expression is only induced for a short period and is not the main driver of the remodeling response after vein graft surgery. This early induction of Vegf mRNA expression can be a result of the hypoxic period during surgery.

Atherosclerotic plaque angiogenesis can be manipulated as we show here by intervening in the VEGF pathway: locally applied VEGF enhanced neovessel density. We found that low

concentration of VEGFR2 blocking antibodies induced pericyte coverage in the aortic ring assay. This is comparable to the observation of increased pericyte coverage in murine and human tumors after VEGF signal blockade [28]. Blockade of VEGFR2 has been shown to facilitate the recruitment of pericytes to tumor vessels by enhancing Ang-1 expression and increasing perivascular matrix metalloproteases activity [29]. Ang-1 decreases endothelial cell permeability and increases vascular stabilization via enhancing endothelial cell interactions with the surrounding matrix and recruitment of pericytes to growing blood vessels. Ang-2 functions as a competitive Ang-1 antagonist in a VEGF-depend manner and mediates angiogenic sprouting and vascular regression [19]. This concurs with our finding that in regions of intraplaque hemorrhage the expression of both Ang-1 and Ang-2 is increased. VEGFR2 blockade by DC101 treatment reduced intraplaque hemorrhage, reduced *Ang-2* expression, and improving gap junctions as shown by the increased *Cx40* expression, pointing towards more mature neovessels. Post *et al*. showed that in plaques with high neovessel density, the local balance between Ang-1 and Ang-2 is in favor of Ang-2 [30]. Unfortunately, vascular maturation and intraplaque hemorrhage was not studied in this context.

Recently, it was shown that treatment with axitinib (inhibitor of VEGFR1,2, and 3) attenuated plaque angiogenesis [31]. Treating vein grafts with VEGFR2 blocking antibodies *in vivo* did not result in a reduction of neovessel density in comparison to control IgG treated animals. Interestingly in a model for breast cancer, tumor vascular density was also not affected with this dose (10 mg/kg DC101) but was significant decreased with a four times higher dose [32]. Furthermore, these authors observed that low dose but not high dose VEGFR2 blocking antibodies treatment resulted in improved vascular maturation. In the aortic ring assay, we observed that the high dose DC101 resulted in reduced sprouting whereas the low dose did not reduce sprouting but did increased pericyte coverage.

VEGF is known to induce re-endothelialization and has been shown to inhibit intimal hyperplasia after vascular injury [33]. Application of VEGF directly after surgery in a rabbit vein graft model showed attenuation of the vessel wall size [34]. We show that local delivery of VEGF directly after surgery results in a non-significant trend towards reduction of intimal hyperplasia. Whereas, blockade of VEGFR2 resulted in significant attenuation of lesion growth. In the VEGFR2 blockade

experiment, treatment with DC101 was started at day 14 after surgery to specifically study the effects on plaque neovessel formation which starts from this time point on as demonstrated in Fig 2I. An important mechanism of action of VEGF is enhancing the re-endothelialtization of the luminal endothelium which occurs primarily in the early period after surgery [35]. The late treatment with DC101 does not interfere with the re-endothelialization process. This was confirmed by the observation that at sacrifice (t=28 days) both the control and DC101 group showed full luminal endothelial coverage. Vein graft lesion formation is largely driven by inflammation [36]. The positive effect of VEGFR2 blockade on this process most likely overrules the VEGF induced attenuation of lesion growth.

It has been shown that VEGFR2 activation can activate and degrade VE-cadherin resulting in vascular permeability [37]. Guo et al showed that CD163+ macrophages promote endothelial permeability via VEGF/VEGFR2 interaction with VE-cadherin [15]. These CD163+ macrophages are clearly present, localized in areas of plaque neovascularization, in the murine vein grafts (Fig 2). Blockade of VEGFR2 could reverse the VE-cadherin induced vascular permeability and induce the observed plaque neovessel maturation and reduced intraplaque hemorrhage.

Phagocytosis of intraplaque erythrocytes and erythrocyte–derived cholesterol by macrophages results in lipid core and plaque expansion, and promotion of plaque instability [12, 38]. Systematic VEGFR2 blockade led to a reduction of intraplaque hemorrhage, lesion size and a reduction in lesion macrophages. Binding of VEGF to VEGFR2 can result in NF-κB induced activation of VCAM-1 and ICAM-1 leading to increased adherence of leukocytes [39]. In various experimental models, inhibition of vascular leakage and NF-κB dependent macrophage influx by DC101 was demonstrated [40, 41]. Although at t28 no effect on inflammatory gene expression could be seen in the vein grafts, blockade of the binding of VEGF to VEGFR2 inhibited macrophage influx and subsequent effects on plaque composition including increased collagen and smooth muscle cell content. The NF-κB signaling cascade is an obvious route, since NF-κB induced inflammation has been previously reported to be a critical pathway to stimulate macrophage influx and plaque instability in vein grafts [24, 36, 42].

In this study we used a vein graft model in hypercholesterolemic mice to study the role of plaque neovessel maturation. This model shows large atherosclerotic lesions with abundant plaque

angiogenesis [23]. Vein graft atherosclerosis differs from native atherosclerosis since the onset (surgery) is acute with endothelial denudation and hypoxia resulting in the accelerated form. The lesions formed are concentric and highly dispersed with inflammatory cells and foam cells [36]. Local processes regarding plaque neovessel maturation in vein grafts show high similarities with native atherosclerosis as demonstrated in figure 1. The findings in this study can be, with cause, extrapolated to other cardiovascular diseases.

In summary, VEGFR2 blocking antibodies inhibit intraplaque hemorrhage and erythrocyte extravasation, resulting in more stable plaque neovascularization, decreased lesion development and increased plaque stabilization in a vein graft model, due to maturation of the plaque neovessels. Our study indicates that vascular maturation (and more specifically VEGFR2) stands as an attractive target to stabilize atherosclerotic (vein graft) disease.

References

[1] de Vries MR, Quax PH. Plaque angiogenesis and its relation to inflammation and atherosclerotic plaque destabilization. *Current opinion in lipidology* 2016; **27**:499-506.
[2] Derksen WJ, Peeters W, van Lammeren GW *et al.* Different stages of intraplaque hemorrhage are associated with different plaque phenotypes: a large histopathological study in 794 carotid and 276 femoral endarterectomy specimens. *Atherosclerosis* 2011; **218**:369-377.
[3] Taqueti VR, Di Carli MF, Jerosch-Herold M *et al.* Increased microvascularization and vessel permeability associate with active inflammation in human atheromata. *Circ. Cardiovasc. Imaging* 2014; **7**:920-929.
[4] Yahagi K, Kolodgie FD, Otsuka F *et al.* Pathophysiology of native coronary, vein graft, and in-stent atherosclerosis. *Nature reviews. Cardiology* 2016**13**:79-98.
[5] de Vries MR, Simons KH, Jukema JW *et al.* Vein graft failure: from pathophysiology to clinical outcomes. *Nature reviews. Cardiology* 2016; **13**:451-470.
[6] Parma L, Baganha F, Quax PHA, de Vries MR. Plaque angiogenesis and intraplaque hemorrhage in atherosclerosis. *European journal of pharmacology* 2017;**5**:107-115.
[7] Lee ES, Bauer GE, Caldwell MP, Santilli SM. Association of artery wall hypoxia and cellular proliferation at a vascular anastomosis. *The Journal of surgical research* 2000; *91*:32-37.
[8] Wan J, Lata C, Santilli A *et al.* Supplemental oxygen reverses hypoxia-induced smooth muscle cell proliferation by modulating HIF-alpha and VEGF levels in a rabbit arteriovenous fistula model. *Annals of vascular surgery* 2014; **28**:725-736.
[9] Sluimer JC, Gasc JM, van Wanroij JL *et al.* Hypoxia, hypoxia-inducible transcription factor, and macrophages in human atherosclerotic plaques are correlated with intraplaque angiogenesis. *J. Am. Coll. Cardiol* 2008; **51**:1258-1265.
[10] Vazao H, Rosa S, Barata T *et al.* High-throughput identification of small molecules that affect human embryonic vascular development. *Proceedings of the National Academy of Sciences of the United States of America* 2017; **114**:E3022-e3031.
[11] Sluimer JC, Kolodgie FD, Bijnens AP *et al.* Thin-walled microvessels in human coronary atherosclerotic plaques show incomplete endothelial junctions relevance of compromised structural integrity for intraplaque microvascular leakage. *J. Am. Coll. Cardiol* 2009; **53**:1517-1527.
[12] Virmani R, Kolodgie FD, Burke AP *et al.* Atherosclerotic plaque progression and vulnerability to rupture: angiogenesis as a source of intraplaque hemorrhage. *Arterioscler. Thromb. Vasc. Biol* 2005; **25**:2054-2061.
[13] Michel JB, Virmani R, Arbustini E, Pasterkamp G. Intraplaque haemorrhages as the trigger of plaque vulnerability. Eur. Heart J 2011;**32**:1977-1985.
[14] Finn AV, Nakano M, Narula J *et al.* Concept of vulnerable/unstable plaque. *Arterioscler. Thromb. Vasc. Biol* 2010; **30**:1282-1292.
[15] Guo L, Akahori H, Harari E *et al.* CD163+ macrophages promote angiogenesis and vascular permeability accompanied by inflammation in atherosclerosis. *The Journal of clinical investigatio*n 2018; **128**:1106-1124.
[16] Carmeliet P, Jain RK. Molecular mechanisms and clinical applications of angiogenesis. *Nature* 2011; **473**:298-307.
[17] Huang Y, Goel S, Duda DG *et al.* Vascular normalization as an emerging strategy to enhance cancer immunotherapy. *Cancer research* 2013; **73**:2943-2948.
[18] Jain RK. Molecular regulation of vessel maturation. *Nat. Med* 2003; **9**:685-693.
[19] Jain RK. Antiangiogenesis strategies revisited: from starving tumors to alleviating hypoxia. *Cancer Cell* 2014; **26**:605-622.
[20] Moulton KS, Heller E, Konerding MA *et al.* Angiogenesis inhibitors endostatin or TNP-470 reduce intimal neovascularization and plaque growth in apolipoprotein E-deficient mice. *Circulation* 1999; **99**:1726-1732.
[21] Lucerna M, Zernecke A, de NR *et al.* Vascular endothelial growth factor-A induces plaque expansion in ApoE knock-out mice by promoting de novo leukocyte recruitment. *Blood* 2007; **109**:122-129.
[22] Xu X, Mao W, Chai Y *et al.* Angiogenesis Inhibitor, Endostar, Prevents Vasa Vasorum Neovascularization in a Swine Atherosclerosis Model. *Journal of atherosclerosis and thrombosis* 2015; **22**:1100-1112.
[23] de Vries MR, Niessen HW, Lowik CW *et al.* Plaque rupture complications in murine atherosclerotic vein grafts can be prevented by TIMP-1 overexpression. *PLoS. One* 2012; **7**:e47134.

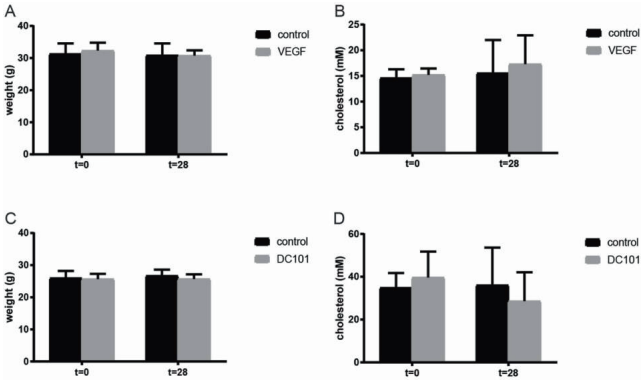
[24] Wezel A, de Vries MR, Maassen JM *et al.* Deficiency of the TLR4 analogue RP105 aggravates vein graft disease by inducing a pro-inflammatory response. *Scientific reports* 2016; **6**:24248.
[25] Witte L, Hicklin DJ, Zhu Z *et al.* Monoclonal antibodies targeting the VEGF receptor-2 (Flk1/KDR) as an anti-angiogenic therapeutic strategy. *Cancer Metastasis Rev* 1998; **17**:155-161.
[26] Eefting D, Bot I, de Vries MR *et al.* Local lentiviral short hairpin RNA silencing of CCR2 inhibits vein graft thickening in hypercholesterolemic apolipoprotein E3-Leiden mice. *J. Vasc. Surg* 2009; **50**:152-160.
[27] Hamdan AD, Aiello LP, Misare BD *et al.* Vascular endothelial growth factor expression in canine peripheral vein bypass grafts. *Journal of vascular surgery* 1997; **26**:79-86.
[28] Falcon BL, Chintharlapalli S, Uhlik MT, Pytowski B. Antagonist antibodies to vascular endothelial growth factor receptor 2 (VEGFR-2) as anti-angiogenic agents. *Pharmacology & therapeutics* 2016; **164**:204-225.
[29] Winkler F, Kozin SV, Tong RT *et al.* Kinetics of vascular normalization by VEGFR2 blockade governs brain tumor response to radiation: role of oxygenation, angiopoietin-1, and matrix metalloproteinases. *Cancer Cell* 2004; *6*:553-563.
[30] Post S, Peeters W, Busser E *et al.* Balance between angiopoietin-1 and angiopoietin-2 is in favor of angiopoietin-2 in atherosclerotic plaques with high microvessel density. J. Vasc. Res 2008; 45:244-250.
[31] Van der Veken B, De Meyer GRY, Martinet W. Axitinib attenuates intraplaque angiogenesis, haemorrhages and plaque destabilization in mice. *Vascular pharmacology* 2018; **100**:34-40.
[32] Huang Y, Yuan J, Righi E *et al.* Vascular normalizing doses of antiangiogenic treatment reprogram the immunosuppressive tumor microenvironment and enhance immunotherapy. *Proceedings of the National Academy of Sciences of the United States of America* 2012; **109**:17561-17566.
[33] Asahara T, Bauters C, Pastore C *et al.* Local delivery of vascular endothelial growth factor accelerates reendothelialization and attenuates intimal hyperplasia in balloon-injured rat carotid artery. *Circulation* 1995; **91**:2793-2801.
[34] Luo Z, Asahara T, Tsurumi Y *et al.* Reduction of vein graft intimal hyperplasia and preservation of endothelium-dependent relaxation by topical vascular endothelial growth factor. *J. Vasc. Surg* 1998; **27**:167-173.
[35] Lardenoye JH, de Vries MR, Lowik CW *et al.* Accelerated atherosclerosis and calcification in vein grafts: a study in APOE*3 Leiden transgenic mice. Circ. Res 2002; 91:577-584.
[36] de Vries MR, Quax PHA. Inflammation in Vein Graft Disease. *Frontiers in cardiovascular medicine* 2018; **5**:3.
[37] Bates DO. Vascular endothelial growth factors and vascular permeability. *Cardiovascular research* 2010; **87**:262-271.
[38] Kockx MM, Cromheeke KM, Knaapen MW *et al.* Phagocytosis and macrophage activation associated with hemorrhagic microvessels in human atherosclerosis. *Arterioscler. Thromb. Vasc. Biol* 2003; **23**:440-446.
[39] Kim I, Moon SO, Kim SH *et al.* Vascular endothelial growth factor expression of intercellular adhesion molecule 1 (ICAM-1), vascular cell adhesion molecule 1 (VCAM-1), and E-selectin through nuclear factor-kappa B activation in endothelial cells. *The Journal of biological chemistry* 2001; **276**:7614-7620.
[40] Watanabe H, Mamelak AJ, Wang B *et al.* Anti-vascular endothelial growth factor receptor-2 (Flk-1/KDR) antibody suppresses contact hypersensitivity. *Experimental dermatology* 2004; **13**:671-681.
[41] Barbay V, Houssari M, Mekki M *et al.* Role of M2-like macrophage recruitment during angiogenic growth factor therapy. *Angiogenesis* 2015; **18**:191-200.
[42] Karper JC, de Vries MR, van den Brand BT *et al.* Toll-like receptor 4 is involved in human and mouse vein graft remodeling, and local gene silencing reduces vein graft disease in hypercholesterolemic APOE*3Leiden mice. *Arterioscler. Thromb. Vasc. Biol* 2011; **31**:1033-1040.

Supplemental material

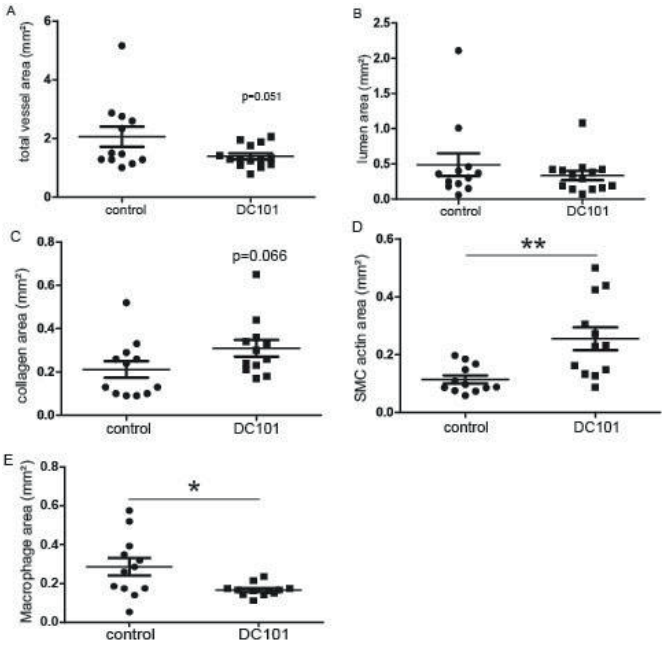
STable 1. **Patient characteristics saphenous vein grafts**

Age	Sex	% stenosis	%stenosis bypass	Stage	Smoker	Diabetes I	Diabetes II	HLP	Previous MI	Heart Failure	CAD	Renal failure	Hypertension
58	male	60	30	Intermediate	no	no	no	no	yes	no	yes	no	yes
54	male	80-90	80	Late	no	no	no	no	no	no	no	no	no
37	male	60	75	Late	no	no	no	no	no	no	no	no	no
58	male	60	75	Late	no	no	no	no	no	no	no	no	no
92	male	40	40	Intermediate	no	no	no	no	no	no	yes	no	no
76	male	70	70	Late	no	no	no	no	no	no	yes	no	no
62	male	50	70	Late	no	no	yes	yes	no	no	yes	no	yes
62	male	50	25	Early	yes	no	no	no	no	no	yes	no	yes
62	male	80	70	Late	yes	no	no	no	no	no	yes	no	yes
70	female	60	40	Intermediate	no	no	no	no	no	no	no	no	no
70	female	30	30	Early	no	no	no	no	no	no	no	no	no
76	male	70	35	Intermediate	no	no	no	no	no	no	no	no	no

Abbreviations: HLP – hyperlipoproteinemia; MI – myocardial infarction; CAD – coronary artery disease. I n red photographs in figure 1, panel 1.



S1. **Bodyweight and cholesterol levels**. (**A**). Bodyweight before (t=0) and 28 days after surgery (t=28) of VEGF treated and control mice. (**B**). Plasma cholesterol levels before (t=0) and 28 days after surgery (t=28) of VEGF treated and control mice. (**C**). Bodyweight before (t=0) and 28 days after surgery (t=28) of VEGFR2 blocking antibodies (DC101) treated and control mice. (**D**). Plasma cholesterol levels before (t=0) and 28 days after surgery (t=28) of DC101 treated and control mice.



S2. **Vein graft morphometry**. Quantitative measurements of vein graft area and lesion composition in vein grafts in hypercholesterolemic ApoE3*L mice treated with control IgG antibodies (10 mg/kg) n=12 and VEGFR2 blocking antibodies (DC101, 10 mg/kg) n=14, 28 days after surgery. Quantitative measurements of (A) total vessel area, (B) luminal area, (C) collagen area, (D) smooth muscle cell (SMCA) area, (E)macrophage content. * p<0.05, **p<0.01.

CHAPTER 5

bFGF BLOCKADE REDUCES INTRAPLAQUE ANGIOGENESIS AND MACROPHAGE INFILTRATION IN ATHEROSCLEROTIC VEIN GRAFT LESIONS IN APOE3*LEIDEN MICE

L Parma[1,2], HAB Peters[1,2], TJ Sluiter[1,2], KH Simons[1,2], P Lazzari[3], MR de Vries[1,2], PHA Quax[1,2]

[1]Department of surgery; [2]Einthoven laboratory for experimental vascular medicine, Leiden University Medical center, Leiden, The Netherlands; [3]KemoTech SrL, Build 3, Loc. Piscinamanna, 09010 Pula, Italy

Manuscript under review

Abstract

Intraplaque angiogenesis increases the chance of unstable atherosclerotic plaque rupture and thrombus formation leading to myocardial infarction. Basic Fibroblast Growth Factor (bFGF) plays a key role in angiogenesis and inflammation and is involved in the pathogenesis of atherosclerosis. Therefore, we aim to test K5, a small molecule bFGF-inhibitor, on remodelling of accelerated atherosclerotic vein grafts lesions in ApoE3*Leiden mice.

K5-mediated bFGF-signalling blockade strongly decreased intraplaque angiogenesis and intraplaque hemorrhage. Moreover, it reduced macrophage infiltration in the lesions by modulating CCL2 and VCAM1 expression. Therefore, K5 increases plaque stability.

To study the isolated effect of K5 on angiogenesis and SMCs-mediated intimal hyperplasia formation, we used an in vivo Matrigel-plug mouse model that reveals the effects on in vivo angiogenesis and femoral artery cuff model to exclusively looks at SMCs. K5 drastically reduced in vivo angiogenesis in the matrigel plug model while no effect on SMCs migration nor proliferation could be seen in the femoral artery cuff model. Moreover, in vitro K5 impaired endothelial cells functions, decreasing migration, proliferation and tube formation.

Our data show that K5-mediated bFGF signalling blockade in hypercholesterolemic ApoE3*Leiden mice reduces intraplaque angiogenesis, haemorrhage and inflammation. Therefore, K5 is a promising candidate to stabilize advanced atherosclerotic plaques.

Introduction

Atherosclerosis is a chronic disease that culminates with plaque rupture often leading to acute cardiovascular events. Crucial factors for plaque instability and therefore for plaque rupture are not the size, but rather the composition of the atherosclerotic plaques [1]. Distinctive features like large necrotic cores, intraplaque angiogenesis, intraplaque haemorrhage, high macrophage content and a thin fibrous cap are known for their role in plaque destabilization [2].

Basic fibroblast growth factor (bFGF) is involved in the pathogenesis of atherosclerosis [3] and especially in the regulation of processes that drive plaque instability [4,5]. It is a known regulator of angiogenesis, macrophage infiltration as well as smooth muscle cells (SMCs) fate [6,7]. A member of the fibroblast growth factors family, bFGF is secreted by SMCs and macrophages [8,9] and exerts its activities by binding to one of the four FGF receptors (FGFR1-4) on the cell surface of different cell types, among which endothelial cells (ECs) and SMCs. bFGF exploits its function on ECs mostly via binding to FGFR1 [10,11]. Upon bFGF binding the receptor dimerizes, gets phosphorylated and the complex ligand/receptor is internalized, resulting in signalling for cell motility, proliferation and survival, leading to angiogenesis [12].

In atherosclerotic lesions, bFGF was shown to promote intraplaque angiogenesis [13]. Intraplaque angiogenesis is driven by local hypoxia that triggers the formation of neovessels from the vasa vasora in the adventitia [14,15]. These newly formed neovessels are immature and leaky. They lack a continuous pericyte coverage and regular tight junctions between endothelial cells, leading to intraplaque haemorrhage. Intraplaque haemorrhage, the extravasation of red blood cells into the plaque, along with inflammatory cells fuels the ongoing inflammation. At the same time, the invading inflammatory cells and in particular macrophages promote the synthesis of various angiogenic factors [16,17], further triggering plaque angiogenesis [15]. bFGF also enhances the infiltration of macrophages in the lesions via stimulating the expression of chemokines and adhesion molecules like MCP-1 and VCAM-1 [6]. Accumulation of (macrophage derived) foam cells contributes to lipid storage, atherosclerotic plaque growth and drives the plaque pro-inflammatory phenotype [18]. As a result, intraplaque angiogenesis and inflammation are strongly connected in atherosclerosis and form a vicious

cycle that drives the atherosclerotic plaque toward an unstable phenotype and possibly rupture.

For many years bFGF has been known to promote SMC proliferation and migration [19] and it was a major target in the prevention of post-interventional intimal hyperplasia [3,20]. SMCs play a complex role in the stability of atherosclerotic lesions. They are involved in lesion formation by inducing intimal proliferation, but are also crucial in the formation of the fibrous cap covering the lesion. Upon vascular injury or endothelial cell activation SMCs display a switch from a contractile phenotype towards a proliferative phenotype characterized by enhanced cell proliferation and migration [21]. SMCs in the fibrous cap mainly show a contractile phenotype [22] and the thickness of the cap is crucial for plaque stability since plaque rupture is increased by cap thinning [23]. bFGF was found to be higher expressed in SMCs of unstable plaques when compared to stable plaques [5] and is known to stimulate a proliferative phenotype [19].

We hypothesize that blocking bFGF signalling would potentially reduce intraplaque angiogenesis, macrophage infiltration and SMCs proliferation, resulting in stabilization of atherosclerotic plaques.

3,3'-(propane-1,3-diyilbis(azanediyl)bis(oxomethylene)bis(1-(2,4-dichlorophenyl)-1,4-dihydro-thieno[3',2':4,5]cyclohepta[1,2-c]pyrazole-8-sulfonic acid), namely K5 (Fig.1) a small molecule developed by Kemotech Srl (Parco Scientifico di Pula, Cagliari, Italy), is able to bind bFGF and act as inhibitor of bFGF signalling [24].

The effect of K5-mediated bFGF signalling blockade on intraplaque angiogenesis, inflammation and SMCs proliferation in atherosclerosis was studied in accelerated atherosclerotic lesions vein graft in hypercholesterolemic ApoE3*Leiden mice. We previously showed that such lesions deeply resemble atherosclerotic unstable plaques found in humans, containing hypoxia, intraplaque angiogenesis and haemorrhage, profound intimal hyperplasia with a strong SMCs proliferation component and extensive inflammation [25]. In this murine model intraplaque angiogenesis can be detected as early as 14 days and after 28 days neovessels can be found throughout all layers of the vein graft. These neovessels have either a basement membrane and a pericyte coverage [26], characteristics of mature plaque neovessels, or they lack a complete pericyte coverage, peculiarity of immature neovessels,

both found in native atherosclerosis. These characteristics allow for the study of both intraplaque angiogenesis and intraplaque haemorrhage in this murine model.

To study the isolated effect of K5 on angiogenesis and SMC proliferation, we evaluated also the effects of K5 in vivo in a matrigel plug mouse model that exclusively reveals the effects on in vivo angiogenesis and on in vivo femoral artery cuff model that looks solely at the effects of SMCs mediated intimal hyperplasia formation. Moreover, we investigated the effect of K5 on cultured endothelial cells using in vitro angiogenesis models.

Hence, we hypothesized that K5 treatment will reduce intraplaque angiogenesis, inflammation and SMCs proliferation in vein graft lesions in hypercholesterolemic ApoE3*Leiden mice and therefore increase lesion stability.

Results

K5 prevents bFGF internalization and inhibits FGFR1 phosphorylation

We first analysed whether K5 (chemical structure in Fig.1A) prevents the receptor binding and internalisation of bFGF by measuring the levels of bFGF in the culture medium of H5V endothelial cells treated with K5 and comparing it to untreated cells. In the conditioned medium of K5 treated cells we observed a significant accumulation of bFGF, that reached with the highest dose tested of 100µM a four-fold difference when compared to control (Fig. 1B, p=0.01).

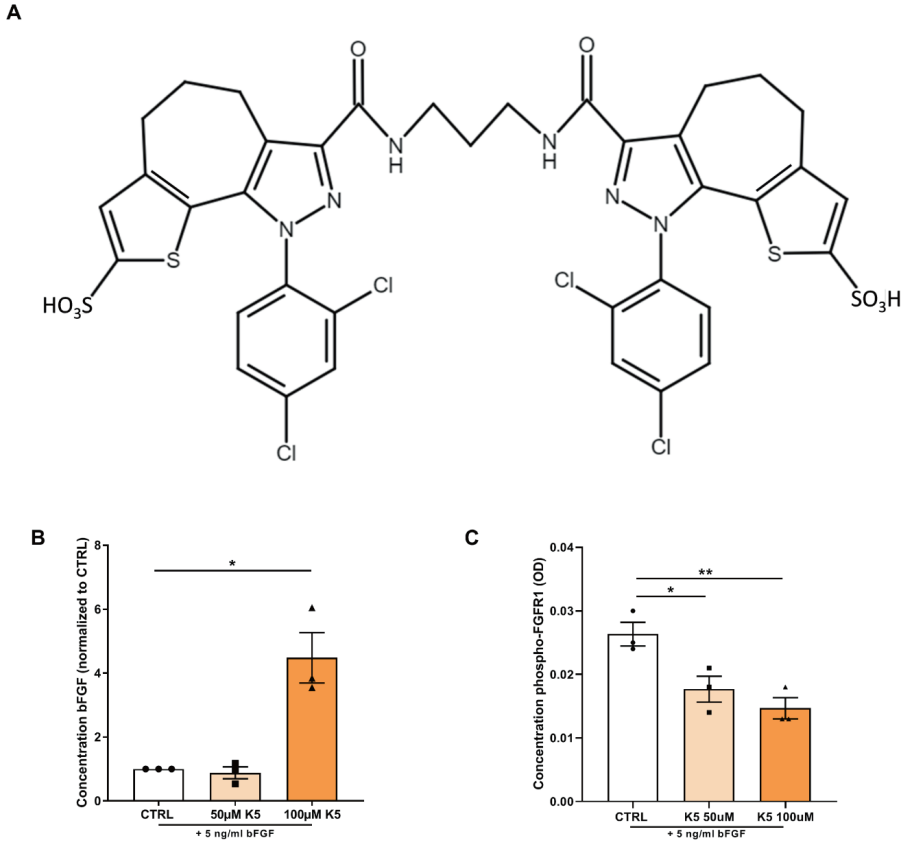


Fig.1 K5 prevents bFGF internalization and inhibits FGFR1 phosphorylation. (A) Chemical structure of K5. (B) Quantification of the concentration of bFGF in cell culture medium of H5V cells incubated with increasing doses of K5 and 5 ng/ml of bFGF (n=3 technical replicates). (C) Concentration of phosphorylated FGFR1 in HUVECs

treated with two different concentration of K5 (n=3 technical replicates). Data are presented as mean±SEM. *p<0.05, **p<0.01, *** p<0.001. **** p<0.0001; by 2-sided Student t test

Moreover, in order to demonstrate that K5 treatment resulted in reduced activation and therefore reduced phosphorylation of FGFR1, we quantified the degree of phosphorylation of FGFR1 in HUVECs treated with K5 or control treatment. As shown in figure 1C, both doses tested resulted in a significant dose dependent (p=0.03 and 0.009 respectively) reduction, by 35% and 46%, in phosphorylation of the receptor compared to the control group.

Effects of K5 on vessel wall remodelling and lesion composition in vein grafts

We studied the effect of K5 on vessel wall remodelling in an in vivo model of accelerated atherosclerosis in hypercholesterolemic ApoE3*Leiden mice which underwent vein graft surgery.

Treatment with K5 at the dose of 25 mg/kg was well tolerated by the mice and did not affect weight nor cholesterol levels (Supplementary information 1). Mice treated with K5 (n=10) had comparable vessel wall thickening to mice of the vehicle treated control group (n=14) (Fig. 2A,B. p=0.4) . Moreover, when looking in detail at the vascular remodelling in the lesions, no differences in circumference of the vessel, lumen area or lumen perimeter could be detected in the K5 treated mice when compared to controls (Fig. 2C).

bFGF is known to regulate SMCs migration and proliferation and inhibition or lack of these processes are crucial drivers toward the formation of advanced unstable atherosclerotic lesions. To assess the effect of K5 on SMCs content in atherosclerotic lesions, we performed an anti-αSMA immunohistochemical staining. αSMA^+ cells were found, both in the K5 treated and in the control groups, mainly in the intimal layer of the vessel around the lumen (Fig. 2E). When quantified, the total amount of SMCs in the K5 treated group showed no differences compared to control (Fig. 2D. p=0.97), not was the number of proliferating SMCs (Fig. 2I) different between the lesions of K5 treated and control mice (Fig.2H).

Since SMCs are the main producers of collagen, we analysed the collagen content in the lesions. Sirius red positive areas were detected in both groups and the total positive area showed no differences between the groups (Fig. 2G, Fig. 2F, p=0.75).

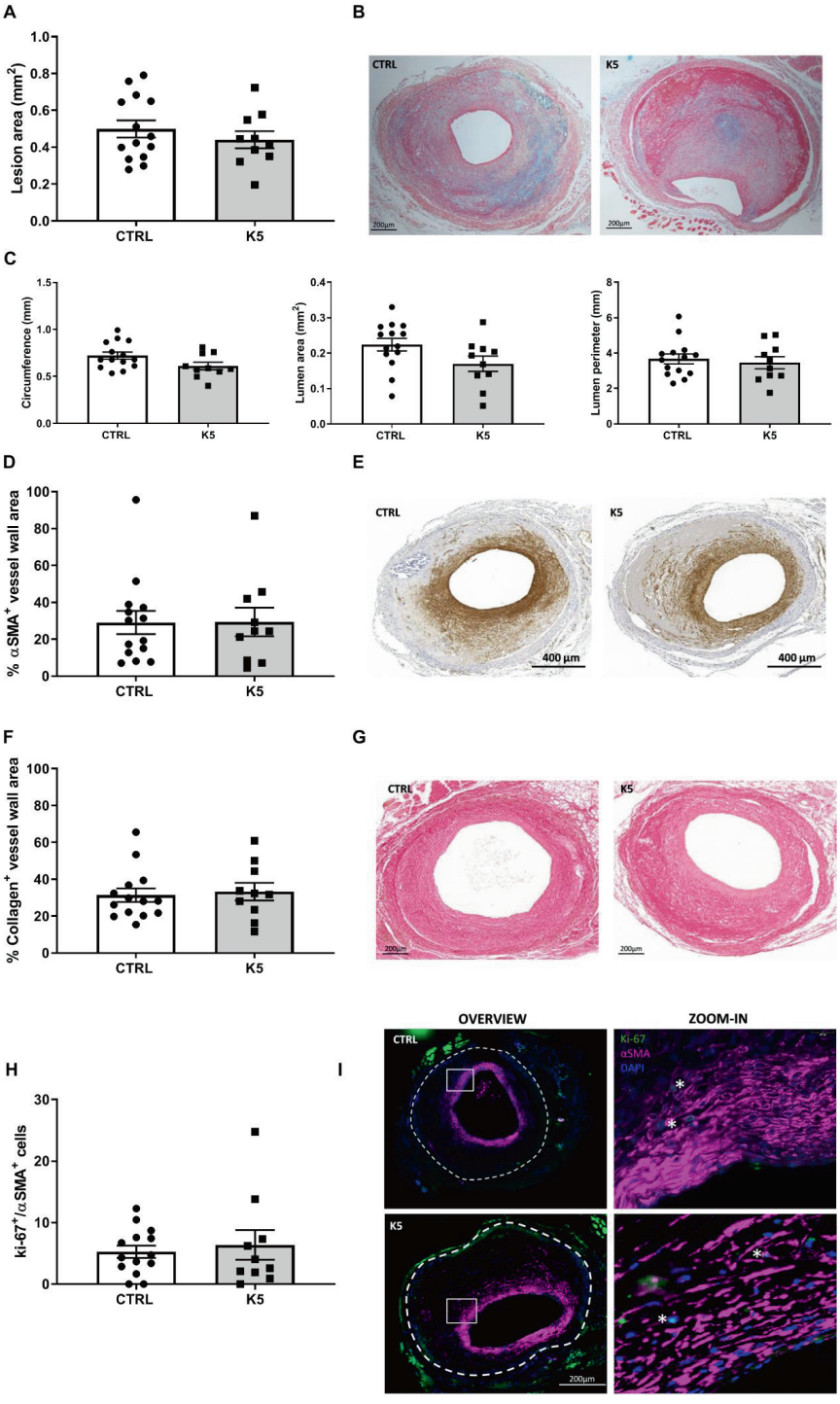

A
Lesion area (mm²)
CTRL
K5
B
CTRL
K5
C
Circumference (mm)
Lumen area (mm²)
Lumen perimeter (mm)
D
% αSMA⁺ vessel wall area
E
400 µm
F
% Collagen⁺ vessel wall area
G
H
ki-67⁺/αSMA⁺ cells
I
OVERVIEW
ZOOM-IN
Ki-67
αSMA
DAPI
200µm

Fig.2 K5 does not affect neointima formation nor SMCs content in advanced vein graft atherosclerotic plaques in ApoE3*Leiden mice. (A) Quantification of lesion area 28 days after vein graft surgery in ApoE3*Leiden mice and (B) representative pictures of the lesions of control and K5 treated mice (n=14 in CTRL group and n=10 in K5 group). (c) Quantification of lesion circumference, lumen area and perimeter (n=14 in CTRL group and n=10 in K5 group). (D) Quantification of αSMA positive area in the vessel wall and (E) representative examples of CTRL and K5 groups lesions (n=14 in CTRL group and n=10 in K5 group). (F) Quantification of sirius red positive lesion area and (G) examples of the staining in vein graft of CTRL and K5 treated groups (n=14 in CTRL group and n=10 in K5 group). (H) Quantification of Ki-67 and αSMA double positive cells and (I) examples of immunofluorescent staining for CTRL and K5 treated groups (n=14 in CTRL group and n=10 in K5 group). The white dotted line delineates the perimeter of the lesion. Data are presented as mean±SEM *p<0.05, **p<0.01, *** p<0.001. **** p<0.0001; by 2-sided Student t test

K5 effects on vascular toxicity and SMCs content in neointima formation in vivo in the femoral artery cuff model

To determine whether K5 had an effect on SMCs driven neointima formation in vivo, we induced neointima formation in the femoral artery of C57BL/6 mice using a non-constrictive cuff and treated the mice with three different doses of K5 (25, 75 and 200 mg/kg). The lesions formed in these mice after cuff placement mainly consists of SMCs accumulating in the intimal layer (Fig. 3B, area between dotted lines).

Moreover, to determine whether K5 in different concentrations has toxic effects on the vessel wall, we studied the media size and breaks in the internal lamina as these parameters in this model are described as indicators of toxicity of the drug tested [27]. We did not observe differences in the medial area of mice treated with different concentrations of K5 and in the control group (Fig. 3C) nor could we detect differences in breaks in the internal lamina (examples of intact internal laminas in Fig. 3B). Taken together these parameters indicate that K5 used in these doses can be used safely and has no toxic side effects on the vessel wall.

We distinguished between lamina elastica externa and lamina elastica interna using an elastin immunohistochemical staining (Fig. 3B) and studied the neointima area. Comparable to the results obtained in the experiment with ApoE3*Leiden mice which underwent vein graft surgery, no differences could be detected in the neointima area of the treated groups when compared to the area of the control group, even with higher doses of K5 (Fig. 3A).

We found αSMA positive areas throughout the intimal and medial layers in all the K5 treated groups and in the control group (Fig. 3E). Quantification of the total area (media and intima) αSMA^+ showed no differences in treated groups when compared to control (Fig. 3D).

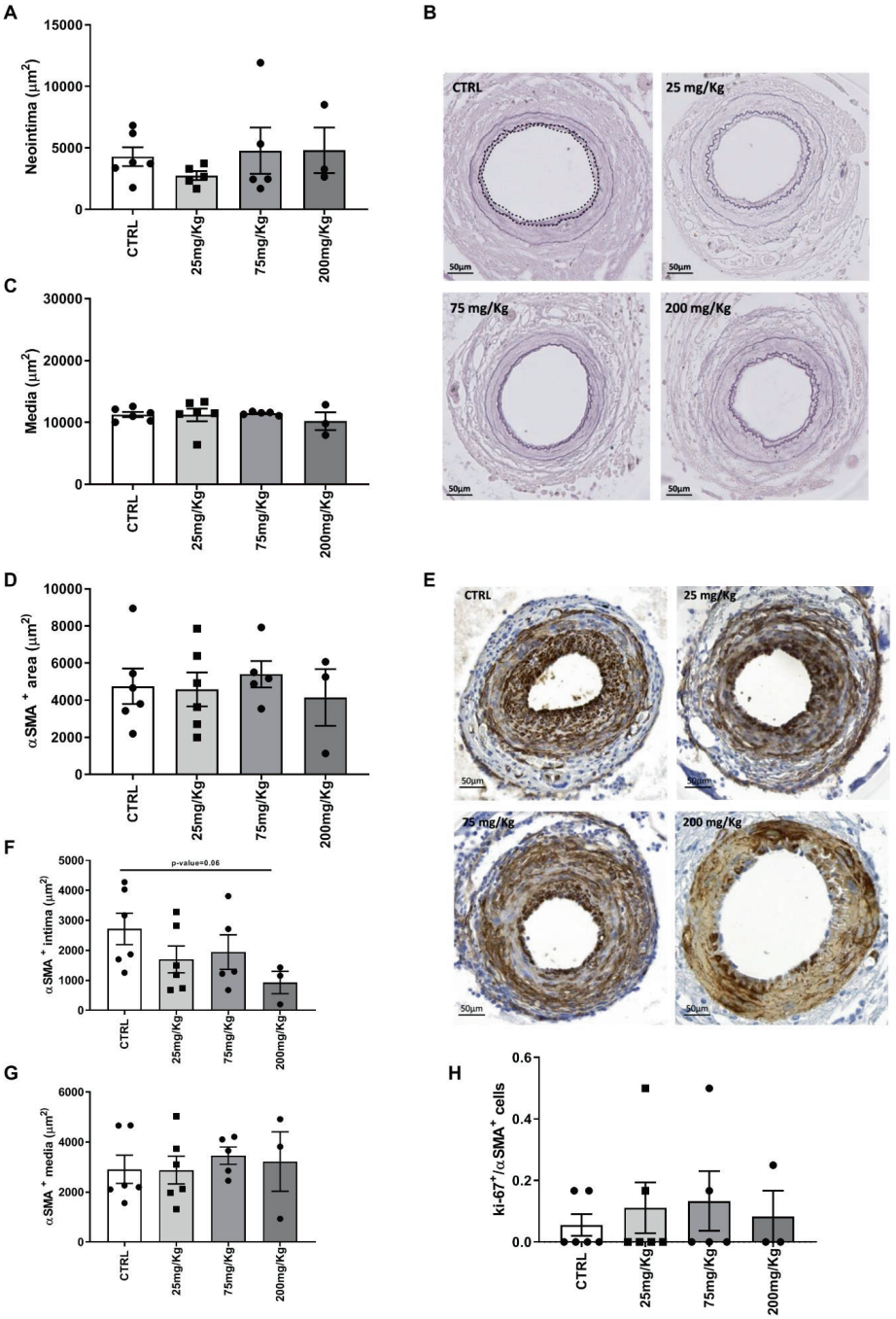

A
Neointima (µm²)
15000
10000
5000
0
CTRL
25mg/Kg
75mg/Kg
200mg/Kg
B
CTRL
25 mg/Kg
75 mg/Kg
200 mg/Kg
50µm
C
Media (µm²)
30000
20000
10000
0
D
αSMA⁺ area (µm²)
10000
8000
6000
4000
2000
E
F
αSMA⁺ intima (µm²)
p-value=0.06
5000
4000
3000
2000
1000
G
αSMA⁺ media (µm²)
6000
4000
2000
H
ki-67⁺/αSMA⁺ cells
0.6
0.4
0.2
0.0

Fig.3 K5 does not affect SMCs driven neointima formation nor induce toxicity in femoral artery cuff lesions. (A) Quantification of the neointima area in control and K5 treated groups and (B) representative pictures of elastin staining of ctrl and K5 treated groups. The white dotted line delineates the perimeter of the lesion (C) Quantification of media area. (D) Quantification of αSMA positive area in the cuff-induced neointima model and (E) examples of pictures of αSMA IHC staining in control and K5 treated groups. (F) Quantification of αSMA positive area in intima and (G) media area of lesions from control and K5 treated mice. (H) Quantification of the number of proliferating smooth muscle cells in control and K5 treated groups. Data are presented as mean±SEM. of n=6 independent measurements per group *p<0.05, **p<0.01, *** p<0.001. **** p<0.0001; by 2-sided Student t test

When looking at the two layers separately, we observed that SMCs content in the media of the control group was comparable to the content of the treated groups (Fig. 3G). The doses tested did not induce a significant reduction of intimal SMCs content when compared to the control group, although the highest dose tested of 200 mg/kg showed a trend toward a reduction in SMCs (p=0.06) when compared to control (Fig. 3F). The number of proliferating SMCs was also comparable between the two groups (Fig. 3H) and no apoptotic SMC could be detected in the control group nor in the K5 treated groups (Supplementary figure 2).

Effects of K5 on intraplaque angiogenesis and intraplaque hemorrhage in advanced atherosclerotic plaques

Since endothelial cells play a crucial role in the development and progression of atherosclerotic lesions we zoomed in on the effect of K5-mediated bFGF receptor binding blockade on endothelial cells in accelerated atherosclerotic vein graft lesions in ApoE3*Leiden mice.

An important aspect in this murine model of advanced atherosclerotic lesions is lumen re-endothelialisation. During the vein graft surgery procedure, the venous graft undergoes high distension due to high pressure of the arterial blood flow which results in loss of the endothelial cells at the luminal side. Restoration of the endothelial monolayer begins quickly after the initial damage and the endothelium surrounding the lumen is found to be intact four weeks after the surgery [28]. We found that the control mice had a complete lumen coverage, represented as a continuous ECs layer surrounding the lumen (Fig. 4A) and the same was visible also in the mice from the K5 treated group (Fig. 4B).

Endothelial cells not only are crucial for the coverage of the luminal side of the grafts, they also are the main cell type driving intraplaque angiogenesis. Therefore the effects of K5 on intraplaque angiogenesis was studied too.

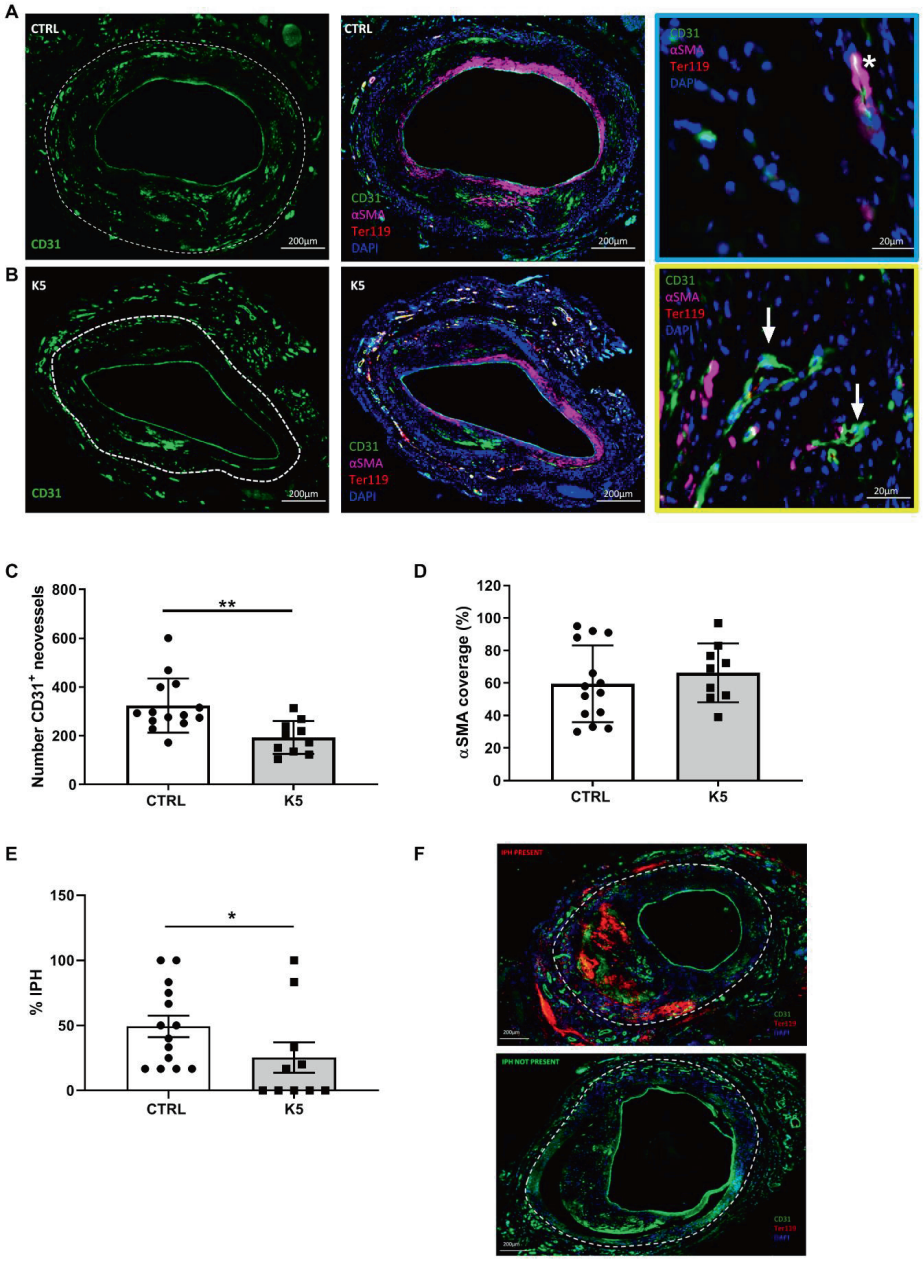


Fig.4 K5 impairs IP angiogenesis in advanced vein graft atherosclerotic plaques in ApoE3*Leiden mice. (A,B) Examples of atherosclerotic lesions stained for CD31 in the left panel, overview of the quadruple IHC staining for CD31, Ter119, αSMA and DAPI in the middle panel and example of mature (marked with a white star in the blue box) and immature vessels (marked with white arrows in the yellow box) in the right panel are shown (n=14 in

CTRL group and n=10 in K5 group). (C) Quantification of IP angiogenesis in the control and K5 groups (n=14 in CTRL group and n=10 in K5 group). (D) Quantification of αSMA coverage (n=14 in CTRL group and n=10 in K5 group). (E) Quantification of IPH and (F) examples of IPH present (top panel) and IPH not present (bottom panel) (n=14 in CTRL group and n=10 in K5 group). Data are presented as mean±SEM *p<0.05, **p<0.01, *** p<0.001. **** p<0.0001; by 2-sided Student t test

Thus we analysed the content of $CD31^+$ neovessels in advanced atherosclerotic plaques in ApoE3*Leiden mice which underwent vein graft surgery and were treated with 25 mg/kg K5 (Fig. 4B) and compared it to the content of the control group (Fig. 4A).

CD31 positive neovessels were found throughout the vessel wall area of both control and treated mice (area outlined with white dotted lines in Fig. 4A and B), but interestingly K5 treated mice showed reduced numbers of neovessels when compared to the control group (p =0.003, Fig. 4C).

Next, we evaluated the maturity of the neovessels and quantified the percentage of vessels that presented a pericyte coverage on top of the ECs layer. Mature vessels present an EC layer fully covered by a SMCs layer (example in Fig.4, zoom-in box outlined in blue) and immature vessels present only an ECs layer (example in Fig.4, zoom-in box outlined in yellow). No significant difference in the amount of SMCs coverage was found when comparing mice of the control group to the mice of the K5 group (Fig. 4D, p-value=0.4)

A complication of immature neovessels is the extravasation of red blood cells, phenomenon known as intraplaque haemorrhage (IPH). We determined the degree of intraplaque haemorrhage in the lesions of control and K5 treated mice and scored them as present (Fig. 4F, top panel) or not present (Fig. 4F, bottom panel). As shown in the quantification in Fig. 4E, we observed a reduction in the amount of IPH in the lesions of mice treated with K5 when compared to controls (p=0.04).

K5 reduces circulating monocytes and macrophage content in accelerated atherosclerotic lesions

bFGF was previously shown to be a mitogen for multipotent progenitors from bone marrow, mostly in the myeloid lineage [29-31]. Although ineffective by itself, it is thought to potentiate the effects of other growth factors and thus act as a permissive factor [32]. Therefore, we assessed the effect of bFGF blockage on systemic inflammation, examining the number of circulating monocytes.

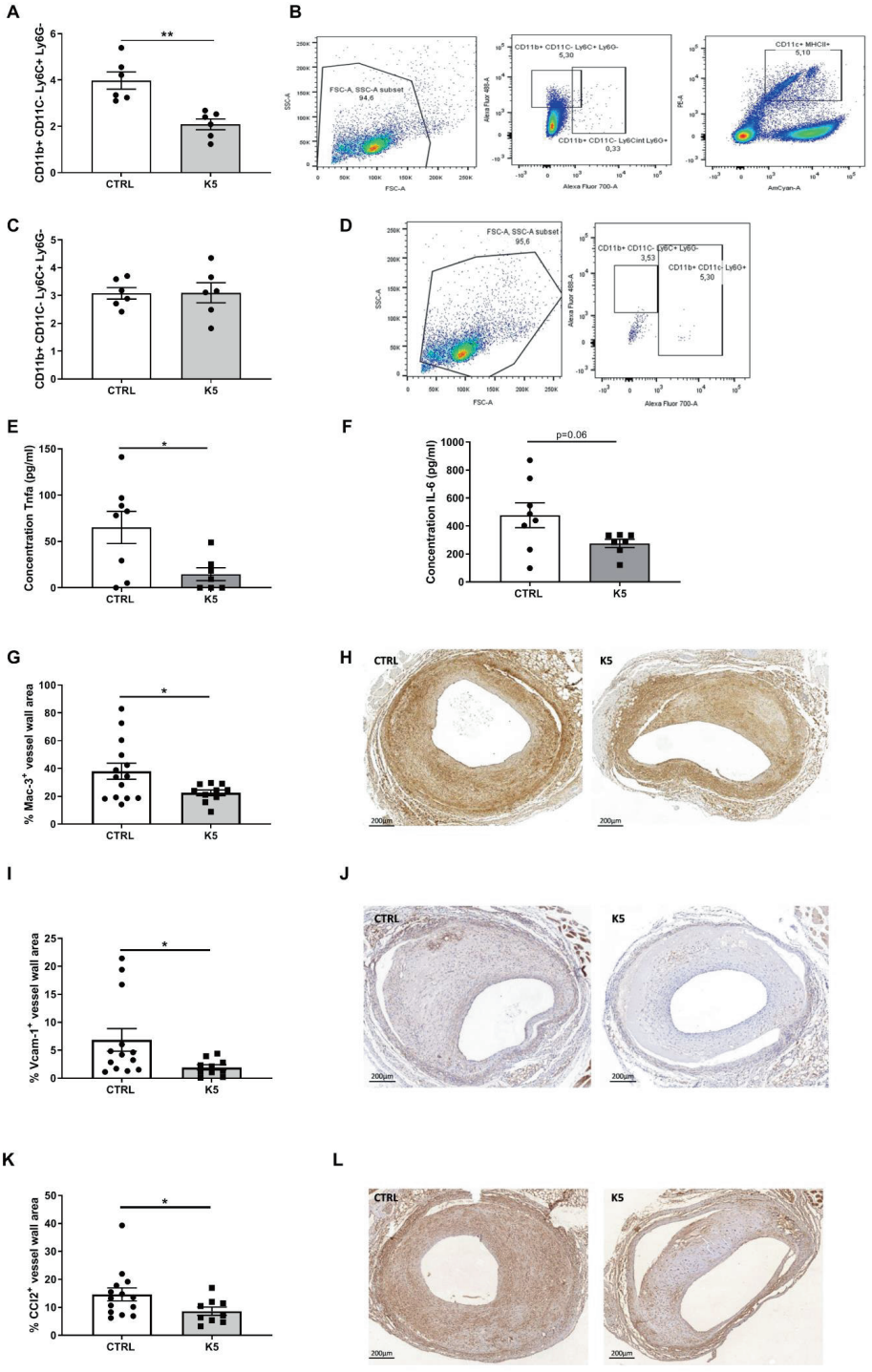

A
CD11b+ CD11C- Ly6C+ Ly6G-
**
CTRL
K5
B
FSC-A, SSC-A subset
94,6
CD11b+ CD11C- Ly6C+ Ly6G-
5,30
CD11b+ CD11C- Ly6Cint Ly6G+
0,33
CD11c+ MHCII+
5,10
C
CD11b+ CD11C- Ly6C+ Ly6G-
D
FSC-A, SSC-A subset
95,6
CD11b+ CD11C- Ly6C+ Ly6G-
3,53
CD11b+ CD11c- Ly6G+
5,30
E
Concentration Tnfa (pg/ml)
*
F
Concentration IL-6 (pg/ml)
p=0.06
G
% Mac-3+ vessel wall area
H
CTRL
K5
200µm
I
% Vcam-1+ vessel wall area
J
K
% CCl2+ vessel wall area
L

Fig.5 K5 reduces circulating monocytes and macrophage infiltration in advanced vein graft atherosclerotic lesions in ApoE3*Leiden mice. (A) FACS quantification of circulating monocytes in the blood of control and K5 treated mice and (B) gating strategy (n=6 mice per group). (C) FACS quantification of monocytes in the spleen of control and K5 treated mice and (D) gating strategy (n=6 mice per group). Quantification of the concentration of Tnf (E) and IL-6 (F) in samples from whole blood assay incubated with LPS (n=8 mice per group). (G) Quantification of Mac3 positive area in the control and K5 groups and (H) respective example of the staining on the right (n=14 in CTRL group and n=10 in K5 group). (I) Quantification of Vcam-1 and (K) Ccl-2 positive area in the control and K5 groups (n=14 in CTRL group and n=10 in K5 group). (J) Representative pictures for Vcam-1 IHC staining and (L) Ccl2 IHC staining in mice from ctrl and K5 groups (n=14 in CTRL group and n=10 in K5 group). Data are presented as mean±SEM. *p<0.05, **p<0.01, *** p<0.001. **** p<0.0001; by 2-sided Student t test

$CD11b^{+}$,$CD11C^{-}$,$Ly6C^{+}$,$Ly6G^{-}$ cells were found to be present in both control and K5 treated mice in the blood and spleen (Fig.5B and D respectively). Quantification of the number of cells showed that circulating monocytes were significantly reduced in the K5 treated group when compared to control (Fig.5A, p=0.001) while no differences were detected between groups when quantifying the amount of monocytes in the spleen (Fig.5C).

To examine the activity of the available cells we examined the amount of pro-inflammatory cytokines in the blood of mice from the control and K5 treated groups. One of the main functions of monocytes is to secrete cytokines so we looked at the amount of pro-inflammatory cytokines after 24 hours treatment with LPS *in vitro*. TNF-alpha production in whole blood in mice treated with K5 was significantly reduced when compared to whole blood from mice of the control group (Fig. 5E p=0.02). The production of IL-6 also decreased in whole blood from mice of the K5 group when compared to the control group upon stimulation with LPS (Fig. 5F. p=0.06).

To analyse the consequences of lower numbers of circulating monocytes on plaque composition and inflammation, we studied the effect of K5 on intraplaque inflammation in the vein graft lesions. Mac3 Positive cells were found throughout the lesion in both control and K5 treated group (Fig.5H), but in the lesions of K5 treated mice macrophages were significantly reduced by 15% when compared to control (Fig.5G, p=0.03).

Since it is known that bFGF upregulates the expression of the cell adhesion molecule VCAM-1 in ECs, increasing polymorphonuclear leukocyte adhesion and trans-endothelial migration [33] and moreover, it can also upregulate the expression of a number of chemokines involved in the recruitment of different inflammatory cells like CCL2, we investigated whether the decrease in macrophages could also be due to reduced infiltration of monocytes in the lesions, by reduction of VCAM-1 expression or reduced CCL2 expression.

VCAM-1 was found to be expressed in the lumen endothelium, as well as in the neovessels in the medial and intimal layers of the vessel wall (Fig.5J). CCL2 was present throughout the vessel wall in both control and treated groups (Fig.5L). Interestingly both VCAM- 1 and CCL2 were found to be significantly decreased, by 5 and 6 % respectively, in the lesions of K5 treated mice when compared to control (Fig.5I and K).

Effect of K5 on the number of neovessels in an in vivo Matrigel plug model

Since the effects on intraplaque angiogenesis in the vein graft model may depend on direct and indirect factors including the size of the lesions, inflammation and degree of ischemia in those lesions, we evaluated the effects of K5 on angiogenesis directly. For this we used an in vivo Matrigel plug model in C57BL/6, in which we tested the effect of K5 in multiple doses (25, 75 and 200 mg/Kg) on angiogenic vessel influx in the plugs.

Mice treated with K5 showed a reduction in $CD31^{+}$ neovessels when compared to control (shown in figure 6). Quantification of the staining confirmed the difference observed and resulted in a significant reduction of CD31 positive vessels in all the treated group when compared to control (p-value=0.008).

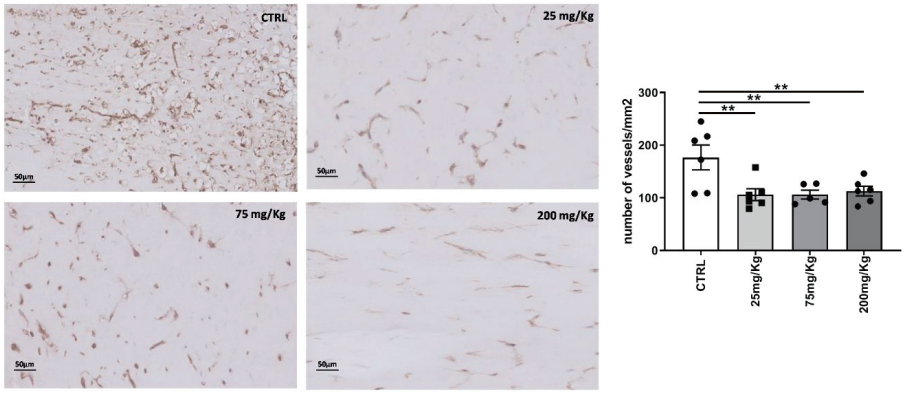


Fig.6 K5 reduces the number of vessels formed in a Matrigel plug model. Examples of CD31 positive neovessels in Matrigel plugs from control mice and mice treated with different increasing doses of K5. On the right quantification of the number of neovessels in the control and treated groups. Data are presented as mean±SEM. of n=6 independent measurements per group *p<0.05, **p<0.01, *** p<0.001. **** p<0.0001; by 2-sided Student t test

Differently from the results obtained in the vein graft model in ApoE3*Leiden mice, no differences could be found in the expression of VCAM-1 and CCL-2 in the Matrigel plugs of the mice treated with K5 when compared to control (Supplementary figure 3 and 4 respectively), while we observed a significant reduction in the number of macrophages in the group treated with the highest dose of K5 (200mg/Kg) when compared to control (Supplementary figure 3, p=0.02)

In vitro angiogenesis is reduced upon K5 treatment

To understand how K5 impairs ECs functions, we investigated its effect in different ECs functional assays in vitro. Namely MTT assay to study ECs proliferation, scratch wound healing assay to evaluate ECs migration, and tube formation assay to assess the ability of ECs to form tubular structures that resemble new vessels.

K5 significantly reduced H5V proliferation rate when compared to control as shown in figure 7A. In fact ECs proliferation was reduced by 24.5% and 40.6% in the cells treated with 50µM and 100 µM K5 respectively (p=0.0014 and <0.0001).

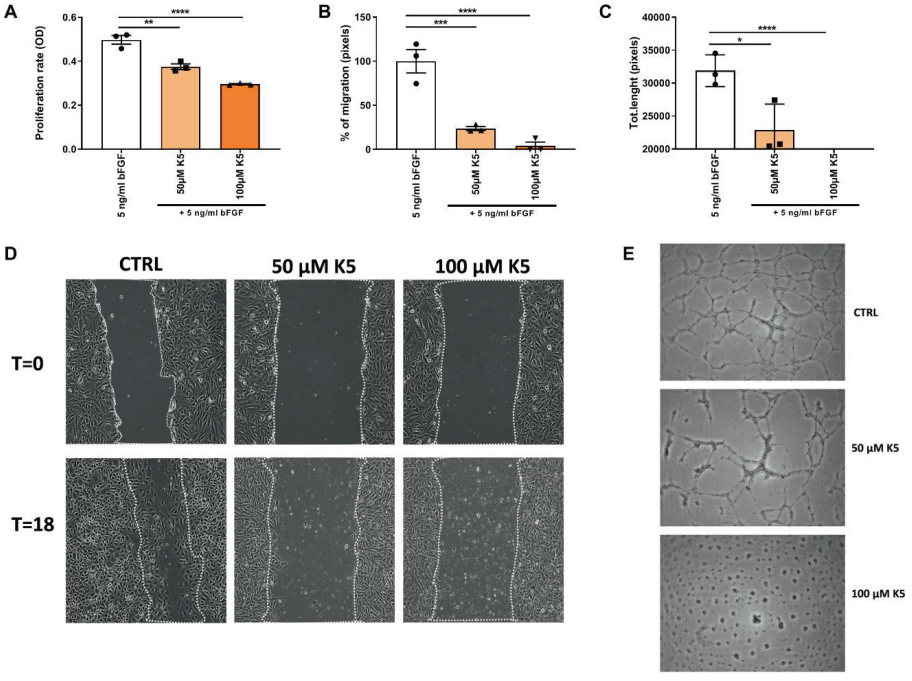


Fig.7 K5 impairs in vitro angiogenesis. (A) Quantification of proliferation rate of H5V cells treated with K5 compared to control (n=3 technical replicates). (B) Quantification of migration rate of H5V cells at T18 (n=3 technical replicates) and (D) representative pictures of wound healing scratches at T0 and after 18 hours. (C) Quantification of total length of tube formed after 12 hours of control and K5 treated groups (n=3 technical replicates). (E) Examples of HUVECs tube formation in control and K5 treated groups and quantification method. Data are presented as mean±SEM. *p<0.05, **p<0.01, *** p<0.001. **** p<0.0001; by one way ANOVA

We next performed a scratch wound healing assay in H5V cells and treated the cells with increasing doses of K5. Treatment with K5 significantly decreased scratch wound closure when compared to control by 76.3% and 95.8% in the groups treated with 50 and 100 µM respectively (Fig. 7B and D). Quantification of the migration rate showed a dose dependent significant reduction in ECs migration ability with all the doses of K5 tested when compared to control (Fig. 7B and D, p =0.0002 and <0.0001 respectively).

We further looked at the ability of K5 to impair the capability of ECs to form capillary like structures and evaluated the total length of tubes formed (Fig. 7C and E). K5 resulted to be able to strongly reduce HUVECs tube formation by 14% with the lowest dose tested of 50µM (p=0.01) and to completely inhibit tube formation with the dose of 100µM (Fig. 7C and E, p=<0.0001) reducing the formation of tubes by 100%.

Discussion

In the present study we found that K5 mediated inhibition of bFGF reduces intraplaque angiogenesis and intraplaque haemorrhage in a model for accelerated atherosclerosis using vein graft surgery in ApoE3*Leiden mice. Additionally, K5 reduced *in vivo* angiogenesis in a Matrigel plug model. We demonstrate that K5 is able to impair EC migration, proliferation and tube formation due to a reduced FGFR1 activation *in vitro*. Moreover, we found that K5 is able to reduce macrophage infiltration in the plaque via modulating the expression of VCAM-1 and CCL-2.

bFGF is known to play a crucial role during angiogenesis. bFGF was shown to be present in complicated atherosclerotic plaques and in higher amounts in patients who presented symptomatic carotid disease when compared to stable plaques [5]. High expression of bFGF/FGFR-1 was also associated with immature and inflammatory intraplaque angiogenesis and plaque instability in a rabbit model of atherosclerosis [13]. In this study we demonstrate that the small molecule K5 can block bFGF signalling, which leads to a decrease in *in vitro* angiogenesis via inhibition of ECs migration, proliferation and tube formation due to a reduction of FGFR1 phosphorylation. The above mentioned features lead to a decrease of *in vivo* angiogenesis in a Matrigel plug model and more importantly a reduction of intraplaque angiogenesis in accelerated atherosclerotic lesions in vein grafts in hypercholesterolemic ApoE3*Leiden mice. Our findings are in line with a study by Tanaka et al, in which FGF-2 treatment increased the number of vasa vasorum in atherosclerotic lesion formation [34]. Moreover FGF-2/FGFR-1 signalling was found to be critical for providing a pattern for the vasa vasorum to form a plexus-like network of neovessels in the atherosclerotic lesions in hypercholesterolemic low-density lipoprotein receptor–deficient/apolipoprotein $B^{100/100}$ mice [35].

A mature neovessel is formed by a basement membrane, a layer of ECs and pericyte coverage. The amount of intraplaque haemorrhage decreased in the treated group when compared to the control. It was suggested that exposure to bFGF hampers endothelial cell-cell junctions [36]. This could explain why bFGF blockade via K5 lead to reduction in intraplaque haemorrhage, probably via enhancing cell-cell connections between endothelial cells.

In 1991 Reidy & Lindner showed that an antibody raised against bFGF could reduce the proliferation of SMCs in a rat model in which carotid arteries where denuded of endothelium with a balloon catheter [20]. Interestingly, in their study this treatment did not lead to any significant decrease in the intimal lesion. Although in the present study, in both the murine model for accelerated atherosclerosis and in the model for SMCs driven neointima formation, we could not observe any difference in SMCs proliferation in the treated groups compared to control, we show that the blockade of bFGF signalling by K5 did not affect intimal lesion area similarly to what observed by Reidy et al. More recently Chen et al., showed that blockage of the signalling of all four FGFRs (FGFR1, 2, 3 and 4) through inhibition of Frs2α, a fibroblast growth factor receptor substrate, resulted in decrease SMCs content and reduced lesion size in ApoE$^{-/-}$ mice [37]. In our study we demonstrate that small molecule mediated blockade of only bFGF does not affect the lesion's SMCs content while still reducing intraplaque angiogenesis.

In the present study we showed that K5-mediated bFGF signalling blockade induces a reduction in systemic levels of monocytes. This is in accordance with previous studies, which demonstrated that bFGF acts as a mitogen for multipotent progenitors from bone marrow, mostly in the myeloid lineage [29-31]. Moreover, we demonstrate that K5 reduced the amount of macrophages present in the lesions via reducing the expression of VCAM-1 and CCL-2, both proteins correlated with macrophage infiltration. Similarly, Liang et al, 2018 showed that knockout of FGF2 reduced infiltration and accumulation of macrophages at different stages of atherosclerosis. They also showed that the knockout induced a reduction in CCL-2 and VCAM-1 expression in the atherosclerotic plaques [6]. Therefore the observed reduced macrophages content in the ApoE3*Leiden mice treated with K5 could be either due to the reduced number of circulating monocytes or a reduced monocyte infiltration in the lesion probably due to a reduced CCL-2 and VCAM-1 expression or a combination of both processes. However the effect of K5 on intraplaque angiogenesis and its effect on the expression of CCL-2 and VCAM-1 could be unrelated to its effect on monocytes and macrophages.

The accelerated atherosclerosis vein graft model used in the present study is a unique model to study plaque angiogenesis. Intraplaque angiogenesis is a feature that is uncommon in murine models of native atherosclerosis except for very old mice. The lesions observed in the ApoE3*Leiden mice vein grafts show many features that can also be observed in advanced human lesions, including intraplaque hypoxia, angiogenesis and intraplaque haemorrhage.

However this is a model in which a vein is inter-positioned in the arterial circulation which makes it an acute model, with high grade inflammation and extensive remodelling. Extrapolation of the effects of K5 in this model to native atherosclerosis should be carefully performed with taking the previous mentioned processes into account. Based on the results obtained in the present study we can conclude that K5 is able to stabilize the atherosclerotic plaque by enhancing plaque stability via reducing intraplaque angiogenesis and decreasing intraplaque haemorrhage. Moreover, it reduces systemic circulating monocytes and decreases macrophages infiltration in the plaque. Taken together, our results show that K5 is a promising therapeutic candidate for the treatment of unstable atherosclerotic plaques.

Materials and methods

Mice

This study was performed in compliance with Dutch government guidelines and the Directive 2010/63/EU of the European Parliament. All animal experiments were approved by the animal welfare committee of the Leiden University Medical Center.

For vein graft surgery male ApoE3*Leiden mice (n=14 for the control group and n=10 for the K5 treated group), crossbred in our own colony on a C57BL/background, 8-16 weeks old, were fed a diet containing 15% cacao butter, 1% cholesterol and 0.5% cholate (100193, Triple A Trading, Tiel, The Netherlands) from 3 weeks prior to surgery until sacrifice. Mice were randomized based on their plasma cholesterol levels (kit 1489437, Roche Diagnostics, Basel, Switzerland) and body weight.

For femoral artery cuff model (n=3 per group) and Matrigel plug model (n=3 per group) 8 weeks old male C57BL/6J mice were used and were fed a chow diet. Mice were randomized in four different groups.

Anesthesia

For all the above-mentioned surgical procedures, on the day of surgery and on the day of sacrifice mice were anesthetized as previously described [25,38]. Briefly, mice were anesthetized with midazolam (5 mg/kg, Roche Diagnostics, Basel, Switzerland), medetomidine (0.5 mg/kg, Orion, Espoo, Finland) and fentanyl (0.05 mg/kg, Janssen Pharmaceutical, Beerse, Belgium). The adequacy of the anesthesia was monitored by keeping track of the breathing frequency and the response to toe pinching of the mice. After surgery, mice were antagonized with atipamezol (2.5 mg/kg, Orion, Espoo, Finland) and fluminasenil (0.5 mg/kg, Fresenius Kabi, Bad Homburg, Germany). Buprenorphine (0.1 mg/kg, MSD Animal Health, Keniworth, NJ, USA) was given after surgery to relieve pain. On the day of sacrifice mice underwent deep anesthesia with midazolam (5 mg/kg, Roche Diagnostics, Basel, Switzerland), medetomidine (0.5 mg/kg, Orion, Espoo, Finland) and fentanyl (0.05 mg/kg, Janssen Pharmaceutical, Beerse, Belgium) and were then euthanized by exsanguination.

Vein graft surgery

Vein graft surgery was performed by donor mice caval vein interposition in the carotid artery of recipient mice as previously described [25]. Briefly, thoracic caval veins from donor mice were harvested. The right carotid artery of the recipient mouse was dissected and cut in the middle. The artery was everted around the cuffs that were placed at both ends of the artery and ligated with 8.0 sutures. The caval vein was sleeved over the two cuffs, and ligated. After 28 days, mice were anesthetized and sacrificed via perfusion with 4% formaldehyde. Vein grafts were harvested, fixed in formaldehyde and paraffin-embedded.

Femoral artery cuff mouse model

C57BL/6 mice underwent a non-constrictive cuff placement around the femoral artery to induce vascular remodeling as previously described [39]. Briefly, the left and right femoral arteries were isolated and a rigid, non-constrictive polyethylene cuff was placed around the artery. Thereafter, the wound was closed by a continuous suture. After 21 days, mice were anesthetized and sacrificed via perfusion with 4% formaldehyde. Cuffed femoral arteries were harvested, fixed in formaldehyde and paraffin-embedded.

Matrigel plugs

In vivo angiogenesis analysis was performed using a Matrigel plug assay in male C57BL/6 mice as previously described [40,41]. Matrigel extracellular matrix (Ref. 354262, Corning, NY, USA) was mixed at 4°C with PBS and supplemented with 50 ng/ml bFGF (Ref. 579606, Biolegend, California, USA). The solution was then injected into the subcutaneous space on the dorsal side of mice on both the left and right flank (350 µl per flank). Mice were sacrificed 21 days post-implantation. Matrigel plugs were excised, fixed in formaldehyde, paraffin-embedded and processed for histological analysis.

K5 synthesis and application

The bFGF signalling blockade inhibitor K5 was synthesized according to the procedure described in Example 10 of US Patent 9,181,196 [24]. ^{1}HNMR, ^{13}CNMR, and FT-IR spectroscopies were adopted to ascertain correspondence of the synthesized compound employed in this

study to 3,3'-(propane-1,3-diyilbis(azanediyl)bis(oxomethylene)bis(1-(2,4-dichlorophenyl)-1,4-dihydro-thieno[3',2':4,5]cyclohepta[1,2-c]pyrazole-8-sulfonic acid), namely K5 (Fig.1).

K5 was dissolved in water for injections (Fresenius, Kabi) at a final concentration of either 25, 75 or 200 mg/kg. For the accelerated atherosclerosis vein graft model mice were treated with IP injections of 25 mg/kg K5 or vehicle (water for injections, Fresenius Kabi) every other day starting at day 14 until the sacrifice on day 28. For the cuff model and the Matrigel plug model mice were treated with IP injections of either 25, 75 or 200 mg/kg K5 or vehicle (water for injections, Fresenius Kabi) every other day starting at day 3 until the sacrifice on day 21.

Histological and immunohistochemical assessment of vein grafts, cuffs and Matrigel plugs

Histological and immunohistochemical assessment of vein grafts, cuffs and Matrigel plugs was performed as previously described [25,38]. In detail, vein grafts, cuffs and Matrigel plugs histological samples were embedded in paraffin, and sequential cross-sections (5 µm thick) were made throughout the specimens. For each mouse, six equal spaced cross-sections over the total vein graft, cuffs and Matrigel plugs length were used for analysis. To quantify the vein graft thickening (vessel wall area), MOVAT pentachrome staining was performed. Total size of the vein graft and lumen were measured. Thickening of the vessel wall (measured as intimal thickening + media thickening) was defined as the area between lumen and adventitia and determined by subtracting the luminal area from the total vessel area. Intraplaque angiogenesis was measured as the amount of $CD31^+$ vessels in the vessel wall area and the percentage of neovessels CD31+αSMA+ was defined as % αSMA coverage. Intraplaque hemorrhage (IPH) was monitored by the amount of erythrocytes outside the (neo)vessels and scored as either present or not present. Antibodies directed at alpha smooth muscle cell actin (αSMActin, Sigma, Santa Clara, CA, USA), Mac-3 (BD Pharmingen, Franklin Lakes, NJ, USA), CD31 (77699S, Cell Signaling, Danvers, MA, USA), Ter119 (116202, Biolegend, San Diego, CA, USA), Ki67 (ab16667, Abcam, Cambridge, UK), MCP-1 (sc-1784, Santa Cruz Biotechnology, Dallas, TX, USA), VCAM-1 (ab134047, Abcam, Cambridge, UK) and cleaved caspase 3 (9661-S, Cell SignalingDanvers, MA, USA) were used for immunohistochemical staining. Sirius red staining (80115, Klinipath, Amsterdam, The Netherlands) was performed to quantify the amount of collagen present in the vein grafts. The immuno-positive areas are expressed as a percentage of the lesion area.

Paraffin sections of femoral arteries from the cuff model experiment were stained with Weigert's Elastin to visualize the elastic laminae to determine intimal hyperplasia. Smooth muscle cells were stained using anti-alpha smooth muscle cell actin (αSMActin, Sigma, Santa Clara, CA, USA) and their proliferation was examined using anti-Ki-67 (ab16667, Abcam, Cambridge, UK) antibody.

Matrigel plugs paraffin sections were stained using anti-CD31 antibody (sc-1506-r, Santa Cruz Biotechnology, Dallas, TX, USA) to evaluate the number of $CD31^+$ neovessels.

Stained slides were photographed using Pannoramic MIDI II digital slide scanner (3DHISTECH, Budapest, Hungary) and image analysis softwares were used to quantify the vein graft intimal hyperplasia and composition (Qwin, Leica, Wetzlar, Germany and Imagej, Bethesda, MD, USA).

Flow cytometry

Flow cytometry was performed on spleen and blood of n=6 mice per group 28 days after vein graft surgery. Single cells suspensions were prepared from spleens by mincing the tissue through a 70 µm cell strainer (BD Biosciences, San Jose, CA, USA). Cells were washed with 10 ml IMDM Glutamax (ThermoFisher, Waltham, Massachusetts, USA) with 8% heat inactivated fetal bovine serum (PAA, Australia) and 100 U/mL Penicillin/streptomycin. Erythrocytes were lysed in red blood cell lysis buffer (hypotonic ammonium chloride buffer). Conjugated monoclonal antibodies to mouse CD11b (V450), Ly6C (FITC/Alexa488), Ly6G (Alexa Fluor 700), CD11c (PE), were purchased from eBioscience or BD Biosciences. Dead cells were excluded by positivity for 7-aminoactinomycinD (7-AAD) (Invitrogen, ThermoFisher, Waltham, Massachusetts, USA). Flow cytometric acquisition was performed on a BD LSR II flow cytometer (BD Biosciences). Data were analyzed using FlowJo V10.1 software.

Whole blood assay and determination of cytokine production

Blood was collected from mice of the control group (n=4) and of the K5 treated group (n=4) on the day of sacrifice 28 days after vein graft surgery. Blood was diluted 25X in either RPMI 1640 medium (52400-025, ThermoFisher, GIBCO, Waltham, Massachusetts, USA) or RPMI 1640 medium supplemented with 200 ng/ml LPS (K-235, Sigma-Aldrich, Saint Louis, Missouri, USA) and incubated at 37°C in a humidified 5% CO_2 environment for 24 hours. The

supernatant was then collected and used to perform ELISA for cytokine concentration of TNFa and IL 6 using ELISA kit 558534 (BD Bioscience) and ELISA kit 555240 (BD Bioscience) respectively.

Cell culture

For the isolation of HUVECS anonymous umbilical cords were obtained in accordance with guidelines set out by the 'Code for Proper Secondary Use of Human Tissue' of the Dutch Federation of Biomedical Scientific Societies (Federa), and conform to the principles outlined in the Declaration of Helsinki. Isolation and culturing of primary vein human umbilical cells was performed as described by Van der Kwast et al [42]. HUVECs were cultured in plates coated with 1% fibronectin. Cells were used between passage 2 and 4.

H5V (endothelial cell line derived from murine heart) cells were kindly provided by Dr. I. Bot from the Leiden Academic Centre for Drug Research.

H5V and HUVECs were cultured at 37°C in a humidified 5% CO_2 environment. Culture medium was refreshed every 2 days. Cells were passed using trypsin-EDTA (Sigma, Steinheim, Germany) at 90-100% confluency.

Detection of bFGF in culture medium

bFGF concentrations in the culture medium of H5V cells treated with 5 ng/ml bFGF (Ref.579606, Biolegend) or 5 ng/ml bFGF plus either 50 or 100 µm K5, were determined using the Mouse FGF basic/FGF2 DuoSet ELISA Kit (DY3139-05, R&D Systems, Minneapolis, MN, USA), according to the manufacturer's instructions.

FGFR1 phosphorylation assay

HUVECs were seeded in 12-well plates with EBM-2 Basal medium (CC-3156, Lonza) supplemented with EGM-2 SingleQuots Supplements (CC-4176, Lonza) for 24 h. Cells were then stimulated with 5 ng/ml bFGF (Biolegend) or 5 ng/ml bFGF in combination with either 50 or 100 µm K5 for 60 minutes. The cells were rinsed with PBS and lysed in cell lysis buffer containing IC diluent #12 (Reagent diluent concentrate 2 DY995, R&D Systems, Minneapolis, MN, USA, in distilled water), plus 10 µg/ml aprotinin (Ref.4139, R&D Systems, Minneapolis, MN, USA) and 10 µg/ml leupeptin (Ref.1167, R&D Systems, Minneapolis, MN, USA). FGFR1

phosphorylation was measured by a sandwich ELISA (DYC5079-2, R&D Systems, Minneapolis, MN, USA) according to the manufacturer's instructions.

Cell proliferation

Cell proliferation (n=3 individual replicates) was measured using MTT assay. H5V cells were plated at 5.000 cells/well in a 96 well plate and grown until 80-85% confluency in complete culture medium (DMEM GlutaMAX (Invitrogen, GIBCO, Auckland, New Zealand), 10% heat inactivated fetal bovine serum (PAA), 1% penicillin/streptomycin, after which they were incubated with low serum medium (DMEM GlutaMAX (Invitrogen, GIBCO, Auckland, New Zealand), 0.1% heat inactivated fetal bovine serum (PAA), 1% penicillin/streptomycin) for 24 hours. The medium was then replaced by treatment mixes consisting of low serum medium plus 5 ng/ml bFGF (Ref.579606, Biolegend), low serum medium plus 5 ng/ml bFGF (Ref.579606, Biolegend) with the addition of either 50 or 100 µM K5. After 24 hours incubation, 10µL MTT (Thiazolyl blue tetrazolium bromide, Sigma M5655) was added directly to each well and cells were incubated at 37°C in a humidified 5% CO_2 environment for 4 hours. Subsequently, 75µL medium was removed from each well and 75µL isopropanol/0.1N HCL was added per well. After incubating the plate for 90 minutes on a shaker platform, absorbance was read at 570nm with a Cytation 5 spectrophotometer (BioTek, Vermont, USA).

Scratch wound healing assay

For the scratch wound healing assay (n=3 individual replicates), H5V cells were plated on a 12 well plate and grown until 80% confluence in complete culture medium (DMEM GlutaMAX (Invitrogen, GIBCO, Auckland, New Zealand), 10% heat inactivated fetal bovine serum (PAA), 1% penicillin/streptomycin). Cells were then treated with low serum medium (DMEM GlutaMAX (Invitrogen, GIBCO, Auckland, New Zealand), 0.1% heat inactivated fetal bovine serum (PAA), 1% penicillin/streptomycin) for 24 hours. After 24h, medium was removed and a scratch-wound was introduced across the diameter of each well of a 12 wells plate using a p200 pipette tip. Subsequently, the cells were washed with PBS and medium was replaced by new low serum culture medium containing low serum medium plus 5ng/ml bFGF (Ref.579606, Biolegend), and low serum medium plus 5 ng/ml bFGF (Ref.579606, Biolegend) with the addition of either 50 or 100 µM K5. Two locations along the scratch-wound were marked per well and scratch-wound closure at these sites was imaged by taking pictures at time 0h and

18h after scratch-wound introduction using live phase contrast microscopy (Axiovert 40C, Carl Zeiss Microscopy, White Plains, NY, USA). Average scratch-wound closure after 18h was objectively calculated per well by measuring difference in cell coverage at 18h vs 0h using the wound healing tool macro for ImageJ.

Tube formation assay

HUVECs were seeded in 12-well plates with EBM-2 Basal medium (CC-3156, Lonza) supplemented with EGM-2 SingleQuots Supplements (CC-4176, Lonza) until confluent. Medium was then replaced with low serum culture medium EBM-2 Basal medium (CC-3156, Lonza) supplemented with 0.2% FCS and 1% GA-1000 (EGM-2 SingleQuots Supplements, CC-4176, Lonza) for 24 hours. A 96-wells was coated using 50 µl/well of Geltrex extracellular matrix (A1413202, Gibco). Cells were then detached using trypsin-EDTA (Sigma, Steinheim, Germany) and diluted at 150.000 cells/ml in low serum medium plus 5 ng/ml bFGF (Ref.579606, Biolegend), or low serum medium plus 5 ng/ml bFGF (Ref.579606, Biolegend) with the addition of either 50 or 100 µM K5. After 12 hours incubation pictures of each well were taken using live phase contrast microscopy (Axiovert 40C, Carl Zeiss). Total length of the tubes formed was analyzed using the Angiogenesis analyzer plugin for ImageJ**.**

Statistical analysis

Results are expressed as mean±SEM. A 2-tailed Student's t-test or a One-Way ANOVA were used to compare individual groups. Non-Gaussian distributed data were analyzed using a Mann-Whitney U test using GraphPad Prism version 6.00 for Windows (GraphPad Software). Probability-values <0.05 were regarded significant.

References

1 Perrotta, P. *et al.* Pharmacological strategies to inhibit intra-plaque angiogenesis in atherosclerosis. *Vascular pharmacology* **112**, 72-78, doi:10.1016/j.vph.2018.06.014 (2019).

2 Chistiakov, D. A., Orekhov, A. N. & Bobryshev, Y. V. Contribution of neovascularization and intraplaque haemorrhage to atherosclerotic plaque progression and instability. *Acta physiologica (Oxford, England)* **213**, 539-553, doi:10.1111/apha.12438 (2015).

3 Lindner, V., Lappi, D. A., Baird, A., Majack, R. A. & Reidy, M. A. Role of basic fibroblast growth factor in vascular lesion formation. *Circ Res* **68**, 106-113, doi:10.1161/01.res.68.1.106 (1991).

4 Takahashi, J. C. *et al.* Adenovirus-mediated gene transfer of basic fibroblast growth factor induces in vitro angiogenesis. *Atherosclerosis* **132**, 199-205, doi:10.1016/s0021-9150(97)00102-0 (1997).

5 Sigala, F. *et al.* Increased expression of bFGF is associated with carotid atherosclerotic plaques instability engaging the NF-kappaB pathway. *Journal of cellular and molecular medicine* **14**, 2273-2280, doi:10.1111/j.1582-4934.2010.01082.x (2010).

6 Liang, W., Wang, Q., Ma, H., Yan, W. & Yang, J. Knockout of Low Molecular Weight FGF2 Attenuates Atherosclerosis by Reducing Macrophage Infiltration and Oxidative Stress in Mice. *Cellular physiology and biochemistry : international journal of experimental cellular physiology, biochemistry, and pharmacology* **45**, 1434-1443, doi:10.1159/000487569 (2018).

7 Bikfalvi, A., Savona, C., Perollet, C. & Javerzat, S. New insights in the biology of fibroblast growth factor-2. *Angiogenesis* **1**, 155-173, doi:10.1023/a:1018325604264 (1998).

8 Yang, X. *et al.* Fibroblast growth factor signaling in the vasculature. *Current atherosclerosis reports* **17**, 509, doi:10.1007/s11883-015-0509-6 (2015).

9 Cordon-Cardo, C., Vlodavsky, I., Haimovitz-Friedman, A., Hicklin, D. & Fuks, Z. Expression of basic fibroblast growth factor in normal human tissues. *Laboratory investigation; a journal of technical methods and pathology* **63**, 832-840 (1990).

10 Javerzat, S., Auguste, P. & Bikfalvi, A. The role of fibroblast growth factors in vascular development. *Trends in molecular medicine* **8**, 483-489, doi:10.1016/s1471-4914(02)02394-8 (2002).

11 Bastaki, M. *et al.* Basic fibroblast growth factor-induced angiogenic phenotype in mouse endothelium. A study of aortic and microvascular endothelial cell lines. *Arterioscler Thromb Vasc Biol* **17**, 454-464, doi:10.1161/01.atv.17.3.454 (1997).

12 Tkachenko, E., Lutgens, E., Stan, R. V. & Simons, M. Fibroblast growth factor 2 endocytosis in endothelial cells proceed via syndecan-4-dependent activation of Rac1 and a Cdc42-dependent macropinocytic pathway. *Journal of cell science* **117**, 3189-3199, doi:10.1242/jcs.01190 (2004).

13 Mao, Y., Liu, X., Song, Y., Zhai, C. & Zhang, L. VEGF-A/VEGFR-2 and FGF-2/FGFR-1 but not PDGF-BB/PDGFR-beta play important roles in promoting immature and inflammatory intraplaque angiogenesis. *PloS one* **13**, e0201395, doi:10.1371/journal.pone.0201395 (2018).

14 Sluimer, J. C. *et al.* Hypoxia, hypoxia-inducible transcription factor, and macrophages in human atherosclerotic plaques are correlated with intraplaque angiogenesis. *J Am Coll Cardiol* **51**, 1258-1265, doi:10.1016/j.jacc.2007.12.025 (2008).

15 Parma, L., Baganha, F., Quax, P. H. A. & de Vries, M. R. Plaque angiogenesis and intraplaque hemorrhage in atherosclerosis. *Eur J Pharmacol* **816**, 107-115, doi:10.1016/j.ejphar.2017.04.028 (2017).

16 Leung, O. M. *et al.* Regulatory T Cells Promote Apelin-Mediated Sprouting Angiogenesis in Type 2 Diabetes. *Cell reports* **24**, 1610-1626, doi:10.1016/j.celrep.2018.07.019 (2018).

17 Liang, C. *et al.* CD8(+) T-cell plasticity regulates vascular regeneration in type-2 diabetes. *Theranostics* **10**, 4217-4232, doi:10.7150/thno.40663 (2020).

18 Bobryshev, Y. V., Ivanova, E. A., Chistiakov, D. A., Nikiforov, N. G. & Orekhov, A. N. Macrophages and Their Role in Atherosclerosis: Pathophysiology and Transcriptome Analysis. *BioMed research international* **2016**, 9582430, doi:10.1155/2016/9582430 (2016).

19 Jackson, C. L. & Reidy, M. A. Basic fibroblast growth factor: its role in the control of smooth muscle cell migration. *The American journal of pathology* **143**, 1024-1031 (1993).

20 Lindner, V. & Reidy, M. A. Proliferation of smooth muscle cells after vascular injury is inhibited by an antibody against basic fibroblast growth factor. *Proceedings of the National Academy of Sciences of the United States of America* **88**, 3739-3743, doi:10.1073/pnas.88.9.3739 (1991).

21 Kawai-Kowase, K. & Owens, G. K. Multiple repressor pathways contribute to phenotypic switching of vascular smooth muscle cells. *American journal of physiology. Cell physiology* **292**, C59-69, doi:10.1152/ajpcell.00394.2006 (2007).

22 Allahverdian, S., Chaabane, C., Boukais, K., Francis, G. A. & Bochaton-Piallat, M. L. Smooth muscle cell fate and plasticity in atherosclerosis. *Cardiovasc Res* **114**, 540-550, doi:10.1093/cvr/cvy022 (2018).

23 Bennett, M. R., Sinha, S. & Owens, G. K. Vascular Smooth Muscle Cells in Atherosclerosis. *Circ Res* **118**, 692-702, doi:10.1161/circresaha.115.306361 (2016).

24 Lazzari P., Z. M., Sani M. United States patent number US9181196B2. (2014).

25 de Vries, M. R. *et al.* Blockade of vascular endothelial growth factor receptor 2 inhibits intraplaque haemorrhage by normalization of plaque neovessels. *Journal of internal medicine* **285**, 59-74, doi:10.1111/joim.12821 (2019).

26 de Vries, M. R. *et al.* Plaque rupture complications in murine atherosclerotic vein grafts can be prevented by TIMP-1 overexpression. *PloS one* **7**, e47134, doi:10.1371/journal.pone.0047134 (2012).

27 Pires, N. M. *et al.* Activation of nuclear receptor Nur77 by 6-mercaptopurine protects against neointima formation. *Circulation* **115**, 493-500, doi:10.1161/circulationaha.106.626838 (2007).

28 de Vries, M. R., Simons, K. H., Jukema, J. W., Braun, J. & Quax, P. H. Vein graft failure: from pathophysiology to clinical outcomes. *Nat Rev Cardiol* **13**, 451-470, doi:10.1038/nrcardio.2016.76 (2016).

29 Brunner, G., Nguyen, H., Gabrilove, J., Rifkin, D. B. & Wilson, E. L. Basic fibroblast growth factor expression in human bone marrow and peripheral blood cells. *Blood* **81**, 631-638 (1993).

30 Gabbianelli, M. *et al.* "Pure" human hematopoietic progenitors: permissive action of basic fibroblast growth factor. *Science (New York, N.Y.)* **249**, 1561-1564, doi:10.1126/science.2218497 (1990).

31 Gabrilove, J. L., White, K., Rahman, Z. & Wilson, E. L. Stem cell factor and basic fibroblast growth factor are synergistic in augmenting committed myeloid progenitor cell growth. *Blood* **83**, 907-910 (1994).

32 Coutu, D. L. & Galipeau, J. Roles of FGF signaling in stem cell self-renewal, senescence and aging. *Aging* **3**, 920-933, doi:10.18632/aging.100369 (2011).

33 Zhang, H. & Issekutz, A. C. Growth factor regulation of neutrophil-endothelial cell interactions. *Journal of leukocyte biology* **70**, 225-232 (2001).

34 Tanaka, K. *et al.* Augmented angiogenesis in adventitia promotes growth of atherosclerotic plaque in apolipoprotein E-deficient mice. *Atherosclerosis* **215**, 366-373, doi:10.1016/j.atherosclerosis.2011.01.016 (2011).

35 Mollmark, J. I. *et al.* Fibroblast growth factor-2 is required for vasa vasorum plexus stability in hypercholesterolemic mice. *Arterioscler Thromb Vasc Biol* **32**, 2644-2651, doi:10.1161/atvbaha.112.252544 (2012).

36 Underwood, P. A., Bean, P. A. & Gamble, J. R. Rate of endothelial expansion is controlled by cell:cell adhesion. *The international journal of biochemistry & cell biology* **34**, 55-69, doi:10.1016/s1357-2725(01)00100-5 (2002).

37 Chen, P. Y., Qin, L., Li, G., Tellides, G. & Simons, M. Smooth muscle FGF/TGFbeta cross talk regulates atherosclerosis progression. *EMBO molecular medicine* **8**, 712-728, doi:10.15252/emmm.201506181 (2016).

38 Parma, L. *et al.* Prolonged Hyperoxygenation Treatment Improves Vein Graft Patency and Decreases Macrophage Content in Atherosclerotic Lesions in ApoE3*Leiden Mice. *Cells* **9**, doi:10.3390/cells9020336 (2020).

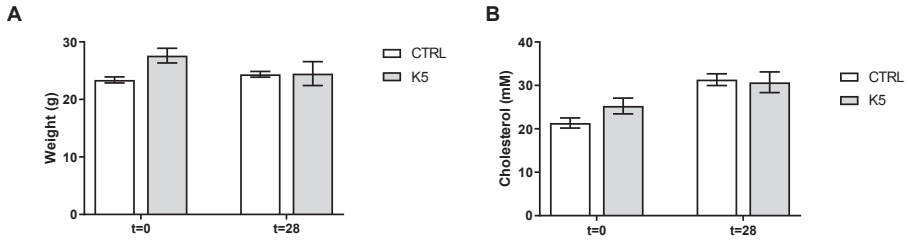
39 de Vries, M. R. *et al.* C57BL/6 NK cell gene complex is crucially involved in vascular remodeling. *Journal of molecular and cellular cardiology* **64**, 51-58, doi:10.1016/j.yjmcc.2013.08.009 (2013).

40 Doorn, J. *et al.* A small molecule approach to engineering vascularized tissue. *Biomaterials* **34**, 3053-3063, doi:10.1016/j.biomaterials.2012.12.037 (2013).

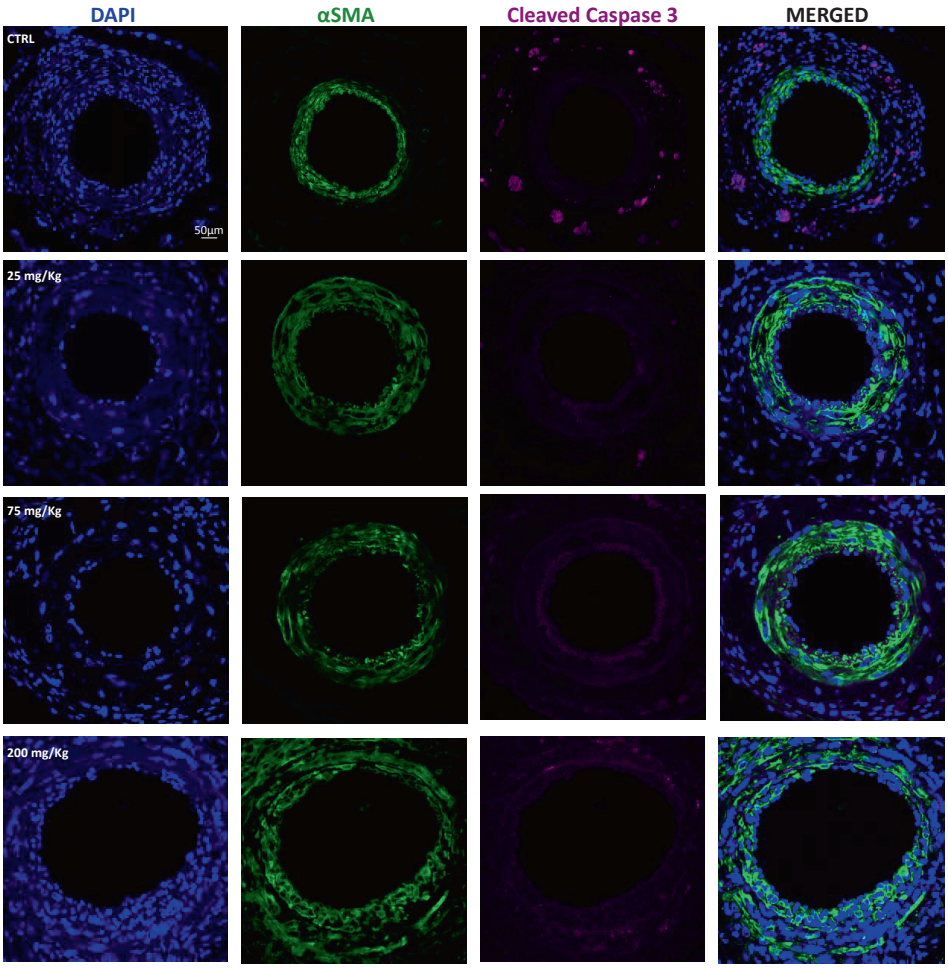
41 Nowak-Sliwinska, P. *et al.* Consensus guidelines for the use and interpretation of angiogenesis assays. *Angiogenesis* **21**, 425-532, doi:10.1007/s10456-018-9613-x (2018).

42 van der Kwast, R. *et al.* Adenosine-to-Inosine Editing of MicroRNA-487b Alters Target Gene Selection After Ischemia and Promotes Neovascularization. *Circ Res* **122**, 444-456, doi:10.1161/circresaha.117.312345 (2018).

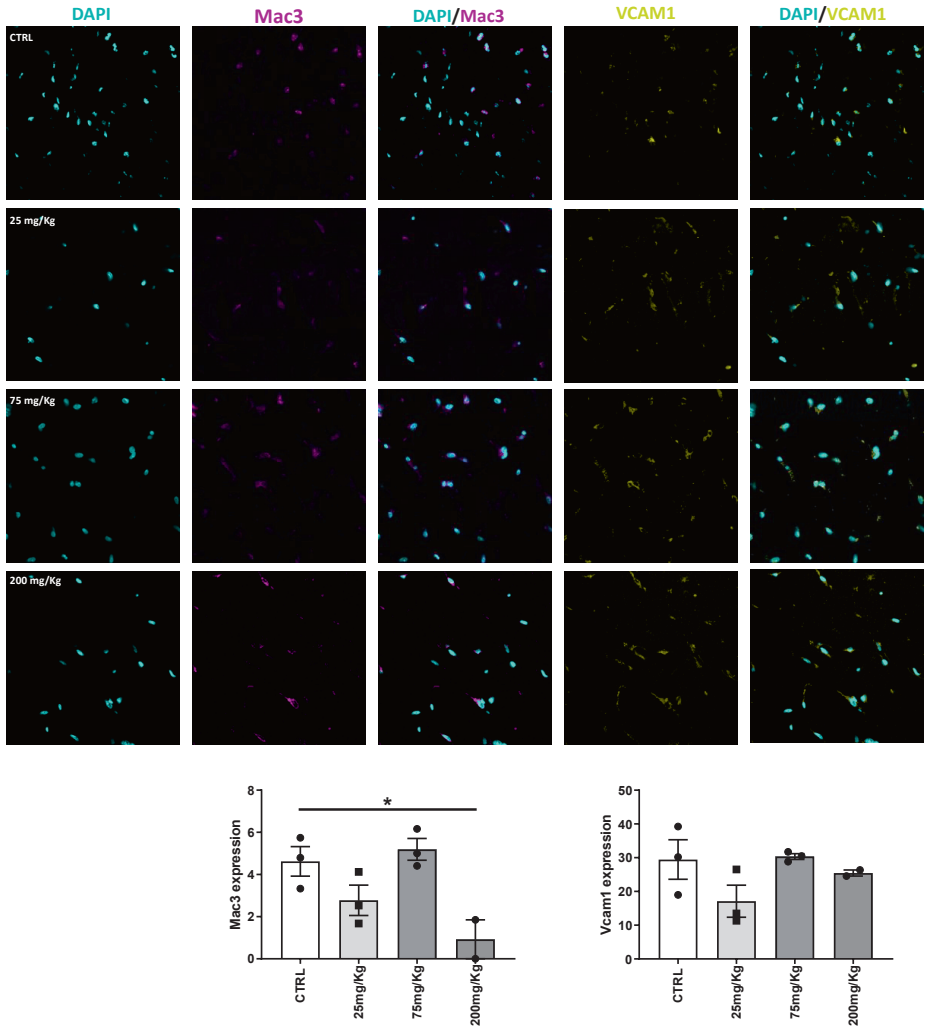
Supplemental material



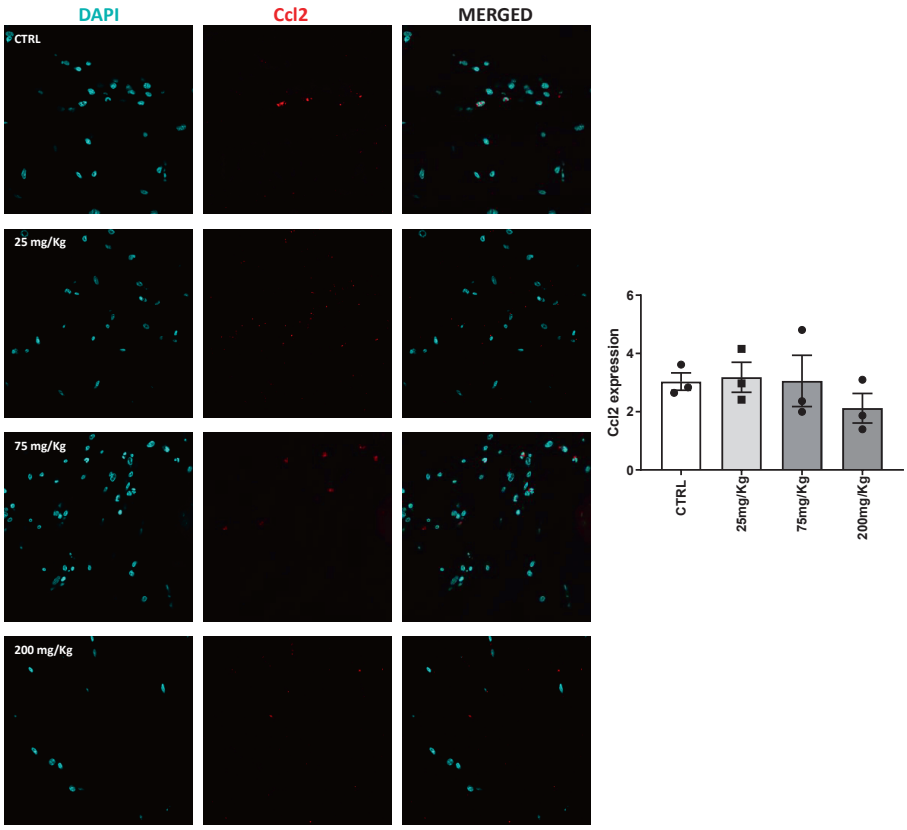
Supplementary figure 1. Bodyweight and cholesterol levels. (A). Bodyweight before (t=0) and 28 days after surgery (t=28) of control and K5 treated mice. (B). Plasma cholesterol levels before (t=0) and 28 days after surgery (t=28) of control and K5 treated mice.



Supplementary information 2. Representative pictures of femoral artery cuffs of ctrl and K5 treated groups stained for DAPI (blue), αSMA (green) and Cleaved caspase 3 (magenta).



Supplementary information 3. Representative pictures of Matrigel plugs of ctrl and K5 treated groups stained for DAPI (cyan), Mac3 (magenta) and VCAM-1 (yellow) and respective quantifications. Data are presented as mean±SEM *p<0.05; by one way Anova.



Supplementary information 4. Representative pictures of Matrigel plugs of ctrl and K5 treated groups stained for DAPI (cyan) and CCL-2 (red) and respective quantification. No significant differences could be observed by one way Anova.

CHAPTER 6

TKT BLOCKADE REDUCES INFLAMMATION AND ANGIOGENESIS IN VITRO

L Parma[1,2], MC Schmit [1,2], S Van Den Bogaert[1,2], MR de Vries[1,2], PHA Quax[1,2]

[1]Department of Surgery and [2]Einthoven Laboratory for Experimental Vascular Medicine, Leiden University Medical Center, Leiden, The Netherlands

Manuscript in preparation

Abstract

Intraplaque angiogenesis and high pro-inflammatory macrophage content increase the chance of unstable atherosclerotic plaque rupture and thrombus formation leading to myocardial infarction. Transketolase (TKT) is an enzyme in the Pentose Phosphate Pathway (PPP) that regulates the production of building blocks necessary for cell proliferation and was found to be upregulated in unstable human atherosclerotic lesions. Therefore, we examined the effect of TKT blockade, using Oxythiamine, on *in vitro* endothelial cell (EC) migration and proliferation and pro-inflammatory M1 macrophage polarization.

We found that TKT was expressed in ECs and macrophages in endarterectomies of unstable human carotid atherosclerotic lesions. When mimicking the ischemic intraplaque environment in cultured HUVECs, TKT protein level was 3-fold increase when compared to normoxic conditions. TKT blockade under these conditions resulted in 40% decrease in ECs migration and 51% decrease in ECs proliferation.

To investigate the metabolic profile of M1 pro-inflammatory macrophages, we measured the mRNA levels of enzymes involved in glycolysis and PPP. Interestingly, TKT was found to be upregulated by 4.5 fold in pro-inflammatory M1 when compared to M0 macrophages. TKT blockade in M1 macrophages resulted in 30% decrease in cell proliferation as well as a strong reduction in mRNA levels of pro-inflammatory cytokines IL-6, TNFα, Ccl2 and IL1b. Pro-angiogenic VEGF and IL8 mRNA levels were also decreased upon TKT blockade. More importantly we found that HUVECs stimulated with supernatant from Oxythiamine-treated M1 macrophages showed a reduced migration by 20% when compared to control.

Our results show that TKT blockade reduces *in vitro* angiogenesis and inflammation by decreasing EC migration and proliferation, both directly and indirectly by reducing M1 macrophage pro-inflammatory and -angiogenic cytokine production. Therefore these preliminary results show that TKT blockade can be an interesting target to reduce angiogenesis and inflammation in atherosclerosis.

Introduction

Atherosclerotic plaques form over a long period of time as a results of accumulation of lipids, immune cells and smooth muscle cells in the arterial wall [1]. Unstable vulnerable plaques are characterized by intraplaque angiogenesis, intraplaque haemorrhage, accumulation of macrophages, a thin fibrous cap and a large necrotic core [2]. The rupture of an unstable atherosclerotic plaque often results in thrombus formation and cessation of the blood flow, leading to the manifestation of severe clinical symptoms like myocardial infarction and stroke [3].

In the early atherosclerotic disease stage, dysfunctional endothelial cells (ECs) regulate the infiltration of monocytes in the intimal layer of the vessel through expression of adhesion molecules and the release of chemoattractant factors [4]. Monocytes adhere to the damaged ECs and accumulate in the vessel wall where they differentiate into macrophages [4]. Macrophages in the plaque can be broadly divided in two groups: M1 pro-inflammatory macrophages and M2 repair associated macrophages [5-7]. M1 pro-inflammatory macrophages play an important role in plaque progression, in monocyte recruitment into the plaque and in the development of unstable plaque [8]. Moreover, M1 macrophages promote atherosclerosis by maintaining chronic inflammation, leading to the formation of foam cell [9].

The release of pro-angiogenic and pro-inflammatory factors by macrophages together with local hypoxia within the atherosclerotic plaque trigger endothelial cell migration and proliferation from the vasa vasora leading to the formation of neovessels, a process called intraplaque angiogenesis [10,11]. The neovessels that are formed are immature and leaky [2]. In fact they are a network of immature endothelial sprouts without a complete supporting pericyte coverage [12]. These newly formed vessels represent an exit point for the extravasation of red blood cells and inflammatory cells, a process called intraplaque haemorrhage [2]. The accumulation of these cells in the plaque contributes to the expansion of the necrotic core of the plaque and the stimulation of local inflammation, leading to plaque instability.

Intraplaque angiogenesis and inflammation are therefore strongly connected in atherosclerosis. The interaction between these two processes forms a vicious cycle that

modifies the microenvironment composition of the plaque and drives the plaque towards an unstable phenotype.

It was previously shown that high-risk human plaques, characterized as being symptomatic, rich in intraplaque haemorrhage and macrophages with elevated inflammatory mediators, had a specific metabolite signature, distinct from the metabolite profile of low-risk plaques [13]. In these plaques the expression of glycolysis and pentose phosphate pathway (PPP) genes was significantly higher compared to asymptomatic plaques [13].

The PPP is one of the metabolic processes used by the cells to break down the glucose for energy production [14]. This pathway has two distinct phases, the oxidative phase and non-oxidative phase. Glucose 6-phosphate (G6P) coming from the glycolysis is converted into ribose 5-phosphate (R5P) in the oxidative branch, generating nicotinamide adenine dinucleotide phosphate (NADPH) [14]. The non-oxidative branch, through the action of the key enzyme transketolase (TKT), supplies precursors for nucleotide synthesis and glycolytic metabolites. TKT, a thiamine-dependent enzyme, reversibly links the non-oxidative branch of the PPP to the glycolysis and is responsible for the production of building blocks necessary for cell proliferation as well as the production of glycolytic intermediates [15].

Due to their role played in driving plaque instability and the fact that they rely on anabolic pathways like glycolysis and PPP to produce energy, we hypothesized that TKT blockade in *in vitro* cultured ECs and macrophages would reduce their proliferation rate and by decreasing the amount of energy available reduce their pro-inflammatory and pro-angiogenic cytokine production.

Therefore in the present study we assessed the presence of TKT in human endarterectomies atherosclerotic lesions and the effect of TKT blockade on ECs migration and proliferation and on in vitro macrophage M1 polarization. Moreover, we studied the functional effect of TKT blockade in macrophages on the migration of ECs.

Material and methods

Tissue preparation and immunohistochemical staining

Anonymous carotid endarterectomy specimens were obtained at the LUMC in accordance with guidelines set out by the 'Code for Proper Secondary Use of Human Tissue' of the Dutch Federation of Biomedical Scientific Societies (Federa) and conform with the principles outlined in the Declaration of Helsinki.

The tissue samples were paraffin embedded, cut in sections of 5μm and fixed on glass slides.

Antibodies directed at TKT (HPA029480, Sigma Aldrich), CD68 (M0876, DAKO) and CD31 (JC70A, DAKO) were used for immunohistochemical staining. Alexa Fluor 647 and Alexa Fluor 488 antibodies (Life Technologies) were used as secondary antibodies and slides were mounted with ProLong Gold mountant with DAPI (P36935, ThermoFisher). Stained slides were scanned using the Pannoramic MIDI II digital slide scanner (3DHISTECH, Budapest, Hungary) and digital photographed with Caseviewer (3DHISTECH, Budapest, Hungary).

Cells and cell culture

For the isolation of HUVECS anonymous umbilical cords were obtained in accordance with guidelines set out by the 'Code for Proper Secondary Use of Human Tissue' of the Dutch Federation of Biomedical Scientific Societies (Federa), and conform to the principles outlined in the Declaration of Helsinki. Isolation and culturing of primary vein human umbilical cells was performed as described by Van der Kwast et al [16]. In brief, umbilical cords were collected from full-term pregnancies and stored in sterile PBS at 4°C and subsequently used for cell isolation within 5 days. For HUVEC isolation, cannulas were inserted on each side of the vein of an umbilical cord and flushed with sterile PBS. The vein was infused with 0.075% collagenase type II (Worthington, Lakewood, NJ, USA) and incubated at 37°C for 20 minutes. The collagenase solution was collected and the vein was flushed with PBS in order to collect all detached endothelial cells. The cell suspension was centrifuged at 300 g for 5 minutes and the pellet was resuspended in HUVEC culture medium (EBM-2 Basal Medium (CC-3156) and EGMTM-2 SingleQuotsTM Supplements (CC-4176), Lonza, Basel, Switzerland). HUVECs were cultured in plates coated with 1% fibronectin. Cells were used between passage 2 and 4. Low serum culture medium consisted of EBM-2 Basal Medium (CC-3156, Lonza) supplemented with 0.2% FBS and 1% GA-1000 (SingleQuotsTM Supplements, CC-4176, Lonza).

Isolation and culturing of primary bone marrow derived macrophages was performed as described by Parma et al [17]. Monocytes were isolated from bone marrow of tibias and femurs of male ApoE3*Leiden mice on normal chow diet (n=4) and cultured in complete medium (RPMI 1640, 52400-025, ThermoFisher, GIBCO, Waltham, MA, USA) supplemented with 25% heat inactivated fetal calf serum (Gibco® by Life Technologies), 100 U/mL Penicillin/Streptomycin (ThermoFisher, GIBCO, Waltham, MA, USA) and 0.1 mg/mL macrophage colony-stimulating factor (14-8983-80, ThermoFisher, E-Bioscience Waltham, MA, USA). After eight days the derived macrophages were used to perform a cell proliferation assay.

THP-1 cells (human monocytic cell line) were cultured in complete medium (RPMI 1640, 52400-025, ThermoFisher, GIBCO, Waltham, MA, USA) supplemented with 25% heat inactivated fetal calf serum (Gibco® by Life Technologies), 100 U/mL Penicillin/Streptomycin (ThermoFisher, GIBCO, Waltham, MA, USA). THP-1 were differentiated into macrophages using phorbol-12-myristate-13-acetate (PMA, Lot#SLBV2992) at a concentration of 10 μg/mL. After 72 hours incubation at 37°C, macrophages were polarized into M1 pro-inflammatory macrophages by adding 100 ng/mL IFNγ (AF-300-02, Peprotech) and 100 ng/mL LPS (*Escherichia coli* K-235, Sigma-Aldrich).

BMM, HUVECs and THP-1 were cultured at 37°C in a humidified 5% CO_2 environment. Culture medium was refreshed every 2 days. Cells were passed using trypsin-EDTA (Sigma, Steinheim, Germany) at 90-100% confluency.

Oxythiamine preparation

For all the experiments performed, Oxythiamine (OT) (Oxythiamine chloride hydrochloride Sigma-Aldrich life science O4000-1G), a known TKT blocker [18], was dissolved in PBS and used at a final concentration of 50 μM, 100 μM and 250 μM.

Immunocytochemistry

HUVECs were cultured in a 12 wells chamber slide (81201, Ibidi) and treated with either complete medium, low serum medium or low serum starve medium combined with oxygen deprived culture conditions (1% O_2, named ischemia) for 24 hours. Cells were then washed

with PBS, fixated with 4% paraformaldehyde (Merck KGaA) per well for 10 minutes and then rinsed with PBS. Next, permeabilization buffer (5% goat serum + 1% BSA (Roche Diagnostics) + 0.1% Triton-X100 (Sigma T8532) in PBS) was added to each well for 60 minutes at room temperature. Cells were washed three times with PBS and afterwards primary antibodies directed at TKT (HPA029480, Sigma Aldrich) and CD31 (M0823, Dako) were applied. Slides were incubated overnight at 4°C and afterward Alexa Fluor 647 and Alexa Fluor 488 secondary antibodies (Life Technologies) were used and slides were mounted with ProLong Gold mountant with DAPI (P36935, ThermoFisher). Stained slides were photographed using Pannoramic MIDI II digital slide scanner (3DHISTECH, Budapest, Hungary) and Fiji image analysis software was used to quantify the mean grey value expression of the targets (ImageJ, Bethesda, MD, USA).

In Vitro Ischemia culture conditions

For in vitro ischemia experiments, HUVECs were seeded in separate 12-well plates at 80% confluency and subsequently cultured in either: normoxia control conditions for 24 h (complete culture medium and ~20% oxygen), 24 h hypoxia conditions (complete medium and hypoxia of 1% oxygen) or 24 h ischemic conditions (low serum medium and hypoxia of 1% oxygen). At the end of the experiment, cells were washed with PBS and harvested with TRIzol Reagent (Invitrogen).

Scratch wound healing assay

For the scratch wound healing assay (n=3 individual replicates), HUVECs were plated on a 12 well plate and grown until 80% confluence in complete culture medium as previously reported [16]. Cells were then treated with low serum medium or low serum supplemented with OT in increasing concentrations for 24 hours. After 24h, medium was removed and a scratch-wound was introduced across the diameter of each well of a 12 wells plate using a p200 pipette tip. Subsequently, the cells were washed with PBS and medium was replaced by new low serum culture medium with OT in increasing concentrations. For the in vitro ischemia model, cells were now placed in hypoxia at 1% O_2 level for 24 hours. Two locations along the scratch-wound were marked per well and scratch-wound closure at these sites was imaged by taking pictures at time 0h and 18h after scratch-wound introduction using live phase-contrast microscopy (Axiovert 40C, Carl Zeiss). Average scratch-wound closure after 18h was

objectively calculated per well by measuring difference in cell coverage at 18h vs 0h using the wound healing tool macro for ImageJ.

MTT assay

Cell proliferation (n=3 individual replicates) was measured using MTT assay. HUVECs and BMM were plated at 5.000 cells/well in a 96 well plate and grown until 80% confluency in complete culture medium, after which they were incubated with low serum medium or low serum supplemented with OT in increasing concentrations for 24 hours. The medium was then replaced by treatment mixtures consisting of low serum medium with or without OT in increasing concentrations. For the in vitro ischemia model, cells were now placed in hypoxia at 1% O_2 level for 24 hours. After 24 hours incubation, 10 µL MTT (Thiazolyl blue tetrazolium bromide, Sigma M5655) was added directly to each well and cells were incubated at 37°C in a humidified 5% CO_2 environment for 4 hours. Subsequently, 75 µL medium was removed from each well and 75 µL isopropanol/0.1 N HCL was added per well. After incubating the plate for 90 minutes on a shaker platform, absorbance was read at 570 nm with a Cytation 5 spectrophotometer (BioTek) and the mitochondrial metabolic activity was quantified as a representative measure of cell proliferation.

Preparation of THP-1 conditioned media and stimulation of HUVECs

THP-1 cells were differentiated in M1 macrophages and treated with or without different concentrations of OT in M199 medium supplemented with 10% heat inactivated fetal calf serum (Gibco® by Life Technologies) and 100 U/mL Penicillin/Streptomycin (ThermoFisher, GIBCO, Waltham, MA, USA) for 24 hours. After stimulation, the cells were pelleted at 1000 g for 5 min, and the supernatants (conditioned media) were collected.

HUVECs were plated in a 12 wells plate and the protocol for scratch wound healing was followed. After a scratch was introduced in each well, the cells were washed with PBS and treated with conditioned medium from M1 macrophages obtained as explained above. Two locations along the scratch-wound were marked per well and scratch-wound closure at these sites was imaged by taking pictures at time 0h and 18h after scratch-wound introduction using live phase-contrast microscopy (Axiovert 40C, Carl Zeiss). Average scratch-wound closure after 18h was objectively calculated per well by measuring difference in cell coverage at 18h vs 0h using the wound healing tool macro for ImageJ.

RNA isolation and cDNA synthesis

Cells were washed with PBS and 700 μL Trizol was added to each well. The RNA was isolated according to the protocol and the RNA concentration was determined by using Nanodrop® ND-1000 spectrophotometer (Isogen).

RNA levels were normalized between samples and the total RNA was converted to cDNA using the High Capacity cDNA Reverse Transcription Kit (Applied Biosystems). The reaction was carried out by the Tetrad® 2 Peltier Thermal Cycler.

qPCR

The expression of mRNAs within cDNA samples was quantified by qPCR using Quantitect SYBR Green (QIAGEN) on the ViiA7 Real-Time PCR System (Applied Biosystems). mRNA expression was measured with intron-spanning primers and normalized against RPLP0 mRNA expression, a household gene that remains stable under ischemic conditions. All primer sequences are provided in Table S1.

Statistical analysis

Statistical analysis were performed using Graphpad Prism. Results are expressed as mean ± SEM. A two-tailed Student's T-test was used to compare individual groups. Non-Gaussian distributed data were analyzed using a Mann-Whitney U test. Probability values of <0.05 were regarded as significant.

Results

Human endarterectomies express TKT in macrophages

We evaluated the presence of TKT in human atherosclerotic endarterectomies. TKT was found to be present throughout the human atherosclerotic lesions studied as shown in Figure 1A.

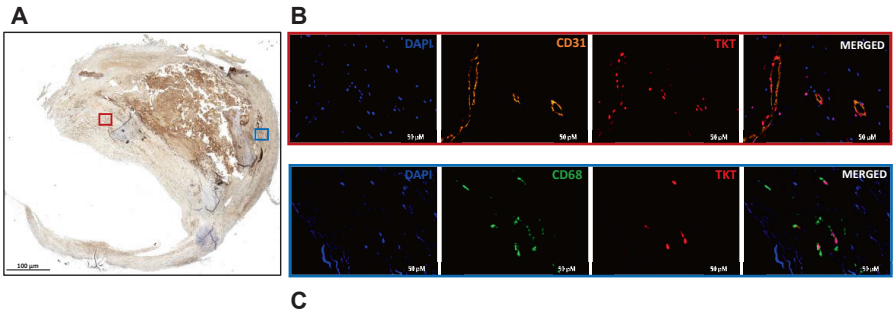


Figure 1. (A) Example of a human atherosclerotic endarterectomy immunohistochemically stained for TKT. In the **RED BOX** examples of neovessels positive for TKT. Cells positive for in blue DAPI, in orange CD31 and in red TKT are present. In the **BLUE BOX** examples of macrophages positive for TKT. Cells positive for in blue DAPI, in green CD68 and in red TKT are present.

When looking at the cellular localization, TKT was found to be lowly expressed in the cytoplasm of ECs and highly expressed in the nuclei of the cells, seen as a double positive signal of TKT and DAPI staining (Fig.1B). Importantly TKT was also found to be expressed with the same pattern, low expression in the cytoplasm and high expression in the nucleus, in macrophages (Fig.1C) throughout the lesion.

TKT is highly expresses in oxygen/serum deprived HUVECs and its blockade reduces HUVECs migration and proliferation

The expression of TKT in HUVECs was studied in different cell culture conditions. Cells were cultured either in normoxia (21% O_2) in complete medium, hypoxia (1% O_2) in complete medium or ischemia (1% O_2 and low serum medium) to mimic the intraplaque environment in which ECs exploit their functions in atherosclerosis. Cytoplasm and nuclei of HUVECs in all three conditions studied were found to be strongly positive for TKT (Fig.2A). Quantification of the staining showed that the expression of TKT was significantly higher in cells in ischemic conditions when compared to cells in normoxia and hypoxia (Fig.2A, p=0.02 and 0.04

respectively). Under ischemic conditions TKT expression was 3-fold higher than in hypoxia and 4.4-fold higher than in normoxia (Fig.2A).

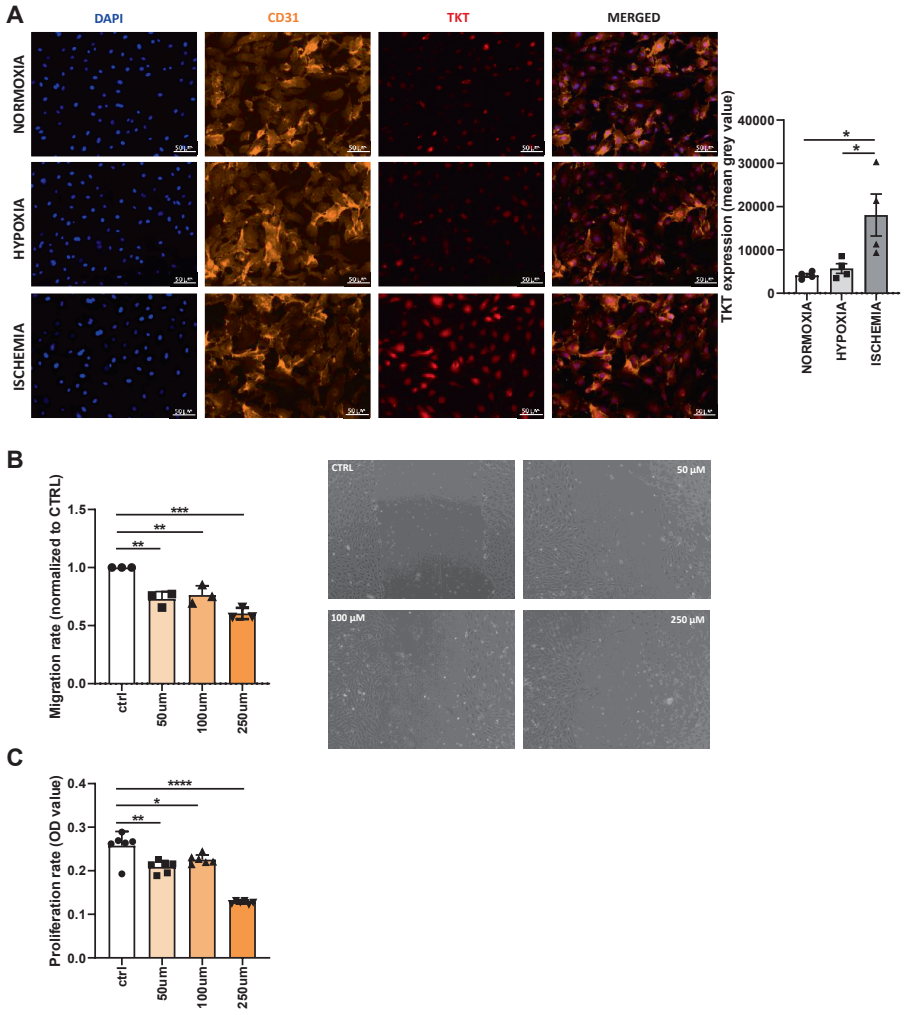


Figure 2. (A) Example of HUVECs ICC staining for DAPI (blue), CD31 (orange) and TKT (red) and quantification of the staining. (B) Quantification of HUVECs migration and representative images and (C) quantification of HUVECs proliferation upon TKT blockade. Data are presented as mean ± SEM. * $p < 0.05$, ** $p < 0.01$; *** $p < 0.001$; **** $p < 0.0001$ by two-sided Student's t-test.

Since intraplaque angiogenesis takes place under deprived oxygen and nutrient conditions and due to the higher expression of TKT in *in vitro* ischemic conditions, we assessed the effect of TKT blockade on ECs migration and proliferation under these specific conditions. Oxythiamine (OT) treatment resulted in a significant reduction of ECs migration with all the

doses tested (50, 100 and 250 µM) by 27%, 24% and 40% respectively when compared to control (p=0.001, 0.006 and 0.0001 respectively. Fig.2B).

ECs proliferation was also reduced upon TKT blockade. Interestingly, all doses of OT tested decreased ECs proliferation by respectively 19%, 13% and 51% when compared to untreated cells (p=0.008, 0.04 and 0.0001, Fig.2C).

Human M1 macrophages show an upregulated expression of genes involved in glycolysis and PPP

To mimic the pro-inflammatory intraplaque environment, we polarized human THP-1 derived macrophages into M1 pro-inflammatory phenotype. To confirm the surface markers profile of the differentiated M1 human THP-1 macrophages, mRNA expression of M1 (CD80, CD86) and M2 (CD206) specific surface markers was evaluated (Fig. 3A, B and C). The expression of CD80 and CD86 was significantly upregulated in the M1 macrophages compared to the M0 control macrophages (Fig. 3A and B. p=0.0005 and 0.001 respectively).

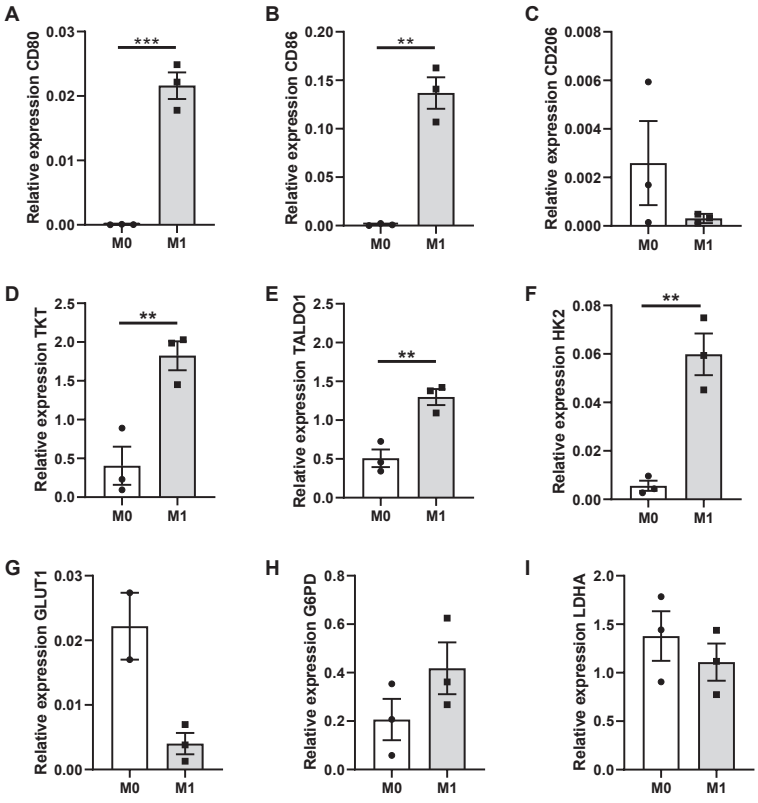


Figure 3. (A) Total mRNA expression of M1 surface marker CD80 and (B) CD86 relative to RPL13. (C) Total mRNA expression of M2 surface marker CD206 relative to RPL13. PPP enzymes (D) TKT and (E) TALDO1 total mRNA expression relative to RPL13. Total mRNA expression of (F) HK2, (G) GLUT1, (H) G6PD and (I) LDHA relative to RPL13. Data are presented as mean ± SEM. * $p < 0.05$, ** $p < 0.01$; *** $p < 0.001$; by two-sided Student's t test.

The M2 specific surface marker CD206, was expressed in low amount in both M1 and M0 macrophages (Fig.3C). mRNA levels of these markers confirm the pro-inflammatory M1 character of the differentiated macrophages.

The mRNA levels of TKT and other enzymes involved in glycolysis and PPP were evaluated to examine the role of these pathways in M1 macrophages. The expression of TKT was significantly upregulated in M1 macrophages compared to M0 by a 4.5 fold increase (Fig.3D. p=0.01). The expression of TALDO1, enzyme in the non-oxidative branch of the PPP, and HK2, responsible for the production of glucose-6-phosphate was also increased in M1 macrophages (Fig.3E and F. p=0.006, 0.003 respectively). No differences could be found in the expression of other glycolysis enzymes, LDHA and GLUT1, as well as G6PD, enzyme in the oxidative branch of the PPP, when comparing M0 and M1 macrophages (Fig.3G, H and I. p=0.4, 0.2 and 0.19 respectively).

TKT blockade reduces proliferation of M1 macrophages derived from bone marrow of ApoE3*Leiden mice

THP-1 monocytes differentiation into macrophages results in increased cell adherence and loss of proliferative activity (Schwende et al., 1996).

Therefore, to study the effect of TKT blockade on macrophage proliferation we used primary Apoe3*Leiden bone marrow derived macrophages. OT treatment significantly reduced BMM proliferation rate when compared to control M1 untreated macrophages (Fig. 4A). Macrophage proliferation was reduced by 15% and 31% in the cells treated with 100µM and 250 µM OT respectively when compared to control M1 macrophages (Fig.4A. p=0.0246 and <0.0001).

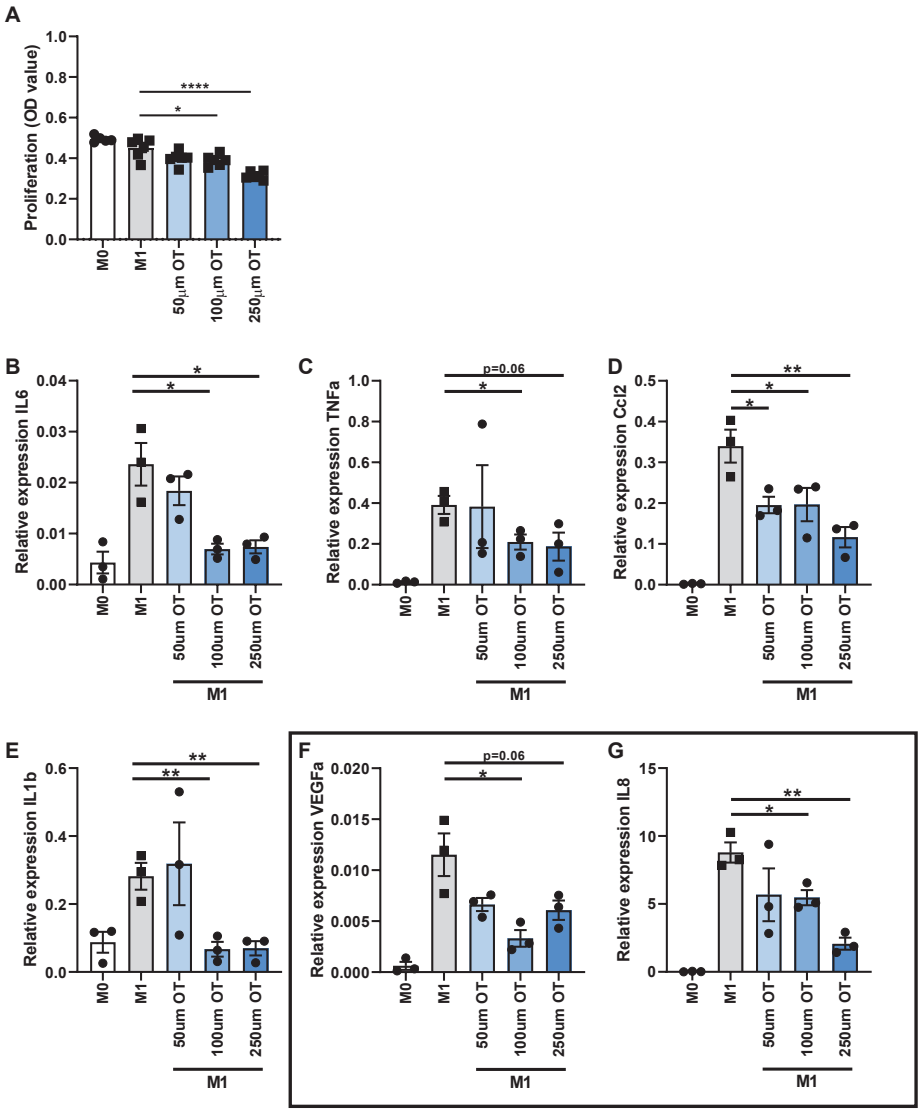


Figure 4. (A) Quantification of BMM proliferation upon TKT blockade. Total mRNA expression of pro-inflammatory cytokines (B) IL6, (C) TNFa, (D) Ccl2 and (E) IL1b relative to RPL13. Dose-dependent of pro-inflammatory cytokines mRNA levels in OT treated groups when compared to M1 untreated macrophages (IL-6 in groups treated with 50, 100 and 250 μM OT p=0.3, 0.01 and 0.02 respectively), (TNFa in groups treated with 50, 100 and 250 μM OT p=0.9, 0.03 and 0.06 respectively), (MCP-1 in groups treated with 50, 100 and 250 μM OT p=0.03, 0.06 and 0.009 respectively), (IL-1b in groups treated with 50, 100 and 250 μM OT p= 0.78, 0.008 and 0.009 respectively).

Pro-angiogenic cytokines total mRNA expression, (F) VEGF-A and (G) IL8 relative to RPL13. Data are presented as mean ± SEM. * $p < 0.05$, ** $p < 0.01$; *** $p < 0.001$; by two-sided Student's t test.

Gene expression of pro-inflammatory and pro-angiogenic cytokines in human THP-1 M1 macrophages are decreased upon TKT blockade

The M1 macrophages mRNA expression profile of pro-inflammatory and pro-angiogenic cytokines was assessed upon TKT blockage. The mRNA expression of the pro-inflammatory cytokines, IL6, TNFα, CCl2 and IL1b was higher in untreated M1 macrophages compared to M0 macrophages (Fig.4B, C, D and E. p=0.01, 0.001, 0.001 and 0.01). More importantly, there was a downregulation in mRNA levels of pro-inflammatory markers in OT treated M1 macrophages compared to untreated M1 (Fig.4B, C, D and E). TKT blockade in M1 macrophages resulted in a dose-dependent reduction in expression of IL-6 (50, 100 and 250 μM OT p=0.3, 0.01 and 0.02 respectively), TNFa (50, 100 and 250 μM OT p=0.9, 0.03 and 0.06 respectively), MCP-1 (50, 100 and 250 μM OT p=0.03, 0.06 and 0.009 respectively) and IL-1β (50, 100 and 250 μM OT p= 0.78, 0.008 and 0.009 respectively) when compared to untreated M1 macrophages. The same pattern was observed in the expression of pro-angiogenic factors. The mRNA expressions of VEGF-A and IL8 were examined. Expression of VEGF-A and IL8 was higher in M1 compared to M0 (Fig.4F and G. p=0.006 and 0.0003 respectively) but more importantly their expression was dose-dependently and significantly reduced upon TKT blockage (VEGF-A in groups treated with 50, 100 and 250 μM OT p=0.08, 0.02 and 0.06 respectively) (IL-8 in groups treated with 50, 100 and 250 μM OT p=0.2, 0.02 and 0.001 respectively).

Functional effect of TKT blockade in M1 macrophages on ECs migration

We next examined if the reduction in production of pro-angiogenic factors by M1 macrophages treated with OT had a functional effect on ECs migration.

The migration rate of HUVECs was dose-dependently and significantly decreased in cells treated with medium deriving from THP-1 derived M1 macrophages in which TKT was blocked when compared to cells treated with medium deriving from untreated M1 control macrophages (Fig.5A. p=0.09 for group treated with 50 μM, p=0.03 for group treated with 100 μM and p=0.04 for group treated with 250 μM). ECs migration was reduced by 14% with the dose of 50 μM and by 20% with the doses of 100 and 250 μM respectively.

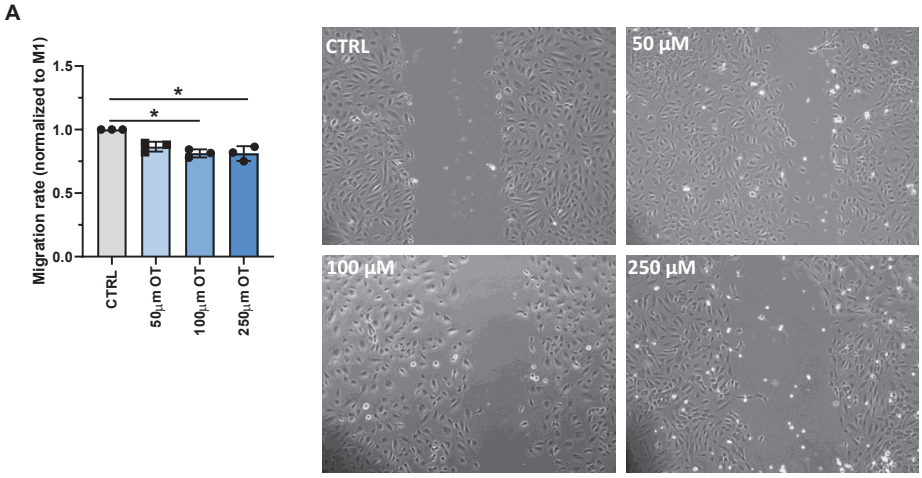


Figure 5. (A) Quantification and representative images of HUVECs migration treated with conditioned media from M1 macrophages in which TKT was blocked. . Data are presented as mean ± SEM. * $p < 0.05$; by two-sided Student's t test.

Discussion

In this study we show that TKT is present in ECs and macrophages in human atherosclerotic lesions. We found that *in vitro* TKT is overexpressed in endothelial cells exposed to reduced oxygen and serum levels and that under these conditions TKT blockade results in decreased ECs migration and proliferation. Moreover, we demonstrate that TKT mRNA level is upregulated in pro-inflammatory M1 macrophages and that upon TKT blockade pro-inflammatory and pro-angiogenic cytokines production is reduced in these cells. We also show that this reduction in production of pro-angiogenic factors has a functional effect by lowering ECs migration.

Tomas et al. found that the expression of glycolysis and PPP genes, including TKT, was significantly higher in plaques from patients displaying clinical symptoms compared to those from asymptomatic patients [13]. These symptomatic plaques were classified as high-risk plaques containing high levels of inflammation, intraplaque angiogenesis and haemorrhage [13]. In line with these observations in the present study we show that TKT was present in endothelial cells and macrophages of human symptomatic atherosclerotic lesions and that *in vitro* TKT mRNA expression, together with the expression of TALDO1 (PPP enzyme) and HK2 (glycolysis enzyme) was upregulated in M1 pro-inflammatory macrophages when compared to M0 macrophages. More importantly we here demonstrate that the protein expression of TKT is upregulated in ECs cells cultured under ischemic conditions, mimicking the intraplaque environment in which these cells form neovessels, when compared to more physiologic normoxic conditions. Our findings point to an altered metabolism in ECs and macrophages under conditions that mimic the intraplaque environment and may imply an important role of TKT in plaque instability.

It is known that altered endothelial cell metabolism is associated with angiogenesis and dysfunctional ECs contribute to atherosclerosis [19]. These ECs mostly rely on glycolysis and pathways connected to glycolysis, such as the PPP, to produce energy and biomass used for migration and proliferation [20]. In a similar way, macrophages use the same pathways to migrate throughout the plaque and proliferate [21]. It was previously shown that TKT blockade using OT resulted in reduced ECs migration and proliferation of Ehrlich's tumor cells [22,23]. Another observation was that fast dividing cells express more TKT than relatively slow

dividing cells [24]. We here found that TKT blockade results in reduced ECs migration and proliferation in HUVECs and decrease proliferation in M1 macrophages. These findings indicate that TKT might be an important target to reduce intraplaque angiogenesis and inflammation.

In the present study we show that cultured M1 pro-inflammatory macrophages present an increased expression of TKT and other enzymes involved in PPP and glycolysis. Our findings confirm what Haschemi et al. previously revealed, that M1 polarization in macrophages results in a functional metabolic adaptation with an enhanced PPP and glycolysis in vitro [25].

A recent study showed the importance of PPP in M1 macrophages, by revealing that selective blockade of G6PD (an enzyme in the oxidative branch of the PPP) in macrophages results in impaired LPS-induced pro-inflammatory cytokine secretion in a hypercholesterolemic mouse model [26]. In accordance with these findings in the present study we show that the expression of pro-inflammatory cytokines significantly decreased upon TKT blockade in human M1 macrophages. More importantly we also found that the blockade of TKT in pro-inflammatory macrophages results in reduced pro-angiogenic factors and that this has a functional effect in reducing ECs migration. These results support the hypothesis that PPP contributes to inflammatory macrophage responses and that its blockade might result in reduced inflammation and angiogenesis translatable to an *in vivo* setting.

Based on the results obtained in this study we can conclude that the blockade of TKT reduces *in vitro* angiogenesis and inflammation by reducing ECs migration and proliferation and M1 macrophage pro-inflammatory and -angiogenic cytokine production. Moreover the reduced cytokines production induced by TKT blockade have a functional effect by decreasing ECs migration. Therefore our results show that TKT is a promising target to stabilize atherosclerotic plaques by reducing intraplaque angiogenesis and inflammation.

References

1. Singh, R.B.; Mengi, S.A.; Xu, Y.J.; Arneja, A.S.; Dhalla, N.S. Pathogenesis of atherosclerosis: A multifactorial process. *Experimental and clinical cardiology* **2002**, *7*, 40-53.
2. Parma, L.; Baganha, F.; Quax, P.H.A.; de Vries, M.R. Plaque angiogenesis and intraplaque hemorrhage in atherosclerosis. *Eur J Pharmacol* **2017**, *816*, 107-115, doi:10.1016/j.ejphar.2017.04.028.
3. Bentzon, J.F.; Otsuka, F.; Virmani, R.; Falk, E. Mechanisms of plaque formation and rupture. *Circ Res* **2014**, *114*, 1852-1866, doi:10.1161/circresaha.114.302721.
4. Otsuka, F.; Kramer, M.C.; Woudstra, P.; Yahagi, K.; Ladich, E.; Finn, A.V.; de Winter, R.J.; Kolodgie, F.D.; Wight, T.N.; Davis, H.R., et al. Natural progression of atherosclerosis from pathologic intimal thickening to late fibroatheroma in human coronary arteries: A pathology study. *Atherosclerosis* **2015**, *241*, 772-782, doi:10.1016/j.atherosclerosis.2015.05.011.
5. Lee, S.G.; Oh, J.; Bong, S.K.; Kim, J.S.; Park, S.; Kim, S.; Park, S.; Lee, S.H.; Jang, Y. Macrophage polarization and acceleration of atherosclerotic plaques in a swine model. *PloS one* **2018**, *13*, e0193005, doi:10.1371/journal.pone.0193005.
6. Bobryshev, Y.V.; Ivanova, E.A.; Chistiakov, D.A.; Nikiforov, N.G.; Orekhov, A.N. Macrophages and Their Role in Atherosclerosis: Pathophysiology and Transcriptome Analysis. *BioMed research international* **2016**, *2016*, 9582430, doi:10.1155/2016/9582430.
7. Llodra, J.; Angeli, V.; Liu, J.; Trogan, E.; Fisher, E.A.; Randolph, G.J. Emigration of monocyte-derived cells from atherosclerotic lesions characterizes regressive, but not progressive, plaques. *Proceedings of the National Academy of Sciences of the United States of America* **2004**, *101*, 11779-11784, doi:10.1073/pnas.0403259101.
8. Davies, M.J. Detecting vulnerable coronary plaques. *Lancet (London, England)* **1996**, *347*, 1422-1423, doi:10.1016/s0140-6736(96)91677-3.
9. Koltsova, E.K.; Hedrick, C.C.; Ley, K. Myeloid cells in atherosclerosis: a delicate balance of anti-inflammatory and proinflammatory mechanisms. *Curr Opin Lipidol* **2013**, *24*, 371-380, doi:10.1097/MOL.0b013e328363d298.
10. Camare, C.; Pucelle, M.; Negre-Salvayre, A.; Salvayre, R. Angiogenesis in the atherosclerotic plaque. *Redox biology* **2017**, *12*, 18-34, doi:10.1016/j.redox.2017.01.007.
11. Sedding, D.G.; Boyle, E.C.; Demandt, J.A.F.; Sluimer, J.C.; Dutzmann, J.; Haverich, A.; Bauersachs, J. Vasa Vasorum Angiogenesis: Key Player in the Initiation and Progression of Atherosclerosis and Potential Target for the Treatment of Cardiovascular Disease. *Frontiers in immunology* **2018**, *9*, 706, doi:10.3389/fimmu.2018.00706.
12. Jain, R.K.; Finn, A.V.; Kolodgie, F.D.; Gold, H.K.; Virmani, R. Antiangiogenic therapy for normalization of atherosclerotic plaque vasculature: a potential strategy for plaque stabilization. *Nature clinical practice. Cardiovascular medicine* **2007**, *4*, 491-502, doi:10.1038/ncpcardio0979.
13. Tomas, L.; Edsfeldt, A.; Mollet, I.G.; Perisic Matic, L.; Prehn, C.; Adamski, J.; Paulsson-Berne, G.; Hedin, U.; Nilsson, J.; Bengtsson, E., et al. Altered metabolism distinguishes high-risk from stable carotid atherosclerotic plaques. *European heart journal* **2018**, *39*, 2301-2310, doi:10.1093/eurheartj/ehy124.
14. Ramos-Martinez, J.I. The regulation of the pentose phosphate pathway: Remember Krebs. *Archives of biochemistry and biophysics* **2017**, *614*, 50-52, doi:10.1016/j.abb.2016.12.012.
15. Horecker, B.L. The pentose phosphate pathway. *J Biol Chem* **2002**, *277*, 47965-47971, doi:10.1074/jbc.X200007200.
16. van der Kwast, R.; van Ingen, E.; Parma, L.; Peters, H.A.B.; Quax, P.H.A.; Nossent, A.Y. Adenosine-to-Inosine Editing of MicroRNA-487b Alters Target Gene Selection After Ischemia and Promotes Neovascularization. *Circ Res* **2018**, *122*, 444-456, doi:10.1161/circresaha.117.312345.
17. Parma, L.; Peters, H.A.B.; Baganha, F.; Sluimer, J.C.; de Vries, M.R.; Quax, P.H.A. Prolonged Hyperoxygenation Treatment Improves Vein Graft Patency and Decreases Macrophage Content in Atherosclerotic Lesions in ApoE3*Leiden Mice. *Cells* **2020**, *9*, doi:10.3390/cells9020336.
18. Wang, J.; Zhang, X.; Ma, D.; Lee, W.P.; Xiao, J.; Zhao, Y.; Go, V.L.; Wang, Q.; Yen, Y.; Recker, R., et al. Inhibition of transketolase by oxythiamine altered dynamics of protein signals in pancreatic cancer cells. *Experimental hematology & oncology* **2013**, *2*, 18, doi:10.1186/2162-3619-2-18.
19. Pircher, A.; Treps, L.; Bodrug, N.; Carmeliet, P. Endothelial cell metabolism: A novel player in atherosclerosis? Basic principles and therapeutic opportunities. *Atherosclerosis* **2016**, *253*, 247-257, doi:10.1016/j.atherosclerosis.2016.08.011.

20. Theodorou, K.; Boon, R.A. Endothelial Cell Metabolism in Atherosclerosis. *Frontiers in cell and developmental biology* **2018**, *6*, 82, doi:10.3389/fcell.2018.00082.
21. Riksen, N.P.; Stienstra, R. Metabolism of innate immune cells: impact on atherosclerosis. *Curr Opin Lipidol* **2018**, *29*, 359-367, doi:10.1097/mol.0000000000000539.
22. Vizan, P.; Sanchez-Tena, S.; Alcarraz-Vizan, G.; Soler, M.; Messeguer, R.; Pujol, M.D.; Lee, W.N.; Cascante, M. Characterization of the metabolic changes underlying growth factor angiogenic activation: identification of new potential therapeutic targets. *Carcinogenesis* **2009**, *30*, 946-952, doi:10.1093/carcin/bgp083.
23. Rais, B.; Comin, B.; Puigjaner, J.; Brandes, J.L.; Creppy, E.; Saboureau, D.; Ennamany, R.; Lee, W.N.; Boros, L.G.; Cascante, M. Oxythiamine and dehydroepiandrosterone induce a G1 phase cycle arrest in Ehrlich's tumor cells through inhibition of the pentose cycle. *FEBS letters* **1999**, *456*, 113-118, doi:10.1016/s0014-5793(99)00924-2.
24. Kathagen-Buhmann, A.; Schulte, A.; Weller, J.; Holz, M.; Herold-Mende, C.; Glass, R.; Lamszus, K. Glycolysis and the pentose phosphate pathway are differentially associated with the dichotomous regulation of glioblastoma cell migration versus proliferation. *Neuro-oncology* **2016**, *18*, 1219-1229, doi:10.1093/neuonc/now024.
25. Haschemi, A.; Kosma, P.; Gille, L.; Evans, C.R.; Burant, C.F.; Starkl, P.; Knapp, B.; Haas, R.; Schmid, J.A.; Jandl, C., et al. The sedoheptulose kinase CARKL directs macrophage polarization through control of glucose metabolism. *Cell metabolism* **2012**, *15*, 813-826, doi:10.1016/j.cmet.2012.04.023.
26. Baardman, J.; Verberk, S.G.S.; Prange, K.H.M.; van Weeghel, M.; van der Velden, S.; Ryan, D.G.; Wust, R.C.I.; Neele, A.E.; Speijer, D.; Denis, S.W., et al. A Defective Pentose Phosphate Pathway Reduces Inflammatory Macrophage Responses during Hypercholesterolemia. *Cell reports* **2018**, *25*, 2044-2052.e2045, doi:10.1016/j.celrep.2018.10.092.

Supplemental material

Target gene	Primer type	Sequence
CD80	FW	ACCTGGCTGAAGTGACGTTA
CD80	RV	TCCAGAGGTTGAGCAAATTATCC
CD86	FW	TTCCCTGATGTTACGAGCAAT
CD86	RV	CCAAGGAATGTGGTCTGGGG
CD206	FW	TTCCCTGATGTTACGAGCAAT
CD206	RV	TGAACGGGAATGCACAGGTT
TKT	FW	ATGGCCTACACCGGCAAATA
TKT	RV	CCATGGCCTCCCATACAGAG
GLUT-1	FW	ACGCTCTGATCCCTCTCAGT
GLUT-1	RV	GCAGTACACACCGATGATGAAG
G6PD	FW	CGAGGCCGTCACCAAGAAC
G6PD	RV	GTAGTGGTCGATGCGGTAGA
LDHA	FW	ATGGCAACTCTAAAGGATCAGC
LDHA	RV	CCAACCCCAACAACTGTAATCT
HK2	FW	TGCCACCAGACTAAACTAGACG
HK2	RV	CCCGTGCCCACAATGAGAC
TALDO-1	FW	CAGCACAGATGCCCGCTTA
TALDO-1	RV	CGGCCCGGAATCTTCTTTAGTA
VEGFa	FW	ATCACCATGCAGATTATGCGG
VEGFa	RV	CCCCTTTCCCTTTCCTCGAAC
IL-6	FW	CCCACACAGACAGCCACTCA
IL-6	RV	CCGTCGAGGATGTACCGAAT
IL-8	FW	CTGGCCGTGGCTCTCTTG
IL-8	RV	CTTGGCAAAACTGCACCTTCA
IL-1β	FW	CGAATCTCCGACCACCACTAC
IL-1β	RV	TCCATGGCCACAACAACTGA
TNFα	FW	GTGCTTGTTCCTCAGCCTCT
TNFα	RV	TTAGAGAGAGGTCCCTGGGG
MCP-1	FW	CTGTGCCTGCTGCTCATAG
MCP-1	RV	AGCTTCTTTGGGACACTTGC
RPL13A	FW	GCTCATGAGGCTACGGAAAC
RPL13A	RV	CCGTACATTCCAGGGCAACA

Table S1. Primer sequences

CHAPTER 7

BIS(MALTOLATO)OXOVANADIUM(IV) INDUCES ANGIOGENESIS VIA PHOSPHORYLATION OF VEGFR2

Laura Parma[1,2], Hendrika A.B. Peters[1,2], Maria E. Johansson[3], Saray Gutiérrez[3], Henk Meijerink[4], Sjef de Kimpe[4], Margreet R. de Vries[1,2], Paul H.A. Quax[1,2]

[1]Department of Surgery and [2]Einthoven Laboratory for Experimental Vascular Medicine, Leiden University Medical Center, Leiden, The Netherlands [3]Department of Physiology, Institute of Neuroscience and Physiology, University of Gothenburg, Gothenburg 43141,Sweden [4]CFM Pharma BV, Industrieweg 40, IJsselstein, The Netherlands

Int J Mol Sci. 2020 Jun 30;21(13):4643.

Abstract

VEGFR2 and VEGF-A play a pivotal role in the process of angiogenesis. VEGFR2 activation is regulated by protein tyrosine phosphatases (PTPs), enzymes that dephosphorylate the receptor and reduce angiogenesis. We aim to study the effect of PTPs blockade using bis(maltolato)oxovanadium(IV) (BMOV) on in vivo wound healing and in vitro angiogenesis. BMOV significantly improves in vivo wound closure by 45% in C57BL/6JRj mice. We found that upon VEGFR2 phosphorylation induced by endogenously produced VEGF-A, the addition of BMOV results in increased cell migration (45%), proliferation (40%) and tube formation (27%) in HUVECs compared to control. In a mouse ex vivo, aortic ring assay BMOV increased the number of sprouts by 3 folds when compared to control. However, BMOV coadministered with exogenous VEGF-A increased ECs migration, proliferation and tube formation by only 41%, 18% and 12% respectively and aortic ring sprouting by only 1-fold. We also found that BMOV enhances VEGFR2 Y951 and p38MAPK phosphorylation, but not ERK1/2. The level of phosphorylation of these residues was the same in the groups treated with BMOV supplemented with exogenous VEGF-A and exogenous VEGF-A only. Our study demonstrates that BMOV is able to enhance wound closure in vivo. Moreover, in the presence of endogenous VEGF-A, BMOV is able to stimulate in vitro angiogenesis by increasing the phosphorylation of VEGFR2 and its downstream proangiogenic enzymes. Importantly, BMOV had a stronger proangiogenic effect compared to its effect in coadministration with exogenous VEGF-A.

Introduction

Angiogenesis is a key process in which new blood vessels grow into ischemic areas and it is mainly defined as the sprouting of new capillaries from existing blood vessels. The process of angiogenesis is regulated by proangiogenic growth factors that act via a family of endothelial receptor tyrosine kinases (RTKs) [1]. Binding of a growth factor to its receptor results in activation of the intracellular kinase domain and autophosphorylation of the receptor on specific tyrosine residues [2]. These events are followed by phosphorylation and activation of different downstream key angiogenic enzymes.

At a cellular level the angiogenic process involves three distinct cell functions: cell-migration, cell proliferation and finally formation of a new mature vessel [3]. These cell functions are carried out by phenotypically different endothelial cells (ECs), respectively: tip cells, stalk cells and phalanx cells [3]. This multistage process involves different RTKs [3,4].

The vascular endothelial growth factor (VEGF) family is composed of five structurally related factors: VEGF-A (also denoted VEGF-A165), VEGF-B, VEGF-C, VEGF-D and placenta growth factor (PLGF). VEGFs act through three structurally related VEGF receptor tyrosine kinases, denoted VEGFR1 (Flt1), VEGFR2 (Flk1) and VEGFR3 (Flt4) [5]. VEGF-A induces angiogenesis via stimulating endothelial cell migration and proliferation, mainly through the binding to the RTK vascular endothelial growth factor receptor 2 (VEGFR2) [6]. Binding of VEGF-A to VEGFR2 induces receptor dimerization and autophosphorylation at multiple tyrosine sites, including Y951, as well as the activation of downstream proangiogenic enzymes such as extracellular signal-regulated kinase (ERK)1/2 and p-38 mitogen-activated protein kinase (MAPK) regulated by the VEGFR2 phosphorylation sites Y1175 and Y1214 respectively [7]. Each tyrosine autophosphorylation site is thought to promote unique downstream signaling pathways, which are linked to different cellular responses such as proliferation, migration and permeability [8].

Tyrosine phosphorylation is controlled by an equilibrium between activation of protein tyrosine kinases and protein tyrosine phosphatases (PTPs). PTPs are a family of endogenous modulators of RTKs-mediated signaling pathways that carry out the dephosphorylation of phospho-tyrosine residues. PTPs act by either direct dephosphorylation of particular receptor

tyrosine residues or of downstream signaling components [9]. Therefore, the blockade of PTPs would be a strategy to increase RTKs activation and subsequently angiogenesis.

The process of angiogenesis, together with arteriogenesis, represents a possible therapeutic strategy to treat patients affected by peripheral arterial disease (PAD) by restoring blood flow to ischemic tissues.

Vanadium compounds are a group of molecules that act as nonselective tyrosine phosphatase inhibitors [10]. Their mechanism of action, the inhibition of PTPs, was first shown on the insulin receptor where vanadium compounds act as insulin-mimic enhancing its phosphorylation [11,12]. In this context bis(maltolato)oxovanadium(IV) (BMOV) was shown to have antidiabetic properties and insulin-mimicking effects and to improve cardiac dysfunctions in diabetic models [13-15]. Previously used as simple inorganic vanadium salts, they were then replaced by larger and more complex compounds with organic ligands, that have shown increased bioavailability [10,16,17].

In the present study we focus on the role of bis(maltolato)oxidovanadium (IV) (BMOV) (Figure 1B), an organic vanadium salt, in wound closure and in angiogenesis and its effect on VEGFR2 signaling, chosen as a representative of the RTKs due to its pivotal role in angiogenesis.

It has previously been shown that different organic vanadium salts have a positive effect in promoting wound healing closure, most likely via increasing angiogenesis. Vanadyl acetylacetonate (VAC) has been shown to increase chondrogenesis and angiogenesis in fracture healing in rats [18-20]. Based on these findings we hypothesized that BMOV would promote wound closure in vivo in C57BL/6JRj mice.

Moreover, based on our findings that human umbilical vein endothelial cells (HUVECs) endogenously produce a baseline amount of VEGF-A and this results in VEGFR2 phosphorylation, we hypothesized that the addition of BMOV would increase in vitro angiogenesis via blocking PTPs-induced receptor de-phosphorylation. Moreover we hypothesized that exogenous addition of VEGF-A would enhance the effect of BMOV resulting in increased VEGFR2 activation and subsequent increased angiogenesis (Figure 1A).

Therefore, in the present study we assessed the effect of BMOV on in vivo wound closure and the effect of BMOV and coadministration of BMOV and exogenous VEGF-A in different in vitro

angiogenesis assays. Moreover, we examined which phospho-residues of VEGFR2 are involved in response to BMOV.

Results

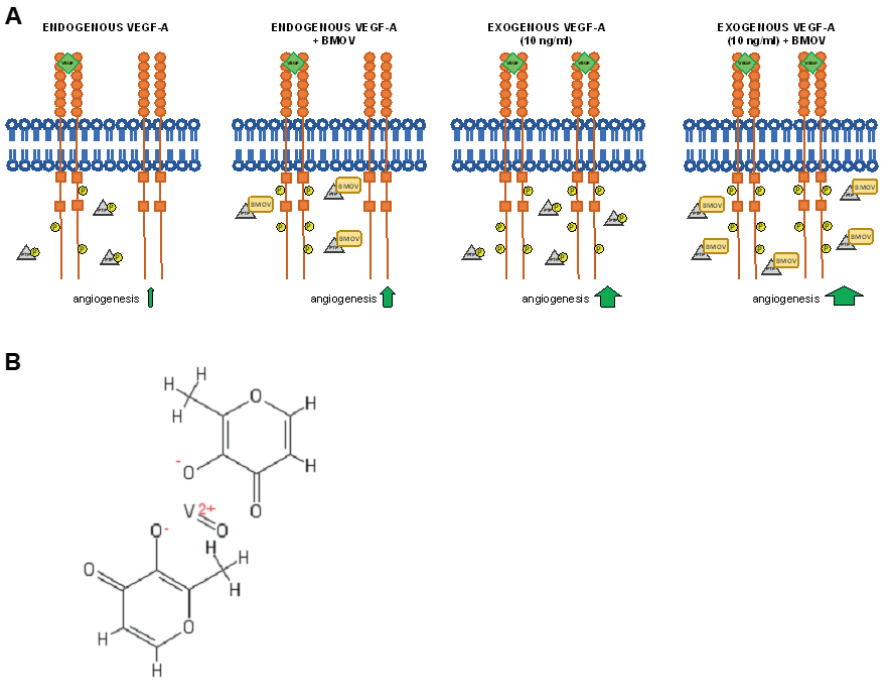


Figure 1. (**A**) Schematic representation of VEGFR2 signaling activation in response to the indicated conditions. (**B**) bis(maltolato)oxovanadium(IV) (BMOV) chemical structure.

BMOV Induces Wound Closure in vivo

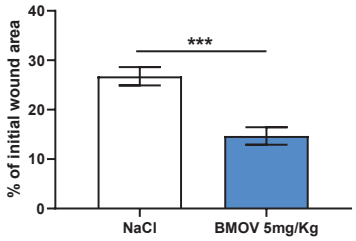


Figure 2. Quantification of in vivo wound area after 4 days' treatment with either saline solution or 5mg/kg BMOV. Wound healing data from two independent experiments were pooled and expressed as estimated marginal means ± SEM. ***p < 0.001, *n* = 11-12/group.

To investigate whether BMOV affects wound healing in vivo we performed two independent wound healing experiments. As shown in Figure 2, 4 days after wound formation, mice treated with 5mg/kg BMOV showed a strong reduction in the wound

area when compared to control mice treated with a saline solution. In fact the wound area of BMOV-treated mice was reduced by 45% when compared to control (Figure 2, $p < 0.001$).

HUVECs Produce Endogenous VEGF-A and this is not Affected by BMOV Treatment

HUVECs endogenously produce low levels of VEGF-A (51 pg/mL) and the amount of VEGF-A in HUVECs that were treated with BMOV for 12 hours was similar to the amount in the nontreated control cells (Figure 3, $p = 0.14$). When looking at the amount of VEGF-A in the culture media of cells treated with exogenous VEGF-A (10 ng/mL) or VEGF-A coadministered with BMOV, no differences could be observed (Figure 3, $p = 0.35$).

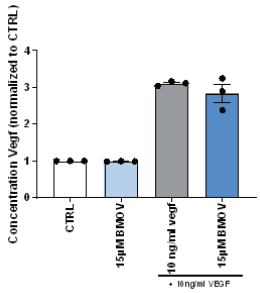


Figure 3. Quantification of the concentration of VEGF-A concentration in the cell culture medium of HUVECs incubated with the indicated conditions. All data points represent normalized averages obtained from 3 independent experiments and are presented as mean ± SEM. Two-sided Student's t test to compare control versus BMOV treatments.

Endothelial Cell Migration is Induced by BMOV Treatment

To understand how BMOV affects the first step toward the formation of a new vessel, we examined its effect on the migration of endothelial cells after 18 hours of treatment. HUVECs treated with increasing doses of BMOV showed dose-dependent enhanced scratch-wound closure when compared to untreated control cells and this induction reached a significant difference with the highest dose tested (Figure 4A and Figure S1A, $p = 0.009$).

Quantification of the migration rate showed an increase in cell migration by 45% in the group treated with 15 µM BMOV when compared to control (Figure 4A and Figure S1A).

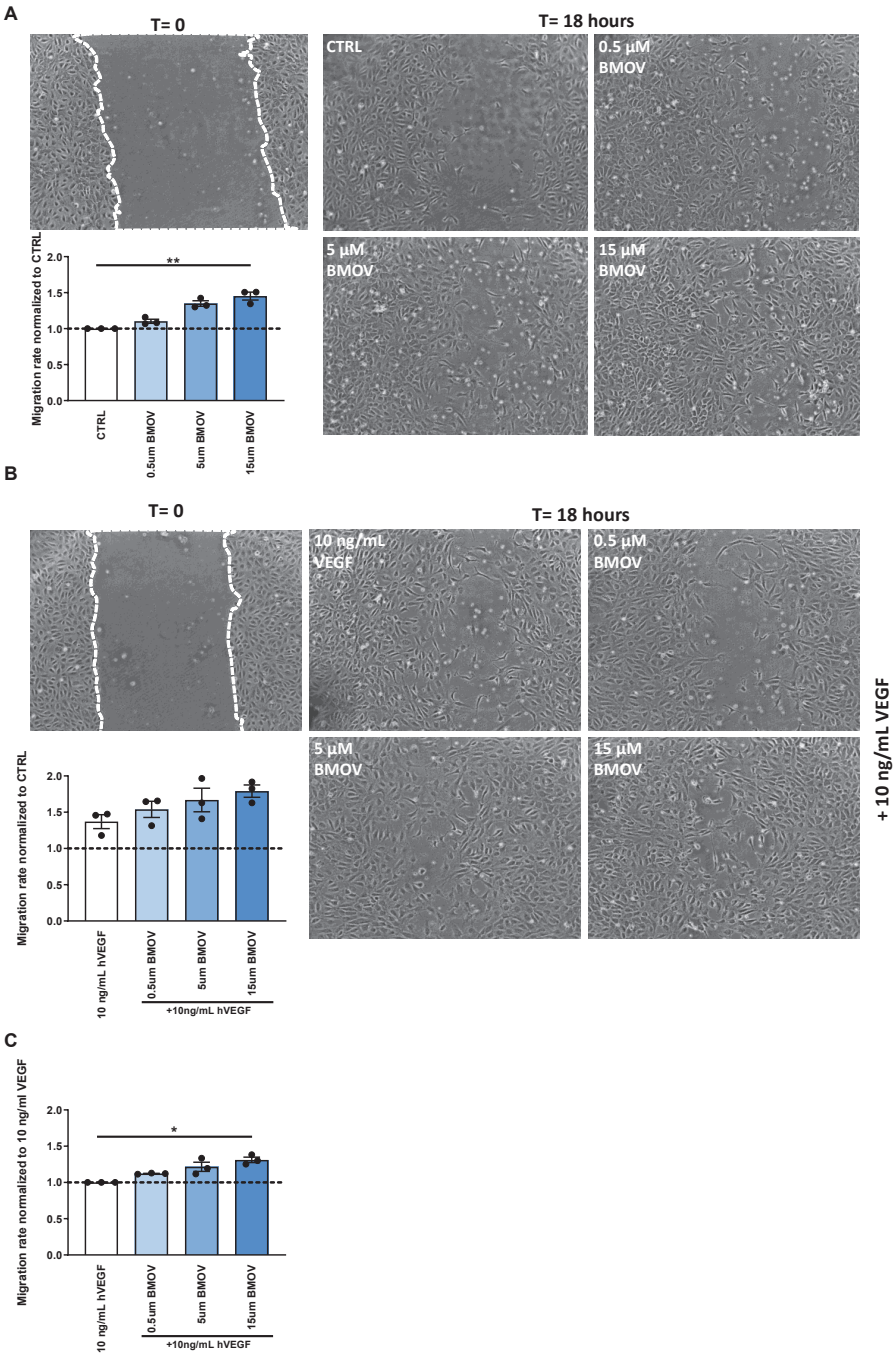


Figure 4. Representative images and quantification of HUVECs scratch-wound healing after treatment with either (**A**) BMOV alone in different concentrations (0.5, 5, 15 µM) or (**B**) different concentrations of BMOV (0.5,

5, 15 µM) supplemented with 10 ng/mL VEGF-A. (**C**) Effect of BMOV in the cell culture supplemented with 10 ng/mL VEGF-A. Datapoints represent averages obtained from 3 independent experiments and are presented as mean ± SEM. *$p < 0.05$; **$p < 0.01$ by Kruskal-Wallis test.

The effect of coadministration of BMOV and VEGF-A on ECs migration was assessed by adding to the cell culture media 10 ng/mL VEGF-A and/or increasing doses of BMOV, 0.5, 5 and 15 µM respectively. In this set-up coadministration of BMOV and VEGF-A was able to increase cell migration rate, reaching a 78% enhanced migration compared to control (10 ng/mL VEGF-A) using exogenous VEGF-A together with BMOV at the dose of 15 µM (Figure 4B and Figure S1B).

However, the effect seen in Figure 4B resulted to be the sum of the effect of BMOV and the effect of VEGF-A. In fact, BMOV gave a 45% increase in cell migration compared to control (untreated cells) (Figure 4A) and when co-administered with VEGF-A the isolated effect of the highest BMOV dose tested resulted in a 41% increase in migration on top of the VEGF-A effect (Figure 4C, $p = 0.01$) compared to cells treated with 10 ng/mL VEGF-A.

BMOV Induces ECs Proliferation

To determine whether BMOV had an effect on ECs proliferation and what would happen to this effect when extra VEGF-A is added to the cells, an MTT assay was performed and cell proliferation was evaluated after 24 hours of treatment.

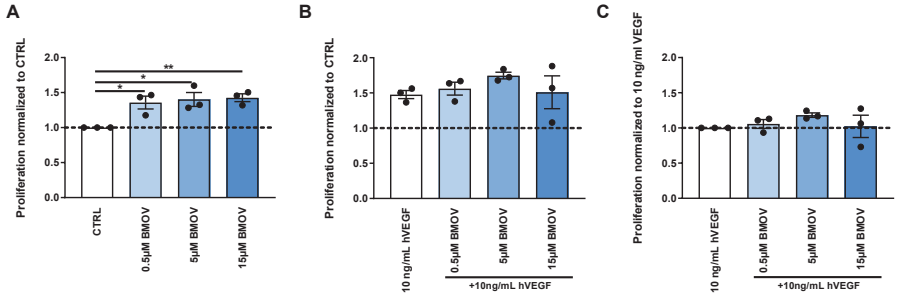


Figure 5. Quantification of HUVECs proliferation after treatment with either (**A**) BMOV alone in different concentrations (0.5, 5, 15 µM) or (**B**) different concentrations of BMOV (0.5, 5, 15 µM) supplemented with 10 ng/mL VEGF-A. (**C**) Effect of BMOV in the cell culture supplemented with 10 ng/mL VEGF-A. Datapoints represent averages obtained from 3 independent experiments and are presented as mean ± SEM. *$p < 0.05$; **$p < 0.01$ by One-Way ANOVA.

All the doses of BMOV tested (0.5, 5 and 15 µM) resulted in a significant increase in ECs proliferation (p = 0.02, 0.01 and 0.008 respectively) reaching a 42% increase in

proliferation with the dose of 15 μM when compared to control (Figure 5A and Figure S2A).

To examine if BMOV and exogenously added VEGF-A work together toward increasing cell proliferation, we repeated the experiment as above coadministering 10 ng/mL VEGF-A and/or BMOV in different doses to the cell culture. As shown in Figure 5B and Figure S2B, cells incubated with BMOV supplemented with exogenous VEGF-A showed an increased proliferation rate compared to cells treated with only 10 ng/mL VEGF-A. BMOV (5 μM) with the addition of 10 ng/mL VEGF-A resulted in an increase in cell proliferation by 27% when compared to control represented by 10 ng/mL VEGF-A (p = 0.02).

As shown in Figure 5C the effect of BMOV in the experiment in which we coadministered it with exogenous VEGF-A resulted to be less pronounced when compared to the experiment in which we added only BMOV to cells. In fact, in Figure 5A, BMOV-treated cells reached an increase of 42% in proliferation when compared to control (untreated cells), while with the supplementation of exogenous VEGF-A cell proliferation induced by BMOV increased by only 18% when compared to control (cells treated with exogenous VEGF-A) (Figure 5C). Therefore, the effect seen in Figure 5B is the sum of individual effects of BMOV and VEGF-A.

Tube Formation is Stimulated by BMOV Treatment

To evaluate whether BMOV can increase the capability of ECs to form capillary-like structures a tube-formation assay was performed and the total length of tubes formed was determined after 12 hours of treatment (Figure 6A and B). BMOV was able to promote HUVECs tube formation by 12% at a dose of 5 μM and by 27% at 15 μM (Figure 6A and Figure S3A, p = 0.003) compared to control (untreated cells).

The effect of coadministration of the highest dose of BMOV and exogenous VEGF-A on tube formation in HUVECs resulted in a 20% increase in total length of the tube formed (Figure 6B and Figure S3B) when compared to control (cells treated with 10 ng/mL VEGF-A). When coadministering BMOV and VEGF-A, the isolated additive effect of BMOV was a 12% increase in tube formation (Figure 6C) on top of the effect of VEGF-A (Figure 6B).

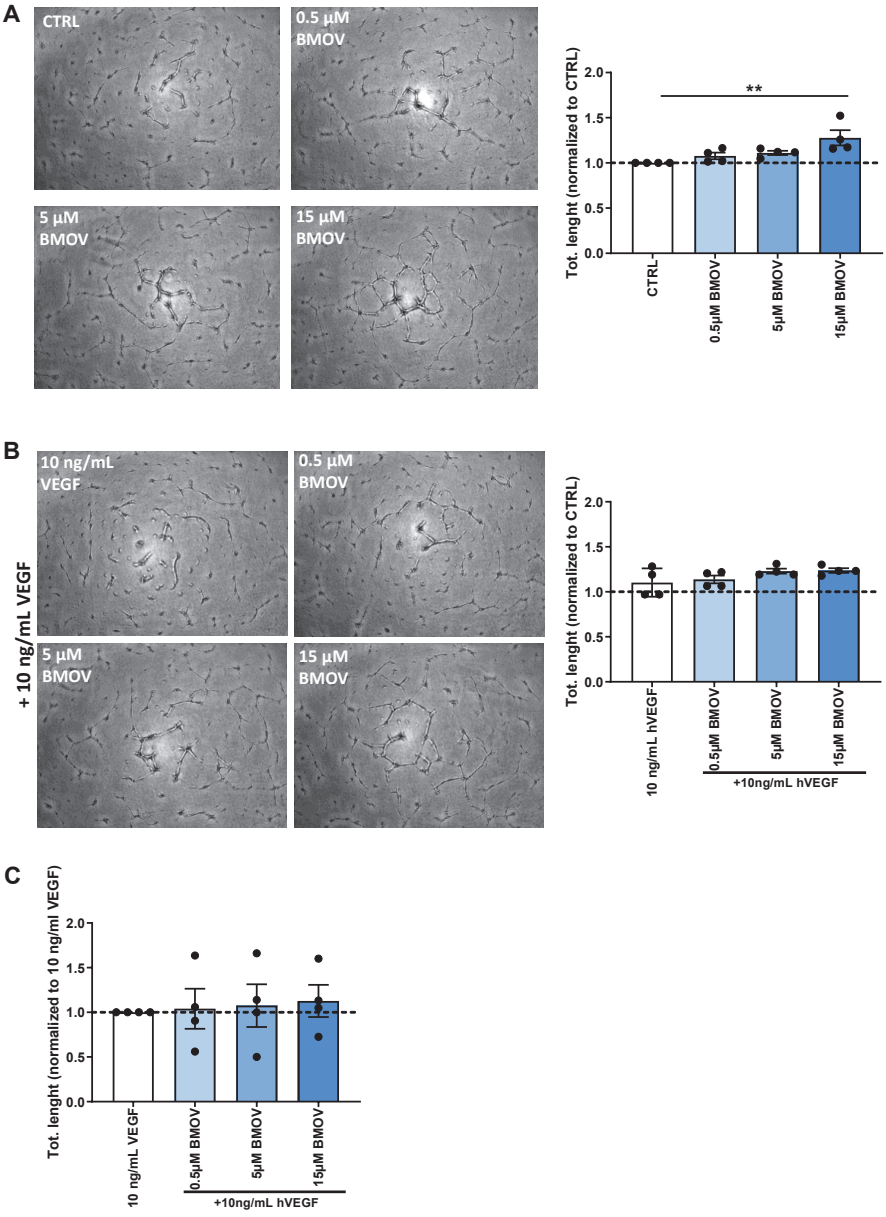


Figure 6. Representative images and quantification of HUVECs tube formation after treatment with either (A) BMOV alone in different concentrations (0.5, 5, 15 µM) or (B) different concentrations of BMOV (0.5, 5, 15 µM) supplemented with 10 ng/mL VEGF-A. (C) Effect of BMOV in the cell culture supplemented with 10 ng/mL VEGF-A. Datapoints represent averages obtained from 3 independent experiments and are presented as mean ± SEM. $^{**}p < 0.01$ by One-Way ANOVA.

Aortic Ring Sprouting is Induced upon BMOV Stimulation

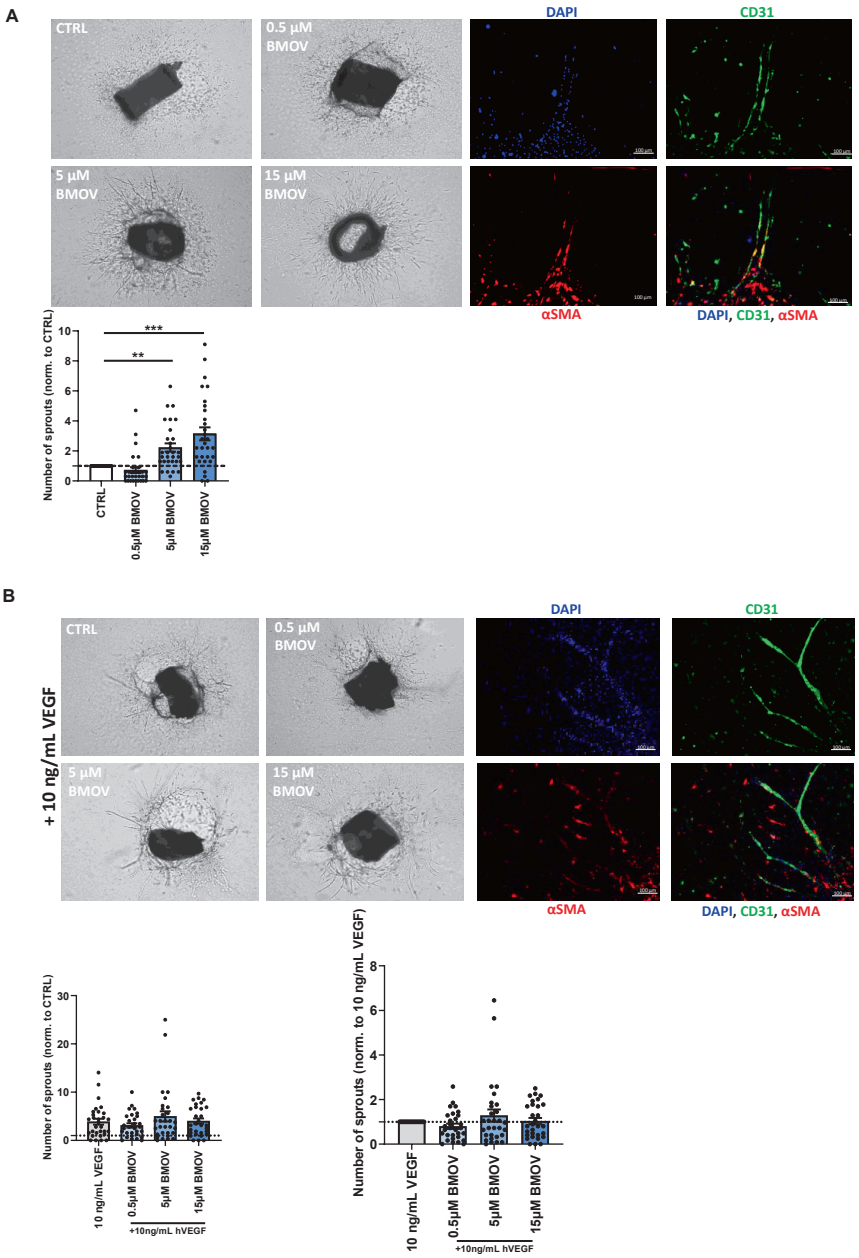


Figure 7. Representative images (top) and quantification of neovessel sprouts (bottom) after treatment with either (**A**) BMOV alone in different concentrations (0.5, 5, 15 µM) or (**B**) different concentrations of

BMOV (0.5, 5, 15 μM) supplemented with 10 ng/mL VEGF-A in an ex vivo aortic ring assay. Top right panels of (**A**) and (**B**) are representative examples of complex aortic ring neovessel sprouts fluorescently stained with cell specific markers. CD31 (green) stains endothelial cells; α-SMA (red) indicates smooth muscle cells; DAPI-stained nuclei (blue). (C) Effect of BMOV in the tissue culture supplemented with 10 ng/mL VEGF-A. Datapoints are presented as mean ± SEM. ** $p < 0.01$; *** $p < 0.001$ by Kruskal-Wallis test.

To examine the effects of BMOV on the sprouting of capillaries we used an ex vivo mouse aortic ring assay, in which not only endothelial cells are present but also other cell types, including smooth muscle cells.

A 2- and 3-fold increase in the number of sprouting neovessels formed in the aortic segments treated respectively with 5 and 15 μM BMOV were found when compared to untreated control (Figure 7A; p = 0.004 and 0.0002, respectively). Cell-type-specific double staining of aortic segments confirmed that the sprouting neovessels are lined with endothelial cells, as described previously [21,22]. The endothelial cells in the sprouts were surrounded by smooth muscle cells, characteristic of mature neovessels (Figure 7A and Figure S4A).

The same vessel structure was observed when co-administering exogenous VEGF-A and increasing doses of BMOV (0.5, 5 and 15 μM) to the cultured rings. Endothelial cells formed the neovessels sprouting from the rings, and they were surrounded by smooth muscle cells (Figure 7B and Figure S4B).

The addition of VEGF-A resulted in almost a 4-fold increase in the number of sprouts when compared to control represented by untreated aortic segments (Figure 7B).

Coadministration of VEGF-A and BMOV in increasing doses enhanced the average number of sprouts formed when compared to the untreated control cultured rings (Figure 7B). However, when administered together with VEGF-A, the isolated effect of BMOV resulted in an increase in sprouting neovessels only with the 5 μM dose when compared to control (aortic segments treated with 10 ng/mL VEGF-A) (28% increase), while the other doses did not show any effect (Figure 7C).

BMOV acts via VEGFR2

As unspecific blocker of protein phosphatases BMOV has been shown to exploit its action on several receptors' downstream signaling [11]. Due to its pivotal role in angiogenesis we

focused on the effect of BMOV on VEFGR2 downstream signaling. To do so we analyzed the phosphorylation and therefore the activation of one of the main VEGFR2 phosphorylation sites (Y951) and two key angiogenic enzymes, ERK1/2 and p-38MAPK regulated by the phosphorylation sites Y1175 and Y1214 respectively (Figure 8A).

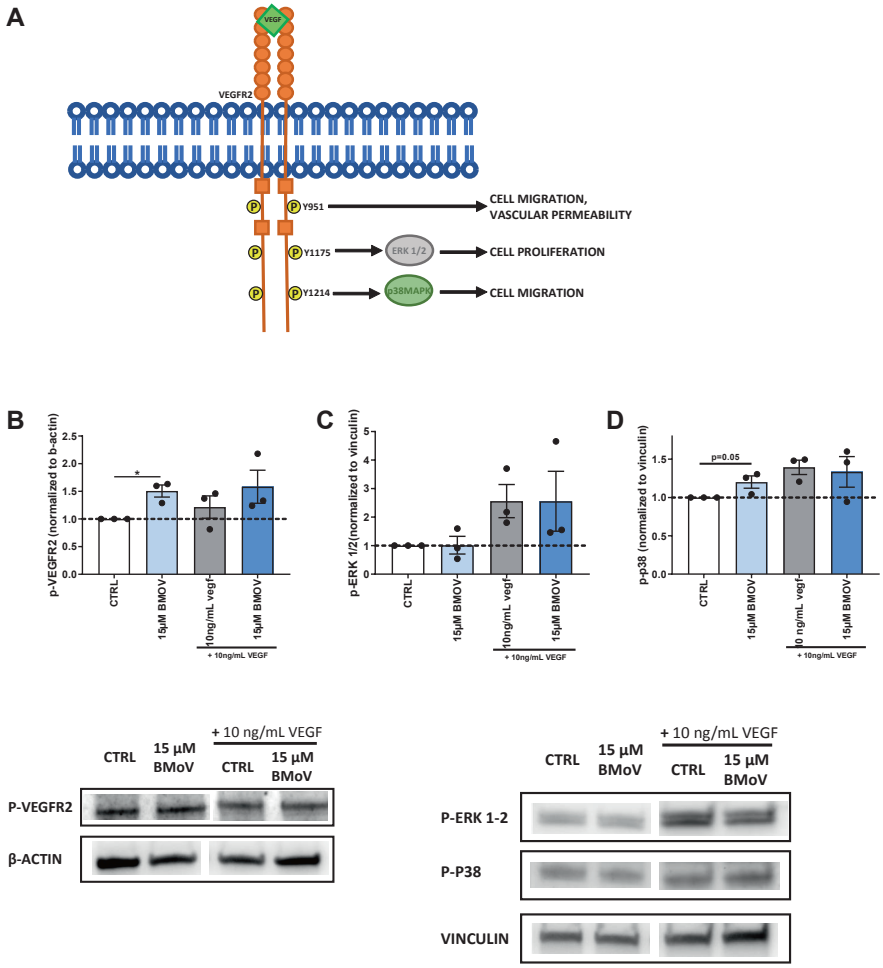


Figure 8. (**A**) Schematic representation of VEGFR2 signaling and downstream enzyme's activation. (**B**) Relative p-VEGFR2, protein expression in HUVECs whole-cell lysates after treatment with indicated conditions as determined by western blot. Expression was normalized per independent experiment to stable household protein β-actin and expressed relative to CTRL. Relative (**C**) p-ERK1/2 and (**D**) p p38, protein expression in HUVECs whole-cell lysates after treatment with indicated conditions as determined by western blot. Expression was normalized per independent experiment to stable household protein vinculin and expressed relative to CTRL. (E) Quantification of the concentration of VEGF-A concentration in the cell culture medium of HUVECs incubated with the indicated conditions. All data points represent normalized averages obtained from 3 independent experiments and are presented as mean ± SEM. *p <

0.05; by one-sample t test versus CTRL or two-sided Student's t test to compare CTRL versus BMOV treatments.

The amount of VEGFR2 phosphorylated on the residue Y951 was increased by 1.5 fold in the group treated with 15 µM BMOV when compared to control (untreated cells) (Figure 8B) (p = 0.04). The phosphorylation on the same residue in the groups costimulated with 15 µM BMOV and exogenous VEGF-A showed no differences between the groups (p = 0.36).

The phosphorylation of ERK1/2 (Figure 8C), downstream signaling of Y1175, showed no differences between control and treated groups. The groups treated with coadministration of exogenous VEGF-A and BMOV showed an increase in phosphorylation of ERK1/2 when compared to control (untreated cells) but no differences were found between BMOV-treated and respective controls (untreated cells and cells treated with 10 ng/mL VEGF-A. p = 0.96 and p = 0.99 respectively) (Figure 8C).

An almost significant increase (p = 0.05) was found in the activation of p38, downstream of Y1214 signaling. BMOV treatment resulted in a 1.2-fold increase in p38 phosphorylation when compared to the control (untreated cells) (p = 0.05. Figure 8D). Coadministration of VEGF-A and BMOV did not show differences when compared to each other (p = 0.8), even though they were 1.4-fold higher than the control (untreated cells) (Figure 8D).

Discussion

In the present study BMOV increases in vivo wound closure and in vitro endothelial cell migration, proliferation and tube formation in HUVECs. Additionally, it increases the number of sprouts formed in an ex vivo aortic ring assay. BMOV increases phosphorylation of VEGFR2 via Y951 and p38MAPK, but not ERK1/2 phosphorylation. We also show that BMOV and exogenous VEGF-A do not work in a synergistic way to increase angiogenesis.

Research from Paglia et al. and Ippolito et al. has shown that a different organic vanadium salt, Vanadyl acetylacetonate (VAC), has a positive effect in promoting chondrogenic wound healing closure, most likely via increasing angiogenesis [18-20]. It was previously described that BMOV could enhance collateral blood flow in a rat model of peripheral vascular disease and increase the diameter of cerebral collateral in rats [9,23]. Interestingly, these latter studies focus primarily on collateral maturation and therefore arteriogenesis, whereas patients with peripheral arterial disease (PAD) benefit by increased blood flow recovery via a combined action of improved angiogenesis and arteriogenesis [24]. Therefore, in this study we examined the role of BMOV in angiogenesis. We show that BMOV stimulates in vivo wound closure and increases in vitro angiogenesis via acting on the whole angiogenic process including the migration and proliferation of ECs and their ability to form a new vessel. Combined, these results indicate that BMOV has an action on both processes of angiogenesis and arteriogenesis.

In the context of PAD, although very promising, VEGF therapy did not show the expected clinical results in patients affected by PAD [25,26]. VEGF was shown to be present and even increased at the site of amputation in patients with critical ischemic PAD but it was not effective enough to restore blood flow and induce angiogenesis [25,26]. These findings show that there is a need for new therapeutic options for the treatment of PAD. Here, we demonstrate that low doses of endogenous VEGF-A activate VEGFR2 and BMOV boosts this induced proangiogenic signaling cascade via PTPs blockade (Figure 9).

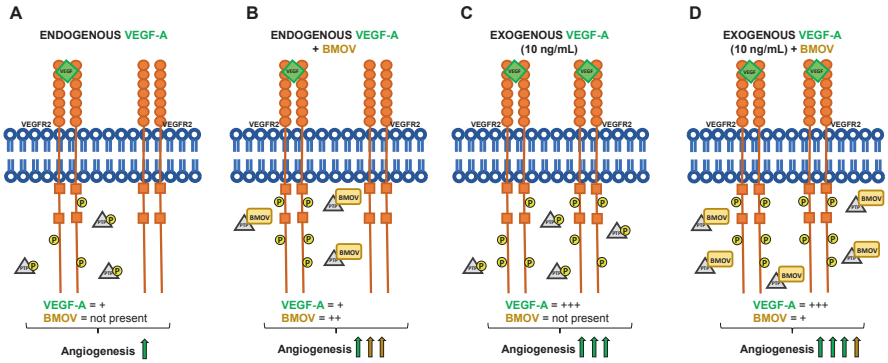


Figure 9. Schematic representation of the results obtained. (A) VEGF-A endogenously produced by HUVECs activates VEGFR2 resulting in its partial phosphorylation and low levels of angiogenesis. No addition of BMOV is carried out in this condition. (B) VEGFR2 is activated by endogenous VEGF-A and BMOV, by blocking PTPs, induces an increase in VEGFR2 phosphorylation that results in increased angiogenesis. (C) Exogenous addition of VEGF-A (10 ng/mL) results in increased angiogenesis via increased VEGFR2 phosphorylation. No addition of BMOV is carried out in this condition. (D) Coadministration of exogenous VEGF-A (10 ng/mL) and BMOV results in increased angiogenesis. The effect of BMOV is indicated with yellow arrow, the effect of VEGF-A is indicated with green arrows.

BMOV increases in vitro and ex vivo angiogenesis by increasing the number of neovessels in a complex angiogenic assay in which all the ECs functions come together toward the formation of a new vessel. Based on these preliminary results BMOV could be a new, interesting therapeutic option to induce angiogenesis in PAD patients in which a low dose of VEGF-A is present but it is not enough to completely restore angiogenesis.

Carr et al have previously shown that coadministered BMOV and exogenous VEGF-A increased HUVECs survival compared to exogenous VEGF-A administered alone [23]. We therefore examined if coadministration of BMOV and exogenous VEGF-A could result in increased angiogenesis. In line with the results from Carr et al we found that coadministration of BMOV and VEGF-A resulted in higher stimulation of in vitro angiogenesis compared to administration of exogenous VEGF-A. However we also found that this was not a synergistic but rather a cumulative effect resulting from the sum of individual BMOV and VEGF-A effects. More importantly, we found that the effect of BMOV when coadministered with exogenous VEGF-A resulted to be less strong in inducing angiogenesis compared to the effect of the single administration of BMOV. Except for the migration assay, in which the effect of BMOV coadministered with VEGF-A resulted to be similar to the effect of BMOV administered alone, in the cell proliferation assay, tube assay and aortic ring assay, the effect of BMOV resulted

to be higher than its effect when used in combination with exogenous VEGF-A (Figure 9). The phosphorylation levels of VEGFR2 (Y951), ERK1/2 and p38MAPK, in HUVECs treated with exogenous VEGF-A and exogenous VEGF-A coadministered with BMOV resulted to be the same. Therefore, due to the fact that high VEGFR2 activation is achieved with exogenous addition of VEGF-A, it is likely that in this situation BMOV does not have a significant effect on angiogenesis induced by VEGFR2 activation because the receptor is already fully active.

In the present manuscript we show not only that VEGFR2 activation is augmented upon BMOV treatment but we also pinpoint the phospho-residues involved in the signaling. In the present set-up BMOV increased the activation of Y-951 and p38MAPK while ERK1/2 was not affected. It was previously shown that BMOV could enhance the phosphorylation of ERK1/2 in skeletal muscle extracts of diabetic rats, suggesting that our results are cell-type specific and dependent on our experimental setup [27]. More importantly Y-951, p38MAPK and ERK1/2 phosphorylation results are not completely in line with the results we obtained in the in vitro assays. It was previously shown that cell migration and sprout formation are regulated by Y-951 and p38MAPK activation, while cell proliferation depends on ERK1/2 activation [28,29]. We here found that BMOV increased HUVECs migration and sprout formation supported by phosphorylation of VEGFR2 Y-951 and p38MAPK, but BMOV also increased HUVECs proliferation and this was not supported by ERK 1/2 activation. As a potential limitation of our study, we used the MTT assay as a proliferation assay whereas it is an assay that measures the mitochondrial activity of the cells [30]. This could be the explanation why the results of our proliferation assay and the phosphorylation of ERK1/2 do not correlate.

Based on the results obtained in this study we can conclude that BMOV alone induces in vitro angiogenesis and does not act synergistically with VEGF in this process. Moreover, BMOV is able to activate VEGFR2 and downstream proangiogenic enzymes without exogenous addition of VEGF. Therefore, our results show that BMOV-mediated inhibition of PTPs is a promising strategy to induce angiogenesis.

Materials and Methods

In vivo Wound Healing

All procedures involving mice were approved by the Regional Animal Ethics Committee at the University of Gothenburg, in accordance with the European Communities Council Directives of 22 September 2010 (2010/63/EU).

Male C57BL/6JRj mice (Janvier Labs, Le Genest-Saint-Isle, France) were anesthetized with isoflurane, hair was removed by shaving using hair removal cream. All animals received Temgesic (0.08 mg/kg BW) prior to creating the wounds. Skin was wiped with 70% ethanol and thereafter two 5-mm-diameter wounds were created at the back of the mouse using a biopsy puncher. BMOV (5mg/kg) or saline was administered via intravenous (iv) injections in the tail vein. Wounds were initially covered with tegaderm band aid (3M, Apoteket AB, Stockholm, Sweden) for the first two days, to avoid sawdust and bedding material getting into the wounds, which were thereafter removed. Wounds were measured using a digital caliper at day 0, 2 and 4 and healing rate is expressed as percentage of initial area. Mice were sacrificed at day 4 by an overdose of pentobarbital (i.p., Apoteket AB).

Animals were housed at 21–24 °C in a room with 12-h light/12-h dark cycle. Water and food were available ad libitum.

Isolation of Human Umbilical Venous Endothelial Cells (HUVECs)

For the isolation of HUVECS anonymous umbilical cords were obtained in accordance with guidelines set out by the 'Code for Proper Secondary Use of Human Tissue' of the Dutch Federation of Biomedical Scientific Societies (Federa, Rotterdam, The Netherlands), and conforming to the principles outlined in the Declaration of Helsinki. Isolation and culturing of primary venous human umbilical cells was performed as described by Van der Kwast et al. [21]. In brief, umbilical cords were collected from full-term pregnancies and stored in sterile PBS at 4 °C and subsequently used for cell isolation within 5 days. For HUVEC isolation, cannulas were inserted on each side of the vein of an umbilical cord and flushed with sterile PBS. The artery was infused with 0.075% collagenase type II (Worthington, Lakewood, NJ, USA) and incubated at 37 °C for 20 min. The collagenase solution was collected and the artery was flushed with PBS in order to collect all detached endothelial cells. The cell suspension was centrifuged at 400 g for 5 min and the pellet was resuspended in HUVEC complete culture

medium (EBM-2 Basal Medium (CC-3156) and EGMTM-2 SingleQuotsTM Supplements (CC-4176), Lonza). HUVECs were cultured in plates coated with 1% fibronectin and used between passage 2 and 4. Low-serum culture medium consisted of EBM-2 Basal Medium (CC-3156, Lonza, Basel, Zwitserland) supplemented with 0.2% Fetal Bovine Serum (FBS) and 1% GA-1000 (SingleQuotsTM Supplements, CC-4176, Lonza).

BMOV Preparation

BMOV was kindly gifted by CFM pharma (Figure 2B). For scratch-wound healing assay, cell proliferation assay, tube formation assay and aortic ring assay, bis(maltolato)oxovanadium(IV) (BMOV) was dissolved in PBS and used for the assays at a final concentration of 0.5, 5 and 15 µm.

For samples used for western blot and ELISA, BMOV was dissolved in PBS and used for the assay at a final concentration of 15 µm.

The selection of the doses of BMOV used for both in vitro and in vivo experiments was based on previous publications that used BMOV or vanadium derivatives in the context of arteriogenesis and wound healing [18,19,23].

Scratch-Wound Healing Assay

For the scratch-wound healing assay (*n*=3 experimental replicates), HUVECs cells were plated on a 12-well plate and grown until 80% confluence in complete culture medium as previously reported [21]. Cells were then treated with low-serum medium or low serum supplemented with BMOV in increasing concentrations for 24 h. After 24 h, medium was removed and a scratch wound was introduced across the diameter of each well of a 12-well plate using a p200 pipette tip. Subsequently, the cells were washed with PBS and medium was replaced by new low-serum culture medium with or without 10 ng/mL VEGF-A (Human VEGF-A165, 718302, Biolegend, Amsterdam, Netherlands) and/or BMOV in increasing concentrations. Two locations along the scratch wound were marked per well and scratch-wound closure at these sites was imaged by taking pictures at time 0 h and 18 h after scratch-wound introduction using live phase–contrast microscopy (Axiovert 40C, Carl Zeiss, Oberkochen, Duitsland). Average scratch-wound closure after 18 h was objectively calculated per well by measuring difference in cell coverage at 18 h vs. 0 h using the wound healing tool macro for ImageJ.

MTT Assay

Cell proliferation (*n* = 3 experimental replicates) was measured using MTT assay. HUVECs cells were plated at 5000 cells/well in a 96-well plate and grown until 80% confluency in complete culture medium, after which they were incubated with low-serum medium or low serum supplemented with BMOV in increasing concentrations for 24 h. The medium was then replaced by treatment mixtures consisting of low-serum medium with or without 10 ng/mL VEGF-A, and/or BMOV in increasing concentrations. After 24 h incubation, 10 µL MTT (Thiazolyl blue tetrazolium bromide, Sigma M5655) was added directly to each well and cells were incubated at 37 °C in a humidified 5% CO2 environment for 4 hours. Subsequently, 75 µL medium was removed from each well and 75 µL isopropanol/0.1N HCL was added per well. After incubating the plate for 90 min on a shaker platform, absorbance was read at 570 nm with a Cytation 5 spectrophotometer (BioTek) and the mitochondrial metabolic activity was quantified as a representative measure of cell proliferation.

Tube Formation Assay

HUVECs were seeded in 12-well plates in complete medium until confluent. Medium was then replaced with low-serum culture medium or low serum supplemented with BMOV in increasing concentrations for 24 h. A 96-wells plate was coated using 50 µL/well of Geltrex extracellular matrix (A1413202, Gibco, Waltham, USA). Cells were then detached using trypsin-EDTA (Sigma, Steinheim, Germany) and diluted at a concentration of 150.000 cells/mL in low-serum medium with or without 10 ng/mL VEGF-A and/or BMOV in increasing concentrations. After 12 hours incubation pictures of each well were taken using live phase–contrast microscopy (Axiovert 40C, Carl Zeiss). Total length of the tubes formed was analyzed using the wound healing tool macro for ImageJ.

Quantification of VEGF-A in Cell Culture Medium

HUVECs were seeded in 12-well plates in 1 mL of complete medium for 24 h until confluent. Medium was then replaced with low-serum culture medium for an additional 24 hours. Cells were stimulated in low-serum medium with or without 10 ng/mL VEGF-A, and/or 15µm BMOV for 60 min. Cell culture medium was collected and stored at -80°C. VEGF-A concentration was measured by a sandwich ELISA (DY293B-05, R&D Systems, Minneapolis, MN, USA) according to the manufacturer's instructions.

Aortic Ring Assay

Mouse aortic ring assay was performed as described previously [31]. In brief, six thoracic aortas were removed from 8- to 10-week old mice, after which the surrounding fat and branching vessels were carefully removed and the aorta was flushed with Opti-MEM medium (Gibco).

Aortic rings of 1 mm were cut and the rings from each mouse aorta were incubated overnight with fresh Opti-MEM.

96-well plates were coated with 75 µL collagen matrix (Collagen (Type I, Millipore, Burlington, USA) diluted in 1x DMEM (Gibco) and pH-adjusted with 5N NaOH. One aortic ring per well was embedded in the collagen matrix, for a total of 30 rings per condition. After letting the collagen solidify for one hour, 150 µL Opti-MEM supplemented with 2.5% FBS (PAA, Pasching, Austria), 1% penicillin-streptomycin (PAA, Pasching, Austria) and with or without 10 ng/mL VEGF-A (R&D systems, Minneapolis, USA) and/or either 0.5, 5 or 15µm BMOV was added to each well. Medium was refreshed every other day. Pictures of each embedded aortic ring and their neovessel outgrowth were taken after 7 days using live phase–contrast microscopy (Axiovert 40C, Carl Zeiss). The number of neovessel sprouts were counted manually. Each neovessel emerging from the ring was counted as a sprout and individual branches arising from each microvessel counted as a separate sprout. For immunohistochemistry the embedded rings were formalin fixed and permeabilized with 0.25% Triton X-100. A triple staining was performed using primary antibodies against smooth muscle cells (α-smooth muscle actin, 1A4, DAKO), endothelial cells (CD31, BD Pharmingen, San Diego, USA) and nuclei (DAPI). Alexa Fluor 647, Alexa Fluor 488 antibodies (Life Technologies) were used as secondary antibodies and slides were mounted with ProLong Gold mountant with DAPI (P36935, ThermoFisher, Waltham, USA). Stained slides were photographed using a Panoramic MIDI II digital slide scanner (3DHISTECH).

Sample Preparation and Western Blot

HUVECs were seeded in 12-well plates in complete medium for 24 h until confluent. Medium was then replaced with low-serum culture medium for additional 24 hours. Cells were stimulated in low-serum medium with or without 10 ng/mL VEGF-A, and/or 15 µm BMOV in PBS for 60 min. Cells were then lysated using modified RIPA buffer [10 mM Tris-HCl pH = 7.4 (10708976001, Sigma-Aldrich, Saint Louis, USA), 150 mM NaCl (S7653, Sigma-Aldrich), 5 mM

EDTA pH = 8.0 (E9884, Sigma-Aldrich), 1% Triton X-100, 1% SDS (L3771, Sigma-Aldrich), 1 mM NaF (S7920, Sigma-Aldrich), 1mM Na3VO4 (S6508, Sigma-Aldrich) and cOmplete™ Protease Inhibitor Cocktail (1169749800, Roche Diagnostics)].

Western blot was performed as described by Van der Kwast et al. [32]. Total protein concentration was quantified using a Pierce BCA ProteinAssay Kit (Thermo Fisher Scientific), after which protein concentration was normalized to 1.25 mg/mL in Laemmli buffer (Bio-Rad Laboratories, Hercules, CA, USA) containing 10%b-mercaptoethanol (Sigma-Aldrich). Proteins were separated in the Vertical Electrophoresis Cell system using pre-mixed Tris/glycine/SDS running buffer (Bio-Rad Laboratories) and were transferred onto a nitrocellulose membrane (GE Health-care Life Sciences, Eindhoven, the Netherlands) using premixed Tris/glycine transfer buffer (Bio-Rad Laboratories, Hercules, USA). Blots were incubated overnight at 4°C with antibodies directed either at p-VEGFR2 (2476s, cell signaling), or p-ERK1/2 (M8159, Sigma-Aldrich) or p-p38 (92115, cell signaling) or stable household protein vinculin (V9131, Sigma-Aldrich) or β-actin (Ab8224, AbCam, Cambridge, UK) diluted to 1:1000 in 5% BSA in TBS-T. The membrane was then incubated with either antimouse (31432, Thermo Fisher Scientific) or antirabbit antibody (31462, Thermo Fisher Scientific) peroxidase-conjugated secondary antibody diluted to 1:10.000 in 5% BSA in TBS-T. Proteins of interest were revealed using SuperSignal West Pico PLUS Chemiluminescent Substrate (ThermoFisher Scientific) and imaged using the ChemiDoc TouchImaging System (Bio-Rad Laboratories). p-VEGFR2 expression was quantified relative to stable household protein β-actin and p-ERK1/2 and p-p38 expression were quantified relative to stable household protein vinculin using ImageJ.

Statistical Analysis

For the in vivo wound healing experiment, to adjust for sacrifice day, data from the two independent experiments, were analyzed and expressed as estimated marginal means ± SEM (IBM SPSS Statistics for windows, Version 25.0, Armonk, NY:IBM Corp).

Results of in vitro assays are expressed as mean ± SEM. A One-Way ANOVA or unpaired T-test were used to compare individual groups. Non-Gaussian distributed data were analyzed using a Kruskal-Wallis test using GraphPad Prism version 6.00 for Windows (GraphPad Software). Probability-values < 0.05 were regarded significant.

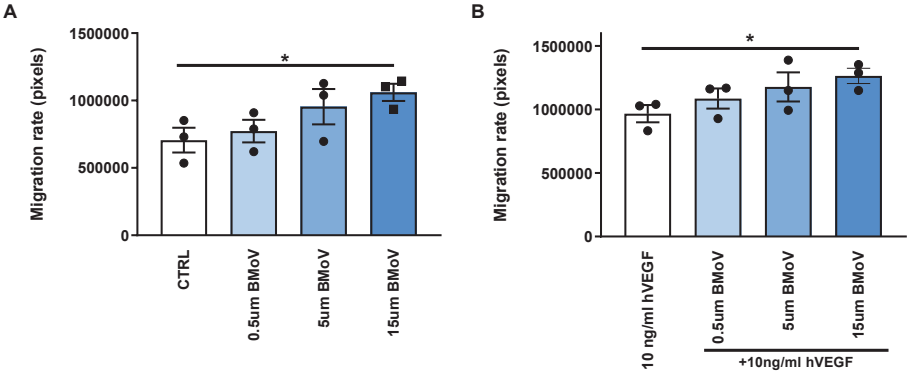
References

1. Jeltsch, M.; Leppanen, V.M.; Saharinen, P.; Alitalo, K. Receptor tyrosine kinase-mediated angiogenesis. *Cold Spring Harbor perspectives in biology* **2013**, *5*, doi:10.1101/cshperspect.a009183.
2. Maruyama, I.N. Mechanisms of activation of receptor tyrosine kinases: monomers or dimers. *Cells* **2014**, *3*, 304-330, doi:10.3390/cells3020304.
3. Carmeliet, P.; Jain, R.K. Molecular mechanisms and clinical applications of angiogenesis. *Nature* **2011**, *473*, 298-307, doi:10.1038/nature10144.
4. Potente, M.; Carmeliet, P. The Link Between Angiogenesis and Endothelial Metabolism. *Annu Rev Physiol* **2017**, *79*, 43-66, doi:10.1146/annurev-physiol-021115-105134.
5. Koch, S.; Claesson-Welsh, L. Signal transduction by vascular endothelial growth factor receptors. *Cold Spring Harbor perspectives in medicine* **2012**, *2*, a006502, doi:10.1101/cshperspect.a006502.
6. Cebe-Suarez, S.; Zehnder-Fjallman, A.; Ballmer-Hofer, K. The role of VEGF receptors in angiogenesis; complex partnerships. *Cellular and molecular life sciences : CMLS* **2006**, *63*, 601-615, doi:10.1007/s00018-005-5426-3.
7. Nakamura, Y.; Patrushev, N.; Inomata, H.; Mehta, D.; Urao, N.; Kim, H.W.; Razvi, M.; Kini, V.; Mahadev, K.; Goldstein, B.J., et al. Role of protein tyrosine phosphatase 1B in vascular endothelial growth factor signaling and cell-cell adhesions in endothelial cells. *Circ Res* **2008**, *102*, 1182-1191, doi:10.1161/circresaha.107.167080.
8. Corti, F.; Simons, M. Modulation of VEGF receptor 2 signaling by protein phosphatases. *Pharmacological research* **2017**, *115*, 107-123, doi:10.1016/j.phrs.2016.11.022.
9. Buschmann, I.; Hackbusch, D.; Gatzke, N.; Dulsner, A.; Trappiel, M.; Dagnell, M.; Ostman, A.; Hooft van Huijsduijnen, R.; Kappert, K. Inhibition of protein tyrosine phosphatases enhances cerebral collateral growth in rats. *Journal of molecular medicine (Berlin, Germany)* **2014**, *92*, 983-994, doi:10.1007/s00109-014-1164-z.
10. Irving, E.; Stoker, A.W. Vanadium Compounds as PTP Inhibitors. *Molecules (Basel, Switzerland)* **2017**, *22*, doi:10.3390/molecules22122269.
11. Mehdi, M.Z.; Pandey, S.K.; Theberge, J.F.; Srivastava, A.K. Insulin signal mimicry as a mechanism for the insulin-like effects of vanadium. *Cell biochemistry and biophysics* **2006**, *44*, 73-81, doi:10.1385/cbb:44:1:073.
12. Peters, K.G.; Davis, M.G.; Howard, B.W.; Pokross, M.; Rastogi, V.; Diven, C.; Greis, K.D.; Eby-Wilkens, E.; Maier, M.; Evdokimov, A., et al. Mechanism of insulin sensitization by BMOV (bis maltolato oxo vanadium); unliganded vanadium (VO4) as the active component. *Journal of inorganic biochemistry* **2003**, *96*, 321-330, doi:10.1016/s0162-0134(03)00236-8.
13. Winter, C.L.; Lange, J.S.; Davis, M.G.; Gerwe, G.S.; Downs, T.R.; Peters, K.G.; Kasibhatla, B. A nonspecific phosphotyrosine phosphatase inhibitor, bis(maltolato)oxovanadium(IV), improves glucose tolerance and prevents diabetes in Zucker diabetic fatty rats. *Exp Biol Med (Maywood)* **2005**, *230*, 207-216, doi:10.1177/153537020523000307.
14. Yuen, V.G.; Orvig, C.; Thompson, K.H.; McNeill, J.H. Improvement in cardiac dysfunction in streptozotocin-induced diabetic rats following chronic oral administration of bis(maltolato)oxovanadium(IV). *Can J Physiol Pharmacol* **1993**, *71*, 270-276, doi:10.1139/y93-042.
15. Yuen, V.G.; Vera, E.; Battell, M.L.; Li, W.M.; McNeill, J.H. Acute and chronic oral administration of bis(maltolato)oxovanadium(IV) in Zucker diabetic fatty (ZDF) rats. *Diabetes Res Clin Pract* **1999**, *43*, 9-19, doi:10.1016/s0168-8227(98)00120-x.
16. Thompson, K.H.; Orvig, C. Vanadium in diabetes: 100 years from Phase 0 to Phase I. *Journal of inorganic biochemistry* **2006**, *100*, 1925-1935, doi:10.1016/j.jinorgbio.2006.08.016.
17. McNeill, J.H.; Yuen, V.G.; Hoveyda, H.R.; Orvig, C. Bis(maltolato)oxovanadium(IV) is a potent insulin mimic. *Journal of medicinal chemistry* **1992**, *35*, 1489-1491, doi:10.1021/jm00086a020.

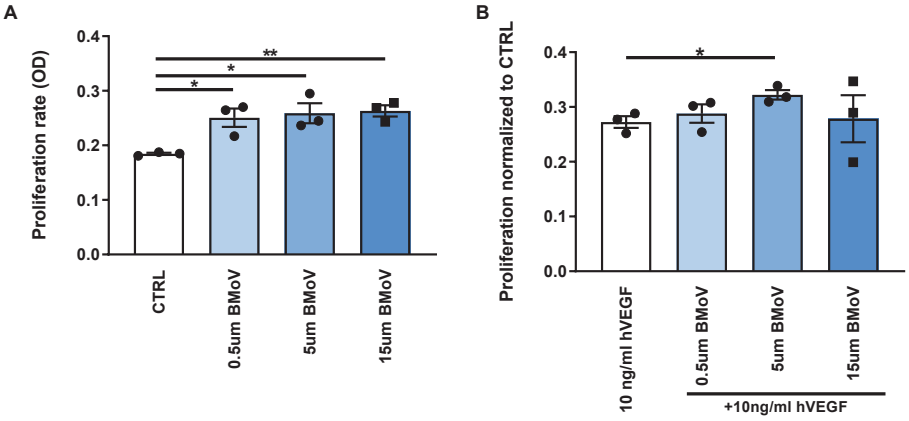
18. Paglia, D.N.; Wey, A.; Park, A.G.; Breitbart, E.A.; Mehta, S.K.; Bogden, J.D.; Kemp, F.W.; Benevenia, J.; O'Connor, J.P.; Lin, S.S. The effects of local vanadium treatment on angiogenesis and chondrogenesis during fracture healing. *Journal of orthopaedic research : official publication of the Orthopaedic Research Society* **2012**, *30*, 1971-1978, doi:10.1002/jor.22159.
19. Paglia, D.N.; Wey, A.; Hreha, J.; Park, A.G.; Cunningham, C.; Uko, L.; Benevenia, J.; O'Connor, J.P.; Lin, S.S. Local vanadium release from a calcium sulfate carrier accelerates fracture healing. *Journal of orthopaedic research : official publication of the Orthopaedic Research Society* **2014**, *32*, 727-734, doi:10.1002/jor.22570.
20. Ippolito, J.A.; Krell, E.S.; Cottrell, J.; Meyer, R.; Clark, D.; Nguyen, D.; Sudah, S.; Munoz, M.; Lim, E.; Lin, A., et al. Effects of local vanadium delivery on diabetic fracture healing. *Journal of orthopaedic research : official publication of the Orthopaedic Research Society* **2017**, *35*, 2174-2180, doi:10.1002/jor.23521.
21. van der Kwast, R.; van Ingen, E.; Parma, L.; Peters, H.A.B.; Quax, P.H.A.; Nossent, A.Y. Adenosine-to-Inosine Editing of MicroRNA-487b Alters Target Gene Selection After Ischemia and Promotes Neovascularization. *Circ Res* **2018**, *122*, 444-456, doi:10.1161/circresaha.117.312345.
22. Baker, M.; Robinson, S.D.; Lechertier, T.; Barber, P.R.; Tavora, B.; D'Amico, G.; Jones, D.T.; Vojnovic, B.; Hodivala-Dilke, K. Use of the mouse aortic ring assay to study angiogenesis. *Nature protocols* **2011**, *7*, 89-104, doi:10.1038/nprot.2011.435.
23. Carr, A.N.; Davis, M.G.; Eby-Wilkens, E.; Howard, B.W.; Towne, B.A.; Dufresne, T.E.; Peters, K.G. Tyrosine phosphatase inhibition augments collateral blood flow in a rat model of peripheral vascular disease. *American journal of physiology. Heart and circulatory physiology* **2004**, *287*, H268-276, doi:10.1152/ajpheart.00007.2004.
24. Simons, K.H.; de Vries, M.R.; de Jong, R.C.M.; Peters, H.A.B.; Jukema, J.W.; Quax, P.H.A. IRF3 and IRF7 mediate neovascularization via inflammatory cytokines. *Journal of cellular and molecular medicine* **2019**, *23*, 3888-3896, doi:10.1111/jcmm.14247.
25. van Weel, V.; Seghers, L.; de Vries, M.R.; Kuiper, E.J.; Schlingemann, R.O.; Bajema, I.M.; Lindeman, J.H.; Delis-van Diemen, P.M.; van Hinsbergh, V.W.; van Bockel, J.H., et al. Expression of vascular endothelial growth factor, stromal cell-derived factor-1, and CXCR4 in human limb muscle with acute and chronic ischemia. *Arterioscler Thromb Vasc Biol* **2007**, *27*, 1426-1432, doi:10.1161/atvbaha.107.139642.
26. Shimamura, M.; Nakagami, H.; Koriyama, H.; Morishita, R. Gene therapy and cell-based therapies for therapeutic angiogenesis in peripheral artery disease. *BioMed research international* **2013**, *2013*, 186215, doi:10.1155/2013/186215.
27. Bhanot, S.; Girn, J.; Poucheret, P.; McNeill, J.H. Effects of bis(maltolato) oxovanadium (IV) on protein serine kinases in skeletal muscle of streptozotocin-diabetic rats. *Molecular and cellular biochemistry* **1999**, *202*, 131-140, doi:10.1023/a:1007001818411.
28. Takahashi, T.; Yamaguchi, S.; Chida, K.; Shibuya, M. A single autophosphorylation site on KDR/Flk-1 is essential for VEGF-A-dependent activation of PLC-gamma and DNA synthesis in vascular endothelial cells. *The EMBO journal* **2001**, *20*, 2768-2778, doi:10.1093/emboj/20.11.2768.
29. Lamalice, L.; Houle, F.; Jourdan, G.; Huot, J. Phosphorylation of tyrosine 1214 on VEGFR2 is required for VEGF-induced activation of Cdc42 upstream of SAPK2/p38. *Oncogene* **2004**, *23*, 434-445, doi:10.1038/sj.onc.1207034.
30. Kumar, P.; Nagarajan, A.; Uchil, P.D. Analysis of Cell Viability by the MTT Assay. *Cold Spring Harbor protocols* **2018**, *2018*, doi:10.1101/pdb.prot095505.
31. de Vries, M.R.; Parma, L.; Peters, H.A.B.; Schepers, A.; Hamming, J.F.; Jukema, J.W.; Goumans, M.; Guo, L.; Finn, A.V.; Virmani, R., et al. Blockade of vascular endothelial growth factor receptor 2 inhibits intraplaque haemorrhage by normalization of plaque neovessels. *Journal of internal medicine* **2019**, *285*, 59-74, doi:10.1111/joim.12821.

32. van der Kwast, R.; Woudenberg, T.; Quax, P.H.A.; Nossent, A.Y. MicroRNA-411 and Its 5'-IsomiR Have Distinct Targets and Functions and Are Differentially Regulated in the Vasculature under Ischemia. *Molecular therapy : the journal of the American Society of Gene Therapy* **2020**, *28*, 157-170, doi:10.1016/j.ymthe.2019.10.002.

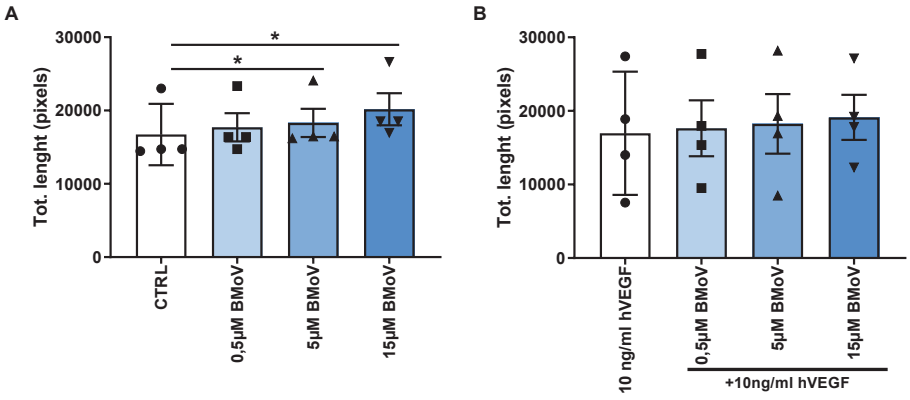
Supplemental material



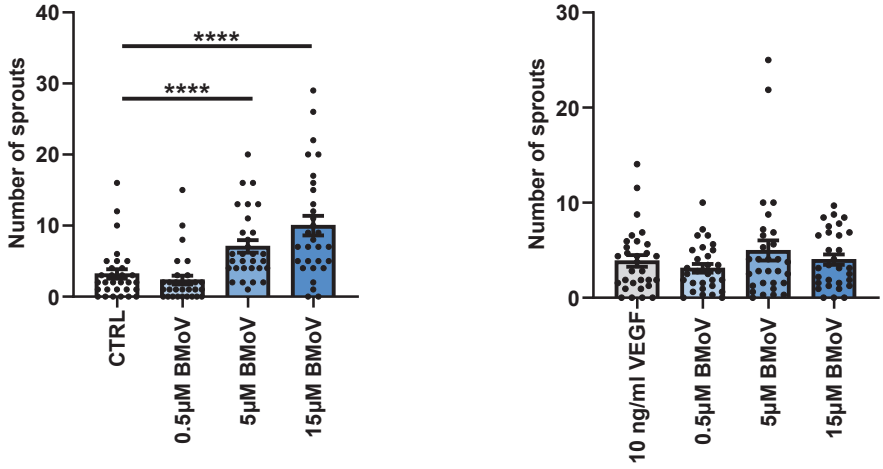
Supplemental 1. Quantification of HUVECs scratch-wound healing after treatment with either (A) BMOV alone in different concentrations (0.5, 5, 15 µM), or (B) different concentrations of BMOV (0.5, 5, 15 µM) supplemented with 10 ng/ml VEGF-A. Datapoints represent averages obtained from 3 independent experiments and are presented as mean±SEM. *p < 0.05 by two-sided Student t test.



Supplemental 2. Quantification of HUVECs proliferation after treatment with either (A) BMOV alone in different concentrations (0.5, 5, 15 µM), or (B) different concentrations of BMOV (0.5, 5, 15 µM) supplemented with 10 ng/ml VEGF-A. Datapoints represent averages obtained from 3 independent experiments and are presented as mean±SEM. *p < 0.05; **p < 0.01 by two-sided Student t test.



Supplemental 3. Quantification of HUVECs tube formation after treatment with either (A) BMOV alone in different concentrations (0.5, 5, 15 µM), or (B) different concentrations of BMOV (0.5, 5, 15 µM) supplemented with 10 ng/ml VEGF-A. Datapoints represent averages obtained from 3 independent experiments and are presented as mean±SEM. *p < 0.05 by two-sided Student t test.



Supplemental 4. Quantification of neovessel sprouts after treatment with either (A) BMOV alone in different concentrations (0.5, 5, 15 µM), or (B) different concentrations of BMOV (0.5, 5, 15 µM) supplemented with 10 ng/ml VEGF-A in an ex vivo aortic ring assay. Datapoints are presented as mean±SEM. **** p<0.0001 by two-sided Student t test.

CHAPTER 8

GENERAL SUMMARY AND FUTURE PERSPECTIVES

General summary

Atherosclerosis is a progressive disease characterized by the formation of plaques in the intima of major arteries with accumulation of lipids, inflammation, fibrosis, cell death and calcification [1]. The stability of atherosclerotic plaques, rather than the size, is the major determinant for acute clinical implications. When a plaque becomes unstable, it is more likely to rupture, leading to myocardial infarction, stroke and sudden death. Characteristics of unstable plaques are intraplaque angiogenesis and haemorrhage, a large lipid core, high macrophage content and a thin fibrous cap. Over the years, due to cholesterol-lowering drugs, the lifespan and well-being of patients have been significantly improved. However, a large group of patients does not fully benefit from current lipid-lowering strategies and plaque rupture remains the leading cause of acute cardiovascular events [2,3]. Therefore, there is a need for new therapeutic targets to stabilize atherosclerotic plaques and prevent plaque rupture.

Intraplaque angiogenesis is a complex process that depends on the equilibrium between different pro- and anti-angiogenic molecules [4]. Sources of pro-angiogenic signals are hypoxia and inflammation. On one side hypoxia is responsible for the transcription of factors promoting angiogenesis like VEGF-A, in an attempt to create new vessels to repristinate oxygen levels in the plaque. On the other side inflammation is also a strong inducer of angiogenesis as it promotes the synthesis of various angiogenic factors. Beside triggering angiogenesis, several pro-angiogenic molecules can also induce vessel permeability, contributing to the infiltration of leukocytes in the inflammatory core and thereby provoking chronic inflammation [5]. These factors contribute to plaque instability and subsequent rupture.

Because intraplaque neovascularization was shown to have a major causative effect on atherosclerosis and plaque destabilization in humans [6], the aim of the first part of this thesis was to investigate whether inhibition of intraplaque neovascularization might be a promising new therapeutic approach for atherosclerotic plaque stabilization. In the second part of this thesis we focused on a new strategy to increase *in vitro* angiogenesis.

In **chapter 2** we describe the pathological processes associated with angiogenesis in atherosclerotic plaques and illustrate how intraplaque angiogenesis and intraplaque

haemorrhage are strongly correlated with atherosclerotic plaque progression, instability and rupture. We also describe in detail the cellular and molecular mechanisms behind intraplaque angiogenesis. We report that intraplaque hypoxia is the main force driving intraplaque angiogenesis promoting the transcription of pro-angiogenic genes and mediating inflammation by promoting pro-inflammatory cytokine expression and consequently inflammatory cell recruitment. As key players in intraplaque angiogenesis we describe the structure of newly formed vessels as immature and leaky due to incomplete endothelial cell tight junction formation and insufficient and disorganized pericyte coverage. Moreover, we delineate the phenomenon of intraplaque haemorrhage, consisting of extravasation of red blood and inflammatory cells from the leaky neovessels, and its relation with inflammatory mediators, and the subsequent effects of intraplaque haemorrhage on plaque instability, both in experimental models and in humans. Moreover, options to target plaque angiogenesis for imaging and therapeutic purposes are discussed.

Due to the role of hypoxia as the main trigger for intraplaque angiogenesis, in **chapter 3** we hypothesized that plaque reoxygenation would result in decreased intraplaque neovessel formation and therefore reduced intraplaque haemorrhage and inflammation leading to increased plaque stability. To achieve this, we used carbogen gas, a gas that is composed of 95% O_2 and 5% CO_2. For this, we used hypercholesterolemic ApoE3*Leiden mice that underwent vein graft surgery and studied the effect of plaque reoxygenation and its outcome on vessel wall remodeling, intraplaque neovascularization, inflammation and patency. Moreover, since prolonged exposure to high levels of oxygen, hyperoxia, has the risk of generating reactive oxygen species in an amount that is higher than what can be cleared by anti-oxidants, we investigated the effect of reactive oxygen species on the plaque environment *in vivo* and on cultured macrophages *in vitro*. Administration of carbogen gas in an acute short-term setting resulted in a profound reduction of intraplaque hypoxia in murine accelerated atherosclerotic lesions *in vivo*. Long-term treatment with carbogen gas resulted in an increased vein graft patency in ApoE3*Leiden mice, but surprisingly, had no effect on intraplaque hypoxia and intraplaque angiogenesis and haemorrhage. At the same time, long-term carbogen gas treatment resulted in hyperoxia-induced ROS accumulation with subsequent induced transcription of HIF1a gene and increased HIF1a mRNA levels and macrophage apoptosis, probably due to their high oxygen consumption. To study the above-

mentioned ROS effect on macrophages we mimicked induction of ROS *in vitro* by using the ROS-mimic t-BHP in murine bone marrow derived macrophages and we observed a strong increment in DNA damage and apoptosis. Overall, despite the beneficial effect of hyperoxygenation treatment on vein graft patency, the treatment also induced ROS accumulation and apoptosis. Both ROS accumulation and apoptosis will possibly be detrimental for the plaque environment in this model under the current conditions. This indicates that in order to define potential therapeutic benefits of hyperoxygenation therapy, further research is needed to the define optimal conditions for the treatment of atherosclerosis.

In the signaling cascade following hypoxia and Hif1a stabilization, the recruitment of VEGF-A plays a critical role in promoting angiogenesis via binding to its receptor VEGFR2 and initiating a pro-angiogenic signaling cascade. Therefore, in **chapter 4** we investigated the results of VEGFR2 blockade using DC101 blocking antibody on intraplaque angiogenesis, maturation status of the neovessels, and atherosclerotic lesion size and composition in accelerated atherosclerotic vein graft lesions in ApoE3*Leiden mice. Upon VEGFR2 blockade, we observed a reduction in lesion size in the treated animals when compared to controls. At the same time collagen and smooth muscle cell (SMC) content were increased and macrophage content was decreased, all together pointing to an increased plaque stability. Surprisingly the treatment did not result in a decrease in $CD31^+$ neovessels. However, when looking at the maturation status of the vessels we could see that the treated group showed a decrease in intraplaque haemorrhage when compared to the controls. To address this aspect, we looked at the expression of genes that are involved in vessel maturation and found that Ang-2, the vessel destabilizing factor, was decreased upon DC101 treatment. Moreover, we observed an increase in Cx40 mRNA level, involved in inter-endothelial cells connections, as a consequence of VEGFR2 blockade. We used an aortic ring assay to study the effect of VEGFR2 blockade on vessel maturation at a cellular level and found that DC101 treatment increased the pericyte coverage around the endothelial cell layer of the formed neovessels. This study points to vascular maturation as an attractive target to stabilize atherosclerotic lesions. In particular VEGFR2 represents a potential target to induce atherosclerotic plaque stabilization.

Another important growth factor that promotes intraplaque angiogenesis in atherosclerosis is bFGF. In **chapter 5** we study the effect of bFGF blockade on intraplaque angiogenesis, SMC

content and inflammation in accelerated atherosclerotic lesions in ApoE3* Leiden mice that underwent vein graft surgery. To achieve this, we synthesized K5, a small molecule that binds to bFGF and results in bFGF signaling blockade. We found that K5 mediated inhibition of bFGF increases plaque stability via strongly reducing intraplaque angiogenesis and intraplaque haemorrhage. Also, K5 treatment reduced the number of circulating monocytes and decreased the expression of adhesion molecule VCAM-1 and chemoattractant protein Ccl2, together resulting in a decreased macrophage content in the atherosclerotic lesions. It was previously shown that bFGF blockade affects SMC proliferation and migration. Surprisingly we could not observe any effect on SMC in the accelerated atherosclerosis vein graft model nor in the femoral artery cuff model, used to study the isolated effect of K5 on SMC migration and proliferation. We also examined more in depth the effect of K5 on angiogenesis and we found that K5 strongly reduced *in vivo* angiogenesis in a Matrigel plug model. We also demonstrate that K5 is able to impair EC migration, proliferation and tube formation due to a reduced FGFR1 activation *in vitro*. K5 was able to enhance plaque stability via reduced intraplaque angiogenesis and decreased intraplaque haemorrhage. Moreover, it reduced systemic circulating monocytes and decreased macrophages infiltration in the plaque and therefore reduced inflammation in the lesions. Taken together, our results show that K5-mediated bFGF signaling blockade is a promising therapeutic candidate for the treatment of unstable atherosclerotic plaques.

Targeting endothelial cell metabolism has been primarily explored for cancer and other diseases characterized by increased angiogenesis e.g., macular degeneration and inflammatory bowel disease [7-9]. Shifting endothelial cells into a more quiescent state, by targeting enzymes involved in cellular metabolism would potentially slow their proliferation, stabilize the endothelial junctions, and reduce the expression of cellular adhesion molecules [10]. Therefore, in **Chapter 6** we study how the inhibition of transketolase (TKT), a key metabolic enzyme involved in the pentose phosphate pathway (PPP), affects EC and macrophage functions. TKT is a thiamine dependent enzyme in the non-oxidative branch of the PPP that controls nucleotide biosynthesis and energy production. Both ECs and macrophages rely on this metabolic pathway for proliferation [10,11]. Due to the tight relationship between angiogenesis and inflammation in atherosclerosis, we studied the *in vitro* effect of TKT blockade, using a thiamine agonist oxythiamine, on EC and macrophages.

We found that TKT is abundantly present in human atherosclerotic lesions, specifically in EC and macrophages. TKT blockade resulted in reduced EC proliferation and migration of HUVEC *in vitro*. More interestingly we found TKT to be upregulated in macrophages with a pro-inflammatory phenotype (M1 macrophages) when compared to resting M0 macrophages. Upon TKT blockade the mRNA expression of pro-inflammatory and pro-angiogenic cytokines in M1 macrophages was reduced when compared to untreated M1 macrophages. Surprisingly we found that this reduction in pro-angiogenic molecules had a functional effect. HUVEC stimulated with supernatant from oxythiamine-treated M1 macrophages acquired a decreased migratory ability when compared to cells stimulated with supernatant from untreated M1 macrophages. These preliminary *in vitro* results show that TKT blockade can be an interesting target to reduce angiogenesis and inflammation in atherosclerosis.

In the second part of this thesis we examined the effect of bis(maltolato)oxovanadium(IV) (BMOV) on *in vitro* angiogenesis. VEGF-A binding to VEGFR2, induces the activation of the receptor and its phosphorylation at different tyrosine sites that triggers the initiation of the signaling cascade leading to the promotion of angiogenesis. Each tyrosine site promotes different cellular responses among which, cell permeability, proliferation and migration. The phosphorylation of these residues is tightly regulated. In this aspect, protein tyrosine phosphatases (PTPs) dephosphorylate VEGFR2 receptor or its downstream signaling enzymes, resulting in decreased angiogenesis. In **chapter 7** we examine the effect of PTPs blockade on VEGFR2 induced angiogenesis on *in vitro* cultured HUVEC using BMOV, a nonselective tyrosine phosphatase inhibitor. Based on our finding that HUVEC produce a basal amount of endogenous VEGF-A and this results in activation of VEGFR2 and subsequently low amount of angiogenesis, in this chapter we hypothesized that upon endogenous VEGF-A receptor activation, BMOV would enhance *in vitro* angiogenesis. Moreover, we hypothesized that exogenous VEGF-A addition would enhance the effect of BMOV resulting in increased VEGFR2 activation and subsequent angiogenesis. We found that BMOV alone strongly increases endothelial cell migration, proliferation and tube formation. Additionally, it stimulates the formation of mature neovessels, lined by EC and covered by pericytes, in an ex vivo aortic ring assay. Moreover, it increases the number of these newly formed vessels when compared to untreated control cultures. To unravel the molecular signaling involved in the observed effect on angiogenesis, we studied the BMOV-induced activation of VEGFR2 in HUVEC. Upon BMOV

treatment, the phosphorylation of the tyrosine residue Y951 was increased when compared to control as well as the phosphorylation of the downstream enzyme p38MAPK. Interestingly the ERK1/2 pathway was not activated by BMOV treatment indicating that the phosphorylation tyrosine residue Y1175 was not altered. In the *in vitro* assays performed we found that BMOV and VEGF-A do not work in a synergistic way in increasing angiogenesis. In fact, in the cell proliferation, tube formation and aortic ring assay the pro-angiogenic effect of BMOV resulted to be higher than its effect when co-administered with exogenous VEGF-A. Our results show that BMOV-mediated inhibition of PTPs is therefore a new promising strategy to induce and stimulate angiogenesis.

Future perspectives

Altogether, the association of intraplaque neovessels and their dysfunction with unstable plaque phenotype presents several therapeutic opportunities for the prevention of plaque rupture. In this thesis we investigated new potential angiogenic targets for the treatment of unstable atherosclerotic plaques and new therapeutic angiogenic targets. Several new therapies have emerged to treat high-risk patients. PCSK9 monoclonal antibodies and inclisiran have been successfully used to reduce cholesterol risk, and canakinumab, a monoclonal antibody against interleukin-1β, was used to reduce plaque inflammation [12-14]. Despite these major advances in cardiovascular research, plaque rupture remains the leading cause of acute events [15]. Therefore, additional therapies aimed at reducing atherosclerotic plaque rupture and its complications are needed.

Anti-angiogenic therapeutics for the treatment of atherosclerosis have not yet entered clinical trials, although promising results have been found in preclinical animal models. However, what we have learned from the treatment of other pathologies in which uncontrolled angiogenesis plays an important role, like cancer or neovascular ocular diseases, is that one of the major challenges in anti-angiogenic therapies is the fine tuning in finding the right dosage of the compound used. In fact using too high dosages could have vessel disruption as a consequence with increased extravasation of erythrocytes and inflammatory cells while a low anti-angiogenic treatment could potentially normalize the neovessels by increasing their pericyte coverage and reducing their leakiness, resulting in a more stable environment (Fig.1) [16]. In the cancer field, the results of different preclinical studies support the beneficial effects of tumor vascular normalization and show that the normalized

vasculature is characterized by vessels that are less leaky with a more normal basement membrane and enhanced coverage by pericytes [17-19]. Moreover, clinical data from a phase I trial comparing a low dose versus a high dose of bevacizumab, an antibody against VEGF, in patients with rectal cancer are consistent with the vascular normalization hypothesis. Therapy with 5 mg/kg Bevacizumab resulted in vessel normalization while the higher dose of 10 mg/kg induced dose-limiting toxicities and excessive disruptions of the vessels [20,21]. In the context of age-related macular degeneration and diabetic retinopathy, in which neovascularization and vascular leakage, including haemorrhage, are major causes of visual loss, it was previously shown that therapeutic antagonism of VEGF results in inhibition of both retinal and choroidal neovascularization, as well as a reduction in vascular permeability [22]. Furthermore, recent clinical trials have shown that treatment with anti-VEGF therapies can improve vision in these patients, probably due to the fact that anti-angiogenic therapy also normalizes and stabilizes immature vasculature in the eye [23-25].

Since it has been shown that pathologically formed vessels in tumors, ocular diseases and atherosclerosis are very similar between each other due to their abnormal structure and leakage of red blood cells [26] and that vascular normalization resulted in improved quality of angiogenesis in tumor and ocular diseases, it is very likely that this therapy could also be successful in patients with advanced unstable atherosclerotic plaques that present intraplaque angiogenesis and haemorrhage.

In advanced plaques, with immature neovessels penetrating into the growing atherosclerotic lesion with high levels of intraplaque haemorrhage, normalization of neovessels by anti-angiogenic molecules should aim at preventing or decreasing leakage of erythrocytes that contribute to plaque progression by stabilizing the neovessels [16,23] (Fig.1). This could be achieved by improving the formation of the basement membrane, increasing the number of cell-cell junctions and/or developing a more mature layer of covering pericytes around the endothelial cells. The resulting less leaky, less haemorrhagic neovessels might then stabilize the plaque microenvironment by delivering intraplaque oxygen and nutrients and therefore alleviating hypoxia [16] (Fig.1). On the other hand, high doses of anti-angiogenic agents are aimed to completely eradicate the abnormal neovessels, but at the same time they could also harm the vasculature of normal tissues. Moreover, blocking intraplaque angiogenesis as a whole could also result in increased hypoxia. In fact, the complete elimination of intraplaque

neovessels would not resolve the intraplaque lack of oxygen and by consequence would result in an even higher hypoxia and stimulation of angiogenesis and inflammation, and therefore a more unstable and prone to rupture plaque phenotype. Another aspect to take into account is that by disrupting intraplaque neovessels, high doses of anti-angiogenic agents could also increase the leakiness of the vessels and cause an increment in intraplaque haemorrhage. In this perspective the right dosage should be aimed at partially reduce the number of intraplaque neovessels and improve their maturation in order to decrease intraplaque haemorrhage rather than entirely eradicate them.

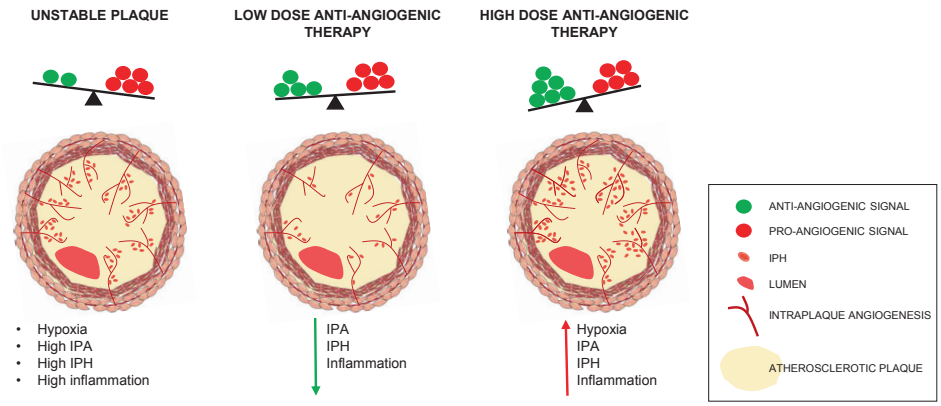


Figure 1. Hypothesis of intraplaque neovessels normalization. Schematic representation of anti-angiogenic treatment in atherosclerosis. **(Left panel)** Atherosclerotic plaque with an unstable phenotype in which pro-angiogenic signals are increased. In unstable plaques hypoxia, high intraplaque angiogenesis and haemorrhage and elevated inflammation are present. **(Middle panel)** Effect of low dose anti-angiogenic therapy on intraplaque environment. More stable plaque with decreased intraplaque angiogenesis, haemorrhage and inflammation. **(Right panel)** High dose anti-angiogenic therapy results in vessel disruption that causes increased hypoxia, intraplaque angiogenesis, haemorrhage and inflammation resulting in more unstable plaque phenotype.

In this thesis we showed this effect in both **chapter 4 and 5**. VEGFR2 blockade on *in vivo* accelerated atherosclerotic lesions in ApoE3*Leiden mice resulted in a decrease intraplaque haemorrhage induced by an increase vessel maturation, possibly due to increased stability of endothelial cells junctions and increased pericyte coverage. bFGF blockade in the same murine model resulted in decreased number of neovessels and intraplaque haemorrhage, and therefore increased lesion stability.

As we learned from the cancer field, another great challenge in anti-angiogenic therapies is that anti-angiogenic therapies often have transient effects as there are multiple compensatory mechanisms that take over [6]. Future strategies for the long-term treatment

of atherosclerosis should take this aspect into account. One possible approach to overcome this problem might be to use a combined therapy that targets not only one single growth factor but two or more. For example, it would be interesting to see the long-term effect of K5 treatment (**chapter 5**) combined with VEGFR2 blockade treatment (**chapter 4**). Another future strategy could be to combine anti-angiogenic factors with anti-inflammatory treatment. Another approach might be targeting cell metabolism. Li et al. proposed that if endothelial cell metabolism is targeted, the blood vessel will no longer be able to grow, regardless of how many pro-angiogenic signals are still present [10]. Based on this rationale, cellular metabolism is considered as the engine of the cell and if targeted and impaired, the endothelial cell would be deprived of energy and therefore would not be able to functionally respond to the pro-angiogenic growth factor signaling. The aim of this kind of therapy should not be to completely shut down cellular metabolism, because that would almost inevitably lead to cellular death but rather shifting the cells in a more quiescent and less proliferative state. In cancer studies, inhibition of the master regulator of glycolysis PFKFB3 decreased glycolysis in pericytes, thereby impairing their migration and proliferation, while increasing quiescence and adhesiveness [27]. This led to a tighter layer of pericytes covering the endothelial cells and contributed to the maturation and normalization of the tumor vasculature [27]. Due to the importance of neovessels and their maturation state in atherosclerosis, targeting cellular metabolism in advanced atherosclerotic plaques may have the added advantage of structurally stabilizing intraplaque neovessels by affecting not only the endothelial cells but also the pericytes. Since we showed in **chapter 6** that TKT blockade reduces endothelial cells and macrophage proliferation and reduces pro-angiogenic and pro-inflammatory cytokines production by M1 macrophages, it would be interesting to evaluate the effect of TKT blockade on vessel maturation.

In conclusion, this thesis presents further understanding in the role of intraplaque angiogenesis and haemorrhage in atherosclerosis. Furthermore, the studies included in this thesis identified new potential angiogenic therapeutic targets. Further research will show if these targets can successfully be used in patients suffering from cardiovascular disease.

References

1. Lusis, A.J. Atherosclerosis. *Nature* **2000**, *407*, 233-241, doi:10.1038/35025203.
2. Libby, P. Mechanisms of acute coronary syndromes and their implications for therapy. *The New England journal of medicine* **2013**, *368*, 2004-2013, doi:10.1056/NEJMra1216063.
3. Perrotta, P.; Emini Veseli, B.; Van der Veken, B.; Roth, L.; Martinet, W.; De Meyer, G.R.Y. Pharmacological strategies to inhibit intra-plaque angiogenesis in atherosclerosis. *Vascular pharmacology* **2019**, *112*, 72-78, doi:10.1016/j.vph.2018.06.014.
4. Potente, M.; Gerhardt, H.; Carmeliet, P. Basic and therapeutic aspects of angiogenesis. *Cell* **2011**, *146*, 873-887, doi:10.1016/j.cell.2011.08.039.
5. Fleiner, M.; Kummer, M.; Mirlacher, M.; Sauter, G.; Cathomas, G.; Krapf, R.; Biedermann, B.C. Arterial neovascularization and inflammation in vulnerable patients: early and late signs of symptomatic atherosclerosis. *Circulation* **2004**, *110*, 2843-2850, doi:10.1161/01.Cir.0000146787.16297.E8.
6. Sedding, D.G.; Boyle, E.C.; Demandt, J.A.F.; Sluimer, J.C.; Dutzmann, J.; Haverich, A.; Bauersachs, J. Vasa Vasorum Angiogenesis: Key Player in the Initiation and Progression of Atherosclerosis and Potential Target for the Treatment of Cardiovascular Disease. *Frontiers in immunology* **2018**, *9*, 706, doi:10.3389/fimmu.2018.00706.
7. Goveia, J.; Stapor, P.; Carmeliet, P. Principles of targeting endothelial cell metabolism to treat angiogenesis and endothelial cell dysfunction in disease. *EMBO molecular medicine* **2014**, *6*, 1105-1120, doi:10.15252/emmm.201404156.
8. Eelen, G.; de Zeeuw, P.; Treps, L.; Harjes, U.; Wong, B.W.; Carmeliet, P. Endothelial Cell Metabolism. *Physiological reviews* **2018**, *98*, 3-58, doi:10.1152/physrev.00001.2017.
9. Schoors, S.; De Bock, K.; Cantelmo, A.R.; Georgiadou, M.; Ghesquiere, B.; Cauwenberghs, S.; Kuchnio, A.; Wong, B.W.; Quaegebeur, A.; Goveia, J., et al. Partial and transient reduction of glycolysis by PFKFB3 blockade reduces pathological angiogenesis. *Cell metabolism* **2014**, *19*, 37-48, doi:10.1016/j.cmet.2013.11.008.
10. Li, X.; Sun, X.; Carmeliet, P. Hallmarks of Endothelial Cell Metabolism in Health and Disease. *Cell metabolism* **2019**, *30*, 414-433, doi:10.1016/j.cmet.2019.08.011.
11. Riksen, N.P.; Stienstra, R. Metabolism of innate immune cells: impact on atherosclerosis. *Curr Opin Lipidol* **2018**, *29*, 359-367, doi:10.1097/mol.0000000000000539.
12. Seidah, N.G.; Abifadel, M.; Prost, S.; Boileau, C.; Prat, A. The Proprotein Convertases in Hypercholesterolemia and Cardiovascular Diseases: Emphasis on Proprotein Convertase Subtilisin/Kexin 9. *Pharmacological reviews* **2017**, *69*, 33-52, doi:10.1124/pr.116.012989.
13. Nishikido, T.; Ray, K.K. Inclisiran for the treatment of dyslipidemia. *Expert opinion on investigational drugs* **2018**, *27*, 287-294, doi:10.1080/13543784.2018.1442435.
14. Ridker, P.M.; Everett, B.M.; Thuren, T.; MacFadyen, J.G.; Chang, W.H.; Ballantyne, C.; Fonseca, F.; Nicolau, J.; Koenig, W.; Anker, S.D., et al. Antiinflammatory Therapy with Canakinumab for Atherosclerotic Disease. *The New England journal of medicine* **2017**, *377*, 1119-1131, doi:10.1056/NEJMoa1707914.
15. Bentzon, J.F.; Otsuka, F.; Virmani, R.; Falk, E. Mechanisms of plaque formation and rupture. *Circ Res* **2014**, *114*, 1852-1866, doi:10.1161/circresaha.114.302721.
16. Jain, R.K.; Finn, A.V.; Kolodgie, F.D.; Gold, H.K.; Virmani, R. Antiangiogenic therapy for normalization of atherosclerotic plaque vasculature: a potential strategy for plaque stabilization. *Nature clinical practice. Cardiovascular medicine* **2007**, *4*, 491-502, doi:10.1038/ncpcardio0979.
17. Winkler, F.; Kozin, S.V.; Tong, R.T.; Chae, S.S.; Booth, M.F.; Garkavtsev, I.; Xu, L.; Hicklin, D.J.; Fukumura, D.; di Tomaso, E., et al. Kinetics of vascular normalization by VEGFR2 blockade governs brain tumor response to radiation: role of oxygenation, angiopoietin-1, and matrix metalloproteinases. *Cancer cell* **2004**, *6*, 553-563, doi:10.1016/j.ccr.2004.10.011.
18. Bierhansl, L.; Conradi, L.C.; Treps, L.; Dewerchin, M.; Carmeliet, P. Central Role of Metabolism in Endothelial Cell Function and Vascular Disease. *Physiology (Bethesda, Md.)* **2017**, *32*, 126-140, doi:10.1152/physiol.00031.2016.
19. Park, J.S.; Kim, I.K.; Han, S.; Park, I.; Kim, C.; Bae, J.; Oh, S.J.; Lee, S.; Kim, J.H.; Woo, D.C., et al. Normalization of Tumor Vessels by Tie2 Activation and Ang2 Inhibition Enhances Drug Delivery and Produces a Favorable Tumor Microenvironment. *Cancer cell* **2016**, *30*, 953-967, doi:10.1016/j.ccell.2016.10.018.

20. Willett, C.G.; Boucher, Y.; di Tomaso, E.; Duda, D.G.; Munn, L.L.; Tong, R.T.; Chung, D.C.; Sahani, D.V.; Kalva, S.P.; Kozin, S.V., et al. Direct evidence that the VEGF-specific antibody bevacizumab has antivascular effects in human rectal cancer. *Nature medicine* **2004**, *10*, 145-147, doi:10.1038/nm988.
21. Willett, C.G.; Boucher, Y.; Duda, D.G.; di Tomaso, E.; Munn, L.L.; Tong, R.T.; Kozin, S.V.; Petit, L.; Jain, R.K.; Chung, D.C., et al. Surrogate markers for antiangiogenic therapy and dose-limiting toxicities for bevacizumab with radiation and chemotherapy: continued experience of a phase I trial in rectal cancer patients. *Journal of clinical oncology : official journal of the American Society of Clinical Oncology* **2005**, *23*, 8136-8139, doi:10.1200/jco.2005.02.5635.
22. Aiello, L.P.; Pierce, E.A.; Foley, E.D.; Takagi, H.; Chen, H.; Riddle, L.; Ferrara, N.; King, G.L.; Smith, L.E. Suppression of retinal neovascularization in vivo by inhibition of vascular endothelial growth factor (VEGF) using soluble VEGF-receptor chimeric proteins. *Proceedings of the National Academy of Sciences of the United States of America* **1995**, *92*, 10457-10461, doi:10.1073/pnas.92.23.10457.
23. Jain, R.K. Normalizing tumor vasculature with anti-angiogenic therapy: a new paradigm for combination therapy. *Nature medicine* **2001**, *7*, 987-989, doi:10.1038/nm0901-987.
24. Gragoudas, E.S.; Adamis, A.P.; Cunningham, E.T., Jr.; Feinsod, M.; Guyer, D.R. Pegaptanib for neovascular age-related macular degeneration. *The New England journal of medicine* **2004**, *351*, 2805-2816, doi:10.1056/NEJMoa042760.
25. Ferrara, N.; Damico, L.; Shams, N.; Lowman, H.; Kim, R. Development of ranibizumab, an anti-vascular endothelial growth factor antigen binding fragment, as therapy for neovascular age-related macular degeneration. *Retina (Philadelphia, Pa.)* **2006**, *26*, 859-870, doi:10.1097/01.iae.0000242842.14624.e7.
26. Herrmann, J.; Lerman, L.O.; Mukhopadhyay, D.; Napoli, C.; Lerman, A. Angiogenesis in atherogenesis. *Arterioscler Thromb Vasc Biol* **2006**, *26*, 1948-1957, doi:10.1161/01.ATV.0000233387.90257.9b.
27. Cantelmo, A.R.; Conradi, L.C.; Brajic, A.; Goveia, J.; Kalucka, J.; Pircher, A.; Chaturvedi, P.; Hol, J.; Thienpont, B.; Teuwen, L.A., et al. Inhibition of the Glycolytic Activator PFKFB3 in Endothelium Induces Tumor Vessel Normalization, Impairs Metastasis, and Improves Chemotherapy. *Cancer cell* **2016**, *30*, 968-985, doi:10.1016/j.ccell.2016.10.006.

APPENDICES

NEDERLANDSE SAMENVATTING
RIASSUNTO IN ITALIANO
LIST OF PUBLICATIONS
CURRICULUM VITAE
ACKNOWLEDGEMENTS

Nederlandse Samenvatting

Atherosclerose is een progressieve ziekte die wordt gekenmerkt door de vorming van plaques in de intima van grote slagaders met ophoping van lipiden, ontstekingscellen, fibrose, en verkalking. De stabiliteit van atherosclerotische plaques, eerder dan de grootte, is de belangrijkste determinant voor acute klinische implicaties. Wanneer een plaque onstabiel wordt, is de kans groter dat deze scheurt, wat leidt tot een myocardinfarct of een beroerte en een plotselinge dood. Kenmerken van onstabiele plaques zijn intraplaque angiogenese en bloeding, een grote lipidenkern, een hoog macrofaaggehalte en een dunne afdekkende kap. In de loop der jaren zijn de levensduur en het welzijn van patiënten door cholesterolverlagende middelen aanzienlijk verbeterd. Een grote groep patiënten heeft echter niet ten volle profijt van de huidige lipidenverlagende strategieën en de plaqueruptuur blijft de belangrijkste oorzaak van acute cardiovasculaire aandoeningen. Daarom is er behoefte aan nieuwe therapeutische doelwitten om atherosclerotische plaques te stabiliseren en plaqueruptuur te voorkomen.

Intraplaque angiogenese is een complex proces dat afhankelijk is van het evenwicht tussen verschillende pro- en anti-angiogenese factoren. Bronnen van pro-angiogenese signalen zijn hypoxie en ontsteking. Aan de ene kant is hypoxie verantwoordelijk voor de transcriptie van factoren die angiogenese bevorderen, zoals VEGF-A, in een poging om nieuwe vaten te creëren om de zuurstofniveaus in de plaque te herstellen. Aan de andere kant is ontsteking ook een sterke oorzaak van angiogenese, omdat het de synthese van verschillende angiogenese factoren bevordert. Naast het uitlokken van angiogenese kunnen verschillende pro-angiogenese moleculen ook vaatpermeabilteit induceren, wat bijdraagt aan de infiltratie van leukocyten in de ontstekingskern en zo een chronische ontsteking veroorzaakt. Deze factoren dragen bij aan de instabiliteit van de plaque en de daaropvolgende breuk.

Omdat intraplaque neovascularisatie een belangrijk oorzakelijk effect bleek te hebben op atherosclerose en plaque destabilisatie bij de mens, was het doel van het eerste deel van dit proefschrift om te onderzoeken of remming van intraplaque neovascularisatie een veelbelovende nieuwe therapeutische benadering zou kunnen zijn voor atherosclerotische plaquestabilisatie. In het tweede deel van dit proefschrift hebben we ons gericht op een nieuwe strategie om de *in vitro* angiogenese te verhogen.

In **hoofdstuk 2** beschrijven we de pathologische processen die gepaard gaan met angiogenese in atherosclerotische plaques en illustreren we hoe intraplaque angiogenese en intraplaque bloeding sterk gecorreleerd zijn met atherosclerotische plaque progressie, instabiliteit en breuk. We beschrijven ook in detail de cellulaire en moleculaire mechanismen achter intraplaque angiogenese. We rapporteren dat intraplaque hypoxie de belangrijkste drijvende kracht is achter intraplaque angiogenese die de transcriptie van pro-angiogenese genen bevordert en de ontsteking bemiddelt door het bevorderen van pro-inflammatoire cytokine productie en bijgevolg het aanwerven van inflammatoire cellen. Als belangrijke spelers in de intraplaque angiogenese beschrijven we de structuur van nieuw gevormde vaten als onvoltooid en lek als gevolg van onvolledige endotheelcel tight-junction vorming en onvoldoende en ongeorganiseerde bedekking met pericyten. Bovendien schetsen we het fenomeen van de intraplaque bloeding, bestaande uit extravasatie van rode bloedcellen en ontstekingscellen uit de lekkende nieuw gevormde vaten en de relatie met ontstekingsmediatoren, en de daaropvolgende effecten van intraplaque bloeding op de instabiliteit van de plaque, zowel in experimentele modellen als bij de mens. Bovendien worden opties besproken om de angiogenese van de plaque aan te pakken voor beeldvorming en therapeutische doeleinden.

Vanwege de rol van hypoxie als de belangrijkste trigger voor intraplaque angiogenese, hebben we in **hoofdstuk 3** de hypothese geformuleerd dat reoxygenatie van de plaque zou resulteren in verminderde intraplaque vorming van neovaten en dus minder intraplaque bloedingen en ontstekingen die leiden tot een grotere stabiliteit van de plaque. Om dit te bereiken, gebruikten we carbogen gas, een gas dat voor 95% uit O_2 en 5% uit CO_2 bestaat. Hiervoor gebruikten we hypercholesterolemische ApoE3*Leiden muizen die een adertransplantatieoperatie ondergingen en bestudeerden we het effect van plaque reoxygenatie en het resultaat daarvan op vaatwandherstructurering, intraplaque neovascularisatie, ontsteking en vaat permeabiliteit. Bovendien, aangezien langdurige blootstelling aan hoge niveaus van zuurstof (hyperoxie) risico geeft tot het genereren van reactieve zuurstofsoorten in een hoeveelheid die hoger is dan wat kan worden verwijderd door anti-oxidanten, hebben we het effect van reactieve zuurstofsoorten op de plaque omgeving *in vivo* en op gekweekte macrofagen *in vitro* onderzocht. Toediening van carbogen gas in een acute kortdurende setting resulteerde in een diepgaande reductie van

intraplaque hypoxie in murine versnelde atherosclerotische laesies *in vivo*. Langdurige behandeling met carbogen gas resulteerde in een verhoogde doorgankelijkheid van de getransplanteerde venen bij ApoE3*Leiden muizen, maar had verrassend genoeg geen effect op intraplaque hypoxie en intraplaque angiogenese en bloeding. Tegelijkertijd leidde de behandeling met carbogene gassen op lange termijn tot hyperoxie-geïnduceerde ROS-ophoping met daaropvolgend geïnduceerde productie van het HIF1a-gen en verhoogde HIF1a mRNA-niveaus en macrofaagapoptose, waarschijnlijk als gevolg van hun hoge zuurstofconsumptie. Om het bovengenoemde ROS-effect op macrofagen te bestuderen hebben we de inductie van ROS *in vitro* nagebootst door gebruik te maken van de ROS-mimische t-BHP in van muizenbotmerg afgeleide macrofagen en hebben we een sterke toename in DNA-schade en apoptose waargenomen. Over het geheel genomen heeft de behandeling, ondanks het gunstige effect van de behandeling met hyperoxygenatie op de doorgangklijkheid van de getransplanteerde venen, ook ROS-ophoping en apoptose geïnduceerd. Zowel ROS-ophoping als apoptose zullen in dit model onder de huidige omstandigheden mogelijk schadelijk zijn voor het plaque-milieu. Dit geeft aan dat om de potentiële therapeutische voordelen van hyperoxygenatietherapie te definiëren, verder onderzoek nodig is om de optimale condities voor de behandeling van atherosclerose te definiëren.

In de signaalcascade na hypoxie en Hif1a stabilisatie speelt de rekrutering van VEGF-A een cruciale rol in het bevorderen van angiogenese via binding aan de receptor VEGFR2 en het initiëren van een pro-angiogenese signaalcascade. Daarom hebben we in **hoofdstuk 4** de resultaten van VEGFR2-blokkade onderzocht met behulp van DC101, een VEGFR2-blokkerend antilichaam, op intraplaque angiogenese en ontwikkeling van de capillairen, atherosclerotische laesiegrootte en -samenstelling in versnelde atherosclerotische veneuze transplantaties in ApoE3*Leiden-muizen. Bij VEGFR2-blokkade zagen we een vermindering van de laesiegrootte in de behandelde dieren in vergelijking met de controlegroep. Tegelijkertijd werd het gehalte aan collageen en gladde spiercellen (SMC) verhoogd en het gehalte aan macrofagen verlaagd, wat wijst op een verhoogde stabiliteit van de plaque. Verrassend genoeg resulteerde de behandeling niet in een afname van CD31+ neovaatjes. Echter, als we kijken naar de ontwikkeling van de vaatjes konden we zien dat de behandelde groep een afname van de intraplaque bloeding

vertoonde in vergelijking met de controlegroep. Om dit aspect verder te onderzoeken, keken we naar de expressie van de genen die betrokken zijn bij de vaatontwikkeling en vonden we dat Ang-2, een vaatdestabiliserende factor, was afgenomen bij de DC101-behandeling. Bovendien zagen we een toename in het Cx40 mRNA niveau, betrokken bij inter-endotheelcel verbindingen, als gevolg van VEGFR2 blokkade. We gebruikten een aorta-ring assay om het effect van VEGFR2-blokkade op de vaatontwikkeling op cellulair niveau te bestuderen en vonden dat de DC101-behandeling de dekking met percyten rond de endotheelcellaag van de gevormde neovaten verhoogde. Deze studie geeft aan dat de vasculaire ontwikkeling een aantrekkelijk therapeutisch doelwit kan zijn om atherosclerotische laesies te stabiliseren. In het bijzonder VEGFR2 vertegenwoordigt een potentieel doelwit om atherosclerotische plaquestabilisatie te induceren.

Een andere belangrijke groeifactor die intraplaque angiogenese bij atherosclerose bevordert, is bFGF. In **hoofdstuk 5** bestudeerden we het effect van bFGF-blokkade op intraplaque angiogenese, SMC-gehalte en ontsteking bij versnelde atherosclerotische laesies in ApoE3* Leiden muizen die een veneuze transplantatieoperatie ondergingen. Om dit te bereiken hebben we K5 gesynthetiseerd, een klein molecuul dat bindt aan bFGF en resulteert in een bFGF-signaalblokkade. We vonden dat K5 gemedieerde remming van bFGF de plaquestabiliteit verhoogt via een sterke vermindering van de intraplaque angiogenese en intraplaque bloeding. Ook verminderde K5 behandeling het aantal circulerende monocyten en verminderde de expressie van het adhesiemolecuul VCAM-1 en het chemoattractant eiwit Ccl2, wat samen resulteerde in een verminderd macrofaaggehalte in de atherosclerotische laesies. Eerder werd aangetoond dat bFGF-blokkade invloed heeft op SMC-proliferatie en -migratie. Verrassend genoeg konden we geen effect op SMC waarnemen in het versnelde atherosclerose veneuze transplantaatmodel of in het femorale slagader-manchetmodel, dat gebruikt wordt om het geïsoleerde effect van K5 op SMC-migratie en -proliferatie te bestuderen. We hebben ook het effect van K5 op de angiogenese nader onderzocht en we vonden dat K5 de *in vivo* angiogenese sterk verminderde in een Matrigel plug model. We hebben ook aangetoond dat K5 in staat is om de endotheel cel migratie, proliferatie en buisvorming te verminderen door een verminderde FGFR1 activering *in vitro*. K5 was in staat om de plaquestabiliteit te verbeteren via verminderde intraplaque angiogenese en verminderde intraplaque bloeding. Bovendien verminderde het de

systemische circulerende monocyten en verminderde het de infiltratie van macrofagen in de plaque en dus ook de ontsteking in de laesies. Onze resultaten tonen aan dat een K5 gemedieerde bFGF signaalblokkade een veelbelovende therapeutische kandidaat is voor de behandeling van onstabiele atherosclerotische plaques.

Het metabolisme van endotheelcellen is voornamelijk onderzocht in kanker en andere ziekten die worden gekenmerkt door een verhoogde angiogenese, zoals maculadegeneratie en inflammatoire darmziekten. Het normaliseren van de activiteit van endotheelcellen, door zich te richten op enzymen die betrokken zijn bij het metabolisme van de cel zou hun proliferatie kunnen vertragen, de endotheelverbindingen kunnen stabiliseren en de expressie van cellulaire adhesiemoleculen kunnen verminderen. Daarom bestuderen we in **hoofdstuk 6** hoe de remming van transketolase (TKT), een belangrijk metabool enzym dat betrokken is bij de pentose-fosfaatroute (PPP), de endotheel cel - en macrofaagfuncties beïnvloedt. TKT is een thiamine-afhankelijk enzym in de niet-oxidatieve tak van de PPP dat de biosynthese van nucleotiden en de energieproductie controleert. Zowel endotheel cellen als macrofagen zijn afhankelijk van deze metabole route voor cel proliferatie. Vanwege het nauwe verband tussen angiogenese en ontsteking bij atherosclerose hebben we het *in vitro* effect van TKT blokkade, met behulp van een thiamine agonist oxythiamine, op endotheel cellen en macrofagen bestudeerd. We vonden dat TKT overvloedig aanwezig is in menselijke atherosclerotische laesies, specifiek in endotheel cellen en macrofagen. TKT-blokkade resulteerde in een verminderde endotheel cel proliferatie en migratie van HUVEC *in vitro*. Interessanter is dat TKT in macrofagen met een pro-inflammatoir fenotype (M1-macrofagen) sterker geïnduceerd wordt in vergelijking tot rustende M0-macrofagen. Bij TKT blokkade werd de mRNA expressie van pro-inflammatoire en pro-angiogenese cytokinen in M1-macrofagen gereduceerd in vergelijking met onbehandelde M1-macrofagen. Verrassend genoeg vonden we dat deze reductie van pro-angiogenese moleculen een functioneel effect had. HUVEC gestimuleerd met supernatant van oxythiamine-behandelde M1-macrofagen vertoonden een verminderd migratievermogen in vergelijking met cellen gestimuleerd met supernatant van onbehandelde M1-macrofagen. Deze *in vitro* resultaten tonen aan dat ook TKT-blokkade een interessant doelwit kan zijn om angiogenese en ontsteking in atherosclerose te verminderen.

In het tweede deel van dit proefschrift hebben we het effect van bis(maltolato)oxovanadium(IV) (BMOV) op *in vitro* angiogenese onderzocht. VEGF-A binding aan VEGFR2, induceert de activering van de receptor en de fosforylering ervan op verschillende tyrosine residuen die de initiatie van de signaalcascade activeert wat vervolgens leidt tot de bevordering van angiogenese. Elke tyrosine residuen bevordert verschillende cellulaire reacties waaronder celpermeabiliteit, proliferatie en migratie. De fosforylering van deze residuen is streng gereguleerd. In dit aspect, eiwit tyrosine fosfatases (PTP's) defosforyleren VEGFR2 receptor of de downstream-signaal enzymen, wat resulteert in verminderde angiogenese. In **hoofdstuk 7** onderzochten we het effect van PTP's blokkade op VEGFR2 geïnduceerde angiogenese op *in vitro* gekweekte HUVEC met behulp van BMOV, een niet-selectieve tyrosine fosfataseremmer. Op basis van onze bevinding dat HUVEC een basale hoeveelheid endogene VEGF-A produceren en dit resulteert in activering van VEGFR2 en vervolgens een lage hoeveelheid angiogenese, hebben we in dit hoofdstuk de hypothese geformuleerd dat bij endogene VEGF-A receptor activering, BMOV *in vitro* angiogenese zou verbeteren. Bovendien veronderstellen we dat exogene VEGF-A toevoeging het effect van BMOV zou versterken, wat zou resulteren in een verhoogde VEGFR2 activering en de daaropvolgende angiogenese. We vonden dat BMOV alleen de endotheelcel migratie, -proliferatie en -buisvorming sterk verhoogt. Bovendien stimuleert het de vorming van functionele neovaatjes, bekleed met endotheel cellen en bedekt met pericyten, in een ex vivo aorta-ringproef. Bovendien verhoogt het aantal van deze nieuw gevormde vaten in vergelijking met onbehandelde controlekweken. Om de moleculaire signalisatie die betrokken is bij het waargenomen effect op de angiogenese te ontrafelen, hebben we de BMOV-geïnduceerde activering van VEGFR2 in HUVEC bestudeerd. Bij BMOV-behandeling werd de fosforylering van het tyrosine residue Y951 verhoogd in vergelijking met de controlegroep en de fosforylering van het downstream-enzym p38MAPK. Interessant is dat het ERK1/2-traject niet werd geactiveerd door de BMOV-behandeling, wat aangeeft dat het fosforyleringsresidu tyrosine Y1175 niet werd gewijzigd. In de uitgevoerde *in vitro* testen vonden we dat BMOV en VEGF-A niet op een synergetische manier werken in het verhogen van de angiogenese. In feite, in de celgroei, buisvorming en aorta-ringtest resulteerde het pro-angiogeen effect van BMOV in een hoger effect dan het effect bij gelijktijdige toediening van exogene VEGF-A. Onze resultaten tonen aan

dat BMOV-gemedieerde remming van PTP's daarom een nieuwe veelbelovende strategie is om angiogenese te induceren en te stimuleren.

Conclusie

Concluderend geeft dit proefschrift meer inzicht in de rol van intraplaque angiogenese en bloeding bij atherosclerose. Bovendien identificeerden de onderzoeken in dit proefschrift nieuwe potentiële angiogeen therapeutische doelen. Nader onderzoek zal uitwijzen of deze therapeutische doelen met succes kunnen worden gebruikt bij patiënten met hart- en vaatziekten.

Riassunto in Italiano

L'aterosclerosi è una malattia progressiva caratterizzata dalla formazione di placche aterosclerotiche nell'intima delle arterie principali con accumulo di lipidi, infiammazione, fibrosi, morte cellulare e calcificazione. La stabilità delle placche aterosclerotiche, piuttosto che la loro dimensione, è il principale fattore determinante per l'insorgere di implicazioni cliniche acute. Quando una placca diventa instabile, è più fragile e può rompersi più facilmente causando infarto del miocardio, ictus e morte improvvisa. Le prinicipali caratteristiche delle placche instabili sono la formazione di nuovi vasi (angiogenesi) ed emorragia intraplacca, un esteso nucleo lipidico, un alto contenuto di macrofagi e un sottile cappuccio fibroso. Nel corso degli anni, grazie ai farmaci per abbassare il colesterolo, la durata della vita e il benessere dei pazienti affetti da aterosclerosi sono notevolmente migliorati. Tuttavia, un ampio gruppo di pazienti non trae pienamente beneficio dalle attuali strategie di riduzione dei lipidi e la rottura della placca aterosclerotica rimane la principale causa di eventi cardiovascolari acuti. Pertanto, nuove terapie sono necessarie per stabilizzare le placche aterosclerotiche e prevenire la loro rottura. Alcuni nuovi possibili bersagli terapeutici sono ipotizzabili.

L'angiogenesi all'interno della placca aterosclerotica è un processo complesso che dipende dall'equilibrio tra molecole pro e anti-angiogeniche. L'ipossia, nel tentativo di creare nuovi vasi sanguigni per repristinare i livelli di ossigeno nella placca, e l'infiammazione rappresentano le principali fonti di segnali pro-angiogenici. Diverse molecole pro-angiogeniche possono anche aumentare la permeabilità dei vasi, contribuendo all'infiltrazione dei leucociti nel nucleo infiammatorio della placca, provocando quindi un processo di infiammazione cronica. Questi fattori contribuiscono all'instabilità della placca e alla sua successiva rottura.

É stato dimostrato che la neovascolarizzazione all'interno della placca aterosclerotica contribuisce al processo aterosclerotico e alla destabilizzazione della placca nell'uomo. Per questo motivo lo scopo della prima parte di questa tesi è stato quello di studiare se l'inibizione della neovascolarizzazione intraplacca potesse essere un nuovo approccio terapeutico per la stabilizzazione delle placche aterosclerotiche. Nella seconda parte di questa tesi ci siamo concentrati su una nuova strategia per indurre l'angiogenesi in vitro.

Nel **capitolo 2** illustriamo come angiogenesi ed emorragia intraplacca siano fortemente correlate con la progressione, l'instabilità e la rottura della placca aterosclerotica stessa. Descriviamo anche in dettaglio i meccanismi cellulari e molecolari alla base della neovascolarizzazione all'interno della placca. Segnaliamo che l'ipossia è la forza principale che guida l'angiogenesi promuovendo la trascrizione di geni pro-angiogenici e mediando l'infiammazione tramite l'espressione di citochine pro-infiammatorie e il reclutamento di cellule infiammatorie. Riportiamo anche che i capillari di nuova formazione hanno una struttura incompleta. Infatti le giunzioni tra le cellule endoteliali dei vasi intraplacca sono frammentarie e la copertura da parte dei periciti è insufficiente e disorganizzata. Queste caratteristiche danno origine al fenomeno dell'emorragia intraplacca, che consiste nello stravaso di globuli rossi e cellule infiammatorie dai vasi sanguigni appena formati verso l'interno della placca. L'emorragia intraplacca promuove l'instabilità della placca, sia nei modelli sperimentali murini sia nell'uomo. Inoltre, in questo capitolo vengono discusse diverse opzioni per evidenziare l'angiogenesi intraplacca con tecniche di imaging favorendo il suo utilizzo come bersaglio terapeutico.

A causa del ruolo dell'ipossia come principale fattore scatenante dell'angiogenesi intraplacca, nel **capitolo 3** abbiamo ipotizzato che la riossigenazione della placca aterosclerotica avrebbe potuto favorire una riduzione della formazione di angiogenesi e quindi una riduzione dell'emorragia e dell'infiammazione con conseguente aumento della stabilità. Per raggiungere questo obiettivo, abbiamo utilizzato il gas carbogen, un gas composto al 95% di O_2 e al 5% di CO_2. Abbiamo utilizzato topi ApoE3*Leiden ipercolesterolemici sottoposti a chirurgia per innesto venoso e studiato l'effetto della riossigenazione sul rimodellamento vascolare, la neovascolarizzazione intraplacca, l'infiammazione e la viabilità dell'innesto. Inoltre, poiché l'iperossia, cioè l'esposizione prolungata a livelli elevati di ossigeno, può generare specie reattive dell'ossigeno (ROS) in una quantità superiore a quella che può essere eliminata dagli antiossidanti, abbiamo studiato l'effetto dei ROS sulla composizione della placca *in vivo* e sui macrofagi *in vitro*. La somministrazione del gas carbogen in un esperimento a breve termine ha determinato una profonda riduzione dell'ipossia intraplacca nelle lesioni aterosclerotiche murine *in vivo*. Il trattamento a lungo termine ha comportato un aumento della vitalità dell'innesto venoso negli animali trattati, ma sorprendentemente non ha avuto alcun effetto sull'ipossia e su

angiogenesi ed emorragia intraplacca. Allo stesso tempo, il trattamento a lungo termine ha provocato l'accumulo di ROS. Questo ha portato a un conseguente aumento dei livelli di mRNA di HIF1a. Un'altra conseguenza del trattamento a lungo termine è stata l'apoptosi dei macrofagi, probabilmente a causa del loro elevato consumo di ossigeno. Per studiare il sopramenzionato effetto dei ROS sui macrofagi abbiamo imitato l'induzione dei ROS *in vitro* usando il ROS-mimic t-BHP nei macrofagi derivati da midollo osseo murino e abbiamo osservato un forte aumento del danno al DNA e dell'apoptosi. Complessivamente, nonostante l'effetto benefico del trattamento di iperossigenazione sulla viabilità dell'innesto venoso, il trattamento ha indotto anche l'accumulo di ROS e apoptosi. Sia l'accumulo di ROS sia l'apoptosi potrebbero essere dannosi per la placca aterosclerotica in questo modello murino nelle condizioni attuali. Ciò indica che, al fine di definire i potenziali benefici terapeutici della terapia di iperossigenazione, sono necessarie ulteriori ricerche per definire le condizioni ottimali per il trattamento dell'aterosclerosi.

Nella cascata di trasduzione del segnale a seguito di ipossia e stabilizzazione di Hif1a, il reclutamento del fattore di crescita dell'endotelio vascolare (VEGF-A) svolge un ruolo fondamentale nel promuovere l'angiogenesi. Infatti, il legame di VEGF-A con il suo recettore, il recettore del fattore di crescita dell'endotelio vascolare (VEGFR2) innesca l'avvio di una cascata di trasduzione intracellulare del segnale che ha un effetto pro-angiogenico. Pertanto, nel **capitolo 4,** utilizzando l'anticorpo DC101, abbiamo studiato gli effetti del blocco di VEGFR2 sull'angiogenesi intraplacca, sullo stato di maturazione dei vasi e sulla dimensione e la composizione delle lesioni aterosclerotiche nei topi ApoE3*Leiden sottoposti ad innesto venoso nella carotide. Abbiamo osservato una riduzione della dimensione della lesione negli animali trattati rispetto ai controlli. Allo stesso tempo, il contenuto di collagene e di cellule muscolari lisce (SMCs) è aumentato e il contenuto di macrofagi è stato ridotto, indicando nell'insieme una maggiore stabilità della placca. Sorprendentemente il trattamento non ha comportato una riduzione dei vasi sanguigni intraplacca $CD31^{+}$. Tuttavia, osservando lo stato di maturazione di questi vasi sanguigni, è stato possibile osservare che il gruppo trattato con DC101 ha mostrato una diminuzione dell'emorragia intraplacca rispetto ai controlli. Per approfondire questo aspetto, abbiamo esaminato l'espressione di geni coinvolti nella maturazione dei vasi sanguigni e abbiamo scoperto che Ang-2, il fattore destabilizzante dei vasi, era diminuito con il trattamento con

DC101. Inoltre, abbiamo osservato un aumento del livello di mRNA di Cx40, coinvolto nelle connessioni tra le cellule endoteliali, come conseguenza del blocco di VEGFR2. Abbiamo poi usato un aortic ring test per studiare l'effetto del blocco di VEGFR2 sulla maturazione dei vasi a livello cellulare e abbiamo scoperto che il trattamento con DC101 aumenta la copertura dei periciti intorno allo strato endoteliale nei vasi formati. Questo studio indica che la maturazione vascolare rappresenta un bersaglio promettente per stabilizzare le lesioni aterosclerotiche. In particolare, VEGFR2 rappresenta un potenziale bersaglio per indurre la stabilizzazione della placca aterosclerotica.

Un altro importante fattore di crescita che promuove l'angiogenesi intraplacca nell'aterosclerosi è il fattore di crescita dei fibroblasti (bFGF). Nel **capitolo 5** abbiamo studiato l'effetto del blocco di bFGF sull'angiogenesi intraplacca, sul contenuto di cellule muscolari lisce e sull'infiammazione nelle lesioni aterosclerotiche nei topi ApoE3*Leiden sottoposti a innesto venoso. Per raggiungere questo obiettivo, abbiamo sintetizzato K5, una piccola molecola che si lega a bFGF. Questo previene il legame tra bFGF e il suo recettore e di conseguenza provoca il blocco della trasduzione intracellulare del segnale che porta allo stimolo dell'angiogenesi. Abbiamo scoperto che l'inibizione di bFGF aumenta la stabilità della placca aterosclerotica riducendo fortemente l'angiogenesi e l'emorragia intraplacca. Inoltre, il trattamento con K5 riduce il numero di monociti circolanti e diminuisce l'espressione della molecola di adesione VCAM-1 e della proteina chemoattraente Ccl2, insieme con una conseguente riduzione del contenuto di macrofagi nelle lesioni aterosclerotiche. In precedenza, era stato dimostrato che il blocco di bFGF influenzava la proliferazione e la migrazione delle SMCs. Sorprendentemente non siamo stati in grado di osservare alcun effetto di K5 sulle cellule muscolari lisce nel modello di aterosclerosi accelerata con innesto venoso né nel modello dell'arteria femorale in topi C57BL/6 utilizzato per studiare l'effetto isolato di K5 sulla migrazione e sulla proliferazione delle SMCs. Abbiamo anche esaminato più in profondità l'effetto di K5 sul processo di angiogenesi e abbiamo scoperto che K5 riduce fortemente l'angiogenesi in vivo in un modello murino con impianti di Matrigel sottocute. Abbiamo dimostrato anche che *in vitro* K5 è in grado di compromettere la migrazione, la proliferazione e la formazione di strutture tubulari delle cellule endoteliali a causa di una ridotta attivazione del recettore del fattore di crescita dei fibroblasti-1 (FGFR1). K5 è in grado di migliorare la stabilità della placca riducendo

angiogenesi ed emorragia intraplacca. Inoltre, riduce il numero dei monociti circolanti a livello sistemico e riduce l'infiltrazione di macrofagi nella placca e quindi diminuisce l'infiammazione nelle lesioni aterosclerotiche. Nel loro insieme, i nostri risultati dimostrano che il blocco di bFGF tramite K5 è un promettente candidato terapeutico per il trattamento di placche aterosclerotiche instabili.

Il targeting del metabolismo delle cellule endoteliali è stato principalmente esplorato per il cancro e altre malattie caratterizzate da un aumento dell'angiogenesi, ad esempio degenerazione maculare e malattia infiammatoria intestinale. Spingere le cellule endoteliali in uno stato più quiescente, prendendo di mira gli enzimi coinvolti nel metabolismo cellulare, potrebbe potenzialmente rallentare la loro proliferazione, stabilizzare le giunzioni endoteliali e ridurre l'espressione delle molecole di adesione cellulare. Pertanto, nel **capitolo 6** abbiamo studiato come l'inibizione della transchetolasi (TKT), un enzima metabolico chiave coinvolto nella via del pentoso fosfati (PPP), influisca sulle cellule endoteliali (ECs) e i macrofagi. TKT è un enzima nel ramo non ossidativo del PPP che controlla la biosintesi dei nucleotidi e la produzione di energia e dipende dal legame con la tiamina per il suo funzionamento. Sia le ECs sia i macrofagi si affidano a questa via metabolica per la proliferazione. A causa della stretta relazione tra angiogenesi e infiammazione nell'aterosclerosi, abbiamo studiato l'effetto del blocco di TKT *in vitro* usando ossitiamina, un analogo della tiamina, su ECs e macrofagi. Abbiamo scoperto che TKT è abbondantemente presente nelle lesioni aterosclerotiche umane, in particolare nelle cellule endoteliali e nei macrofagi. Il blocco di TKT comporta una riduzione della proliferazione e della migrazione di ECs *in vitro*. Abbiamo anche scoperto che TKT è sovraespressa nei macrofagi con un fenotipo pro-infiammatorio (macrofagi M1) rispetto ai macrofagi M0 (a riposo). Il blocco di TKT nei macrofagi M1 riduce i livelli di espressione dell'mRNA di citochine pro-infiammatorie e pro-angiogeniche rispetto ai macrofagi M1 non trattati. Sorprendentemente abbiamo scoperto che questa riduzione delle molecole pro-angiogeniche ha un effetto funzionale. Infatti, cellule endoteliali derivate da cordoni ombelicali umani (HUVECs) stimolate con il surnatante di macrofagi M1 trattati con ossitiamina hanno una ridotta capacità migratoria rispetto alle cellule stimolate con surnatante di macrofagi M1 non trattati. Questi risultati preliminari *in vitro* mostrano che il

blocco di TKT può essere un target interessante per ridurre l'angiogenesi e l'infiammazione nelle placche aterosclerotiche.

Nella seconda parte di questa tesi abbiamo esaminato l'effetto del bis(maltolato) oxovanadio (IV) (BMOV) sull'angiogenesi *in vitro*. Il legame di VEGF-A con VEGFR2, induce l'attivazione del recettore e la sua fosforilazione in diversi residui tirosinici innescando l'inizio della cascata di trasduzione intracellulare del segnale che porta alla promozione dell'angiogenesi. Ogni residuo tirosinico promuove diverse risposte cellulari tra cui, permeabilità cellulare, proliferazione e migrazione. La fosforilazione di questi residui è strettamente regolata dalle proteine tirosin fosfatasi (PTPs). Le proteine tirosin fosfatasi defosforilano VEGFR2 o gli enzimi a valle della cascata di trasduzione del segnale, e di conseguenza riducono l'angiogenesi. Nel **capitolo 7** abbiamo esaminato l'effetto del blocco delle PTPs sul processo di angiogenesi usando HUVECs in coltura *in vitro* trattate con BMOV, un inibitore non selettivo delle proteine tirosin fosfatasi. Sulla base della nostra scoperta che le HUVEC producono una quantità basale di VEGF-A endogena con conseguente attivazione di VEGFR2 e una angiogenesi limitata, abbiamo ipotizzato che dopo l'attivazione endogena di VEGFR2 tramite VEGF-A, BMOV potrebbe aumentare l'angiogenesi *in vitro*. Inoltre, abbiamo ipotizzato che l'aggiunta di VEGF-A esogeno avrebbe migliorato l'effetto di BMOV con conseguente aumento dell'attivazione di VEGFR2 e successiva angiogenesi. Abbiamo scoperto che BMOV da solo aumenta fortemente la migrazione delle cellule endoteliali, la proliferazione e la formazione di strutture tubulari. Inoltre, in un esperimento di aortic ring *ex vivo*, BMOV stimola la formazione di vasi sanguigni maturi, formati da cellule endoteliali ricoperte da periciti. Inoltre, aumenta anche il numero di questi vasi rispetto alle colture di controllo non trattate. Per studiare la trasduzione intracellulare del segnale coinvolta nell'effetto osservato sull'angiogenesi, abbiamo studiato l'attivazione di VEGFR2 indotta da BMOV in HUVECs. Abbiamo trovato che il trattamento con BMOV induce un aumento della fosforilazione del residuo di tirosina Y951 e un aumento della fosforilazione dell'enzima p38MAPK rispetto ai controlli non trattati. È interessante notare che l'enzima ERK1/2 non è attivato dal trattamento con BMOV, il che indica che il residuo di tirosina Y1175 non è alterato dal trattamento. Nei test in vitro eseguiti abbiamo scoperto che BMOV e VEGF-A non funzionano in modo sinergico nell'aumentare l'angiogenesi. Infatti, nella proliferazione cellulare, nella formazione di strutture tubulari e nel test aortic ring, l'effetto

pro-angiogenico di BMOV si è rivelato superiore al suo effetto quando somministrato in associazione con VEGF-A esogeno. I nostri risultati mostrano che l'inibizione delle PTPs mediata da BMOV è quindi una nuova strategia promettente per indurre e stimolare l'angiogenesi.

In conclusione, questa tesi presenta una approfondita visione del ruolo dell'angiogenesi e dell'emorragia intraplacca nel processo di aterosclerosi. Inoltre, gli studi inclusi in questa tesi hanno identificato nuovi potenziali bersagli terapeutici per stabilizzare le lesioni aterosclerotiche a rischio di rottura. Ulteriori ricerche mostreranno se questi bersagli possono essere utilizzati con successo in pazienti affetti da malattie cardiovascolari.

List of publications

Plaque angiogenesis and intraplaque hemorrhage in atherosclerosis.
Parma L*, Baganha F*, Quax PHA, de Vries MR.
Eur J Pharmacology. 2017; 816:107-115.

Inhibition of 14q32 microRNA miR-495 reduces lesion formation, intimal hyperplasia and plasma cholesterol levels in experimental restenosis.
Welten SMJ, de Jong RCM, Wezel A, de Vries MR, Boonstra MC, Parma L, Jukema JW, van der Sluis TC, Arens R, Bot I, Agrawal S, Quax PHA, Nossent AY.
Atherosclerosis. 2017 Jun 261:26-36.

Adenosine-to-Inosine Editing of MicroRNA-487b Alters Target Gene Selection After Ischemia and Promotes Neovascularization.
van der Kwast RVCT, van Ingen E, Parma L, Peters HAB, Quax PHA, Nossent AY.
Circulation Research 2018 Feb 2;122(3):444-456.

Blockade of vascular endothelial growth factor receptor 2 inhibits intraplaque haemorrhage by normalization of plaque neovessels.
de Vries MR*, Parma L*, Peters HAB, Schepers A, Hamming JF, Jukema JW, Goumans MJTH, Guo L, Finn AV, Virmani R, Ozaki CK, Quax PHA.
J Internal Medicine. 2018; 285(1):59-74.

Prolonged hyperoxygenation treatment improves vein graft patency and decreases macrophage content in atherosclerotic lesions in ApoE3*Leiden mice.
Parma L, Peters HAB, Baganha F, Sluimer JC, de Vries MR and Quax PHA.
Cells. 2020 Feb 1;9(2).

Bis(maltolato)oxovanadium(IV) Induces Angiogenesis via Phosphorylation of VEGFR2
Parma L, Peters HAB, Johansson ME, Gutiérrez S, Meijerink H, de Kimpe S, de Vries MR and Quax PHA
Int. J. Mol. Sci. 2020, 21(13), 4643

Adenosine-to-Inosine editing of vasoactive microRNAs alters their targetome and function in ischemia.
van der Kwast RVCT, Parma L, van der Bent ML, van Ingen E, Baganha F, Peters HAB, Goossens EAC, Simons, KH, Palmen M, de Vries MR, Quax PHA, Nossent AY.
Molecular Therapy Nucleic Acids. July 2020

Small molecule mediated inhibition of bFGF reduces intraplaque angiogenesis and macrophage infiltration in accelerated atherosclerotic vein graft lesions in ApoE3*Leiden mice.
Parma L, Peters HAB, Simons KH, Lazzari P, de Vries MR, Quax PHA.
Manuscript under review.

Transketolase blockade reduces inflammation and angiogenesis in vitro.
Parma L, Schmit MC, Van Den Bogaert S, de Vries MR, Quax PHA.
Manuscript in preparation.

Curriculum Vitae

Curriculum Vitae

Laura Parma was born on the 29th of January 1990 in Italy. In July 2009 she graduated from the Liceo Scientifico A. Banfi in Vimercate and she obtained a high school Scientific Lyceum Diploma, including Biology and Physics. That same year, she started studying Biotechnology at the University of Milano. Afterward she studied Medical and Pharmaceutical Biotechnology at the University of Pavia and in September 2014 she obtained her MSc diploma. As a MSc student in medical biotechnology, her passion for molecular biology combined with a growing interest in taking an international challenge. As a result after completing her MSc degree she sought out an Erasmus+ internship fellowship at the surgery group of the Leiden University Medical Center to study new potential target for NIR Image-guided surgery in cancer biology under the supervision of Dr. Kees Sier.

Afterward she was selected for an Horizon2020 MSCA PhD position at the Leiden University Medical Center under the supervision of Prof. dr. Paul Quax and dr. Margreet de Vries. During the four years she studied different approaches to inhibit intraplaque angiogenesis in atherosclerosis and the results of her findings are described in this thesis. On July 1st, 2020, Laura started as a postdoctoral researcher in the lab of dr. Remco Megens at the Institute for Cardiovascular Prevention, Ludwig-Maximilians-University Munich, where she will study the role of CD8+ T-cell based nanomedicines in the local immunomodulation of atherosclerosis.

A

Acknowledgements

Acknowledgements

I would like to thank all the people that helped me in this journey that ends with the creation of this thesis.

Dear **professor Quax**, dear **Paul**, thank you for the past four years. Under your supervision I grew and became a more confident scientist. I really appreciated the freedom you gave me to explore new ideas and at the same time your ability to keep me on track. It was great to be part of your group!

Margreet, thank you for all the things you taught me during our long hours at the PDC. I discovered we had a lot of things in common, starting from our love for horses and our quite strong character. Thanks for the support and the endless help during the writing of this thesis.

Erna, my dear colleague, thanks for all the EC talks and teachings, I could not have had a better teacher. Thanks for all the pancakes, the coffees and for being there anytime I had a down moment and I needed a word with you. Thanks also for listening in the "what can we do?" situations.

My safe C7 room. Karin and **Fab**, thank you for the fun times and the stressful coffee stealing moments! **Valerie** and **Leontien**, you arrived during my last year but I could not imagine finishing my PhD without you. Thank you for the support, the great scientific talks, the late evening dinners at C7 and for always being there ready to help me during the writing of this thesis.

Eveline, **Eva** and **Licheng** my buddies from another floor. Thank you for the "staining trains", for being Beyoncé fans, for trying to teach me some Chinese words and for all the fun we had in the lab.

Thank you also to the other Quaxies **Yaël**, **Alwin**, **Thijs, Sabine** and **Rob** for the time spent together. A big thank you to **Stefano** for supervising me during my secondment and to my students that helped me during the years, **Michele**, **Boyd**, **Sanne**, **Maurits** and **Siel**.

Un grazie alla mia **mamma**, al mio **papà**, a mio fratello **Marco** e alla mia nonna **Angelina** per il continuo supporto e aiuto. Senza di voi probabilmente non sarei qui oggi!

And finally, the biggest thank you goes to my C7 buddy, colleague, friend and boyfriend **Regi**. It's crazy to think that without this PhD I wouldn't have met you and that without you it would have been extremely more difficult to finish this PhD. I'm proud of what we achieved and what we are today!